ALGAL BIOMASS TO HYDROGEN: OPTIMISING CARBON NEGATIVE HYDROGEN PRODUCTION FROM THE SUPERCRITICAL WATER GASIFICATION OF MICROALGAE

by

KIERAN HEELEY

A thesis submitted to the University of Birmingham for the degree of
DOCTOR OF PHILOSOPHY

School of Chemical Engineering

College of Engineering and Physical Sciences

University of Birmingham

September 2024

ABSTRACT

Supercritical water gasification (SCWG) of microalgae is a potentially viable alternative for hydrogen production that can simultaneously remove carbon from the atmosphere, without the environmental challenges associated with other biomass processes. However, due to the high costs of algal production, achieving these environmental benefits requires limiting the feedstock requirement. The work herein addresses this by optimising the hydrogen yield, while ensuring that significant carbon capture is achieved from the SCWG of the microalga *Chlorella vulgaris*.

A continuous SCWG rig was designed, constructed, commissioned and utilised to investigate the influence of operating conditions, catalysts and oxidant to find the optimal values. An initiative of using the algal growth water as the reaction media was adopted, as industrial applications would utilise this as the reaction medium in practice. A significant difference was observed upon using growth water compared to distilled water. Most notable was the decrease in carbon monoxide and increase in hydrogen produced, which was attributed to the elevated pH. Consequently, the algal growth water was utilised as reaction medium in subsequent experiments in this work.

To maximise the hydrogen production, it is important to find the ideal and cost-effective catalyst. Some literature outlined $FeCl_3$ as potentially the most effective catalyst for achieving high hydrogen yields, yet further literature investigating this was scarce. Hence, this work investigates $FeCl_3$ as a potential catalyst for the SCWG of *Chlorella vulgaris,* for a range of temperatures (400 - 600°C) and biomass concentrations (1 – 3wt.%). A significant decrease in hydrogen yield, energy efficiency and the amount of the feedstock carbon that is converted to gas was observed. This was attributed to the reduced pH caused by the Lewis acid activity of $FeCl_3$ which suppressed the water gas shift reaction and increased polymerisation reactions. Accordingly, $FeCl_3$ was deemed an unsuitable catalyst. The more established catalysts of potassium hydroxide (KOH) and ruthenium (Ru/C) were found to be effective and were therefore used for subsequent work in this thesis.

An in-depth study of the influence of temperature (400 - 600°C), biomass concentration (1 - 3wt.%), KOH concentration (0 – 1wt.%), Ru/C catalyst (present or not present) and oxidant (oxidant coefficient 0 - 0.5), including any interactions, was completed. High temperatures, low biomass concentrations, high KOH concentrations and Ru/C catalyst were all found to be favourable for high hydrogen yields. Oxidant enhanced hydrogen yields up to 20% of the stoichiometric concentration for complete oxidation, after which hydrogen was oxidised causing a reduction in hydrogen product yield. Additionally, several significant interactive effects were observed between the catalysts and operating conditions. Hence, in the reaction alone, the greatest hydrogen yield was predicted to be 23 mg/g at 1wt.% biomass, 600°C, 1wt.% KOH, Ru/C and an oxidant coefficient of 0.2.

A whole system model was developed in ASPEN plus ®, which incorporated the experimental work performed as part of this research, to find the true optimum conditions when system losses are considered. The use of experimental data to program the reactor in this model revealed significant deviations from equilibrium reactor models used in literature, which emphasises the importance of incorporation of experimental data in SCWG system analysis. The model of the whole system showed that, as with the reaction alone, higher temperatures and the presence of Ru/C favoured hydrogen yield and efficiency. Oxidant coefficient also showed a similar trend however, greater concentration of oxidant was preferred in the model, due to a larger reaction enthalpy. Higher heating requirements and pumping power required at lower biomass concentrations and poor reaction performance at higher biomass concentrations meant that a moderate 2wt.% was the optimal concentration. Also, KOH was found to be most effective at minimum or maximum concentration (0 or 1wt.%), which differed from the reaction alone. As a result, the optimum hydrogen yield predicted was 12.7mg/g at 2wt% biomass, 600°C, 1wt.% KOH, Ru/C and an oxidant coefficient of 0.3. At these conditions, 68% of the feedstock carbon was captured as CO_2 (38%) or biochar (30%), making the process significantly carbon negative at those conditions.

ACKNOWLEDGEMENTS

Firstly, I'd like to thank my supervisors Bushra Al-Duri and Rafael Orozco for the continued support from the unusual lockdown influenced start of my program all the way to the reviewing of the drafts of this thesis. I would also like to give a special thanks to Lynne Macaskie who despite retirement would always be willing to providing excellent notes on any of my work in her own unique way. I would also like to thank the Sustainable Hydrogen CDT team for funding the project, providing the taught elements and, most importantly, supporting my Get with the H_2ype idea, which allowed me to bring hydrogen research to the best festival in the world (twice).

I also must acknowledge any of the academics, departments and research groups who allowed me access to their equipment and resources with minimal fuss without which, my PhD would have not been possible. This includes Robert Steinberger-Wilckens, Kun Zhang, Osaze Omoregbe and rest of the fuel cell group of UoB for training on and allowing me continued use of their GC-TCD. Bethan Phillips, Nicholas Davidson and the GEES team, for training and use of their TOC and IC equipment, especially as I had absolutely nothing to do with their group. John Love for his support with the algal growth side of the project.

A big shout out to all the friends I've made on the way. The lunch crew in chem eng who made a long day in the lab or writing much more enjoyable and the CDT crew, for many great company at socials and events, with Glastonbury being an obvious standout. And finally, a shoutout to Leeds United, who showed me throughout my PhD, that no matter how hard things got, at least I knew my football team were there to make things worse.

And of course to my Alex, my partner in crime.

TABLE OF CONTENTS

ABSTRACT i

ACKNOWLEDGEMENTS iii

TABLE OF CONTENTS iv

PUBLICATIONS xiii

CONFERENCES xiv

FIGURES xv

Chapter 1 xv

Chapter 2 xv

Chapter 3 xvi

Chapter 4 xvii

Chapter 5 xvii

Chapter 6 xvii

Chapter 7 xix

TABLES xx

Chapter 1 xx

Chapter 2 xx

Chapter 3 xx

Chapter 4 xx

Chapter 5 xxi

Chapter 6 xxi

Chapter 7 xxi

ABBREVIATIONS xxii

SYMBOLS xxiii

CHAPTER 1: INTRODUCTION 1

1.1 Background 1

1.2 Aims and Objectives 2

1.3 Thesis Structure 3

1.4 References 5

CHAPTER 2: LITERATURE REVIEW 8

2.1 Publication: Supercritical water gasification of microalgal biomass for hydrogen production-a review 8

Abstract 8

2.1.1 Introduction 9

2.1.2 Supercritical Water Gasification Reactions 10

2.1.2.1 Main Reactions 10

2.1.2.2 Reaction Pathways 12

2.1.2.2.1 Carbohydrate Gasification 12

2.1.2.2.2 Protein Gasification 13

2.1.2.2.3 Lipid Gasification 14

2.1.3 Influential Factors 16

2.1.3.1 Biomass Composition 16

2.1.3.1.1 Effect of Protein 17

2.1.3.1.2 Effect of Carbohydrates 20

2.1.3.1.3 Effect of Lipids 22
2.1.3.1.4 Tailoring Growth Conditions for Gasification 23
2.1.3.2 Catalysts 24
2.1.3.2.1 Homogeneous Catalysts 25
2.1.3.2.2 Heterogeneous Catalysts 30
2.1.3.2.2.1 Nickel Catalysts 30
2.1.3.2.2.2 Ruthenium Catalysts 33
2.1.3.2.2.3 Other Transition Metals 35
2.1.3.2.2.4 Catalyst Deactivation 36
2.1.3.2.2.5 Effect of the Support 38
2.1.3.2.3 Catalytic Wall Effects 41
2.1.3.3 Temperature 42
2.1.3.4 Biomass Concentration 46
2.1.3.5 Residence or Reaction Time 47
2.1.3.6 Other Factors 53
2.1.3.6.1 Pressure 53
2.1.3.6.2 Heating Rate 54
2.1.4 Supercritical Water Gasification Systems 54
2.1.4.1 Nutrient Recycling 54
2.1.4.2 Integrated systems 57
2.1.5 Conclusion 58
2.1.6 References 60
2.2 Additional Literature 80
2.2.1 Influence of Biomass Composition 80

2.2.2 Catalysts 80
2.2.3 Recovery of Inorganic Nutrients 81
2.2.4 SCWG Reaction Models 82
2.2.5 SCWG System Models 83
2.3 Further Discussion 83
2.4 Additional References 85
CHAPTER 3: EXPERIMENTAL APPARATUS DESIGN, OPERATIONAL AND ANALYTICAL TECHNIQUES 89
3.1 Microalgal Growth 89
3.1.1 Photobioreactor Set-Up 89
3.1.1.1 Initial Experiments 89
3.1.1.2 Finalised Reactor Set-up 90
3.1.2 Analysis Methods 93
3.1.2.1 Culture Monitoring 93
3.1.2.1.1 Growth 93
3.1.2.1.2 pH and Temperature 94
3.1.2.2 Characterisation of Microalgae 95
3.1.2.2.1 Protein 95
3.1.2.2.2 Carbohydrates 95
3.1.2.2.3 Lipid 96
3.1.2.3 Growth Water Analysis 97
3.1.3 Results of Algal Growth 98

3.1.3.1 Algae 98
3.1.3.2 Growth Water 99
3.2 Supercritical Water Gasification 102
3.2.1 Reactor Design Calculations 102
3.2.1.1 Practical Constraints 102
3.2.1.2 Minimum Flowrate 102
3.2.1.3 Reactor Coil design 104
3.2.1.4 Reactor Length 104
3.2.2 Reactor Set-up 106
3.2.3 Experimental Procedure 111
3.2.3.1 Feedstock Preparation 111
3.2.3.2 Operational Procedure 112
3.2.3.2.1 Pre-Experiment Procedure 112
3.2.3.2.2 Experimental Procedure 113
3.2.3.2.3 Post-Experiment Procedure 113
3.2.4 Analysis Methods 114
3.2.4.1 Product Analysis 114
3.2.4.1.1 Gas 114
3.2.4.1.2 Liquid 114
3.2.4.2 Calculations 115
3.2.4.2.1 Gas Yields 115
3.2.4.2.2 Carbon Conversion 116

3.2.4.2.3 Other Parameters 116
3.2.5 Initial Tests 117
3.2.5.1 Flow Tests 117
3.2.5.2 Residence time tests 117
3.2.5.3 Catalyst and Oxidant Concentration Tests 118
3.2.5.4 Oxidant Concentrations 121
3.2.6 Safety Considerations 123
3.3 References 124
CHAPTER 4: THE IMPACT OF THE ALGAL GROWTH WATER ON SUPERCRITICAL WATER GASIFCATION OF *CHLORELLA VULGARIS* 129
4.1 Publication: Supercritical water gasification of microalgae: The impact of the algal growth water 129
Abstract 129
4.1.1 Introduction 130
4.1.2 Materials and methods 135
4.1.2.1 Materials 135
4.1.2.2 Supercritical Water Gasification Reactor Set-Up 137
4.1.2.3 Analysis 138
4.1.3 Results and discussion 139
4.1.3.1 Glucose Gasification Without a Catalyst 139
4.1.3.2 Glucose Gasification With a Catalyst 143
4.1.3.3 Microalgae Gasification 145
4.1.4 Conclusion 147

4.1.5 References 149
4.2 Further Discussion 156
CHAPTER 5: ASSESSMENT OF IRON(III) CHLORIDE AS A CATALYST FOR THE PRODUCTION OF HYDROGEN FROM THE SUPERCRITICAL WATER GASIFICATION OF MICROALGAE 157
Abstract 157
5.1 Introduction 158
5.2 Materials and Methods 163
5.2.1 Materials 163
5.2.2 Supercritical Water Gasification Set-up 165
5.2.3 Analysis 166
5.2.4 Design of Experiments 167
5.3 Theory 168
5.4 Results and Discussion 169
5.4.1 Assessment of $FeCl_3$ 169
5.4.2 Comparison to Other Catalysts 177
5.4.3 pH Analysis 179
5.5 Conclusion 182
5.6 References 183
5.7 Further Discussion 195
CHAPTER 6: ASSESSMENT OF THE OPTIMAL REACTION CONDITIONS AND CATALYST COMBINATIONS FOR THE PRODUCTION OF CARBON NEGATIVE HYDROGEN FROM THE SUPERCRITICAL WATER GASIFICATION OF MICROALGAE 197

Abstract 198

6.1 Introduction 199

6.2 Materials and Methods 203

6.2.1 Materials 203

6.2.2 Supercritical Water Gasification Reactor Set-up 204

6.2.3 Analysis of Experimental Work 206

6.2.4 Design of Experiments 207

6.2.5 System Model 208

6.3 Results and Discussion 217

6.3.1 SCWG Experimental Results 217

6.3.1.1 Impact of Reaction Conditions 225

6.3.1.2 Impact of Catalysts 227

6.3.1.3 Impact of Oxidant 230

6.3.2 SCWG System Model Results 232

6.3.2.1 Comparison to Equilibrium Values 232

6.3.2.2 Consideration of Factors 235

6.3.2.2.1 Biomass Concentration 238

6.3.2.2.2 Impact of Catalysts 240

6.3.2.2.3 Oxidant 242

6.3.2.2.4 Optimal conditions 243

6.4 Conclusion 246

6.5 References 247

CHAPTER 7: CONCLUSIONS AND RECOMMENDATIONS FOR FURTHER WORK 257

APPENDICES ..... a

A- Optical Density and Concentration Relationship ..... a

B- Lipid Measurement Verification ..... a

C- Pump Flowrate Testing ..... b

D. pH of the Liquid Product c

E. Organic Liquid Analysis ..... e

F. Investigation into Recycle Rate and Pressure ..... f

G. pH Change and Influence of KOH ..... g

H. Actual vs Predicted Plots ..... g

PUBLICATIONS

This thesis incorporates the following papers, which are included in the format of the corresponding journal for which they have been submitted to or published in. For these chapters, Al-Duri, Orozco and Macaskie offered support with writing (proof) and conceptualisation of all 4 publications. Love offered support on background knowledge for the algal growth aspect that influenced all 4 publications. Shah and Sheppard provided GC-MS analysis of the liquid phase after reaction in publications 2 and 3. Glover offered support in the production of the ASPEN Plus® model used in the final publication. The remaining work was completed by the author of this thesis. This includes, literature review, conceptualisation, design of experiments, experimental operation, data analysis, visualisation, model construction and writing.

- **K. Heeley**, R. L. Orozco, L. E. Macaskie, J. Love and B. Al-Duri, "Supercritical water gasification of microalgal biomass for hydrogen production-A review," *International Journal of Hydrogen Energy*, vol. 49 Part A, pp. 310-336, 2024. https://doi.org/10.1016/j.ijhydene.2023.08.081
- **K. Heeley**, R. L. Orozco, Z. Shah, L. E. Macaskie, J. Love and B. Al-Duri, "Supercritical water gasification of microalgae: The impact of the algal growth water," *The Journal of Supercritical Fluids*, vol. 205, 2024 https://doi.org/10.1016/j.supflu.2023.106143
- **K. Heeley,** R. L. Orozco, I.Sheppard, L. E. Macaskie, J. Love and B. Al-Duri, "Assessment of iron(Iii) chloride as a catalyst for the production of hydrogen from the supercritical water gasification of microalgae," vol.6, *Next Energy,* 2025 https://doi.org/10.1016/j.nxener.2024.100198
- **K. Heeley,** R. L. Orozco, B. Glover, L. E. Macaskie, J. Love and B. Al-Duri, "Assessment of the optimal reaction conditions and catalyst combinations for the production of carbon negative hydrogen from the supercritical water gasification of microalgae," (in submission)

CONFERENCES

This section outlines the conferences for which oral presentations of this work were performed.

International Solvothermal and Hydrothermal Association Conference **September 2023**

Valladolid, Spain

Supercritical water gasification of microalgae: The impact of the algal growth water

Hydrogen Days **March 2024**

Prague, Czech Republic

Assessment of $FeCl_3$ as a catalyst for hydrogen production from the supercritical water gasification of microalgae.

FIGURES

CHAPTER 1

No Figures

CHAPTER 2

Figure 2.1: Reaction pathways for the supercritical water gasification of glucose……13

Figure 2.2: Protein gasification reaction pathway……14

Figure 2.3: Potential free radical reaction pathways for the gasification of glycerol as a model compound for lipids……15

Figure 2.4: Carbon gasification efficiency of different amino acids at varying temperatures……..20

Figure 2.5: Potential products formed from different bond cleavages in supercritical water gasification……..25

Figure 2.6: Phenol content in the effluent of the supercritical water gasification of glucose……...28

Figure 2.7: Change in carbon gasification efficiency in time on stream of the continuous supercritical water gasification of glycerol and *Phaeodactylum tricornutum* using an activated carbon supported ruthenium catalyst……..37

Figure 2.8: Methane-carbon dioxide ratio at different total carbon gasification efficiencies during the supercritical water gasification of *Chlorella vulgaris* using ruthenium catalysts with different supports……40

Figure 2.9: Dry gas composition and gasification efficiency for the non-catalytic supercritical water gasification of *Chlorella vulgaris* in a batch reactor……44

Figure 2.10: Impact of temperature on the carbon and hydrogen gasification efficiencies for the supercritical water gasification of *Chlorella pyrenoidos*a……45

Figure 2.11: Carbon gasification efficiency at different reaction times for the batch supercritical water gasification of *Chlorella vulgaris*, with and without a charcoal supported ruthenium catalyst…….49

Figure 2.12: Change in gas composition and gasification efficiency over time, for supercritical water gasification of *Chlorella vulgaris* without a catalyst……50

Figure 2.13: Gas composition over time for the supercritical water gasification of glucose with either no catalyst or a ruthenium on alumina catalyst……..52

Figure 2.14: Microalgae growth in the residual water following the supercritical water gasification *of Acutodesmus Obliquus*, comparison of the different treatment methods……..56

Figure 2.15: Potential supercritical water gasification of microalgae system to produce hydrogen and capture carbon dioxide……..57

CHAPTER 3

Figure 3.1: Initial algal growth experiment…….91

Figure 3.2: Photobioreactor set-up schematic diagram……..92

Figure 3.3: Images of photobioreactor set-up……...92

Figure 3.4: Algal mass produced for each 2-week batch growth of Chlorella vulgaris……..98

Figure 3.5: Reactor set-up one feed schematic diagram……..108

Figure 3.6: Reactor set-up two feeds schematic diagram……108

Figure 3.7: SCWG reactor image……..109

Figure 3.8: SCWG downstream processing image: part 1……110

Figure 3.9: SCWG downstream processing image: part 2……110

Figure 3.10: Impact of residence time on the hydrogen yield……118

Figure 3.11: Influence of KOH on hydrogen yield and carbon gasification efficiency……..119

Figure 3.12: Influence of KOH on liquid product……..119

Figure 3.13: Influence of FeCl3 on hydrogen yield and carbon gasification efficiency…….120

Figure 3.14: Influence of FeCl3 on liquid product……..120

Figure 3.15: Influence of oxidant coefficient on hydrogen yield and carbon gasification efficiency.122

Figure 3.16: Influence of oxidant coefficient on liquid product……..122

CHAPTER 4

Figure 4.1: Reaction pathways of the supercritical water gasification of glucose……..134

Figure 4.2: Experimental set-up……...137

Figure 4.3: Results of the supercritical water gasification of glucose without a catalyst……...140

Figure 4.4: Results of the supercritical water gasification of glucose with a catalyst……143

Figure 4.5: Results of the supercritical water gasification of C*hlorella vulgaris* without a catalyst..146

CHAPTER 5

Figure 5.1: Experimental set-up……...165

Figure 5.2: Hydrogen yield, energy efficiency and carbon distribution comparison for FeCl3 as a catalyst……171

Figure 5.3: Non-hydrogen gas yields in mg/g of feedstock……...171

Figure 5.4: Gas yields, carbon product distribution and energy efficiency comparison for different catalysts……..177

Figure 5.5: Effect of pH on the main output variables……180

Figure 5.6: Effect of pH on the CO and H2% in gas and inorganic carbon in the liquid……..180

CHAPTER 6

Figure 6.1: Experimental set-up……..205

Figure 6.2: Modelled System for the Supercritical Water Gasification of Microalgae, with a equilibrium reactor……211

Figure 6.3: Modelled System for the Supercritical Water Gasification of Microalgae, with a reactor modelled on experimental data……..212

Figure 6.4: Equilibrium system model ASPEN PLUS® flowsheet……..213

Figure 6.5: System model including experimental data ASPEN PLUS® flowsheet…….214

Figure 6.6: Interaction between factors on the hydrogen yield……..223

Figure 6.7: Interaction between factors on the energy efficiency……223

Figure 6.8: Interaction between factors on the carbon conversion…….224

Figure 6.9: Interaction between factors on the residual carbon……..224

Figure 6.10: Impact of temperature and biomass concentration on hydrogen Yield, carbon conversion, energy efficiency and residual carbon……..225

Figure 6.11: Impact of KOH and Ru/C catalysts on hydrogen Yield, carbon conversion, energy efficiency and residual carbon……227

Figure 6.12: Impact of oxidant on hydrogen yield, carbon conversion, energy efficiency and residual carbon……230

Figure 6.13: Comparison of the hydrogen yield and energy efficiency of equilibrium model to experimental model……..233

Figure 6.14: Comparison of the carbon capture of equilibrium model to experimental model…….233

Figure 6.15: Interaction between factors on the hydrogen yield of the system model based on experimental data……..236

Figure 6.16: Interaction between factors on the efficiency of the system model based on experimental data…….237

Figure 6.17: Interaction between factors on the carbon capture of the system model based on experimental data…….237

Figure 6.18: Influence of biomass concentration on hydrogen Yield, efficiency and carbon capture of the system model using experimental data……..238

Figure 6.19: Influence of catalysts on hydrogen yield, efficiency and carbon capture of the system model using experimental data……..240

Figure 6.20: Influence of oxidant coefficient on hydrogen yield, efficiency and carbon capture of the system model using experimental data…….242

CHAPTER 7

No figures

TABLES

CHAPTER 1

No Tables

CHAPTER 2

Table 2.1: Microalgae Compositions……..17

Table 2.2: Comparison of gas composition, gas yield and gasification efficiency for supercritical water gasification of *Chlorella vulgaris* with or without increased carbohydrate content….21

Table 2.3: Akali metal catalysts that increase the carbon gasification efficiency of the supercritical water gasification of biomass feedstocks……...26

Table 2.4: Nickel catalysts used in the supercritical water gasification of biomass feedstocks……31

Table 2.5: Ruthenium catalysts used in the supercritical water gasification of biomass feedstocks.34

Table 2.6: Microalgae experiments in which a decrease in hydrogen content was observed with an increase in biomass concentration in the feed……...47

CHAPTER 3

Table 3.1: Composition of Chu-13 growth medium……..91

Table 3.2: Algae characterisation results……..99

Table 3.3: Analysis of algal growth water and Chu-13 media……101

Table 3.4: Equipment constraints……..102

CHAPTER 4

Table 4.1: Supercritical water gasification of microalgae literature summary……131

Table 4.2: Growth water ion composition……..136

Table 4.3: *Chlorella vulgaris* composition……136

CHAPTER 5

Table 5.1: Heterogenous catalysts used in the supercritical water gasification of biomass…….160

Table 5.2: Homogenous catalysts used in the supercritical water gasification of biomass……...161

Table 5.3: Composition of *Chlorella vulgaris* feedstock……..163

Table 5.4: Growth water ion composition……..164

Table 5.5: Logworth of each factor of the model……..170

CHAPTER 6

Table 6.1: Composition of *Chlorella vulgaris* feedstock……..203

Table 6.2: Growth water ion composition……..204

Table 6.3: Experimental results for the SCWG of *Chlorella vulgaris* in a continuous system…….218

Table 6.4: Directional logworth of each factor on the carbon conversion, energy efficiency and gas yields…….222

Table 6.5: Directional logworth of each factor on the carbon conversion, energy efficiency and carbon capture of the system model based on experimental data……236

Table 6.6: System model results for a series of optimisation criteria……...244

CHAPTER 7

No Tables

ABBREVIATIONS

Abbreviation	Meaning
5-HMF	5-(hydroxymethyl)furfural
BECCS	Bioenergy with Carbon Capture and Storage
BPR	Back Pressure Regulator
CGE	Carbon Gasification Efficiency
CoV	Coefficient of Variance
DW	Distilled Water
GC-MS	Gas Chromatography-Mass Spectrometer
GC-TCD	Gas Chromatography with Thermal Conductivity Detector
GW	Algal Growth Water
HGE	Carbon Gasification Efficiency
HHV	Higher Heating Value
IC	Ion Chromatography
ICP	Inductively Coupled Plasma Spectroscopy
ML	Machine Learning
OD_{680}	Optical Density at 680 nanometres
PBR	Photobioreactor
PSRK	Predictive Soave–Redlich–Kwong
Ru/C	Activated Carbon Supported Ruthenium Catalyst
SCW	Supercritical Water
SCWG	Supercritical Water Gasification
TIC	Total Inorganic Carbon
TOC	Total Organic Carbon
UoB	University of Birmingham
WGS	Water Gas Shift Reaction

SYMBOLS

Symbol	Meaning
A_{ov}	Oven Internal Surface Area
A_r	Reactor External Surface Area
B	Biomass
C	Catalyst
C_i	Constant
d	Diameter
d_i	Internal Diameter
d_o	External Diameter
h_i	Internal Heat Transfer Coefficient
h_o	External Heat Transfer Coefficient
h_{oc}	External Heat Transfer Coefficient (due to convection)
h_{or}	External Heat Transfer Coefficient (due to radiation)
H_T	Enthalpy at a Given Temperature
I	Intermediate Product
k	Thermal Conductivity
$\dot{m}$	Mass Flow Rate
pr	Prantl Number
Q	Heat Flow
Re	Reynolds Number
T	Temperature
T_{ov}	Oven Temperature
T_r	Reactor Temperature
T_{ro}	Room Temperature
U	Overall Heat Transfer Coefficient
v	Volumetric flow
W	Work
x	Mass Fraction
x_a	Algal Mass Fraction
Y_x	Yield of Product x
ΔT_{lm}	Log Mean Temperature Difference
ε_{ov}	Emissivity of the Oven
ε_r	Emissivity of the Reactor
μ	Dynamic Viscosity
μ_c	Dynamic Viscosity of Continuous Phase in a Slurry
ρ_a	Algal Cell Density
ρ_p	Algal Powder Density
ρ_T	Total Density
ρ_w	Water Density
ρ_x	Density of Product x
σ	Boltzmann's Constant
φ	Volume Fraction
φ_m	Maximum Packing Fraction
Φ_x	Volume Fraction of Product x

CHAPTER 1: INTRODUCTION

1.1 BACKGROUND

To control global warming and prevent the crossing of catastrophic environmental tipping points, rapid reductions in greenhouse gas emission are required. Carbon removal technologies are expected to be key to this, of which biomass with carbon capture and storage (BECCS) is expected to be a key contributor [1]. BECCS offers the unique double advantage of simultaneously removing CO_2 from the atmosphere and satisfying energy requirements that the majority of which is still fulfilled by fossil fuels. However, biomass production often has unwanted negative environmental and social consequences. The use of pesticides [2], large monocultures [3] and fertilizers [4] are all damaging for biodiversity. Moreover, food prices can be impacted by the competition for land and fertilizers [5].

Microalgae can grow 10 times faster than terrestrial plants [6] and is grown in contained bioreactors. Consequently, the land requirement is reduced, and arable quality of the soil is not required. Also, pesticides and nutrients are contained, mitigating much of the negative impacts of biomass production. However, the high moisture content makes it unfeasible for conventional energy conversion processes such as thermal gasification, combustion and pyrolysis [7]. Alternative methods are required to extract the energy and carbon from the algae to take advantage of its potential as a feedstock for BECCS.

Supercritical water gasification (SCWG) uses water above its critical point as the reaction medium, to convert a biomass feedstock into a hydrogen rich syngas. This syngas can be used to produce energy directly or the hydrogen separated to help decarbonise hard to abate sectors [8]. The use of water as reaction media eliminates any limitations of high moisture feedstocks like microalgae and the properties of supercritical water provide additional advantages. The high diffusivity enhances reaction rates [9] and the low dielectric constant allows organic intermediates to dissolve, decreasing recombination and increasing gas yield [10]. Additionally, the CO_2 can be easily separated with

minimal additional processing [11] and the char biproduct can be utilised in construction materials [12]. This makes SCWG an ideal process to produce carbon negative hydrogen from algal biomass.

Despite these advantages, growth of microalgae comes at a significant cost [13] and, while less than alternative biomass sources, still possesses a significant land footprint [14]. Therefore, to ensure the environmental benefits of microalgae SCWG are realised, optimisation of the process to maximise the hydrogen yield is required. This is work aims to address this.

1.2 Aims and Objectives

The aim of this project is to maximise the hydrogen production from the SCWG of microalgae, while ensuring significant carbon capture is achieved. As a result, the algal feedstock requirement will be reduced. This will suppress costs and negative environmental impacts, increasing the feasibility of SCWG of microalgae as a carbon negative hydrogen source. This aim was achieved through the following objectives and their associated tasks:

1. *Set-up appropriate experimental apparatus and procedures.*
    a. Design, construction and testing of a continuous SCWG rig that is representative of a potential industrial system.
    b. Testing and development of appropriate reaction conditions, variables ranges and operational procedures.
2. *Investigate new and existing catalyst combinations.*
    a. In-depth analysis of new catalysts of interest for SCWG of microalgae at a range of reaction conditions.
    b. Comparison with more established catalysts, including their interactions.

3. *Investigate the Influence of different factors on the SCWG reaction*.
    a. Detailed experimental study and analysis of the effects of key operating parameters, including any interactions.
    b. Regression analysis to produce relationships between these factors and key output variables.
4. *Study the influence different factors on the SCWG system.*
    a. Development of SCWG system model to produce hydrogen and capture carbon that incorporates experimental data.
    b. Analysis of impact of operating conditions, catalysts and oxidant.
    c. Selection of optimal conditions for hydrogen yield, efficiency and carbon capture.

1.3 THESIS STRUCTURE

Chapter 2 contains an in-depth literature review on the SCWG of different biomass sources, including microalgae. This studies the impact of biomass composition, catalysts and reaction conditions, with a focus on their impact on hydrogen production. Much of this chapter is a paper published in the *Internation Journal of Hydrogen Energy*, with additional literature included following this to capture the research completed since its publication.

Chapter 3 outlines the design, development and selection of the experimental apparatus, experimental methods and analytical techniques used in the subsequent chapters.

Chapter 4 presents a detailed analysis of the impact of the growth media that remains after algal growth on the SCWG reaction. Analysis for a range of reaction conditions, catalysts and biomass feedstocks is considered. The work presented is published in the *Journal of Supercritical Fluids*. The results of this chapter are used to select the reaction media utilised in the subsequent work.

Chapter 5 presents a comprehensive analysis of the impact of iron (III) chloride ($FeCl_3$) as a catalyst for the SCWG of *Chlorella vulgaris.* Analysis for a range of reaction conditions and comparison to other catalysts is considered. The work presented is published in *Next Energy*. The results of this chapter are used to select the catalysts studied in the final results chapter.

Chapter 6 presents an extensive analysis of the influence of temperature, biomass concentration, catalysts (potassium hydroxide (KOH) and activated carbon supported ruthenium (Ru/C)) and oxidant on the SCWG of *Chlorella vulgaris*. This work is then integrated into a whole system model in ASPEN Plus®, to select the optimum conditions for hydrogen production and carbon capture. The work presented has been submitted for publication in *Chemical Engineering Journal*.

Chapter 7 summarises the main findings and conclusions of the work, recommending any appropriate further work that may add to this field of research.

1.4 REFERENCES

[1] Intergovernmental Panel on Climate Change: Working Group 3, “Climate Change 2022-Mitigation of Climate Change,” Intergovernmental Panel on Climate Change, Geneva, 2022.

[2] F. Geiger, J. Bengtsson, F. Berendse, W. W. Weisser, M. Emmerson, M. B. Morales, P. Ceryngier, J. Liira, T. Tscharntke, C. Winqvist, S. Eggers, R. Bommarco, T. Pärt, V. Bretagnol, M. Plantegenest, L. W. Clement, C. Dennis, C. Palmer, J. J. Onate and I. Guerrero, “Persistent negative effects of pesticides on biodiversity and biological control potential on European farmland,” *Basic and Appl. Ecology,* vol. 11, no. 2, pp. 97-105, 2010. doi:10.1016/j.baae.2009.12.001.

[3] M. S. Yahya, M. Syafiq, A. Ashton-Butt, A. Ghazali, S. Asmah and B. Azhar, “Switching from monoculture to polyculture farming benefits birds in oil palm production landscapes: Evidence from mist netting data,” *Ecology and Evolution,* vol. 7, no. 16, p. 6, 2017. doi:10.1002/ece3.3205.

[4] M. Dorgham, “Effects of Eutrophication.,” in *Eutrophication: Causes, Consequences and Control*, Dordrecht, Springer, 2014. doi:10.1007/978-94-007-7814-6_3.

[5] J. Tomei and R. Helliwell, “Food versus fuel? Going beyond biofuels,” *Land Use Policy,* vol. 56, pp. 320-236, 2016. doi:10.1016/j.landusepol.2015.11.015.

[6] M. Benedetti, V. Vecchi, S. Barera and L. Dall’Osto, “Biomass from microalgae: the potential of domestication towards sustainable biofactories,” *Microb Cell Factories,* vol. 17, no. 173, 2018. doi:10.1186/s12934-018-1019-3.

[7] Y. Yoshida, K. Dowaki, Y. Matsumura, R. Matsuhashi, D. Li, H. Ishitani and H. Komiyama, “Comprehensive comparison of efficiency and CO2 emissions between biomass energy conversion technologies—position of supercritical water gasification in biomass technologies,” *Biomass and Bioenergy,* vol. 25, no. 3, pp. 257-272, 2003. doi:10.1016/S0961-9534(03)00016-3.

[8] Committee on Climate Change, “Hydrogen in a Low-Carbon Economy,” Committee on Climate Change, London, 2018.

[9] N. Akiya and P. E. Savage, “Roles of Water for Chemical Reactions in High-Temperature Water,” *Chem. Reviews,* vol. 102, no. 8, pp. 2725-2750, 2002. doi:10.1021/cr000668w.

[10] C. Wang, W. Zhu, H. Zhang, C. Chen, X. Fan and Y. Su, “Char and tar formation during hydrothermal gasification of dewatered sewage sludge in subcritical and supercritical water: Influence of reaction parameters and lumped reaction kinetics,” *Waste Management,* vol. 100, pp. 57-65, 2019. doi:10.1016/j.wasman.2019.09.011.

[11] J. A. Withag, J. R. Smeets, E. A. Bramer and G. Brem, “System model for gasification of biomass model compounds in supercritical water – A thermodynamic analysis,” *The Journal of Supercritical Fluids,* vol. 61, pp. 157-166, 2012 doi:doi.org/10.1016/j.supflu.2011.10.012.

[12] S. A. Miller, E. V. Roijen, P. Cunningham and A. Kim, “Opportunities and challenges for engineering construction materials as carbon sinks,” *RILEM Tech. Lett.,* vol. 6, pp. 105-118, 2021 doi:https:10.21809/rilemtechlett.2021.146.

[13] M. Brandenberger, J. Matzenberger, F. Vogel and C. Ludwig, “Producing synthetic natural gas from microalgae via supercritical water gasification: A techno-economic sensitivity analysis,” *Biomass and Bioenergy,* vol. 51, pp. 26-34, 2013 doi:10.1016/j.biombioe.2012.12.038.

[14] P. W. Gerbens-Leenes, L. Xu, G. J. d. Vries and A. Y. Hoekstra, “The blue water footprint and land use of biofuels from algae,” *Water Resour. Res.,* vol. 50, no. 11, pp. 8549-8563, 2014 doi:10.1002/2014WR015710.

CHAPTER 2: LITERATURE REVIEW

2.1 PUBLICATION: SUPERCRITICAL WATER GASIFICATION OF MICROALGAL BIOMASS FOR HYDROGEN PRODUCTION-A REVIEW

The research within this chapter subsection has been published as a review article in the International *Journal of Hydrogen Energy*, as cited on the following page. For consistency with the published material, the content remained the same as the journal article.

ABSTRACT

Due to their potential for a high growth rate microalgae are seen as promising feedstocks for hydrogen production, but their high-water content makes them unsuitable for traditional gasification. An alternative method, such as supercritical water gasification, is required to maximise this potential. This review assesses the literature involving the supercritical water gasification of microalgae and other relevant feedstocks. The impact on hydrogen yield, of biomass composition, catalysts, operating conditions, and the integration of the reactor into larger systems are considered. A high carbohydrate and low protein feed is usually preferable for maximum hydrogen yield. Homogeneous alkali metal salts and heterogeneous transition metals are desirable as catalysts. Issues such as recyclability, deactivation, and poor selectivity towards hydrogen production of these catalysts remain problematic. High temperatures and low biomass concentrations are suitable for high yields but require high energy inputs, so may not be advantageous when considering a whole system energy balance.

2.1.1 Introduction

The release of greenhouse gases, largely through the burning of fossil fuels, has significantly increased the average global temperature to 1.2°C above pre-industrial levels. Unless this warming is limited to 1.5°C, irreversible environmental tipping points could be crossed and devastating consequences for global ecosystems and communities are foreseen. To prevent the crossing of environmental tipping points, net greenhouse gas emissions must be zero by 2050 [1]. Hydrogen could replace fossil fuels in many applications where electrification is difficult, such as heavy industry and long-distance transport. However, to be carbon neutral, highly polluting methods of hydrogen production that currently produce most of the hydrogen today, such as steam methane reforming, must be replaced. Within these alternatives, biomass-derived hydrogen is an attractive option as it has the advantage of not increasing the strain on renewable electricity production, which would occur with widespread production of hydrogen through electrolysis, while also possessing the potential to be carbon negative if combined with carbon capture and storage [2].

Amongst potential biomass feedstocks, microalgae have excellent potential. A much higher photosynthetic efficiency than terrestrial plants [3] results in a growth rate up to tenfold greater [4] and a correspondingly greater rate of carbon sequestration [5]. This allows more efficient use of the land available, a significant advantage because land use is an area of major concern of bioenergy [6]. Microalgae can also simultaneously remove harmful metals from the environment [7]. However, the high-water content of algae has an adverse effect on traditional thermal gasification processes due to the significant energy required for drying [8]. Therefore, it is important to consider conversion processes that can handle feedstocks with a high-water content.

Supercritical water gasification (SCWG) involves the conversion of organic compounds to gaseous products in water under conditions above its critical point (374°C and 22.1MPa) [9]. The use of water as the reaction medium makes it appropriate for high moisture feeds (like microalgae), while the thermophysical properties of supercritical water (SCW) bring a variety of other advantages. Beyond the critical point, the density and viscosity fall, increasing the diffusivity, thus reducing transport

limitations, and increasing reaction rates [10]. Furthermore, the dielectric constant of SCW is significantly lower than that of subcritical water, making it a universal solvent for all organics, polymers and gases whereas the solubility of polar compounds decreases [10]. This allows the organic intermediates formed from the degradation of biomass to dissolve into the water, reducing their chance of recombining to form longer chain tars and chars [11]. Such compounds are usually undesirable as they reduce gasification yield and can block the reactor. Although, the biochar has the potential to be used in Electrochemical Double Layer Capacitors, so may be of value if reactors are designed to capture the solid product [12].

This review aims to summarise the work up to date on the supercritical water gasification of microalgal biomass. It identifies key areas that affect hydrogen production and biomass conversion, drawing on work done on algae as well as other relevant biomass feedstocks. It also looks at potential systems that incorporate SCWG of algae, while maximising their efficiency and reducing waste. This will help to identify areas of further work required to address existing technical challenges and increase the feasibility of this technology.

2.1.2 Supercritical Water Gasification Reactions

2.1.2.1 Main Reactions

In SCWG, several reactions occur, both in series and in parallel with each other. The first reaction is the hydrolysis of the longer chain molecules within the biomass into smaller intermediates, as shown B and I in equation 1 respectively. For example, starch is broken down into glucose and protein is broken down into its constituent amino acids [13].

$$B + H_2O \rightarrow I_1 + I_2 \quad (1)$$

The main reactions considered for the gasification of these intermediates are steam reforming, water gas shift (WGS) and methanation reactions, as shown by equations 2, 3 and 4 respectively [14]. The gaseous products are hydrogen (H_2), carbon dioxide (CO_2), carbon monoxide (CO) and methane (CH_4),

$$C_xH_yO_z + (x-z)H_2O \rightarrow xCO + \left(\frac{y}{2} + x - z\right)H_2 \quad (2a)$$

$$C_xH_yO_z + (2x-z)H_2O \rightarrow xCO_2 + \left(\frac{y}{2} + 2x - z\right)H_2 \quad (2b)$$

$$CO + H_2O \rightarrow CO_2 + H_2 \quad (3)$$

$$CO + 3H_2 \rightarrow CH_4 + H_2O \quad (4a)$$

$$CO_2 + 4H_2 \rightarrow CH_4 + 2H_2O \quad (4b)$$

The steam reforming reaction can produce CO (Equation 2a) [13], CO_2 (Equation 2b) [9] or both as potential reaction pathways [15] [16]. As equation 2b is equal to 2a followed by the water gas shift reaction, it would be difficult to tell whether the CO_2 arose directly from the steam reforming reaction or via a two-step reaction. Hence, either of them could be the correct pathway. However, equation 2a must occur as CO is often found as a product if a catalyst is not used [17]. Hence, it is likely that equation 2b is this combined with the water gas shift reaction. Similarly, a direct formation of CH_4 and CO_2 has also been outlined as a potential reaction [13], which can be explained by reaction 2b followed by 4b, so is not considered here. In some cases, glucose for example, equation 2a does not contain water at all, which suggests that water is also a product of the reaction which in those cases, is produced at the same rate it is used up. Indicating a catalytic effect of the water.

In practice, SCWG involves several other possible side/intermediate reactions, some of which are discussed in more detail in Section 2.1.2.2. Multiple sources have reported that at low temperatures, when gasifying different algal strains without the presence of a catalyst, the gas product consists almost entirely of CO_2 [4] [18]. This means that decarboxylation reactions must predominate. The occurrence of short chain alkanes such as ethane or propane, gives evidence of cracking reactions [15], while the formation of chars shows polymerisation reactions are present [16]. A variety of other molecular rearrangements can also occur in the reactor; particularly problematic being dehydration and ring closure reactions to form phenols [19]. Phenols are very difficult to gasify, reducing the

gasification of other compounds around them and can polymerise into highly toxic compounds [20] [21].

2.1.2.2 Reaction Pathways

The potential reaction pathways in SCWG for some compounds commonly found in biomass have been studied and evaluated in the literature mainly focusing on lignocellulosic biomass, but some of it is relevant to algal biomass. Microalgae consist mainly of proteins, lipids, and carbohydrates [22], with the total products being a result of their breakdown and the interactions between breakdown products. Reaction pathways of model compounds have been studied and, while the real system will be more complex, this helps to understand some of the reactions that describe the SCWG process.

2.1.2.2.1 Carbohydrate Gasification

Glucose is commonly used as a model compound for studying the gasification of carbohydrates as it the 'building unit' of carbohydrates and thus is the decomposition product of many major carbohydrates [9]. Figure 2.1 shows the reaction pathways in SCWG of glucose outlined in the literature [23, 24]. One pathway forms phenols and other aromatics, either directly or through electrocyclic reaction of furans. These are difficult to gasify due to the stability of the benzene ring in SCW, thus are much more likely to form chars, making this route undesirable. To maximise the gas produced, the formation of readily gasified short chain acids, alcohols and ketones, formed through C-C scission of larger ketones, aldehydes, and furans, is preferred. This can be achieved through the addition of catalysts, as discussed later in Section 2.1.3.2. Despite this, furans such as 5-Hydroxymethylfurfural or furfural are useful chemical precursors in biorefinery processes [25], so the formation of these may be preferred in some cases.

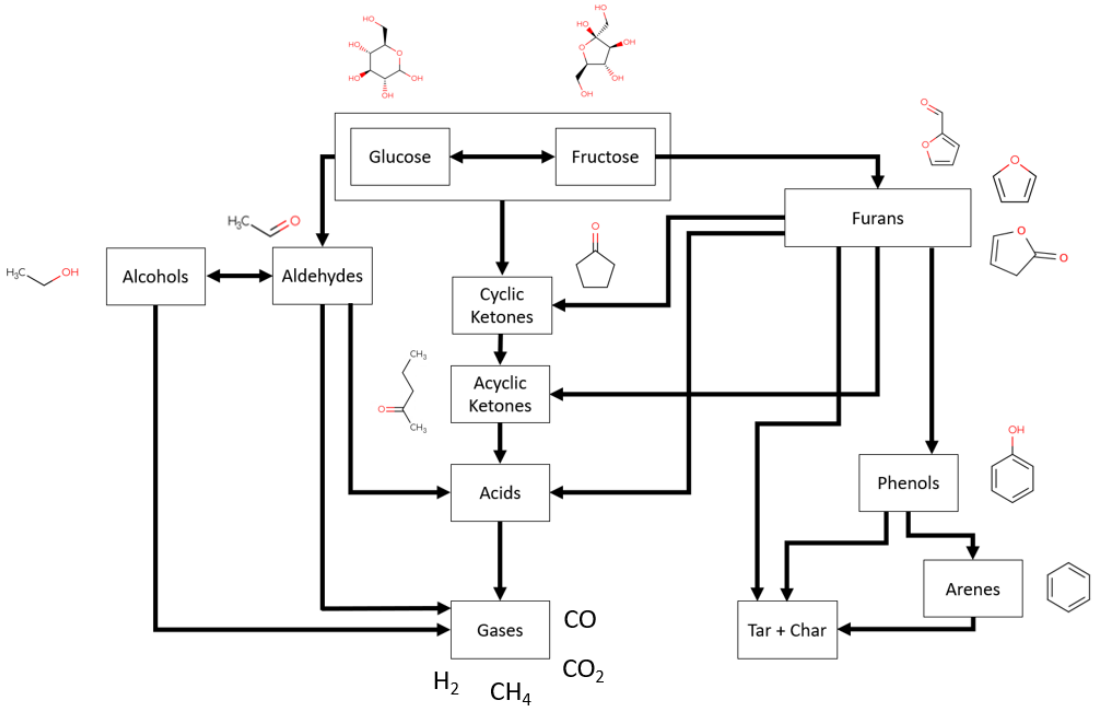

Figure 2.1-Reaction pathways for the supercritical water gasification of glucose [15] [16]

2.1.2.2.2 Protein Gasification

Proteins commonly hydrolyse in supercritical water to form amino acids and peptides which subsequently undergo further reactions [26] but, compared with carbohydrates, the hydrolysis of proteins is up to 12 times slower and proteins are hydrolysed from the microalgae at approximately half the rate [27]. Possible pathways include the decarboxylation route to form amines and carbon dioxide or deamination to form ammonia and organic acids. These have both been noted extensively in the subcritical region [28] [29] [30] and remain the main pathways in the supercritical region [31], and hence are likely to occur in SCWG both during heating and in the reactor. The stable nature of amines makes that pathway undesirable and the formation of ammonia and organic acids, the favourable pathway for hydrogen production. Additionally, amino acids can react with carbonyl intermediates in the Maillard reaction to form N-heterocyclic compounds such as pyridine [32] [33], which are also stable and thus undesirable for gas production. The peptides can hydrolyse into amino acids or decompose into aromatic hydrocarbons, diketopiperazine, aliphatic amines or

aldehydes [33]. Many of these are undesirable as they can polymerise into tar and chars [26], which are difficult to gasify and can block the reactor. This pathway is summarised in Figure 2.2.

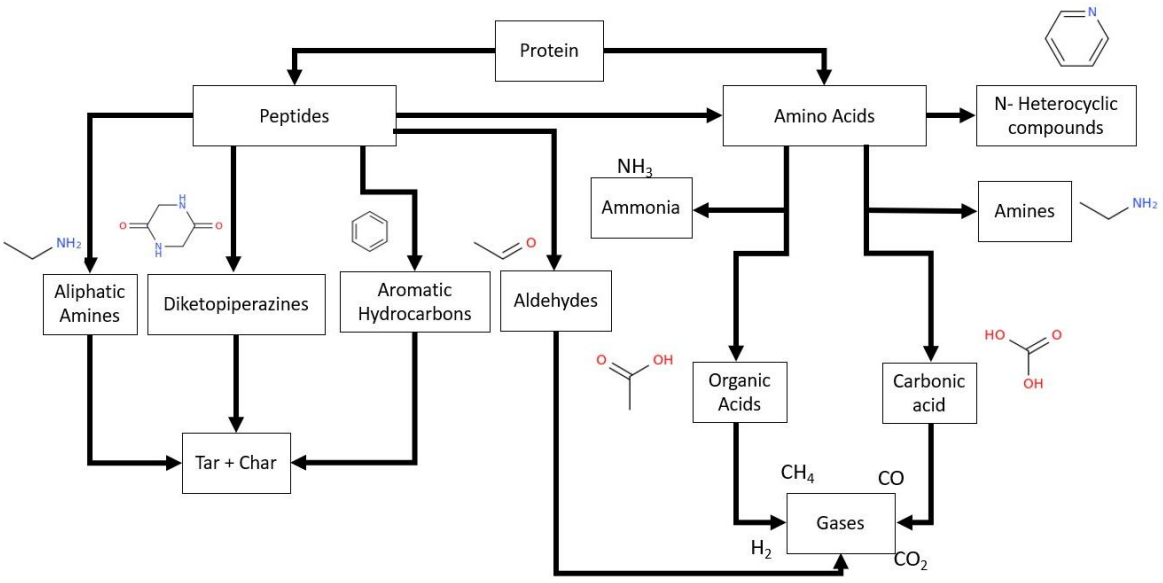

Figure 2.2-Protein gasification reaction pathway. Adapted from. [15]

2.1.2.2.3 Lipid Gasification

Literature on the mechanisms for lipid gasification has been studied less than that for carbohydrates or proteins, however, some work on model compounds to represent lipids has been carried out. Lipids hydrolyse rapidly in sub or supercritical water, to form fatty acids and glycerol. Oleic acid, a model fatty acid, initially decomposes either through decarboxylation or decarbonylation to large aliphatic hydrocarbons, or through the cracking of C-C bonds to form shorter fatty acids. Some of the aliphatic hydrocarbons can rearrange to form cycloalkanes, precursors to aromatic compounds [34], which are undesirable as they can polymerise into tar and chars [26]. Further decompositions of both oxygenated and aliphatic hydrocarbon intermediates into gaseous products also occur, particularly at longer reaction times, at higher temperatures and in the presence of a catalyst [34] [35].

The degradation of glycerol in hydrothermal conditions can occur through competing ionic or free radical pathways, where the reactions are driven by charged ions and molecules with unpaired electrons respectively. Above the critical point, the low ionic product means that there are few ionic compounds available, so the free radical pathways dominate [36]. This makes these the most relevant pathways for SCWG, although some intermediates from the ionic pathways may be present in smaller quantities due to the subcritical conditions during heating. Buhler et al. [36] and Ortiz et al. [37] both outlined the dehydration pathway for free radical dominated gasification. In this, glycerol is dehydrated to either hydroxy acetone or 3-hydroxypropanal. The former then undergoes C-C bond scission, to acetaldehyde and formaldehyde, which decompose further into gas under supercritical conditions, while 3-hydroxypropanal dehydrates further to form acrolein, which decomposes further into ethylene and CO. However, the dehydrogenation pathway, another free radical pathway, would also fit the data observed by Ortiz et al. [37], so further work is needed to fully understand whether either or perhaps a combination of the two is correct. For hydrogen production, the dehydrogenation pathway would be preferable, as 6 moles of hydrogen are produced per mole of glycerol, compared to just one in the dehydration pathway. These are shown in Figure 2.3.

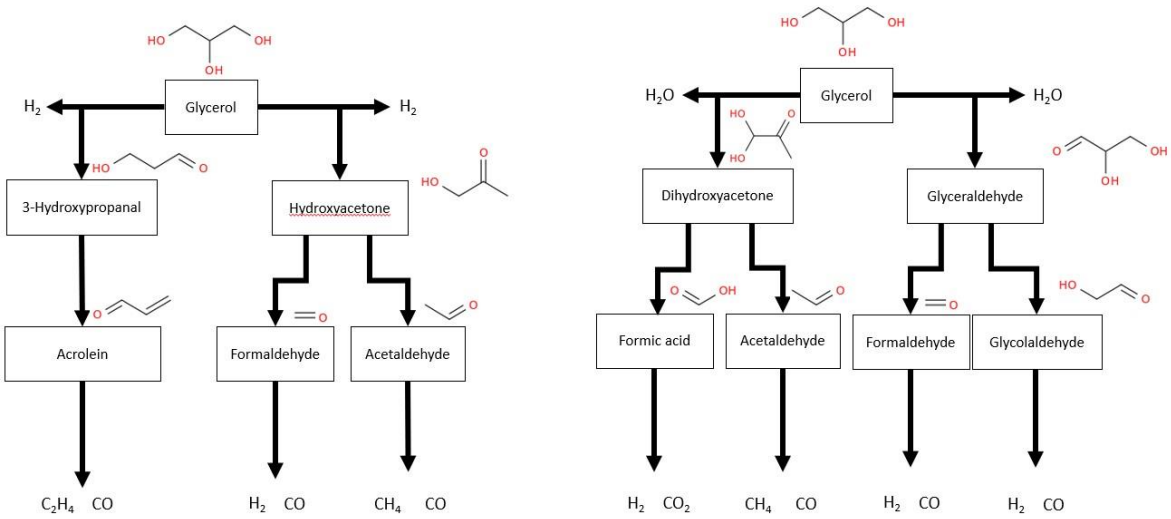

Figure 2.3-Potential free radical reaction pathways for the gasification of glycerol as a model compound for lipids. Adapted from [37]

2.1.3 Influential Factors

The operating conditions and catalysts can all have a significant impact on the reaction pathways discussed in Section 2.1.2 and other reactions in a SCWG system, thus impacting upon the composition of the product streams [38]. Moreover, different biomass types have different mixes of biochemical components, all of which react differently in SCW and can have significant interactions with each other, thereby having a substantial impact on the final product [9] [17].To produce hydrogen, it is important to maximise selectivity by increasing hydrogen producing reactions like steam reforming and WGS, while limiting hydrogen consuming reactions like methanation. It is also important to avoid unwanted, stable compounds, such as char or phenol, that reduce the overall yield and can block the reactor.

2.1.3.1 Biomass Composition

Microalgae mostly consists of the three groups of compounds: carbohydrates, proteins, and lipids. The precise composition is a function of both the strain and the growth conditions [39], meaning that a wide range of compositions can be found, as shown Table . Advantageously, microalgae do not contain lignin, which is known to be particularly difficult to gasify, reducing the conversion and yield of hydrogen in both real biomass and mixtures of model compounds [19] [20] [38] [41].

Table 2.1-Microalgae Compositions

Strain	Alga Type	Composition (wt%)			Source
		Carbohydrate	Lipids	Protein	
Chlorella vulgaris	Chlorophyceae (Green)	15	13	50	[15]
Chlorella vulgaris	Chlorophyceae (Green)	10	7	67	[42]
Chlorella vulgaris	Chlorophyceae (Green)	10.	12	65	[17]
Chlorella vulgaris (under light and nutrient stresses)	Chlorophyceae (Green)	61	9	7	[42]
Scenedesmus quadricauda	Chlorophyceae (Green)	43	20	27	[17]
Auxenochlorella pyrenoidosa	Chlorophyceae (Green)	19	21	55	[43]
Porphyridium cruentum	Porphyridiophyceae (Red)	40	8	43	[44]
Nannochloropsis oculata	Eutomatophyceae	8	32	57	[44]
Nannochloropsis gaditana	Eutomatophyceae	12	32	38	[20]
Nannochloropsis oceanica	Eutomatophyceae	28	21	41	[43]
Spirulina	Cyanophyceae (Blue-Green/Cyanobacterium)	20	5	65	[44]
Arthrospira platensis	Cyanophyceae (Blue-Green/Cyanobacterium)	15	6	67	[43]
Synechocystis sp. (low dilution rate)	Cyanophyceae (Blue-Green/Cyanobacterium)	11	66	20	[45]
Synechocystis sp. (high dilution rate)	Cyanophyceae (Blue-Green/Cyanobacterium)	10	62	11	[45]

2.1.3.1.1 Effect of Protein

As shown in Table 2.1, some of these strains, such as *Chlorella vulgaris* or *Spirulina,* contain very high levels of protein and are therefore used as a potential alternative protein source in food supplements [46]. For *Chlorella vulgaris*, this protein content was maximised in the fastest growing (exponential) phase of growth [47]. However, this high protein content can be detrimental to the gasification performance. Kruse et al. [48] observed that a high protein feed, mostly chicken and rice, resulted in a significantly lower gas yield than glucose or a plant-based feedstock of carrots and onions. They hypothesised that the amines and aldose sugars formed in protein decomposition react in the Maillard reaction to form relatively stable free radical ions (cyclic N compounds such as

pyridine or pyridium [49]), which act as free-radical scavengers, inhibiting the free radical reactions involved in gasification. This same effect was also found in their subsequent experiments when the amino acid alanine or urea were added to glucose both of which form free radical scavenging compounds [50]. Other amino acids, proline and histidine were found to decompose into stable free radical compounds, which would have a similar negative effect on gasification [51] [52].

Chakinala et al. [4] found that adding the amino acid alanine to glycerol actually increased the gas produced, though this does not disprove the theory proposed by Kruse et al [48]. In the second case, the alanine was added without the addition of an alkali metal salt catalyst. This is significant as the release of ammonia from amino acid degradation catalyses the reaction and can increase gas yield in the same way as the salts [22]. This effect would be lost when the salts are already present, so only the negative effect of the free radical scavenging is observed. In a real system, these catalysts are likely to be present, so the effect of proteins would be negative overall and should be avoided if possible. Moreover, the slower hydrolysis of proteins to the amino acids, compared to carbohydrates and lipids [9], should result in real proteins having a more significant negative impact of gasification than their constituents at shorter reaction times.

As with alanine, Chakinala et al. [4] noted that the addition of another amino acid, glycine, to glycerol increased gas yield. This is a contradiction with Caputo et al. [22] who found that gasifying glycine in its pure form and with glucose, both produced a lower gas yield than pure glucose or the microalga Nannochloropsis gaditana. Both had similar reactor setups, with the latter being at a higher temperature (550-650°C vs 663°C) and longer residence time (3-12s vs 128s), which are known to increase the gas yield (as discussed in Sections 2.1.3.3 and 2.1.3.5). The main difference appears to be the reactor feedstock. In the first example, a small amount of glycine (0.5%wt) was added to a feed of 10%wt glycerol, while the second was 3% glycine with 1% glucose. As a result, the contribution to the gas from the glycine was small in the first instance, so the difficulty gasifying the latter could be masked by the glycerol and the potential increase in gas produced due to the catalytic

effect of the ammonia. Additionally, glucose and glycerol could interact with the amino acid differently and a study with comparable concentrations would be required to determine the extent of this factor.

Despite this discrepancy both papers showed that under the same conditions different impacts can occur from different amino acids. Proline, known for being a free radical scavenger in plant tissue, had a much larger detrimental effect on glycerol gasification than glycine or alanine [4], while glycine was much harder to gasify than leucine or glutamic acid [22]. Under different conditions, this may alter, as some amino acids are less affected by these changes, for example, proline is less sensitive to an increase in the temperature [53], as shown in Figure 2.4. Moreover, the alkyl group, which forms the backbone of amino acid valine, caused an increase in hydrocarbon intermediates with more than two carbons, when compared with other amino acids or glucose. These intermediates were effectively converted to hydrogen and methane in the presence of a catalyst [54], resulting in a positive impact on the gas yield. This outlines further complexities that show the effect on the gasification of the protein content will also depend on the composition of the proteins. So, while in general, protein will decrease gas yield, there may be some cases (small amounts of protein, without the presence of alkali metal salts [4]) that ‘break the rule’ and some that have a larger impact.

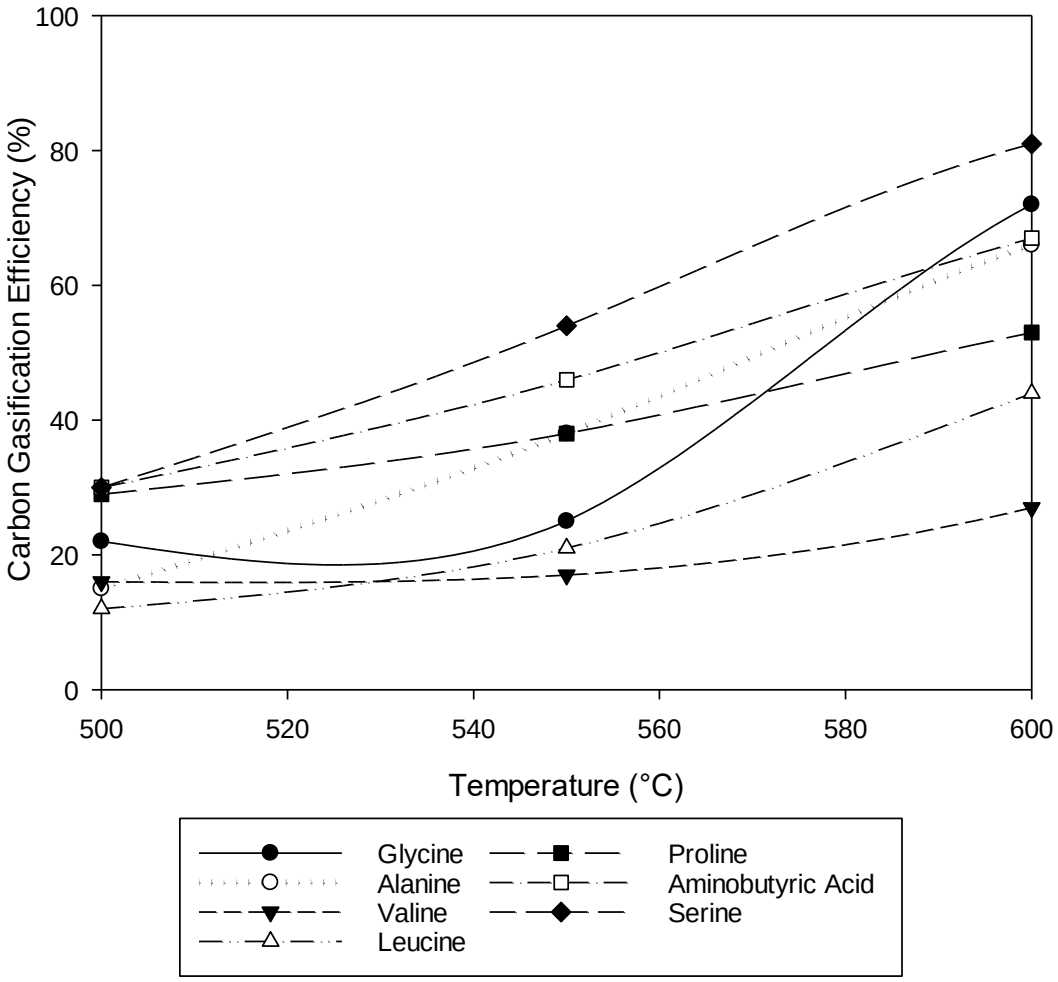

Figure 2.4- Carbon gasification efficiency of different amino acids at varying temperatures. Adapted from [53]

2.1.3.1.2 Effect of Carbohydrates

When gasifying glucose, albumin and canola oil, at low temperatures without a catalyst, as model compounds for carbohydrates, protein, and lipids respectively, glucose had the highest carbon conversion to gas [18]. The carbon conversion is often stated as carbon gasification efficiency (CGE), defined as moles of carbon in gas/moles of carbon in feed. Without a catalyst, glucose had a CGE of close to 100% much higher than the three amino acids glycine, leucine and glutamic acid (40-75%) or *Nannochloropsis gaditana* (82%) [22]. This indicates that a higher carbohydrate content in the algae may increase the conversion of biomass into gas and therefore facilitate high hydrogen yields.

Samiee-Zafarghandi et al. [42] found that increasing the carbohydrate content at the expense of protein by altering the growth conditions on *Chlorella vulgaris* increased both conversion and hydrogen content in the gas significantly, as shown in Table 2.2. Fozer et al. [55] confirmed increasing the carbohydrate content of *Chlorella vulgaris*, through altering the light intensity and dilution rate, increased hydrogen content and total gas yield. Similarly, when comparing *Chlorella vulgaris*, *Spirulina platensis* and *Saccharina latissimi*, the higher carbohydrate content (in *Saccharina latissimi*) gave a higher CGE and hydrogen content [17]. However, this is not always the case, *Chlorella vulgaris* (high protein) and *Scenedesmus quadricauda* (high carbohydrate) had a similar conversion, with the latter having a higher hydrogen content in the product stream [18]. Jiao et al. [56] found that *Nannochloropsis sp.* had the lowest carbon conversion despite the highest carbohydrate content, when compared with *Chlorella pyrenoidosa*, *S. platensis* and *Schizochytrium limacinum*, but again gave the highest hydrogen content.

Table 2.2- Comparison of gas composition, gas yield and gasification efficiency for supercritical water gasification of Chlorella vulgaris with or without increased carbohydrate content. Taken from [42]

Biomass	Gas composition (mole%)				Gas yield (mmol/g)	Hydrogen Yield (mmol/g)	Gasification Efficiency
	H_2	CO	CH_4	CO_2			
Chlorella vulgaris with a high protein content	3.95	18.97	1.9	75.18	1.46	0.0577	5.67%
Chlorella vulgaris with a high carbohydrate content	9.42	11.7	0.83	78.05	2.7	0.254	10.25%

There could be several reasons for this disparity. Firstly, as with the proteins, different carbohydrates can also have different CGE and hydrogen yields under similar reaction conditions. Williams and Onwudili [57] found that glucose, starch, cellulose, and a starchy real biomass (cassava) all gave very different conversions and hydrogen yields, even though the materials were all based on glucose. Secondly, Tiong et al. [18] stated the lower tenacity of the cell membrane in *Chlorella vulgaris* than *Scenedesmus quadricauda* as the reason for a higher conversion at short residence times. Factors like this can also be influential, particularly under milder conditions and shorter

timeframes, where it may be harder to overcome these effects and break down the biomass. This was the case with the low temperature and residence time in that example or the very high biomass concentration used by Jiao et al. [56]. Finally, in some cases the carbohydrate content is lower, but lipid content might be higher. Lipids are less problematic to gasify than protein, so should not have as great an impact on conversion but may impact gas composition (as noted in Section 2.1.3.1.3). In all these cases the hydrogen content was increased, and in many cases, conversion was also increased, therefore a higher carbohydrate content is likely to increase the hydrogen yield. Consequently, a higher carbohydrate content is usually preferred for hydrogen production, but not in every case.

2.1.3.1.3 Effect of Lipids

There is far less literature available assessing the effect of lipids in microalgal gasification or the gasification of lipids in general. This is likely to be a result of the potential for biodiesel production from the high lipid content of some microalgae [58], leading to more research into that area. However, as a key component in most algal strains, it is important to know the impact of lipids on gasification. Nurcahyani et al. [59] compared the gasification of *Chlorella vulgari*s with and without its lipids component, which was extracted using hexane. They found that the original algae had a higher gas yield and lower solid residue, with more methane and less hydrogen than the residual algae (without lipid). A subsequent kinetic study, in the same paper, revealed that when gasifying *Chlorella vulgaris*, the part of the algae extractable with hexane (lipids) produced gas 3.5 times faster than the remaining biomass (mostly carbohydrate and protein). This was confirmed by Jiao et al. [56] who gasified the extracted oil and residual solids from *Chlorella pyrenoidosa*. They found that the oil extracted gave a higher gas yield than the residuals and higher methane content than either the residuals or the original algae. The total methane yield was also higher than the total for the algae or any other algae tested.

These show that the lipid proportion is less resistant to gasification than the remaining solids, which consist of mostly carbohydrates and protein. As discussed earlier, it is likely that protein is the main cause of this lower production, meaning lipids are less resistant to gasification than proteins, being more comparable to carbohydrates. Lipids also have the tendency to produce a large amount of methane, which can be undesirable for a hydrogen production system as it would reduce the selectivity to hydrogen. However, in a system where the methane is used for heating the reactor or chemical looping is used to purify the syngas (as mentioned in Section 2.1.5), some methane will not be problematic and in that case higher lipid contents would be acceptable. In some cases, a mixture of hydrogen and methane (Hythane), is seen as advantageous when compared with the individual gases [60].

2.1.3.1.4 Tailoring Growth Conditions for Gasification

The information detailed above outlines the composition of biomass that would be most suitable for hydrogen production through SCWG. This will influence the choice of algal strain and the growth conditions as both are can significantly affect the final biomass composition. One way in which the composition of the algae can be altered is through nutrient limitation; the way in which an alga responds depends on the strain. As nitrogen is a vital component of proteins, limiting this reduces the protein content [39] and, depending on the strain, increases the content of carbohydrate and lipids in some cases [61] [62] but only the carbohydrate content in others [63] [64]. Similarly, phosphorus limitation alters the algal composition, but less predictably, reducing the protein in some cases [65] [66] and reducing the lipids content in others [67]. In addition to these, limiting micronutrients like iron [68], silicon [63] and sulphur [66], can alter the composition. However, in all these cases, especially under nitrogen and phosphorus limitation, the algal growth was reduced. This would mean a larger area is required to grow the same quantity of algae, creating issues with land use and capital cost. A balance of the growth and composition of the algae, potentially using a two-stage system, should be considered.

One case where the growth wasn't limited was the limiting of calcium, which increased biomass productivity in both the green alga *Chlorella sorokiniana str* [61] and the blue green alga (Cyanobacterium) *Spirulina platensis* [69], while increasing carbohydrate and lipid content. The increased productivity is due to weaker cell walls [61], which facilitated easier gasification *of Chlorella vulgaris* at short residence times [18], which could be beneficial to gasification. Hence, calcium limitation offers the potential double benefit of increased growth and increased gas production, so should be further investigated. The effect of salinity also has potential because for *Spirulina platensis*, increasing salinity increased the carbohydrate content without reducing the growth [69]. However, this is not the case for all strains as the growth can be reduced in some cases [68] [70]. Likewise, an increased pH can increase the availability of inorganic carbon which increases growth of strains that can use bicarbonate as a source of carbon [71] but high pH levels are detrimental to the growth of other algal strains that cannot [72]. Being able to operate at higher pH is desirable as the higher solubility of bicarbonate allows a higher uptake of CO2 from the gas stream [73] and reduces the chance of contamination from other organisms [74]. This should be considered when selecting the alga strain.

Variations in the light intensity can also be used [55], however in outdoor settings the light source is often sunlight so is difficult to control. The use of artificial lights can be used to overcome this but that requires additional input of energy, which will reduce the benefits of the increased hydrogen production. Considering how to optimise the suitability of a feedstock and the growth of the algae is an important area that can help increase the hydrogen yield per unit of area needed to growth the algae. It should therefore be a key area of further research into the SCWG of microalgae.

2.1.3.2 Catalysts

Catalysts can be used to reduce the activation energy of reactions, hence reducing the operating temperatures and increasing the biomass concentration ranges that could still achieve high conversion and high hydrogen selectivity [75]. A lower temperature can reduce the potential corrosive effects of the medium, reducing the cost of equipment [76], while lower temperatures and

higher biomass concentrations reduce the energy losses upon heating the water [77]. Heat recovery systems can reduce the heat losses but not entirely remove them [78]; minimising the heating requirements is still vital. The high costs, both capital and operating, are major barriers to commercialisation of supercritical technologies [79], and hence catalysts will be key to overcoming them. To achieve this, the catalysts should increase the C-C bond cleavage, increasing reactions like hydrolysis and steam reforming that break down the biomass, hence increasing the carbon conversion. They should also increase the WGS reaction, while suppressing C-O bond cleavage (reactions such as methanation), increasing hydrogen selectivity [80] as shown in Figure 2.5.

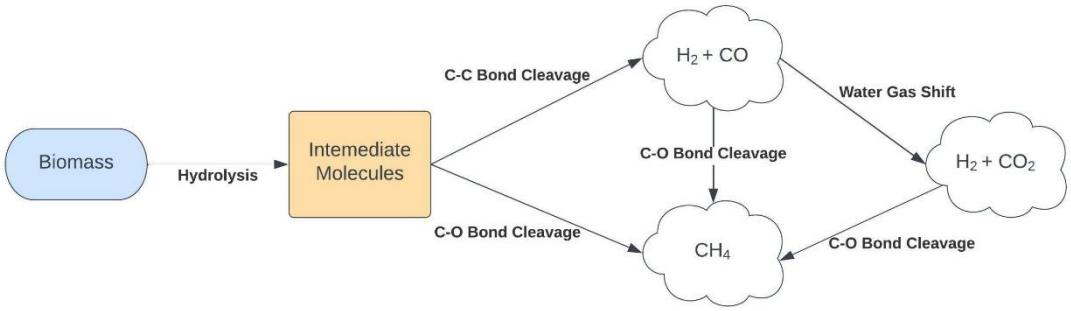

Figure 2.5- Potential products formed from different bond cleavages in supercritical water gasification. For hydrogen production, C-C bond cleavage and water gas shift are diesitable, C-O bond cleavage is undesirable. Adapted from [81]

2.1.3.2.1 Homogeneous Catalysts

Homogeneous catalysts are catalysts that are in the same phase as the reaction media, in this case water. The most common of which for SCWG is alkali metal salts, which have widely been used in the SCWG of various feedstocks for both real biomass (including microalgae) and model compounds. An increase in the CGE is commonly observed, indicating an increase in carbon conversion and therefore increased C-C bond cleavage. Onwudili et al. [17] suggest that nucleophilic attack of hydroxide ions in the subcritical region drives this increased degradation. However, Caputo et al. [22] observed significant increases in CGE with the addition of Na_2CO_3, despite a rapid heating rate and thus a very short time in the subcritical region, so this seems unlikely to be the main driver. More work is required to fully understand the driver behind this in the supercritical region.

Table 2.3-Akali Metal Catalysts that Increase the Carbon Gasification Efficiency of the Supercritical Water Gasification of Biomass Feedstocks

Catalyst	Biomass or Model Compound	Increase in CGE?	Increase in Hydrogen Yield?	Increase in Hydrogen content in gas?	Sources
Potassium Hydroxide (KOH)	Sawdust, straw, sewage sludge, lignin, glycine, glucose, catechol, fructose, xylose, cellulose, sugarcane bagasse	All cases, except sugarcane bagasse	All cases	All cases	[15] [16] [17] [18] [19]
Sodium Hydroxide (NaOH)	*Chlorella vulgaris, Spirulina platensis, Saccharina latissimi,* Fructose, sugarcane bagasse	Fructose only	All	all	[16] [20] [19]
Potassium Carbonate (K_2CO_3)	*Nannochloropsis gaditana, Acutodesmus obliquus,* sawdust, straw, sewage sludge, lignin, glycine, glucose, catechol, xylose, sugarcane bagasse, cauliflower residue, acorn, tomato residue, extracted acorn, hazelnut shell, glycerol	All but glycine, sugarcane bagasse	All but glycine	All but glycine	*[*21] [15] [17] [19] [41] [23] [24] [25*]*
Sodium Carbonate (Na_2CO_3)	*Nannochloropsis gaditana,* leucine, glutamic acid, glycine	All but glutamic acid, glycine	All but glutamic acid, glycine	All but glutamic acid, glycine	[21]
Trona ($Na_2CO_3 \cdot NaHCO_3 \cdot 2H_2O$)	Cauliflower residue, acorn, tomato residue, extracted acorn, hazelnut shell	All cases	All cases	All cases	[41]
Sodium Bicarbonate($NaHCO_3$)	Sugarcane bagasse	All cases	All cases	All cases	[19]
Potassium Bicarbonate ($KHCO_3$)	Sugarcane bagasse	All cases	All cases	All cases	[19]
Iron Chloride ($FeCl_3$)	Humic acid	All cases	All cases	All cases	[89]

Table 2.3 shows the wide range of biomass feedstocks for which alkali metal salts increase the conversion in SCWG, yet this is not always the case. Glutamic acid (an amino acid) was unaffected both in conversion and gas composition by the addition of the catalyst (Na_2CO_3) [22].This could be attributed to the ammonia being released during the reaction, as with the alkali metal salts, it can create an alkaline environment in water [90]. Consequently, further addition of alkali has a less significant effect on the reaction pathways and thus the gas yield. Onwudili et al. [17] found less gas was produced when gasifying algae in the presence of NaOH than without. This was due to the reaction of CO_2 with NaOH to form carbonates and bicarbonates. This is something that needs to be considered when comparing catalysts, as it could show a low CGE even though the reaction was successfully catalysed, as the carbon could remain in the liquid effluent in inorganic form.

Alkali salts also significantly enhance the WGS reaction, thus having a significant positive impact on hydrogen yield, as shown in Table 2.3. This is achieved through the reaction of the hydroxide such as KOH reacting with CO, to produce formate, which easily reacts with water to form hydrogen. This creates a more favourable route, thus accelerating the reaction. Equations (5-8) show the pathway when K_2CO_3 is added as catalyst, with KOH as an intermediate product. A similar pathway should be also found when other alkali metal carbonates and hydroxides are used [91].

$$K_2CO_3 + H_2O \rightarrow KHCO_3 + KOH \quad (5)$$

$$KOH + CO \rightarrow HCOOK \quad (6)$$

$$HCOOK + H_2O \rightarrow KHCO_3 + H_2 \quad (7)$$

$$2KHCO_3 \rightarrow K_2CO_3 + H_2O + CO_2 \quad (8)$$

Evidence of this is shown with the low (often negligible) CO content and high hydrogen content observed, when alkali metal salts are added to a wide range of biomass and model compounds [22] [41] [82] [83] [86] [92]. One exception is some amino acids such as glycine and glutamic acid, where the impact of the released ammonia has already progressed the WGS reaction to such an extent that the catalyst has minimal effect on the gas yield or composition [17]. In the case of microalgae

gasification, the concentration of ammonia released will be lower, due to biomass containing components (carbohydrates and lipids), making the ammonia produced more diluted when compared with a similar concentration of pure protein or amino acid. Therefore, alkali metal salts should still have a significant effect.

Alkali metal salts also impact upon the liquid phase reactions; the addition of either K_2CO_3 and KOH produced a lower furan but higher phenol content in the liquid product when gasifying glucose [91] [82], as shown in Figure 2.6. This could be through rapid conversion of furans into smaller molecules and phenol, or direct conversion of glucose to phenol rather than via 5-HMF (5-(hydroxymethyl)furfural) and other furans. However, phenols are undesirable, and hence this is a disadvantage of these catalysts.

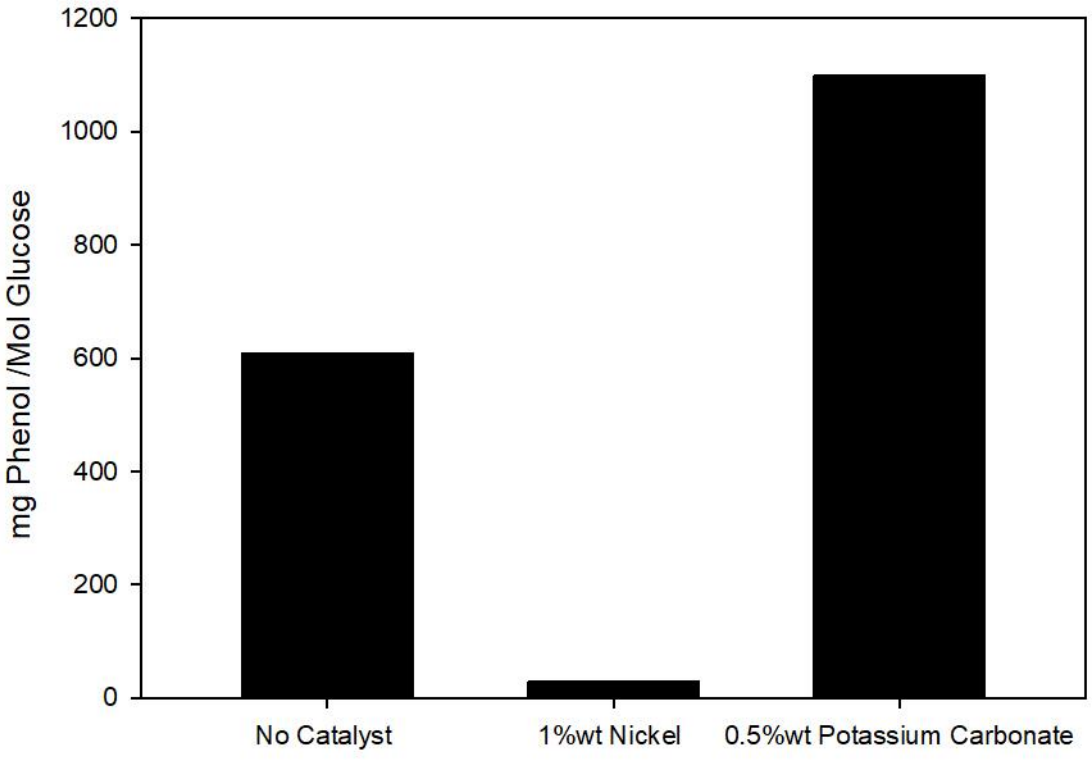

Figure 2.6-Phenol content in the effluent of the supercritical water gasification of glucose. Adapted from [15]

For the different alkali metal salts, while all increase the hydrogen yield, the extent to which this takes place, varies. Except for glycine [22], potassium salts outperformed sodium salts on gasifying a particular feedstock. KOH gave a higher hydrogen yield than NaOH when gasifying fructose [83] and sugarcane bagasse [86], while K_2CO_3 produced a higher hydrogen yield than Na_2CO_3 on sugarcane bagasse [86] and most significantly Nannochloropsis gaditana [22]. Additionally, it is often found that in terms of hydrogen yield, they follow the order of hydroxides > carbonates > bicarbonates [92] [86]. This would indicate, given the role of formates in the WGS reaction, that potassium salts (especially KOH) more readily produces formates. However, there could be many other factors involved, requiring further work to fully understand it.

The above makes salts ideal catalysts to maximise hydrogen production from SCWG. However, other factors must be considered. Alkali catalysts also catalyse phenol production [92] which, as discussed in Section 2.1.2, is highly undesirable. They can also increase the corrosion in the system [91], which may mitigate against the reduction in corrosion achieved through lower temperatures. This can also alter the product distribution (as mentioned in 3.2.3). Both increased phenol content and corrosion can limit the ability to recycle the inorganic portions of the biomass to be used in microalgae growth, increasing costs and wastes (see Section 2.1.4.1). Moreover, the low solubility of salts in supercritical water can lead to precipitation, plugging of the reactor and are much more difficult to recover than heterogeneous catalysts [80]. This results in reduced operability and homogenous increased cost due to increased downtime from blockages and frequent supply of a new catalyst for each run. Therefore, to mitigate such disadvantages diligent reactor design is required for catalytic reactions. The use of alloys with a high nickel content or sacrificial liners can help minimise the impacts of corrosion [76] and the use of downflow reactors or hydro cyclone reactors can reduce solid deposition [93] [94].

In addition to this, $FeCl_3$ has also been studied for the SCWG of humic acid, as a model compound for the humic compounds sewage sludge [89]. This was found to be more effective at increasing the hydrogen yield and total gas yield of alkali or transition metal catalysts (K_2CO_3, nickel, $ZnCl_2$). Furthermore, a machine learning aided study of literature for SCWG of wet waste feedstocks by Li et al [95] found that $FeCl_3$ was more effective than other transition metals. Despite this, far less literature is available on these catalysts and further work is needed to study these effects on other feedstocks such as microalgae before a more conclusive picture can be drawn.

2.1.3.2.2 Heterogeneous Catalysts

2.1.3.2.2.1 Nickel Catalysts

Heterogeneous catalysts form another phase to the reaction media, often a solid in a packed bed or suspended in media. Transition metal catalysts, often supported on another material, are commonly used as heterogeneous catalysts in SCWG. Due to their low cost, nickel catalysts are most commonly used, in pure form or supported on different compounds. nickel catalysts are effective at increasing C-C bond cleavage, which results in a higher conversion and thus higher hydrogen yields in most cases. The catalysts used on algae and other biomass feedstocks is summarised in Table 2.4.

Table 2.4-Nickel Catalysts Used in the Supercritical Water Gasification of Biomass Feedstocks

Catalyst	Biomass or Model Compound	Increase in CGE?	Increase in Hydrogen Yield?	Increase in Hydrogen content in gas?	Sources
Nickel on Alumina (Al_2O_3), pure and modified with lanthanum or Cerium	*Chlorella vulgaris, Scenedesmus quadricauda, Spirulina platensis, Nannochloropsis oculata,,* Glucose, fermentation stillage, cellulose, xylan, lignin, bark	All cases	All cases except *Scenedesmus quadricauda, Spirulina platensis*	All cases	[15] [96] [17] [18] [19] [20] [21]
Nickel oxide on Silica (SiO_2)	*Chlorella sp.*	All cases	All cases	All cases	[22]
Nickel on Silica-Alumina	Oleic Acid	All cases	All cases	All cases	[23]
Nickel on Zirconia (ZrO_2)	Switchgrass Biocrude	Not stated	Not stated	Not stated	[24]
Nickel on Zeolite	*Chlorella pyrenoidosa*	All cases	All cases	All cases	[25]
Nickel on Activated Carbon	Xylose, Valine	All Cases	All cases	True when stated	[26] [27]
Nickel on Graphene oxide	*Chlorella sp.*	All cases	All cases	All cases	[28]
Nickel on hydrotalcite	Glucose, cellulose, xylan, lignin, bark	All cases	All cases	All cases	[19]
Raney Nickel	*Chlorella vulgaris, Scenedesmus quadricauda* Fermentation Stillage, sugarcane bagasse, glucose, fructose, cellulose, xylan, lignin, bark	All cases	All cases	All cases	[15] [18] [29] [19]
Raney Nickel with Molybdenum	Sewage sludge	All cases	All cases	All cases	[30]
Nickel Wire	*Chlorella vulgaris*	All cases	All cases	All cases	[31]
Inconel Powder	*Chlorella vulgaris*	All cases	All cases	All cases	[31]
Ni-5132P	Cellulose, lignin, sawdust, rice straw	All cases	All cases	All cases	[104]
Nickel and Iron on Alumina	*Enteromorpha intestinalis*	All cases	All cases	All cases	[105]

An increased conversion was seen universally for nickel catalysts, when compared with similar reactions without a catalyst. However, the impact on the composition of the gas produced was less consistent than that of the homogeneous catalysts. Sinag et al. [91] stated that the interaction between hydrogen and nickel makes it a good hydrogenation catalyst which would enhance methanation. The hydrogen dissociates on the nickel surface and combines with the carbon to form methane, as shown in equations 9-11.

$$H_2 \leftrightarrow 2(H)_m \tag{9}$$

$$2(H)_m + C \rightarrow (CH_2)_m \rightarrow (CH_4)_m \tag{10}$$

$$(CH_4)_m \rightarrow CH_4 \tag{11}$$

Where m denotes the entity adsorbed onto the metal. This strong hydrogenation activity also has a significant impact on the composition of the liquid effluent. Far less phenol was present in the gasification of glucose with a Raney nickel catalyst than without [91], as shown in Figure 2.6. Given the refractory nature and tendency of phenol to polymerise, reduction in phenol content is likely to be a major contributor to the increased gasification efficiency in the presence of nickel catalysts. On the other hand, the hydrogenation effect would result in a higher methane content and lower hydrogen. Some of the literature reinforces this assertion. Azadi et al. [99] found while gasifying glucose, cellulose and xylan, that increasing the nickel dispersion increased the methane formed and reduced hydrogen selectivity, indicating that nickel does catalyse the methanation reaction. Similar effects were also seen with nickel on activated carbon gasifying xylose [84] and when Raney nickel was used to gasify sugarcane bagasse [86]. However, while using nickel on lanthanum-modified alumina when gasifying glucose [96], on yttrium-modified activated carbon when gasfiying valine [54], on zeolite when gasifying *Chlorella pyrendiosa* [24] and on graphene oxide when gasifying *Chlorella sp* [103], the methane content decreased, favouring more hydrogen and CO_2. This indicates that in these cases methanation was suppressed and the water gas shift reaction was favoured, Sinag at al. [91] who claimed nickel increased methanation.

In other works, it was commonly observed that the addition of a nickel catalyst increased both hydrogen and methane. This was the case upon gasifying glucose when Raney Nickel, nickel on cerium-modified alumina and nickel-aluminium-magnesium catalysts, were employed [91] [97] [106]. It was also true for nickel and molybdenum on alumina, Inconel powder and nickel wire gasifying *Chlorella vulgaris* [4], as well as nickel oxide on silica, gasifying *Chlorella sp* [101]. Moreover, when gasifying cellulose, Ni-5132P catalyst increased the hydrogen in product gas/hydrogen in organic feed (hydrogen gasification efficiency (HGE)) above 100%, showing that the water played a significant role, while also increasing methane [104].

One factor for this is that at milder temperatures decarboxylation dominates, making CO_2 the main product, with little hydrogen or methane [107] [15] [108]. The catalyst allows other reactions to progress at these conditions leading to further degradation of the biomass and therefore an increase in both hydrogen and methane contents. However, this cannot explain every case and thus suggests that nickel catalysts increase methane forming reactions (such as methanation or cracking of hydrocarbons) and hydrogen producing reactions (such as steam reforming and WGS) reactions, even though, in some cases one dominates, so it can appear to catalyse one or the other. It is difficult to be certain of the reason for why one can dominate in different situations, as a wide range of feeds, supports and operating conditions were used all of which, can significantly impact the gas composition. If this can be used advantageously, nickel catalysts offer a low-cost way of increasing the hydrogen yield and selectivity in SCWG of algal biomass.

2.1.3.2.2.2 Ruthenium Catalysts

Ruthenium catalysts have also been extensively used to successfully increase conversion and hydrogen yields, with a variety of supports and on a wide range of feeds, including various species of microalgae, as summarised in Table 2.5. As with nickel, the literature summarised in the table shows the proficiency of ruthenium catalysts at accelerating the C-C bond cleavage. Chakinala et al. [4] compared ruthenium to nickel catalysts and found that nickel was more proficient at increasing CGE. However, they all contained varying amounts of metal, so this was not standardised, making

it difficult to draw conclusions. Nguyen et al. [98] did compensate for the quantity of metal, claiming that ruthenium catalysts were superior to nickel at converting fermentation stillage. This is a much more appropriate comparison, especially as they considered industrially available catalysts with the same supports. While this may differ for microalgae, this indicates the ruthenium being the superior catalyst when considering performance. However, the much higher cost of ruthenium (approximately 970 times that of nickel in April 2023 [109]) means nickel may still be more economically viable. The rate of deactivation must also be considered when comparing the catalysts, as discussed in Section 2.1.3.2.2.4.

Table 2.5-Ruthenium catalysts used in the supercritical water gasification of biomass feedstocks

Catalyst	Biomass or Model Compound	Increase in CGE?	Increase in Hydrogen Yield?	Increase in Hydrogen content in gas?	Sources
Ru on alumina (Al_2O_3)	*Chlorella vulgaris*, *Enteromorpha intestinalis*, *L. digitata, L. hyperborea, Saccharina latissimi and A. esculenta,* glucose, cellulose, fructose, xylan, pulp, alkali lignin, bark, fermentation stillage, xylose, oleic acid	All cases	All cases	All cases	[15] [16] [17] [18] [19] [20] [21] [22]
Ru on zirconia (ZrO_2)	*Spirulina platensis*	All cases	All cases	no	[23]
Ru on charcoal	*Chlorella vulgaris, Phaeodactylum tricornutumpr*	True when stated (*Ch Vulgaris)*	True when stated *(Ch Vulgaris)*	True when stated *(Ch Vulgaris)*	[15] [24]
Ru on activated carbon	*Chlorella vulgaris*, *Chlorella pyrenoidosa* , *Spirulina platensis, Nannochloropsis species, Schizochytrium limacinum, g*lucose, cellulose, fructose, xylan, pulp, alkali lignin, bark, xylose	All cases	All cases except lignin	All cases except *Spirulina platensis*	[15] [25] [23] [16] [17] [18] [26]
Ru and Rh (Rhodium) on activated carbon	*Chlorella pyrenoidosa*	All cases	All cases	All cases	[27]
Ru on titanium oxide (TiO_2)	*Chlorella vulgaris,* switchgrass biocrude	All cases	All cases	All cases	[4] [102]

As with nickel catalysts, ruthenium appear to enhance both the WGS and methanation reactions. Ruthenium supported on activated carbon increased hydrogen selectivity when gasifying xylose or *Chlorella pyrendiosa* [84] [15], as did ruthenium on graphene oxide, gasifying *Chlorella sp* [103]. However, Azadi et al. [99] found that ruthenium supported on either carbon or alumina, reduced hydrogen selectivity favouring methanation and produced larger amounts of methane. An increase in both hydrogen and methane content was also observed with ruthenium supported on charcoal, alumina and carbon [23] [35] [110]. This means that, as with nickel, ruthenium can catalyse WGS and methanation reactions. The one example where only methanation was observed, was at a low temperature (380°C) [99], which suggests that at lower temperatures the catalyst favours methanation. However, as with the nickel catalysts, many other factors make it more difficult to be certain and further investigation is needed.

To achieve a higher gas yield and reduced char formation, ruthenium catalysts have a significant impact on the reaction pathways that form both the intermediates and final products. In the gasification of glucose, alumina supported ruthenium catalysts were found to inhibit the formation of furans, pre-cursors to the formation of phenols, a refractory intermediate which leads to char formation (as shown in Figure 2.1). Moreover, the high hydrogenation and C-C bond scission activity promoted the degradation of phenols, which did not occur without the presence of this ruthenium catalyst [23]. However, when gasifying oleic acid, ruthenium on alumina facilitated the diels-alder addition, increasing the phenol content when compared to no catalyst or a nickel catalyst [35]. Hence, for high lipid algae strains, ruthenium catalyst may be less effective.

2.1.3.2.2.3 Other Transition Metals

Other transition metals have also been tested for the SCWG of biomass. Cobalt-molybdenum and platinum-palladium were both used successfully to increase CGE and hydrogen yield when gasifying *Chlorella vulgaris* [4]. Copper, cobalt, chromium, and manganese were all used successfully when supported on graphene oxide [103]. However, in these cases, they had a smaller impact on hydrogen

yield than the equivalent nickel or ruthenium catalyst. Copper nanoparticles were also found to be effective at increasing hydrogen yield from methanol gasification [115]. It would be interesting to investigate if nickel or ruthenium are more effective than copper when in nanoparticle form, given that they are more effective when as part of a supported catalyst, but that has not been tested to date.

In some studies, the higher activity of nickel and ruthenium is less apparent. Cobalt outperformed nickel and ruthenium in terms of CGE when gasifying switchgrass biocrude. However, it did not progress the WGS reactions, leading to large amounts of CO being present in that case and a lower hydrogen yield [102] so would not be suitable for hydrogen production without further alterations. Manganese oxide was more effective than nickel oxide at gasifying *Chlorella sp,* although this can be attributed to the lower activity of nickel oxide compared with nickel metal [101]. Therefore, while other transition metals are effective, the higher activity towards hydrogen production of nickel and ruthenium, means they are still the preferred metals for use in heterogeneous catalysts.

2.1.3.2.2.4 Catalyst Deactivation

A major issue with heterogeneous catalysts is deactivation. The activity of the catalyst reduces over time, thus requiring it to be replaced or regenerated to regain the original activity. This is undesirable as it adds cost and complexity to the process, so should be limited as much as possible. Poisoning of a catalyst through the adsorption of a chemical species in the feed, is a common cause. This is often caused by sulphur, which is present in many organic feeds, including microalgae. Peng et al. [114] and Bagnoud-Velásquez et al. [113] found significant sulphur poisoning when gasifying microalgal biomass (*Chlorella vulgaris* and *Phaeodactylum tricornutum* respectively), using a carbon supported ruthenium catalyst. The latter authors found that adsorption had dropped to zero after the reaction, so the activity had been completely lost by the poisoning. The effect of poisoning is shown in Figure 2.7 by the rapid drop in CGE observed a short period after switching from a low sulphur feed of glycerol to a higher sulphur microalgae feed [113]. Sulphur was also found to poison copper nanoparticles and nickel catalysts gasifying other feedstocks [99] [115]. Techniques to overcome

this such as adsorbents before the catalyst [114] or regeneration of the catalysts through oxidation [116] can be used. However, these add downtime and cost to the process, so must be considered when proposing heterogeneous catalysts, especially ruthenium, as an option.

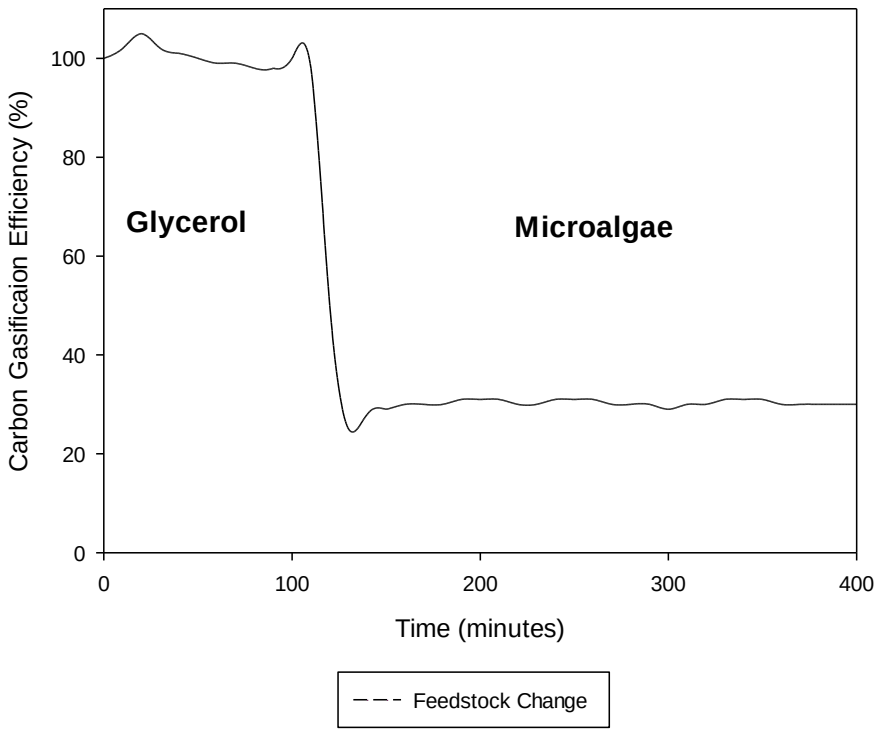

Figure 2.7-Change in carbon gasification efficiency in time on stream of the continuous supercritical water gasification of glycerol and Phaeodactylum tricornutum using an activated carbon supported ruthenium catalyst. glycerol is gasified from time 0-100minutes, Phaeodactylum tricornutum thereafter. Adapted from [15].

Another common deactivation mechanism is coking, where solid char is deposited on the catalyst, blocks the active sites and hence reduces the activity. Significant coking was found when gasifying *Chlorella pyrendiosa* with zirconia supported nickel catalysts, with the acidic nature of the catalyst being a significant driver [24]. Coking was also experienced with nickel on γ-alumina supports when gasifying glucose [97]. Given the abundance of acid sites (proton donating sites) on γ-alumina [117], this was likely to also be a factor and therefore, supports containing large amounts of acid sites should be avoided to prevent excessive coke build up. Feedstocks such as switchgrass biocrude and lignin both promoted issues with coking, but they are much more susceptible to carbon

deposition on the catalyst during SCWG than microalgae so are less relevant in the latter context [102] [99].

Irreversible changes to the catalyst can also occur because of the extreme conditions in SCWG. Ruthenium on charcoal catalysts showed a significantly reduced CGE after 3 runs. This was due to metal leaching into the reaction media, reducing the total metal available from the catalyst [110]. This effect is also detrimental the recovery of inorganic nutrients (as mentioned in Section 2.1.4.1). Alternatively, Raney nickel, nickel on alumina and nickel on zirconia, all showed an increase in nickel crystal size [98] [24]. This reduces the active surface area of the metal, lowering the activity. The effect was outlined by Xie et al. [24] where the hydrogen yield fell with each run of a nickel on a zirconia support when gasifying *Chlorella pyrenoidosa*, even when the coke was removed. Nickel has also been shown to react with the alumina support, reducing its surface area and activity [96] [100]. These are all examples of the catalysts being unstable at supercritical conditions, with nickel catalysts being particularly problematic. This would mean replacing the catalyst more frequently, without being able to easily regenerate them. While this is a significant barrier, the lower cost of nickel catalysts may make them still more economically viable than the ruthenium alternatives.

2.1.3.2.2.5 Effect of the Support

As well as the active metal, the support can play a major role in the gasification reaction. Many materials used in support can be used as catalysts for SCWG. Activated carbon has been used to successfully increase the CGE on sugarcane bagasse [86], valine [54] and glucose [118] with the source of the activated carbon significantly affecting its performance. Similarly, zirconia was found to increase the conversion of glucose and cellulose, while also increasing the WGS reaction [119]. Titanium dioxide also increased hydrogen yield, if combined with calcium oxide [38]. While these catalysts were less effective than the alkali metal salts and transition metal catalysts mentioned previously, they show how support material can contribute to the overall performance of a catalyst.

This is evident in the significant variation in CGE between different forms of alumina and carbon supported ruthenium catalysts gasifying *Chlorella vulgaris* where γ-alumina and charcoal

outperformed α-alumina and activated carbon, converting approximately 20% more carbon to gas. Moreover, the CH_4/CO_2 ratio in the products, significantly varied, indicating differing methanation performances. This shows that, despite changing with different conversions, the CH_4/CO_2 ratio is always higher for γ-alumina than charcoal supported catalysts, indicating the enhancement of methanation with γ-alumina supported catalyst [110], as shown in Figure 2.8. Additionally, lanthanum-modified alumina supports were found to adsorb CO_2, which impacted the gas composition in glucose gasification [96]. This shows that the support is a factor in the disparity between ruthenium catalysts in terms of gas composition (as observed in Section 2.1.3.2.2.2). Xie et al. [24] provided further evidence to the support impact, showing that the zeolites with more strong acid sites had a higher CGE and HGE when supporting nickel in the gasification of *Chlorella pyrendiosa*, despite the same quantity of metal.

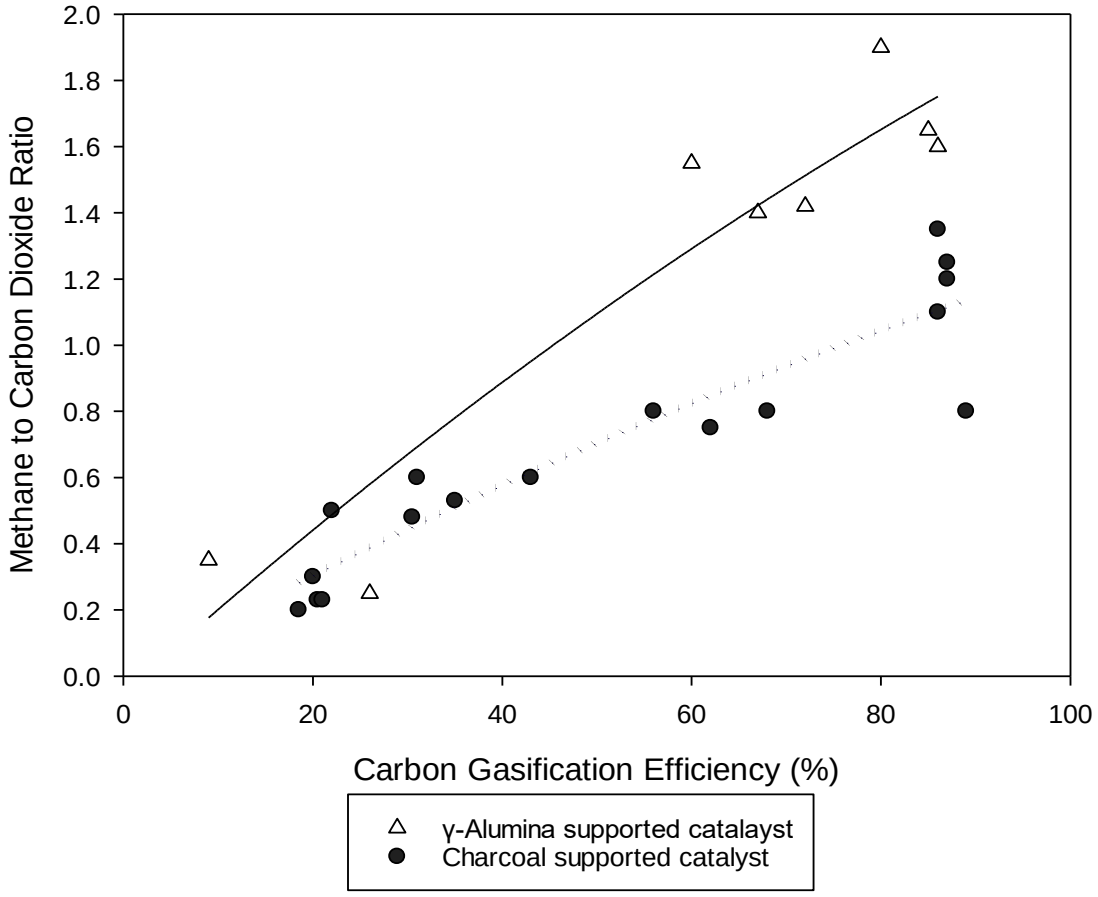

Figure 2.8-methane-carbon dioxide ratio at different total carbon gasification efficiencies during the supercritical water gasification of Chlorella vulgaris using ruthenium catalysts with different supports. Adapted from [15]

The support material can significantly impact upon the favourability of different reaction pathways, a major contributing factor for the impact on overall gasification performance observed. When gasifying the amino acid valine in the presence of activated carbon as catalyst or support for nickel, no nitrogenous organic compounds were observed. This indicates that the decarboxylation route is suppressed, favouring deamination to form ammonia and organic acids. As these acids are more easily gasified than nitrogenous compounds such as amine, the CGE increased in the presence of activated carbon [54]. This could mitigate the negative effects of protein content on gasification (see Section 2.1.3.1.1), thus activated carbon catalysts are desirable for high protein feedstocks such as many species of microalgae. Moreover, this would allow algae to be grown in the exponential phase,

where the protein content is higher [47], with a reduced detrimental effect on the hydrogen yield and therefore a reduced land requirement.

The supports can also play an important role in the deactivation of the catalyst. The nature of the catalysts such as number of acid sites (see Section 2.1.3.2.2.4) or the interaction between the metal and support, can significantly affect deactivation. Modifications can be attempted to minimise this. Modifying alumina supports with lanthanum reduced the interaction with nickel, hence reducing deactivation through sintering, which allows more active metal to be available for longer, increasing the activity [96] [100]. Similarly, modifying activated carbon with platinum or palladium reduced crystallisation of nickel, which reduces the active surface area and therefore deactivates the catalyst [54]. Modifying alumina with cerium oxide also limited deactivation by reducing the coke deposition and lowering the temperature needed to remove the easily removable coke, allowing easier recycling of the catalyst [97]. However, these modifications will increase the costs of the catalyst. It is important, when choosing a catalyst support, to balance the need for increased hydrogen yield and reduced deactivation, with the cost of the catalyst.

2.1.3.2.3 Catalytic Wall Effects

Nickel based alloys, including Inconel, are often used in SCWG, due to their high resistance to corrosion, high strength at elevated temperatures and resistance to hydrogen embrittlement [76]. Chakinala et al. [4] observed that Inconel powder or nickel wire at elevated temperatures had a significant positive impact on both the CGE and the yield when gasifying the microalga *Chlorella vulgaris.* Therefore, it is likely that the reactor wall will have an impact on the reaction, which must be considered. While, to the authors' knowledge, no work has been carried out to investigate this effect on microalgal gasification, other relevant work studying the effects of the wall material has been carried out.

Yu et al. [120] observed a higher hydrogen yield in an Inconel tubular reactor than in an identical Hastelloy reactor, for the SCWG of acetic acid or glucose. When the Hastelloy reactor was corroded with potassium chloride, the hydrogen yields increased. However, it is better to compare the new

(uncorroded) reactors as it is hard to differentiate whether this is due to an increased surface area, or the salts being released which also catalyse the reaction. Castello et al. [121] compared stainless steel and Inconel 625 batch reactors for the gasification of glucose and beech sawdust. They found that the Inconel reactor produced a higher gas yield, with a higher methane and lower hydrogen yield, indicating enhanced C-C bond scission and methanation, when compared with the stainless-steel reactor. Additionally, they found that beech sawdust was less affected than glucose, due to the natural salts within the biomass dominating the wall catalytic effect. Microalgae, like sawdust, contain natural salts, so the impact of the reactor walls is expected to be less significant. However, the results described above identify that the wall can have an effect, which should be considered if comparing results from different reactors.

2.1.3.3 Temperature

Temperature is a major operating condition, which has the most significant impact on the reactions in SCWG [95], strongly affecting the biomass conversion and product distribution in the gas. The overall reaction to form hydrogen and CO_2 from biomass (equation 2b) is endothermic (346kJ mol-1 for glucose), while the overall reaction to form methane (equation 2a followed by 4a) is exothermic (-148kJ mol-1 for glucose) [122] [105]. According to Le Chatelier's principle, higher temperatures favour the formation of hydrogen and suppress methane [123]. Thermodynamic models of microalgae and other biomass also agree with this, stating that at equilibrium, a higher temperature increases hydrogen concentration and reduces methane concentration [124] [77] [125] [126]. The models also predict that the solid carbon produced is also reduced at higher temperatures [124], which increases CGE and reduces negative effects of plugging or catalyst deactivation.

The models listed above only include the equilibrium conditions and do not consider the kinetics. Guan et al. [16] modelled the kinetics of SCWG based on experimental data where *Nannochloropsis sp.* was gasified at temperatures ranging from 450-550°C (723-823K). This showed that increasing the temperature increases the CGE and the total energy in the product gases. Increasing temperature always increases the reaction rate and leads to shorter reaction times. However, this

study showed that the higher conversion was seen obtained at longer reaction times too. This was attributed to temperature having a larger effect on the rate of formation of intermediates less resistant to gasification, reducing the biomass converted into the recalcitrant intermediates such as phenols, which are difficult to gasify, and are more likely to polymerise into chars, reducing the overall conversion. These models show that, in theory, a higher temperature is preferred to maximise the hydrogen yield from microalgal SCWG.

In real systems, Chakinala et al. [4], Duan et al. [15] and Zhang et al. [108] all observed that without a catalyst, increasing the temperature significantly increased conversion. Increasing the temperature from 400 to 700°C (673-973K) increased the CGE of *Chlorella vulgaris* from 14 to 82% [4], increasing from 380 to 600°C (653-873K) increased the CGE of *Chlorella pyrenoidosa* from 31.59 to 68.02% [15] and increased the total gas yield from 4 to 13 mol/kg on a mix of cyanobacteria [108]. However, at low temperatures (653 or 673K), all authors observed almost entirely CO2. This indicates that decarboxylation reactions prevailed, showing that the kinetics of the other main reactions, such as steam reforming, WGS or other intermediate reactions were significantly slower. As a result, in all three, higher temperatures, despite increasing the hydrogen content, this also significantly increased the methane content of the gas. This shows how kinetics can explain the large deviations from equilibrium values. Duan et al. [15] suggested the increased pressure at higher temperatures favoured methanation. While this could be factor in that case, especially with a longer reaction time, the other two cases were performed at constant pressure, so a kinetic explanation is more likely.

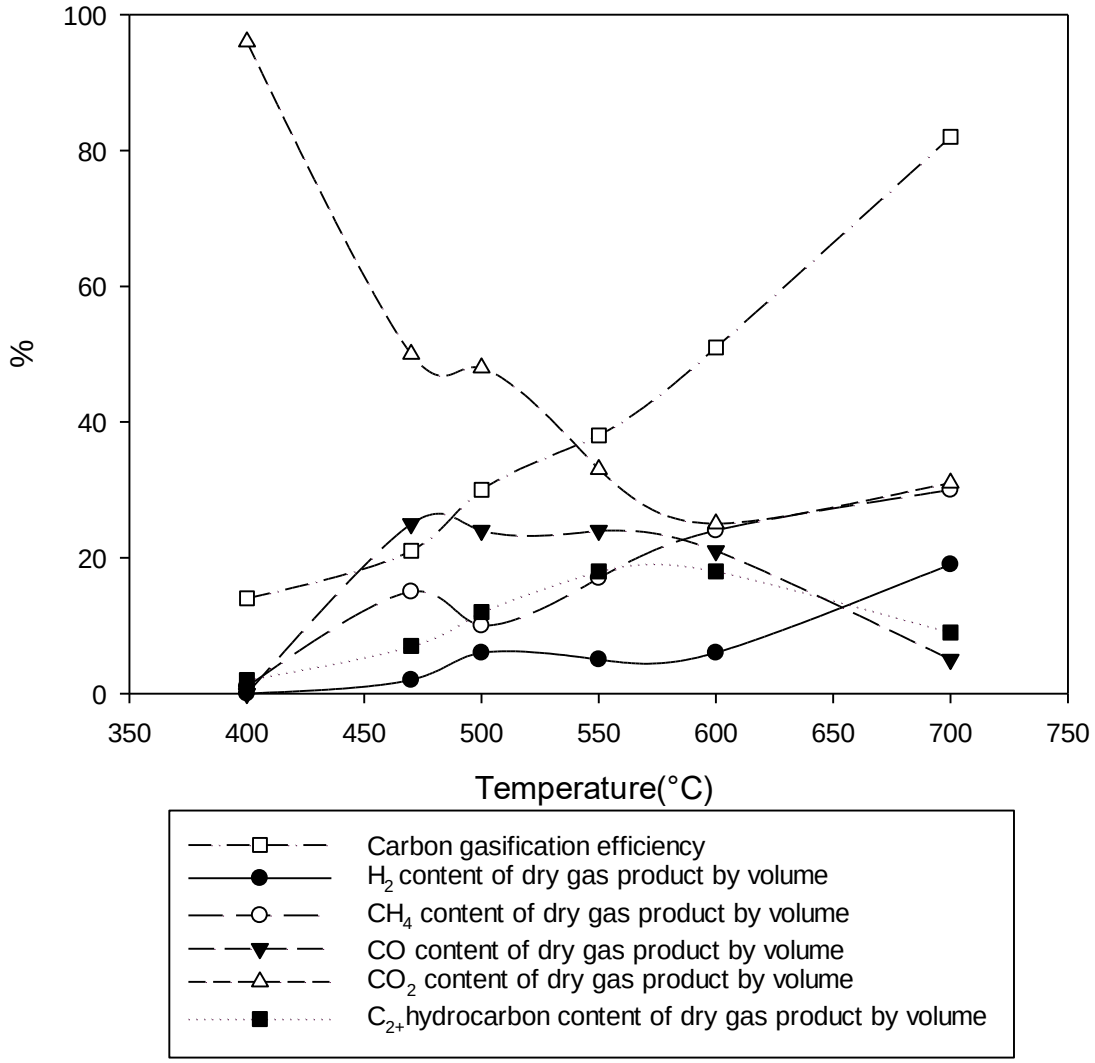

Figure 2.9-Dry gas composition and gasification efficiency for the non-catalytic supercritical water gasification of Chlorella vulgaris in a batch reactor at 240bar, 7.3wt%, 2minutes reaction time . Adapted from. [15]

The effect of temperature on conversion with a catalyst followed a similar trend. Duan et al. [15] observed a similar increase of the CGE with temperature, with or without a ruthenium and rhodium catalyst. The exception was that the conversion was higher for a given temperature than the non-catalytic equivalent, as shown in Figure . The increase in gasification efficiency at higher temperatures, both with and without a catalyst, was also observed in other biomass feedstocks [127]. However, the effect on gas composition on catalytic SCWG of real biomass can vary.

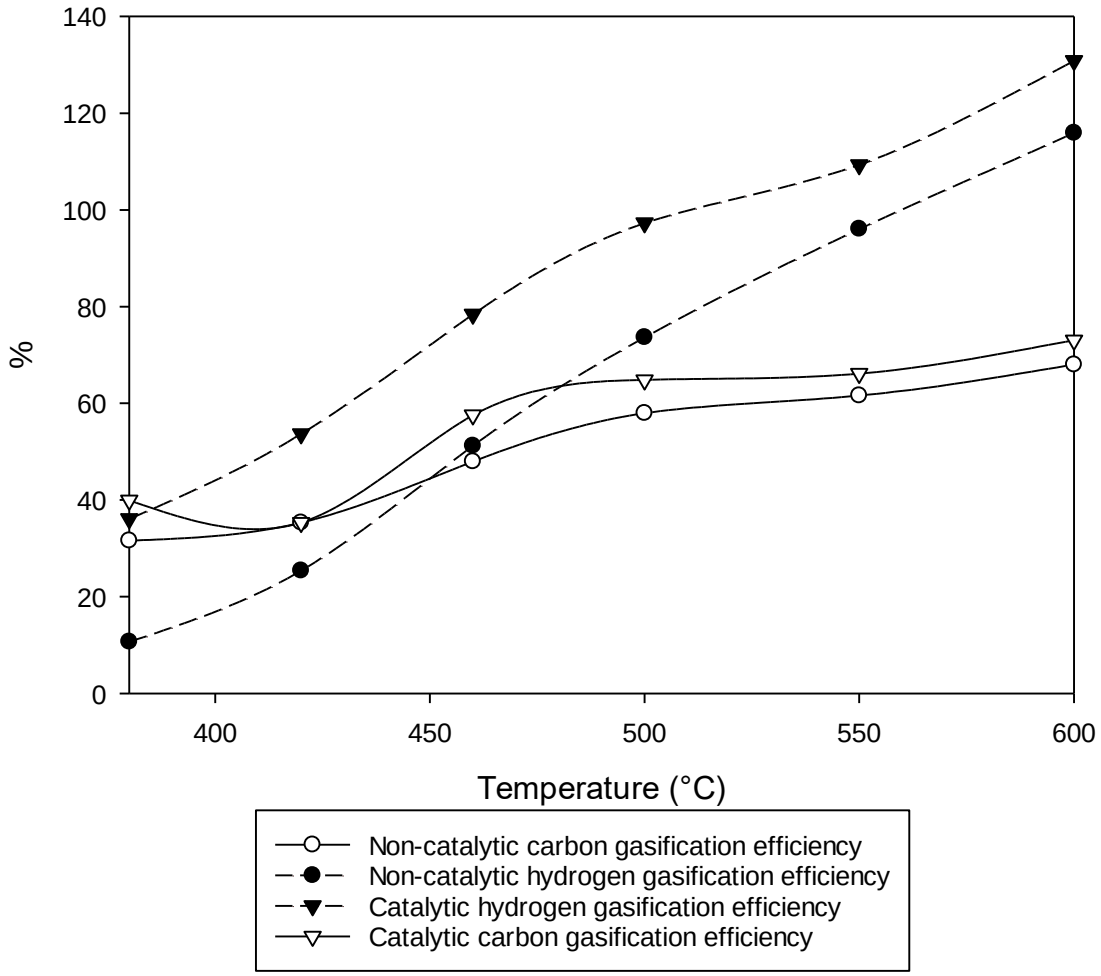

Figure 2.10-Impact of temperature on the carbon and hydrogen gasification efficiencies for the supercritical water gasification of Chlorella pyrenoidosa. Reaction time 1h, 10wt%, Ru/C+ Rh/C catalysts. Adapted from [15]

Elsayed et al. [15] found that, when gasifying *Acutodesmus obliquus* with a K_2CO_3 catalyst, increasing the temperature between 600 and 700°C (873 and 973K) increased the hydrogen content of the gas and reduced the methane. This is similar to that predicted in the mathematical models, indicating it was close to equilibrium. This was not the case reported by Duan et al. [16] when increasing the temperature between 380-600°C (653-873K) in the gasification of *Chlorella pyrenoidosa*, with Ru/C and Rh/C catalysts. These authors observed that increasing the temperature increased methane and short alkanes at the expense of CO_2, with almost constant hydrogen content and yield. This indicates that increasing the temperature favoured more cracking reactions and methanation, with any hydrogen created in the process being converted to methane. These

examples used different catalysts, temperatures, and feedstocks, which can potentially impact upon the effect of temperature. Therefore, it is hard to predict the impact of an increased temperature on the gas product composition and further work should be completed to investigate the interaction between these parameters.

Nonetheless, the yield of hydrogen almost always increases with temperature, to the higher conversion achieved and higher equilibrium concentration. Therefore, higher temperatures are usually preferred. However, this requires more energy to heat up the reactor contents, which cannot be fully recovered [17] and requires more expensive materials to withstand the temperatures [18], so it is important to consider the whole system when selecting a reaction temperature. Catalysts and feedstock selection can be used to help minimise the required temperature to achieve high yields, increasing the overall efficiency.

2.1.3.4 Biomass Concentration

Water plays an important role in many of the main reactions involved in SCWG. Le Chatelier's principle means that if the concentration of water is high, the equilibrium will shift to remove it. This would increase hydrolysis, WGS and steam reforming, where water is a reactant, while reducing the methanation reaction, where water is a product [128]. This favours an increased conversion, high content of hydrogen in the feed and thus a high hydrogen yield. This explains the reduction in hydrogen and the increase in methane content observed in thermodynamic models of the gasification of microalgae and other biomass feedstocks at higher biomass concentrations [124] [125] [126]. Moreover, Guan et al. [16] found that first order kinetics were insufficient to show the effect of biomass concentration on hydrogen production. This shows that biomass concentration also has a strong role in kinetics too.

In real systems, Elsayed et al. [15], Samiee-Zafarghandi et al. [24] and Guan et al. [129] found that increasing the biomass concentration significantly reduced the concentration of hydrogen and increased the concentration of methane in the product gas during the SCWG of microalgae. This

was a unanimous finding, for different algae strains, temperatures, catalysts, and range of biomass concentration (outlined in Table 2.6Table). Moreover, the former two authors observed a significant decrease in CGE. Guan et al. [129] observed that, while the hydrogen yields significantly fell with concentration, the carbon compounds had consistent yields, so CGE changed minimally. In this case a major production of carbon gas (CO, CO_2 and CH_4) may be from direct conversion of biomass in processes like decarboxylation [16], so the loss of CO_2 from reduced steam reforming is compensated by increases production from these sources. Higher biomass concentrations can also lead to an increase of undesirable compounds such as phenol [19].

Feedstock	Catalyst	Temperature (K)	Biomass concentration (wt.%)	Hydrogen yield at min wt.% (mmol/g)	Hydrogen yield at max wt.% (mmol/g)	Source
Acutodesmus obliquus	K_2CO_3	963	2.5-20	299.33	63.3	[15]
Chlorella sp.	None	628-653	1-8	1.2	0.714	[24]
Nannochloropsis sp.	Ru/C	683	2-13.5	11.6	2.8	[129]

Table 2.6-Microalgae experiments in which a decrease in hydrogen content was observed with an increase in biomass concentration in the feed.

These observations verify the models by demonstrating that a lower biomass concentration increases hydrogen yield, which would be preferable for hydrogen production. However, as with temperature, this increases the energy lost, due to the larger quantities of water requiring heating to supercritical temperatures and pumped through the system [17]. The heat is often provided from the product gas, so reduces the overall yield. Furthermore, the concentration of microalgal slurry can be highly energy intensive, so a lower concentration reduces the energy required to produce the feedstock [130]. Therefore, the whole system should be considered when choosing the ideal feedstock concentration.

2.1.3.5 Residence or Reaction Time

Longer reaction times naturally allow the reactions to proceed further. Since the hydrolysis step is fast [16], longer reaction time allows further conversion of the intermediates to final products and therefore it is expected that gasification efficiency is increased. This was the case described by Miller

et al. [131] when continuously gasifying *Spirulina* and by Samiee-Zafarghandi et al. [24] when gasifying *Chlorella sp*. in a batch reactor. However, the case is not quite that simple as some chemicals formed (such as amino acids or phenols, which are both found to occur in SCWG of algae) are very difficult to gasify and/or favour polymerisation to tar and chars than gas [29] [16]. Hence, under the milder conditions they may not gasify in a reasonable time frame. This was evidenced by the asymptotic curve that never reaches 100% when longer reaction times were used [30], as shown in Figure 2.11. This was the case with and without the ruthenium catalyst, although the catalyst promoted a higher maximum yield and achieved this more rapidly (30 minutes instead of 90). This shows that the catalyst accelerates the reactions allowing the “easier” reactions occur more rapidly and some of the more difficult reactions to progress in a more reasonable time.

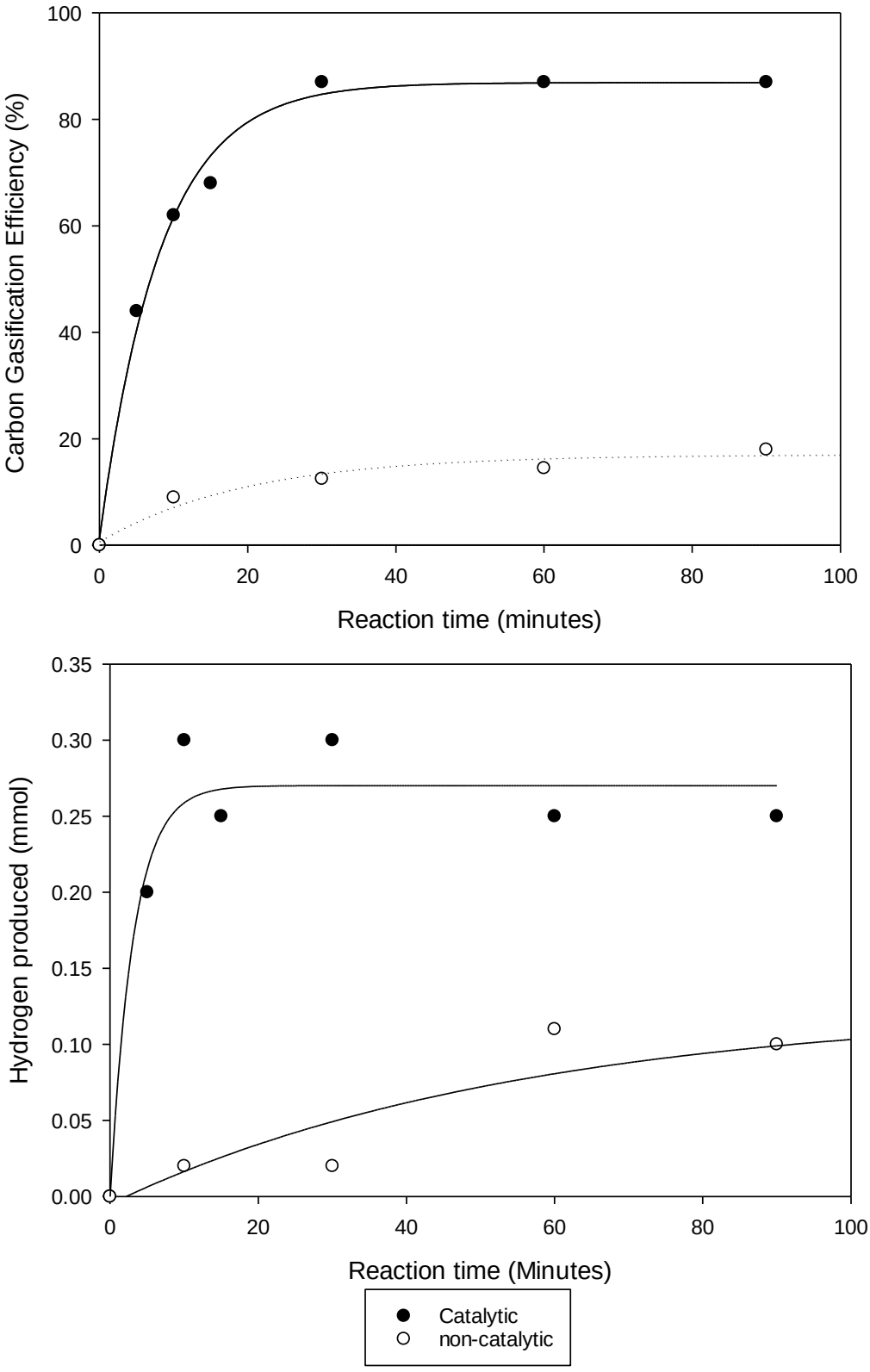

Figure 2.11-Carbon gasification efficiency at different reaction times for the batch supercritical water gasification of Chlorella vulgaris, with and without a charcoal supported ruthenium catalyst. 4.8%wt biomass, 385°C and 0.83g of catalyst (if used). Adapted from [30]

Even after the gasification efficiency has plateaued, a further increase in reaction time can alter the gas composition. Once the faster reactions that affect gasification efficiency (steam reforming and decarboxylation) have reached a maximum, the slower gas reactions (WGS and methanation) progress with time, until the gas has reached equilibrium. This is illustrated in Figure 2.12, where the CO content reduces over time with hydrogen and methane contents increasing correspondingly [29], in this case CO_2 remains constant as the extra created in WGS is consumed in methanation reactions. Similarly, an increase in the residence time increased both hydrogen and methane content at the expense of CO in non-catalytic continuous SCWG of *Chlorella sp*. and *Chlorella vulgaris* [24] [31].

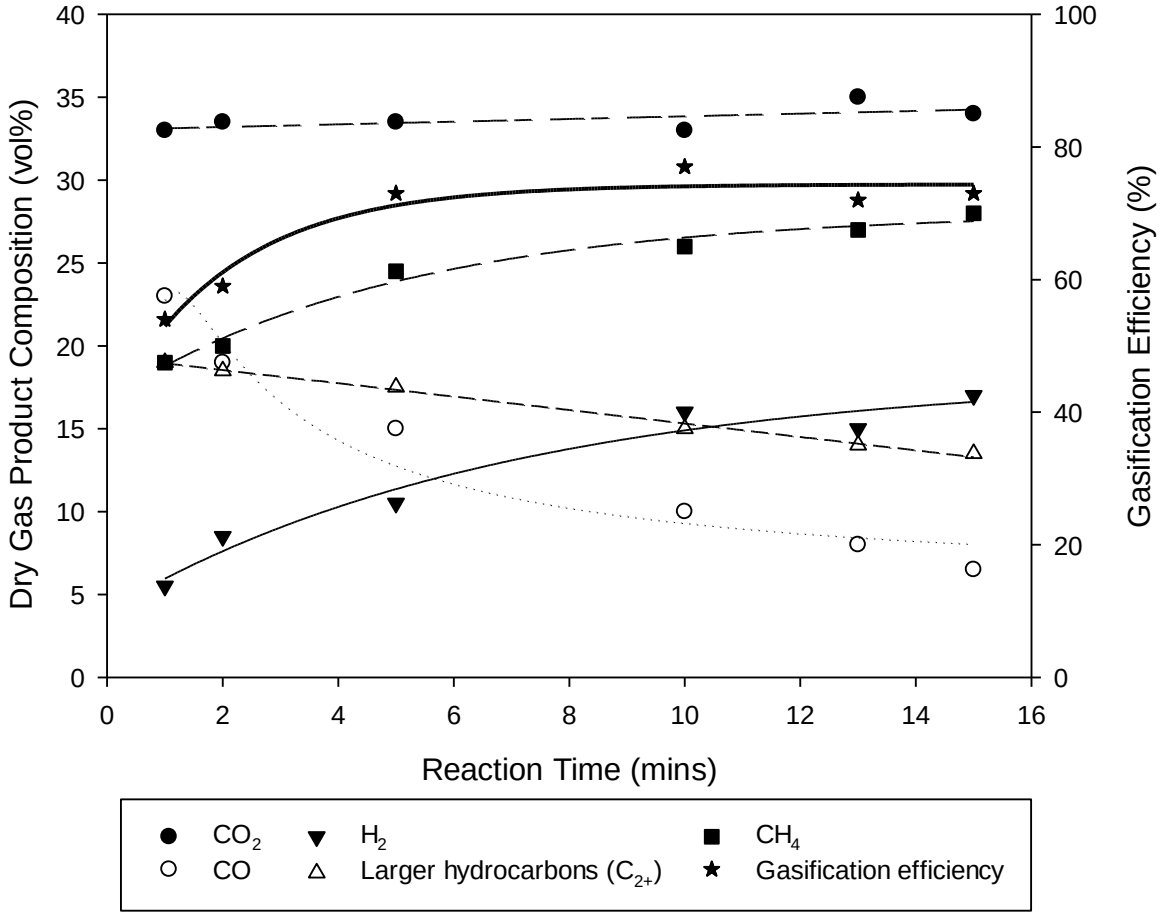

Figure 2.12-Change in gas composition and gasification efficiency over time, for supercritical water gasification of Chlorella vulgaris without a catalyst. Temperature: 580°C, Concentration 7.3%wt, pressure 24MPa. Adapted from [29]

In catalytic gasification, similar effects occur but at a faster rate. Zhu et al. [32] gasified glucose with and without a ruthenium catalyst for reaction time ranges of 30-1800s and the effect on gas composition is shown in Figure 2.13. Without a catalyst, at short reaction times CO_2 dominated, with CO increasing (steam reforming) up to 600s where the CO content reduced, producing more hydrogen and methane. With a catalyst, the WGS and methanation reactions progressed more rapidly, being more significant at shorter times but the hydrogen and methane content also increased with time. However, there was little change after 300s indicating the system had reached equilibrium. As the reaction time increases, the gas composition will progress towards the equilibrium values. As the position of equilibrium is dictated by reaction conditions, the effect of higher residence times on composition of the gas will be dependent on these. This was shown by Samiee-Zafarghandi et al. [24], who found the increase in hydrogen yield with longer residence times was more significant at higher temperatures (where the equilibrium hydrogen fraction in the gas is higher [124]).

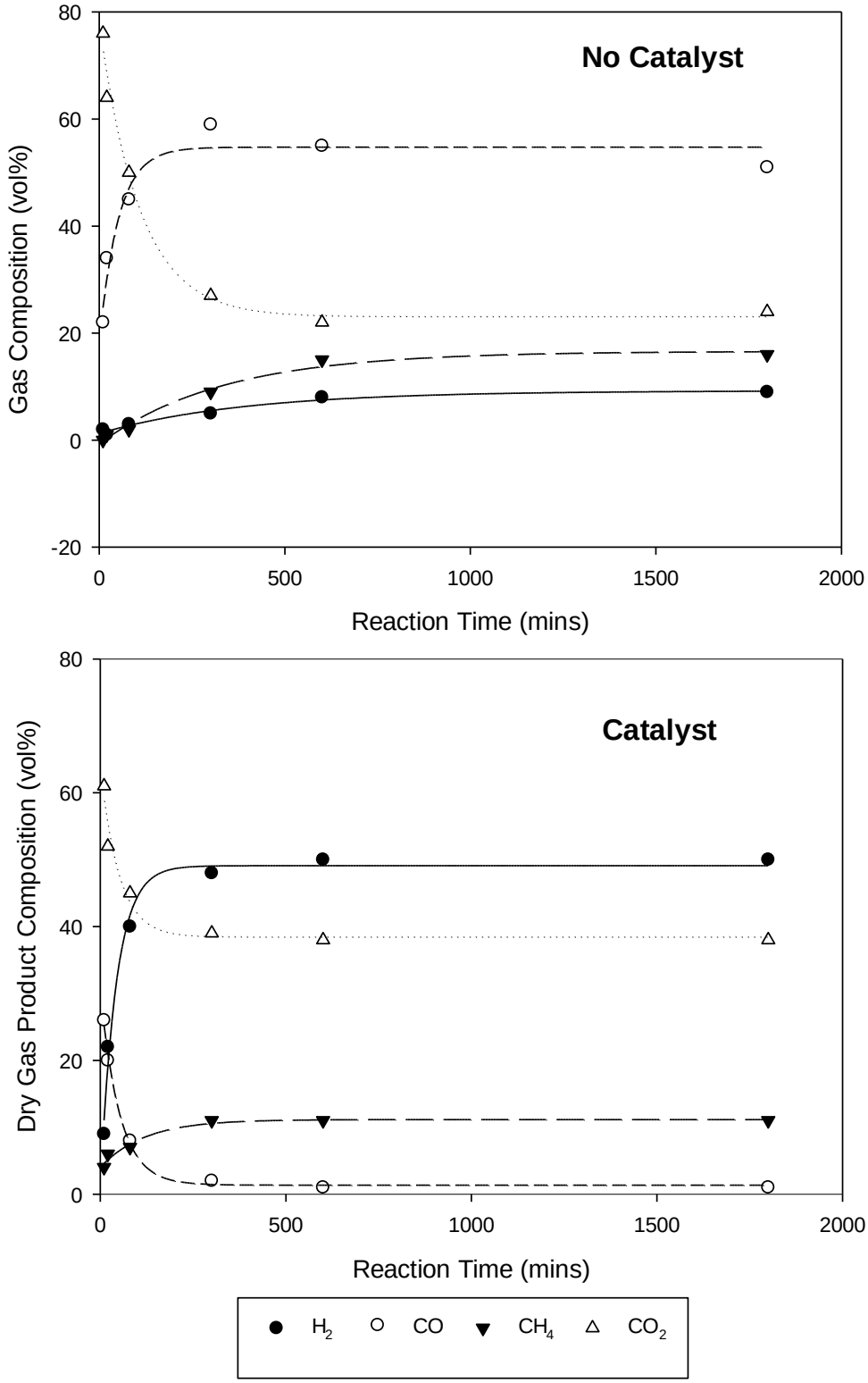

Figure 2.13-Gas composition over time for the supercritical water gasification of glucose with either no catalyst or a ruthenium on alumina catalyst. Temperature 500°C, Concentration 5%wt Adapted From [32].

2.1.3.6 Other Factors

2.1.3.6.1 Pressure

Le Chatelier's principle implies that lower pressures favour reactions with more moles of products than reactants. This would suit the steam reforming and WGS reactions while suppressing methanation at low pressures, leading to a higher hydrogen concentration. This is observed in thermodynamic models of SCWG of microalgae and other biomass [124] [125]. Although the effect was small, relative to that of temperature, this was investigated in some literature. Duan et al. [16] observed an increase in hydrogen content at lower water density (higher biomass concentration but lower pressure). As noted in Section 2.1.3.4, a lower biomass concentration increases hydrogen, so the pressure effect must have promoted the higher hydrogen.

In contrast, work on other feedstocks has found that increasing pressure marginally increased hydrogen and reduced methane [132]; there was an optimum pressure above or below which the hydrogen yield was reduced [133]; or pressure had little impact [134]. This is caused by the change in reaction kinetics due to the increased water density. This can increase collisions and solvent cage effects, which increase reaction rates and reactions involving water (such as WGS). However, it also increases the dielectric constant that reduces the free-radical reactions [36], key reactions in SCWG. Hence positive and negative impacts can come from increased pressure. These impacts are seen where kinetics play more of a key role, with harder to gasify feedstocks, when there is no catalyst or short residence times. Although, the impact is far less significant than that of the temperature, biomass concentration and feedstock composition [135]. It is also important to consider that increased pressure increases the pumping energy required [136] and the required strength of the reactor material [18].Therefore, in many cases, particularly with a catalyst, lower pressures (still above the critical point) are preferred. However, in some cases the pressure may be significant and effect of pressure should be considered.

2.1.3.6.2 Heating Rate

The heating rate is an important factor in SCWG as it dictates the time the feed spends in the subcritical region. In this region, different intermediates are favoured, that may have a negative impact on the overall gasification performance. For example, a slower heating rate using glucose increases the formation of furfurals and phenol, which are difficult to gasify and are more likely to polymerise to form unwanted tar and chars. This reduces the gas and hydrogen yields [39]. As glucose is a major component in many carbohydrates in microalgae, this effect should also occur in this case. Caputo et al. [40] observed that preheating the feed reduced gasification efficiency and increased solid residue, when gasifying *Nannochloropsis gaditana*. This has the same effect as a slower heating rate, thus showing the effect found on glucose should also be applicable for microalgae. Therefore, heating rate should be maximised in SCWG of microalgae. Using a hot water stream that rapidly mixes with a cold microalgal feed, providing extremely fast mixing is a potential method to achieve this [93]. However, it will be more difficult to regain the heat from the product stream and will require a higher feed concentration. A whole system approach is needed to assess whether the added benefits of this approach outweigh the increased energy requirement from heating and pumping the feed.

2.1.4 Supercritical Water Gasification Systems

2.1.4.1 Nutrient Recycling

To grow large amounts of algae requires nutrients such as nitrogen and phosphorus, as well as inorganic carbon (usually CO_2) for growth. These (particularly CO_2) contribute significantly to the cost of the algae production, which is a major cost in the whole of the process, and a barrier to the development of microalgal SCWG systems [42] [137]. Furthermore, many of the fertilisers used today to provide these nutrients are energy intensive to produce [138] or are already limited in supply. Thus, large scale algal production could put further strain on the fertilizer supply, threatening food supplies in an expanding world population [139]. Therefore, it is important to limit nutrient use as much as possible. SCWG is advantageous as it can completely mineralise the inorganic parts of the

algae, allowing it to be recycled more easily [46]. Moreover, the gas product does not contain toxic pollutants such as hydrogen sulphide. Thus, minimal processing is required to recycle the CO_2. Achieving the maximum CO2 recovery is vital for minimising costs, as it remains the highest operating cost in the algal growth even at 90% recovery [42]. This would allow a large reduction in nutrients required, without affecting the algae growth.

Elsayed et al. [15] and Patzelt et al. [140] found that a very high percentage (85-100%) of the nitrogen in *Acutodesmus obliquus* was recovered in the aqueous phase after SCWG, mostly in the form of ammonium ions. Phosphorus and the trace metals were largely precipitated out in the reactor due to their low solubility in supercritical water. Therefore, it is important that regular purging of the reactor with subcritical water is required to recover these salts is included, otherwise the nutrients would be lost, and the reactor would be plugged. When the purge was included, over 85% recovery was achieved for phosphorus, nitrogen, potassium, calcium, magnesium, sulphur, sodium, with a recovery close to 100% in many cases [15] . Despite high nutrient recovery, several toxic organic compounds such as phenols would be present in the aqueous phase, so algal growth was not achieved if the untreated aqueous phase is used as the growth media [15] [140]. Dilution as treatment method worked in both cases [140] and for growing *Chlorella vulgaris* in the aqueous phase of following the SCWG of the macroalga *Saccharina latissimi,* but that remained impractical as it would overfill the growth vessel. Activated carbon and ultraviolet (UV) treatment were both successfully used to reduce the toxic compounds and achieve growth, but UV also destroyed some of the nitrogen. [15] [140]. Elsayed et al. [15] found that the aqueous phase treated with activated carbon outperformed the original media used for growth, as shown in Figure 2.14. Moreover, in other tests involving phenol, activated carbon filters were easily regenerated using a mixture of ethanol and sodium hydroxide [141]. Hence, the use of activated carbons offers a promising solution to remove toxic compounds and allow for nutrient recycling.

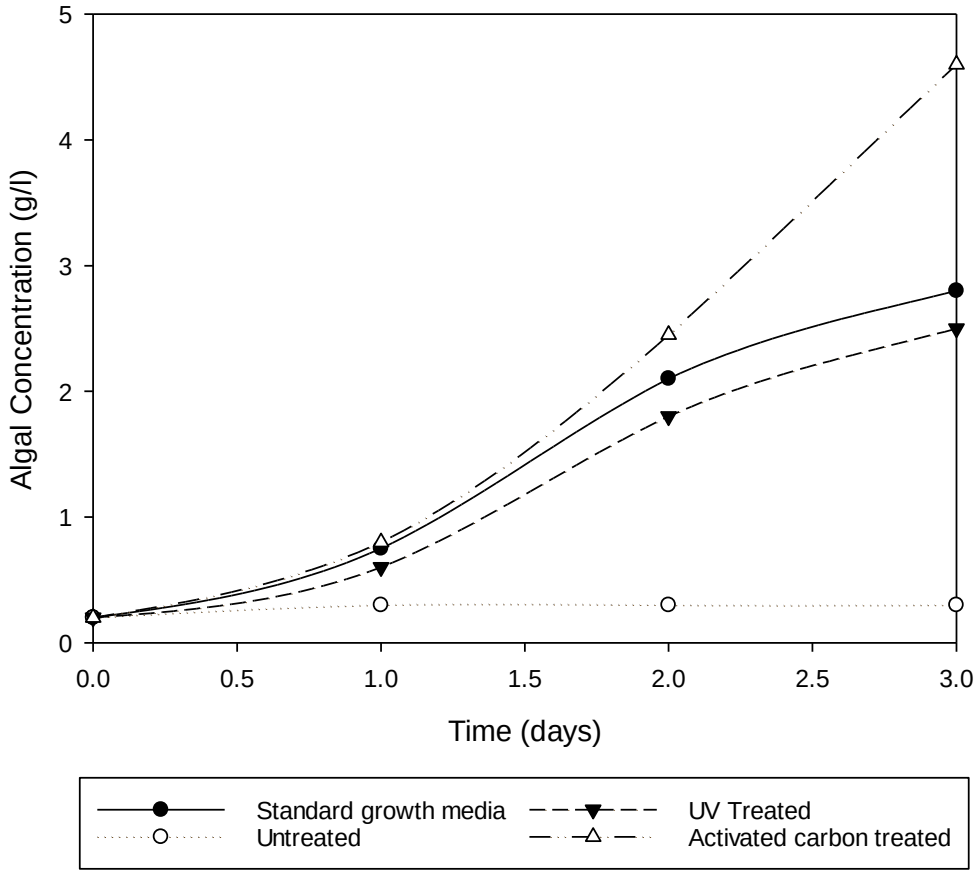

Figure 2.14- Microalgae growth in the residual water following the supercritical water gasification of Acutodesmus Obliquus, comparison of the different treatment methods. Adapted from: [15]

The SCWG reactions themselves are also important to achieving successful nutrient recycling and limiting the steps required after the reaction. Gokkaya et al. [49], observed that ruthenium catalysts reduced the phenol content and alkali catalysts increased it in the gasification of xylose. While the reverse has been observed in some microalgae examples [30] [46], this shows that the choice of catalyst can significantly affect the recyclability of the aqueous phase and should be considered in the choice of a catalyst. Further work should focus on the effect of the catalysts on the recyclability of the aqueous phase. Furthermore, metals such as nickel and aluminium, often used in catalysts and the wall material, are known to limit microalgal growth [46] [50] [142]. Both were found in large quantities when both nickel on alumina and NaOH were used due to reaction between the catalysts [46]. It is therefore important to ensure supported metal catalysts are stable in the reaction environment and corrosion is minimised, to keep the metal content in the aqueous phase to a minimum.

2.1.4.2 Integrated systems

The SCWG reactor will not stand alone and must be placed within a whole system that includes algal growth, purification of the gas stream and storage of produced gases. It is possible to recover energy from parts of the process and therefore increase the efficiency of the system. A general system of this is shown in Figure 2.15. Nurdiawati et al. [42] proposed a system that included chemical looping for purification, hydrogenation of liquid organic carriers (in this case toluene) for hydrogen storage and gas turbines to recover excess pressure as electricity. Chemical looping is particularly advantageous as it has a high process efficiency and produces highly concentrated CO_2 and hydrogen from the mix of gases produced in SCWG [143]. This allows the hydrogen to be used in any application without further purification and the CO_2 to be easily recycled or stored. Also, system allows the heat from chemical looping regained, as well as maximising energy recovery of the SCWG system. The result predicted total efficiencies of over 50% in some cases, exceeding that of the more mature technology of dry gasification although, this may differ in real life applications. In other cases, with suitable climates, concentrated solar heating can be used to heat the reaction and reduce losses [144] [145].

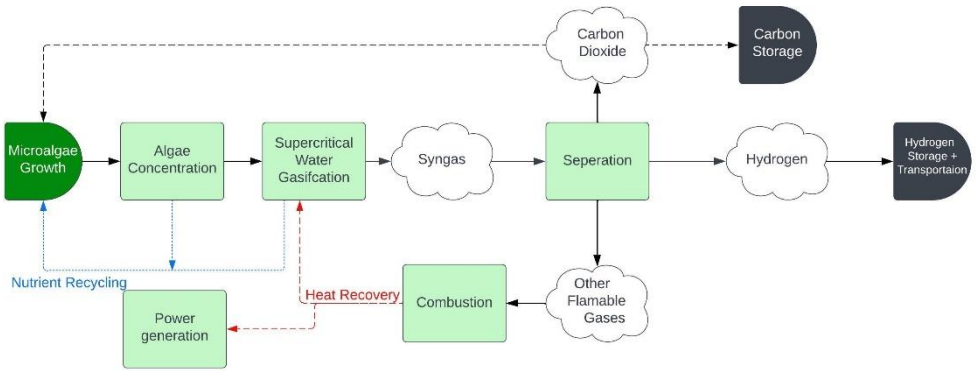

Figure 2.15-Potential supercritical water gasification of microalgae system to produce hydrogen and capture carbon dioxide.

Systems as such are vital to maximising efficiency and reducing costs in the process, with models being important for seeing the impacts of operating conditions on the whole model. Nurdiawati et al. [42] found that the optimum reaction temperature depended on the biomass concentration into the reactor; a higher temperature was preferred at a higher biomass concentration and conversely lower

temperature at lower biomass concentrations. However, this does not include the difference in energy requirement for concentrating the algae. This must be incorporated to obtain the ideal operating conditions. Aziz [136] proposed a similar system except with a membrane separation in place of chemical looping and a fluidised bed reactor. In this model, pressure and fluidisation velocity were investigated. Both were found to reduce energy efficiency when they were increased, due to higher pumping energy. However, this model did not consider kinetics which can be influenced by the pressure and levels of turbulence from the higher velocities. Thus, a real system may differ from this. Combination with a direct use of the hydrogen, such as ammonia production [146], can also help maximise efficiencies.

2.1.5 Conclusion

Supercritical water gasification of microalgal biomass offers an alternative source of green hydrogen that does not rely on the electrical grid and can potentially be carbon negative. It also brings several other advantages, when compared to other biomass conversion processes, such as reduced char formation, no drying requirement, possibility of energy recovery and reuse, and the potential for recycling the inorganic nutrients and CO_2 required for algal growth. These are important to minimise costs and strain on the fertiliser supply so should be considered in the system. This includes choosing an appropriate catalyst and the use of post reaction treatment such as activated carbon filters.

The composition of the algae, catalyst selection and operating conditions all impact upon the gasification performance. A higher carbohydrate content is usually favourable for a high hydrogen yield, a high protein content usually reduces the gas produced and lipids are easily gasified but tend to produce methane. However, this is not always the case, due to the large range of compounds within those categories and other factors such as algal cell wall thickness. Alkali metal salts can be used as a homogeneous catalyst to increase the hydrogen yield and selectivity but can be difficult to recover and increase corrosion. Supported nickel and ruthenium catalyst can increase hydrogen yield but often increase the methane produced at the expense of hydrogen. They also are prone to

deactivation and careful selection of the support is needed to minimise this. Adjustments to the catalysts and or the reactor systems are required to maximise their positive impact.

A high temperature and low biomass concentration in the reactor both favour a higher biomass conversion, hydrogen yield and hydrogen selectivity. However, in real systems these require a greater energy input in heating and pumping of the water, which reduces the overall efficiency of the process. Moreover, the feed should be heated rapidly to maximise efficiency and minimise char. A longer residence time can also increase conversion and yield but only up to a point where further increases have little effect. Despite a low pressure often being preferred, in some cases the increased kinetics from higher pressure may be the better option. These factors are all important to consider for the design of a supercritical water gasification system, to produce hydrogen from microalgae. Further work should investigate how the catalysts, biomass composition and the overall system can be optimised to maximise efficiency and reduce the cost of hydrogen produced in this way.

2.1.6 References

[1] M. R. Allen, O. Dube, W. Solecki, F. Aragón-Durand, W. Cramer, S. Humphreys, M. Kainuma, J. Kala and N. Mahowald, “Global Warming of 1.5°C,” IPCC, Geneva, 2018.

[2] Committee on Climate Change, “Hydrogen in a Low-Carbon Economy,” Committee on Climate Change, London, 2018.

[3] A. Scragg, A. MIllman, A. Carden and S. Shales, “Growth of microalgae with increased calorific values in a tubular bioreactor,” *Biomass and Bioenergy,* vol. 23, no. 1, pp. 67-73, 2002.

[4] A. G. Chakinala, D. W. F. (. Brilman, W. P. v. Swaaij and S. R. A. Kersten, “Catalytic and Non-catalytic Supercritical Water Gasification of Microalgae and Glycerol,” *Industrial and Engineering Chemistry Research,* vol. 49, no. 3, pp. 1113-1122, Septemeber 2010.

[5] M. K. Lam, K. T. Lee and A. R. Mohamed, “Current status and challenges on microalgae-based carbon capture,” *International Journal of Greenhouse Gas Control,* vol. 10, pp. 456-469, 2012.

[6] J. Tomei and R. Helliwell, “Food versus fuel? Going beyond biofuels,” *Land Use Policy,* vol. 56, pp. 320-236, 2016.

[7] Y. K. Leong, W.-H. Chen, D.-J. Lee and J.-S. Chang, “Supercritical water gasification (SCWG) as a potential tool for the valorization of phycoremediation-derived waste algal biomass for biofuel generation,” *Journal of Hazardous Materials,* vol. 418, 2021.

[8] Y. Yoshida, K. Dowaki, Y. Matsumura, R. Matsuhashi, D. Li, H. Ishitani and H. Komiyama, “Comprehensive comparison of efficiency and CO2 emissions between biomass energy conversion technologies—position of supercritical water gasification in biomass technologies,” *Biomass and Bioenergy,* vol. 25, no. 3, pp. 257-272, 2003.

[9] C. R. Correa and A. Kruse, “Supercritical water gasification of biomass for hydrogen production – Review,” *The Journal of Supercritical Fluids,* vol. 133, no. 2, pp. 573-590, March 2018.

[10] N. Akiya and P. E. Savage, “Roles of Water for Chemical Reactions in High-Temperature Water,” *Chemical Reviews,* vol. 102, no. 8, pp. 2725-2750, 2002.

[11] C. Wang, W. Zhu, H. Zhang, C. Chen, X. Fan and Y. Su, “Char and tar formation during hydrothermal gasification of dewatered sewage sludge in subcritical and supercritical water: Influence of reaction parameters and lumped reaction kinetics,” *Waste Management,* vol. 100, pp. 57-65, 2019.

[12] C. Wang, M. Du, H. Feng and H. Jin, “Experimental investigation on biomass gasification mechanism in supercritical water for poly-generation of hydrogen-rich gas and biochar,” *Fuel,* vol. 319, 2022.

[13] D. A. Cantero, M. D. Bermejo and M. J. Coceroa, “Reaction engineering for process intensification of supercritical water biomass refining,” *The Journal of Supercritical Fluids,* vol. 96, pp. 21-35, January 2015.

[14] Q. Yan, L. Guo and Y. Lu, “Thermodynamic analysis of hydrogen production from biomass gasification in supercritical water,” *Energy Conversion and Management,* vol. 47, no. 11-12, pp. 1515-1528, July 2006.

[15] P.-G. Duan, S.-C. Li, J.-L. Jiao, F. Wang and Y.-P. Xu, “Supercritical water gasification of microalgae over a two-component catalyst mixture,” *Science of The Total Environment,* vol. 630, pp. 243-253, 2018.

[16] Q. Guan, C. Wei and P. E. Savage, “Kinetic model for supercritical water gasification of algae,” *Physical Chemistry Chemical Physics,* vol. 14, no. 9, pp. 3140-3147, 2012.

[17] J. A. Onwudili, A. R. Lea-Langton, A. B. Ross and P. T. Williams, “Catalytic hydrothermal gasification of algae for hydrogen production: Composition of reaction products and potential for nutrient recycling,” *Bioresource Technolgoy,* vol. 127, pp. 72-80, January 2013.

[18] L. Tiong, M. Komiyama, Y. Uemura and T. T. Nguyen, “Catalytic supercritical water gasification of microalgae: Comparison of Chlorella vulgaris and Scenedesmus quadricauda,” *The Journal of Supercritical Fluids,* vol. 107, pp. 408-413, January 2016.

[19] A. Kruse, T. Henningsen, A. Sınağ and J. Pfeiffer, “Biomass Gasification in Supercritical Water: Influence of the Dry Matter Content and the Formation of Phenols,” *Industrial & engineering chemistry research,* vol. 42, no. 16, pp. 3711-3717, 2003.

[20] E. Weiss-Hortala, A. Kruse, C. Ceccarelli and R. Barna, “Influence of phenol on glucose degradation during supercritical water gasification,” *The Journal of Supercritical Fluids,* vol. 53, no. 1-3, pp. 42-47, June 2010.

[21] H. Zhang, C. Wang, X. Zhang, R. Zhang and L. Ding, “Formation and inhibition of polycyclic aromatic hydrocarbons from the gasification of cyanobacterial biomass in supercritical water,” *Chemosphere,* vol. 253, 2020.

[22] G. Caputo, M. Dispenza, P. Rubio, F. Scargiali, G. Marotta and A. Brucato, “Supercritical water gasification of microalgae and their constituents in a continuous reactor,” *The Journal of Supercritical Fluids,* vol. 118, pp. 163-170, December 2016.

[23] C. Zhu, L. Guo, H. Jin, J. Huang, S. Li and X. Lian, “Effects of reaction time and catalyst on gasification of glucose in supercritical water: Detailed reaction pathway and mechanisms,” *International Journal of Hydrogen Energy,* vol. 41, no. 16, pp. 6630-6639, May 2016.

[24] L.-F. Xie, P.-G. Duan, J.-L. Jiao and Y.-P. Xu, “Hydrothermal gasification of microalgae over nickel catalysts for production of hydrogen-rich fuel gas: Effect of zeolite supports,” *International Journal of Hydrogen Energy,* vol. 44, no. 11, pp. 5114-5124, 2019.

[25] Z.-H. Zhang, Z. Sun and T.-Q. Yuan, “Recent Advances in the Catalytic Upgrading of Biomass Platform Chemicals Via Hydrotalcite-Derived Metal Catalysts,” *Transactions of Tianjin University,* vol. 28, pp. 89-111, 2022.

[26] N. Wei, D. Xu, B. Hao, S. Guo, Y. Guo and S. Wang, “Chemical reactions of organic compounds in supercritical water gasification and oxidation,” *Water Research,* vol. 190, 2021.

[27] Q. Fu, C. Xiao, Q. Liao, Y. Huang, A. Xia and X. Zhu, “Kinetics of hydrolysis of microalgae biomass during hydrothermal pretreatment,” *Biomass and Bioenergy,* vol. 149, 2021.

[28] N. Sato, A. T. Quitain, K. Kang, H. Daimon and K. Fujie, “Reaction Kinetics of Amino Acid Decomposition in High-Temperature and High-Pressure Water,” *Industrial and Engineering Chemistry Research,* vol. 43, no. 13, pp. 3217-3222, 2004.

[29] J. D. Sheehan and P. E. Savage, “Reaction pathways and kinetics of tryptophan in hot, compressed water,” *Chemical Engineering Journal,* vol. 390, 2020.

[30] S. Changi, M. Zhu and P. E. Savage, “Hydrothermal Reaction Kinetics and Pathways of Phenylalanine Alone and in Binary Mixtures,” *ChemSusChem,* vol. 5, no. 9, pp. 1743-1757, 2012.

[31] D. Klingler, J. Berg and H. Vogel, “Hydrothermal reactions of alanine and glycine in sub- and supercritical water,” *The Journal of Supercritcal fluids,* vol. 43, no. 1, pp. 112-119, 2007.

[32] D. Xu, L. Liu, N. Wei, Y. Guo, S. Wang, Z. Wu and P. Duan, “Catalytic supercritical water gasification of aqueous phase directly derived from microalgae hydrothermal liquefaction,” *International Journal of Hydrogen Energy,* vol. 44, no. 48, pp. 26181-26192, 2019.

[33] W. Ma, G. Du, J. Li, Y. Fang, L. Hou, G. Chen and D. Ma, “Supercritical water pyrolysis of sewage sludge,” *Waste Management,* vol. 59, pp. 371-378, 2017.

[34] D. W. de-Leeuw, “Supercritcal Water Gasifcation: Decompositon of lipids forming a substantial part of sewage sludge,” Delft Unviersity of Technology , Delf, 2017.

[35] E. A. Youssef, G. Nakhla and P. A. Charpentier, “Oleic acid gasification over supported metal catalysts in supercritical water: Hydrogen production and product distribution,” *International Journal of Hydrogen Energy,* vol. 36, no. 8, pp. 4830-4842, April 2011.

[36] W. Bühler, E. Dinjus, H. J. Ederer, A. Kruse and C. Mas, “Ionic reactions and pyrolysis of glycerol as competing reaction pathways in near- and supercritical water,” *The Journal of Supercritcal Fluids,* vol. 22, no. 1, pp. 37-53, 2002.

[37] F. J. G. Ortiz, A. Serrera, S. Galera and P. Ollero, “Experimental study of the supercritical water reforming of glycerol without the addition of a catalyst,” *Energy,* vol. 56, pp. 193-206, 2013.

[38] E. Youssef, G. Nakhla and P. Charpentier, “Co-gasification of catechol and starch in supercritical water for hydrogen production,” *International Journal of Hydrogen Energy,* vol. 37, no. 10, pp. 8288-8297, May 2012.

[39] G. Markou, I. Angelidaki and D. Georgakakis, “Microalgal carbohydrates: an overview of the factors influencing carbohydrates production, and of main bioconversion technologies for production of biofuel,” *Applied Microbiology and Biotechnology volume,* vol. 96, pp. 631-645, 2012.

[40] T. Yoshida and Y. Matumura, “Gasification of cellulose, xylan, and lignin mixtures in supercritical water,” *Industrial and Engineering Chemistry Research,* vol. 40, no. 23, pp. 5469-5474, 2001.

[41] T. G. Madenoğlu, N. Boukis, M. Sağlam and M. Yüksel, “Supercritical water gasification of real biomass feedstocks in continuous flow system,” *International Journal of Hydrogen Energy,* vol. 36, no. 22, pp. 14408-14415, 2011.

[42] R. Samiee-Zafarghandi, J. Karimi-Sabet, M. A. Abdoli and A. Karbassi, “Increasing microalgal carbohydrate content for hydrothermal gasification purposes,” *Renewable energy,* vol. 116, no. A, pp. 710-719, February 2018.

[43] P.-G. Duan, S.-K. Yang, Y.-P. Xu, F. Wang, D. Zhao, Yu-JingvWeng and X.-L. Shi, “Integration of hydrothermal liquefaction and supercritical water gasification for improvement of energy recovery from algal biomass,” *Energy,* vol. 155, pp. 734-745, July 2018.

[44] P. Biller and A. Ross, “Potential yields and properties of oil from the hydrothermal liquefaction of microalgae with different biochemical content,” *Bioresource Technology,* vol. 102, no. 1, pp. 215-225, January 2011.

[45] E. Touloupakis, B. Cicchi and G. Torzillo, “A bioenergetic assessment of photosynthetic growth of Synechocystis sp PCC 6803 in continuous cultures,” *Biotechnology biofuels,* vol. 8, no. 133, 2015.

[46] A. L. Lupatini, L. M. Colla, C. Canan and E. Colla, “Potential application of microalga Spirulina platensis as a protein source,” *Journal of the Science of food and agriculture,* vol. 97, no. 3, pp. 724-732, 2017.

[47] A. Sánchez-Bayo, V. Morales, R. Rodríguez, G. Vicente and L. F. Bautista, “Cultivation of Microalgae and Cyanobacteria: Effect of Operating Conditions on Growth and Biomass Composition,” *Molecules,* vol. 25, no. 12, 2020.

[48] A. Kruse, A. Krupka, V. Schwarzkopf, C. Gamard and T. Henningsen, “Influence of Proteins on the Hydrothermal Gasification and Liquefaction of Biomass. 1:Comparison of Different Feedstocks,” *Industrial and Engineering Chemical Research,* vol. 44, no. 9, pp. 3013-3020, 2005.

[49] G. P. Rizzi, “Free Radicals in the Maillard Reaction,” *Food Reviews International,* vol. 19, pp. 375-395, 2007.

[50] A. Kruse, P. Maniam and F. Spieler, “Influence of Proteins on the Hydrothermal Gasification and Liquefaction of Biomass. 2: Model Compounds,” *Industrial & Engineering Chemistry Research,* vol. 46, no. 1, pp. 87-96, December 2006.

[51] T. Samanmulya, O. Farobie and Y. Matsumura, “Gasification characteristics of histidine and 4-methylimidazole under supercritical water conditions,” *Biomass Conversion and Biorefinery,* vol. 7, pp. 487-494, 2017.

[52] T. Samanmulya, S. Inoue, T. Inoue, Y. Kawai, H. Kubota, H. Munestsuna, T. Noguchi and Y. Matsumura, “Gasification Characteristics of Amino Acids in Supercritical Water,” *Journal of the Japan Institute of Energy,* vol. 93, no. 9, pp. 936-943, 2013.

[53] T. Samanmulya, O. Farobie and Y. Matsumura, “Gasification characteristics of aminobutyric acid and serine as model compounds of proteins under supercritical water conditions,” *Journal of the Japan Petroleum Intitute,* vol. 60, no. 1, pp. 34-40, 2017.

[54] I.-G. Lee, A. Nowacka, C.-H. Yuan, S.-J. Park and J.-B. Yang, “Hydrogen production by supercritical water gasification of valine over Ni/activated charcoal catalyst modified with Y,

Pt, and Pd," *Internation Journal of Hydrogen Energy,* vol. 40, no. 36, pp. 12078-12087, September 2015.

[55] D. Fozer, B. Kiss, L. Lorincz, E. Szekely, P. Mizsey and A. Nemeth, "Improvement of microalgae biomass productivity and subsequent biogas yield of hydrothermal gasification via optimization of illumination," *Renew. Energy,* vol. 138, pp. 1262-1272, August 2019 doi:10.1016/j.renene.2018.12.122.

[56] J. Jiao, F. Wang, P. Duan, Y. Xu and W. Yan, "Catalytic hydrothermal gasification of microalgae for producing hydrogen and methane-rich gas," *Energy Sources, Part A: Recovery, Utilization, and Environmental Effects,* vol. 39, no. 9, pp. 851-860, 2017.

[57] P. T. Williams and J. Onwudili, "Subcritical and Supercritical Water Gasification of Cellulose, Starch, Glucose, and Biomass Waste," *Energy Fuels,* vol. 20, no. 3, pp. 1259-1265, 2006.

[58] L. Brennan and P. Owende, "Biofuels from microalgae—A review of technologies for production, processing, and extractions of biofuels and co-products," *Renewable and Sustainable Energy Reviews,* vol. 14, no. 2, pp. 557-677, 2010.

[59] P. R. Nurcahyani, S. Hashimoto and Y. Matsumura, "Supercritical water gasification of microalgae with and without oil extraction," *The Journal of Supercritical Fluids,* vol. 165, 2020.

[60] B. David, B. Federico, C. Cristina, G. Marco, M. Federico and P. Paolo, "Biohythane Production From Food Wastes," in *Biohydrogen*, Elsevier, 2019, pp. 347-368.

[61] M. M. Hanifzadeh, E. C. Garcia and S. Viamajala, "Production of lipid and carbohydrate from microalgae without compromising biomass productivities: Role of Ca and Mg," *Renewable Energy,* vol. 127, pp. 989-997, 2018.

[62] C. Sassano, L. Gioielli, L. S. Ferreira, M. Rodrigues, S. Sato, A. Converti and J. Carvalho, “Evaluation of the composition of continuously-cultivated Arthrospira (Spirulina) platensis using ammonium chloride as nitrogen source,” *Biomass and Bioenergy,* vol. 34, no. 12, pp. 1732-1738, 2010.

[63] S. G. Lynn, S. S. Kilham, D. A. Kreeger and S. J. Interlandi, “Effect of Nutrient Availability on the Biochemical and Elemental Stoichiometry in the Freshwater Diatom Stephanodiscus Minutulus,” *Journal of Phycology,* vol. 36, no. 3, 2003.

[64] M. J. Zarrinmehr, O. Farhadian, F. P. Heyrati, J. Keramat, E. Koutra, M. Kornaros and E. Daneshvar, “Effect of nitrogen concentration on the growth rate and biochemical composition of the microalga, Isochrysis galbana,” *The Egyptian Journal of Aquatic Research,* vol. 46, no. 2, pp. 153-158, 2020.

[65] G. Markou, I. Chatzipavlidis and D. Georgakakis, “Carbohydrates Production and Bio-flocculation Characteristics in Cultures of Arthrospira (Spirulina) platensis: Improvements Through Phosphorus Limitation Process,” *BioEnergy Research volume,* vol. 5, pp. 915-925, 2012.

[66] C.-F. Ji, X.-J. Yu, Z.-A. Chen, S. Xue, J. Legrand and W. Zhangad, “Effects of nutrient deprivation on biochemical compositions and photo-hydrogen production of Tetraselmis subcordiformis,” *International Journal of Hydrogen Energy,* vol. 36, no. 10, pp. 5817-5821, 2011.

[67] A. P. Dean, B. Estrada, J. M. Nicholson and D. C. Sigee, “Molecular response of Anabaena flos-aquae to differing concentrations of phosphorus: A combined Fourier transform infrared and X-ray microanalytical study,” *Phycological Research,* vol. 56, no. 3, 2008.

[68] C. Yeesang and B. Cheirsilp, “Effect of nitrogen, salt, and iron content in the growth medium and light intensity on lipid production by microalgae isolated from freshwater sources in Thailand,” *Bioresource Technology,* vol. 102, no. 3, pp. 3034-3040, 2011.

[69] M. Zaparoli, F. G. Ziemniczak, L. Mantovani, J. A. V. Costa and L. M. Colla, “Cellular Stress Conditions as a Strategy to Increase Carbohydrate Productivity in Spirulina platensis,” *BioEnergy Research,* vol. 13, pp. 1221-1234, 2020.

[70] M. Takagi, Karseno and T. Yoshida, “Effect of salt concentration on intracellular accumulation of lipids and triacylglyceride in marine microalgae Dunaliella cells,” *Journal of Bioscience and Bioengineering,* vol. 101, no. 3, pp. 223-226, 2006.

[71] N. Chandra, P. Shukla and N. Mallick, “Role of cultural variables in augmenting carbohydrate accumulation in the green microalga Scenedesmus acuminatus for bioethanol production,” *Biocatalysis and Agricultural Biotechnology,* vol. 26, 2020.

[72] H. Singh, J. L. Varanasi, S. Banerjee and D. Das, “Production of carbohydrate enrich microalgal biomass as a bioenergy feedstock,” *Energy,* vol. 188, 2019.

[73] K. A. Canon-Rubio, C. E. Sharp, J. Bergerson, M. Strous and H. D. I. H. Siegler, “Use of highly alkaline conditions to improve cost-effectiveness of algal biotechnology,” *Applied Microbiology and Biotechnology volume,* vol. 100, pp. 1611-1622, 2016.

[74] E. Touloupakis, B. Cicchi, A. M. S. Benavides and G. Torzillo, “Effect of high pH on growth of Synechocystis sp. PCC 6803 cultures and their contamination by golden algae (Poterioochromonas sp.),” *Appl Microbiol Biotechnol,* vol. 100, no. 3, pp. 1333-1341, 2016.

[75] Y. Guo, S. Wang, D. Xu, Y. Gong, H. Ma and X. Y. Tang, “Review of catalytic supercritical water gasification for hydrogen production from biomass,” *Renewable and Sustainable Energy Reviews,* vol. 14, no. 1, pp. 334-342, 2010.

[76] P. A. Marrone and G. T. Hong, “Corrosion control methods in supercritical water oxidation and gasification processes,” *The Journal of Supercritical Fluids,* vol. 51, no. 2, pp. 83-103, 2009.

[77] O. Yakaboylu, J. Harinck, K. G. Smit and W. de Jong, “Supercritical Water Gasification of Biomass: A Detailed Process Modeling Analysis for a Microalgae Gasification Process,” *Industrial and Engineering Chemistry Research,* vol. 54, no. 21, pp. 5550-5562, May 2015.

[78] A. Nurdiawati, I. N. Zaini, A. R. Irhamna, D. Sasongkod and M. Aziz, “Novel configuration of supercritical water gasification and chemical looping for highly-efficient hydrogen production from microalgae,” *Renewable and Sustainable Energy Reviews,* vol. 112, pp. 369-381, 2019.

[79] F. J. G. Ortiz, “Techno-economic assessment of supercritical processes for biofuel production,” *The Journal of Superitical Fluids ,* vol. 160, 2020.

[80] S. N. Reddy, S. Nanda, A. K. Dalai and J. A. Kozinski, “Supercritical water gasification of biomass for hydrogen production,” *International Journal of Hydrogen Energy,* vol. 39, no. 13, pp. 6912-6926, April 2014.

[81] G. Peng, “Methane Production from Microalgae via Continuous Catalystic Super Crtical Water Gasification: Development of Catalysts and Sulfur removal Technques,” Lausanne, 2015.

[82] H. Schmieder, J. Abeln, N. Boukis, E. Dinjus, A. Kruse, M. Kluth, G. Petrich, E. Sadri and M. Schacht, “Hydrothermal gasification of biomass and organic wastes,” *The Journal of Supercritical Fluids,* vol. 17, no. 2, pp. 145-153, April 2000.

[83] S. Nanda, S. N. Reddy, H. N. Hunter, A. K. Dalai and J. A. Kozinski, “Supercritical water gasification of fructose as a model compound for waste fruits and vegetables,” *The Jounal of Supercritical fluids,* vol. 104, pp. 112-121, September 2015.

[84] D. S. Gökkaya, M. Sağlam, M. Yüksel, T. G. Madenoğlu and L. Ballice, “Characterization of products evolved from supercritical water gasification of xylose (principal sugar in hemicellulose),” *Energy Sources, Part A: Recovery, Utilization, and Environmental Effects,* vol. 38, no. 11, pp. 1503-1511, 2016.

[85] M. B. García-Jarana, J. R. Portela, J. Sánchez-Oneto, E. J. M. d. l. Ossa and B. A.-D. 2, “Analysis of the Supercritical Water Gasification of Cellulose in a Continous System Using Short Residence times,” *Applied Sciences,* vol. 10, no. 15, p. 5185, 2020.

[86] l. J. Sheikhdavoodi, M. Almassi, M. Ebrahimi-Nik, A. Kruse and H. Bahrami, “Gasification of sugarcane bagasse in supercritical water; evaluation of alkali catalysts for maximum hydrogen production,” *Journal of the Energy Institute,* vol. 88, no. 4, pp. 450-458, November 2015.

[87] S. Elsayed, N. Boukis, D. Patzelt, S. Hindersin, M. Kerner and J. Sauer, “Gasification of Microalgae Using Supercritical Water and the Potential of Effluent Recycling,” *Chemical Engineering & Technology,* vol. 38, no. 2, November 2015.

[88] Y. Che, L. Yi, W. Wei, H. Jin and L. Guo, “Hydrogen production by sewage sludge gasification in supercritical water with high heating rate batch reactor,” *Energy,* vol. 238, no. A, 2022.

[89] M. Gong, S. Nanda, M. J. Romero, W. Zhu and J. A. Kozinski, “Subcritical and supercritical water gasification of humic acid as a model compound of humic substances in sewage sludge,” *The Journal of Supercritical Fluids,* vol. 119, pp. 130-138, 2017.

[90] T. Samanmulya, S. Inoue, T. Inoue, Y. Kawai, H. Kubota, H. Munetsuna, T. Noguchi and Y. Matsumura, “asification Characteristics of Alanine in Supercritical Water,” *Journal of the Japan Petroleum Institute,* vol. 57, no. 5, pp. 225-229, 2014.

[91] A. Sinag, A. Kruse and J. Rathert, “Influence of the Heating Rate and the Type of Catalyst on the Formation of Key Intermediates and on the Generation of Gases during Hydropyrolysis of

Glucose in Supercritical Water in a Batch Reactor," *Industrial and engineering chemistry research,* vol. 43, no. 2, pp. 502-508, 2004.

[92] D. Gokkaya, M. Saglam, M. Yuksel and L. Ballice, "Supercritical water gasification of phenol as a model for plant biomass," *The International Journey of Hydrogen Energy,* vol. 40, no. 34, pp. 11133-11139, Septemeber 2015.

[93] G. Caputo, P. Rubio, F. Scargiali, G. Marotta and A. Brucato, "Experimental and fluid dynamic study of continuous supercritical water gasification of glucose," *The Journal of Supercritical Fluids,* vol. 107, pp. 450-461, January 2016.

[94] B. R. Pinkard, D. J. .Gorman, K. Tiwari, E. G. Rasmussen, J. C. Kramlich, P. G. Reinhall and I. V. Novosselov, "Supercritical water gasification: practical design strategies and operational challenges for lab-scale, continuous flow reactors," *Helliyobn,* vol. 5, no. 2, 2019.

[95] J. Li, L. Pan, M. Suvarna and X. Wang, "Machine learning aided supercritical water gasification for H2-rich syngas production with process optimization and catalyst screening," *Chemical Engineering Journal,* vol. 426, 2021.

[96] S. Adamu, H. Binous, S. A. Razzak and M. M. Hossain, "Enhancement of glucose gasification by Ni/La2O3-Al2O3 towards the thermodynamic extremum at supercritical water conditions," *Renewable Energy,* vol. 111, pp. 399-409, October 2017.

[97] Y. Lu, S. Li, L. Guo and X. Zhang, "Hydrogen production by biomass gasification in supercritical water over Ni/γAl2O3 and Ni/CeO2-γAl2O3 catalysts," *International Journal of Hydrogen Energy,* vol. 35, no. 13, pp. 7161-7168, 2010.

[98] H. T. Nguyen, E. Yoda and M. Komiyama, "Catalytic supercritical water gasification of proteinaceous biomass: Catalyst performances in gasification of ethanol fermentation stillage

with batch and flow reactors," *Chemical Engineering Science,* vol. 109, pp. 197-203, April 2014.

[99] P. Azadi, S. Khan, F. Strobel, F. Azadi and R. Farnood, "Hydrogen production from cellulose, lignin, bark and model carbohydrates in supercritical water using nickel and ruthenium catalysts," *Applied Catalysis B: Environmental,* Vols. 117-118, pp. 330-338, May 2012.

[100] M. M. Hossain, "Production of H2 from Microalgae Biomass in Supercritical Water Using a Ni/La-γAl2O3 Catalyst," *Energy Procedia,* vol. 110, pp. 384-389, 2017.

[101] R. Samiee-Zafarghandi, J. Karimi-Sabet, M. A. Abdoli and A. Karbassi, "Supercritical water gasification of microalga *Chlorella PTCC* 6010 for hydrogen production: Box-Behnken optimization and evaluating catalytic effect of MnO2/SiO2 and NiO/SiO2," *Renewable Energy,* vol. 126, pp. 189-201, 2018.

[102] A. J. Byrd, S. Kumar, L. Kong, H. Ramsurn and R. B. Gupta, "Hydrogen production from catalytic gasification of switchgrass biocrude in supercritical water," *International Journal of Hydrogen Energy,* vol. 36, no. 5, pp. 3426-3433, March 2011.

[103] R. Samiee-Zafarghandi, A. Hadi and J. Karimi-Sabet, "Graphene-supported metal nanoparticles as novel catalysts for syngas production using supercritical water gasification of microalgae," *Biomass and Bioenergy,* vol. 121, pp. 13-21, 2019.

[104] T. Yoshida, Y. Oshima and Y. Matsumura, "Gasification of biomass model compounds and real biomass in supercritical water," *Biomass and Bioenergy,* vol. 26, no. 1, pp. 71-78, January 2004.

[105] O. Norouzi, F. Safari, S. Jafarian, A. Tavasoli and A. Karimi, "Hydrothermal gasification performance of Enteromorpha intestinalis as an algal biomass for hydrogen-rich gas

production using Ru promoted Fe–Ni/γ-Al2O3 nanocatalysts," *Energy Conversion and Management,* vol. 141, pp. 63-71, June 2017.

[106] S. Li, L. Guo, C. Zhu and Y. Lu, "Co-precipitated Ni–Mg–Al catalysts for hydrogen production by supercritical water gasification of glucose," *Interanl Journal of Hydrogen Energy,* vol. 38, no. 23, pp. 9688-9700, August 2013.

[107] A. G. Chakinala, D. W. F. Brilman, W. P. v. Swaaij and S. R. A. Kersten, "Catalytic and Non-catalytic Supercritical Water Gasification of Microalgae and Glycerol," *Industrial and Engineering Chemistry Research,* vol. 49, no. 3, pp. 1113-1122, Septemeber 2010.

[108] H. Zhang, W. Zhu, Z. Xu and M. Gong, "Gasification of cyanobacterial in supercritical water," *Environmental Technology,* vol. 35, no. 22, pp. 2788-2795, 2014.

[109] Daily Metal Prices, "Metal Spot Price Charts," 11 April 2023. [Online]. Available: https://www.dailymetalprice.com/. [Accessed 2023 April 12].

[110] L. Tiong and M. Komiyama, "Supercritical water gasification of microalga *Chlorella vulgaris* over supported Ru," *The Journal of Supercritical Fluids,* vol. 144, pp. 1-7, 2019.

[111] R. Cherad, J. Onwudili, U. Ekpo, P. Williams, A. R. Lea-Langton, M. Carmargo-Valero and A. Ross, "Macroalgae supercritical water gasification combined with nutrient recycling for microalgae cultivation," *Environmental Process and Sustainable energy,* pp. 186-185, 2013.

[112] S. Stucki, F. Vogel, C. Ludwig, A. G. Haiduc and M. Brandenberger, "Catalytic gasification of algae in supercritical water for biofuel production and carbon capture," *Energy and Environemntal Science,* vol. 2, pp. 535-541, 2009.

[113] M. Bagnoud-Velásquez, M. Brandenberger, F. Vogel and C. Ludwig, “Continuous catalytic hydrothermal gasification of algal biomass and case study on toxicity of aluminum as a step toward effluents recycling,” *Catalysis Today,* vol. 223, pp. 35-43, 2014.

[114] G. Peng, F. Vogel, D. Refardt and C. Ludwig, “Catalytic Supercritical Water Gasification: Continuous Methanization of *Chlorella vulgaris*,” *Industrial and Engineering Chemistry Research,* vol. 56, no. 21, pp. 6256-6265, 2017.

[115] J. B. Gadhe and R. B. Gupta, “Hydrogen production by methanol reforming in supercritical water: Catalysis by in-situ-generated copper nanoparticles,” *International Journal of Hydrogen Energy,* vol. 32, no. 13, pp. 2374-2381, 2007.

[116] M. Dreher, M. Steib, M. Nachtegaal, J. Wambach and F. Vogel, “On-Stream Regeneration of a Sulfur-Poisoned Ruthenium–Carbon Catalyst Under Hydrothermal Gasification Conditions,” *ChemCatChem,* vol. 6, no. 2, pp. 623-633, 2013.

[117] S. Kiatphuengporn, A. Junkaew, C. Luadthong, S. Thongratkaew, C. Yimsukanan, S. Songtawee, T. Butburee, o. Khemthong, S. Namuangruk, M. Kunaseth and K. Faungnawakij, “Roles of acidic sites in alumina catalysts for efficient d-xylose conversion to lactic acid,” *Green Chemistry,* vol. 22, no. 24, pp. 8572-8583, 2020.

[118] X. Xu, Y. Matsumura, J. Stenberg and M. J. Antal, “Carbon-Catalyzed Gasification of Organic Feedstocks in Supercritical Water,” *Industrial and Engineering Chemistry Research,* vol. 35, no. 8, pp. 2522-2530, 1996.

[119] M. Watanabe, H. Inomata and K. Arai, “Catalytic hydrogen generation from biomass (glucose and cellulose) with ZrO2 in supercritical water,” *Biomass and Bioenergy,* vol. 22, no. 5, pp. 405-410, 2002.

[120] D. Yu, M. Aihara and J. Michael Jerry Antal, “Hydrogen production by steam reforming glucose in supercritical water,” *Energy Fuels,* vol. 7, no. 5, pp. 574-577, Septemeber 1993.

[121] D. Castello, A. Kruse and L. Fiori, “Biomass gasification in supercritical and subcritical water: The effect of the reactor material,” *Chemical Engineering Journal,* vol. 228, pp. 535-544, July 2013.

[122] H. Tang and K. Kitagawa, “Supercritical water gasification of biomass: thermodynamic analysis with direct Gibbs free energy minimization,” *Chemical Engineering Journal,* vol. 106, no. 3, pp. 261-267, 2005.

[123] A. Kruse, “Supercritical water gasification,” *Biofuels, Bioproducts and Biorefining,* vol. 2, no. 5, pp. 415-437, 2008.

[124] A. C. D. Freitas and R. Guirardello, “Thermodynamic Analysis of Supercritical Water Gasification of Microalgae Biomass for Hydrogen and Syngas Production,” *Chemical Engineering Transaction,* vol. 32, 2013.

[125] C. Yang, S. Wang, Y. Li, Y. Zhang and C. Cui, “Thermodynamic analysis of hydrogen production via supercritical water gasification of coal, sewage sludge, microalga, and sawdust,” *International Journal of Hydrogen Energy,* vol. 46, no. 34, pp. 18042-18050, 2021.

[126] J. Gomes, J. Mitoura and R. Guirardello, “Thermodynamic analysis for hydrogen production from the reaction of subcritical and supercritical gasification of the C. Vulgaris microalgae,” *Energy,* vol. 260, 2022.

[127] C. S. Lee, A. V. Conradie and E. Lester, “Review of supercritical water gasification with lignocellulosic real biomass as the feedstocks: Process parameters, biomass composition, catalyst development, reactor design and its challenges,” *Chemical Engineering Journal,* vol. 415, 2021.

[128] A. Kruse and N. Dahmen, “Water – A magic solvent for biomass conversion,” *The Journal of Supercritical Fluids,* vol. 96, pp. 36-45, January 2015.

[129] Q. Guan, C. Wei and P. E. Savage, “Hydrothermal Gasification of Nannochloropsis sp. with Ru/C,” *Energy Fuels,* vol. 26, no. 7, pp. 4575-4582, 2012.

[130] D. Vandamme, S. Cláudia, V. Pontes, K. Goiris, I. Fouber, L. Jozef, J. Pinoy and K. Muylaert, “Evaluation of electro-coagulation–flocculation for harvesting marine and freshwater microalgae,” *Biotechnology and Bioengineering,* vol. 108, no. 10, May 2011.

[131] A. Miller, D. Hendry, N. Wilkinson, C. Venkitasamy and W. Jacoby, “Exploration of the gasification of Spirulina algae in supercritical water,” *Bioresource Technology,* vol. 119, pp. 41-47, 2012.

[132] Y. J. Lu, L. J. Guo, C. M. Ji, X. M. Zhang, X. H. Hao and Q. H. Yan, “Hydrogen production by biomass gasification in supercritical water: A parametric study,” *International Journal of Hydrogen Energy,* vol. 31, no. 7, pp. 822-831, 2006.

[133] Y. Lu, L. Guo, X. Zhang and C. Ji, “Hydrogen production by supercritical water gasification of biomass: Explore the way to maximum hydrogen yield and high carbon gasification efficiency,” *International Journal of Hydrogen Energy,* vol. 37, no. 4, pp. 3177-3185, 2012.

[134] Y. Matsumura, T. Minowa, B. Potic, S. R. A. Kersten, W. Prins, W. P. M. v. Swaaij, B. v. d. Beld, D. C. Elliott, G. G. Neuenschwander, A. Kruse and M. J. A. Jr., “Biomass gasification in near- and super-critical water: Status and prospects,” *Biomass and Bioenergy,* vol. 29, no. 4, pp. 269-292, 2005.

[135] L. Tiong and M. Komiyama, “Statistical analysis of microalgae supercritical water gasification: Reaction variables, catalysis and reaction pathways,” *The Journal of Supercritical Fluids,* vol. 183, 2022.

[136] M. Aziz, “Integrated hydrogen production and power generation from microalgae,” *International Journal of Hydrogen Energy,* vol. 41, no. 1, pp. 104-112, 2016.

[137] A. Onigbajumo, A. Taghipour, J. Ramirez, G. Will, T.-C. Ong, S. Couperthwaite, T. Steinberg and T. Rainey, “Techno-economic assessment of solar thermal and alternative energy integration in supercritical water gasification of microalgae,” *Energy Conversion and Management,* vol. 230, 2021.

[138] J. Woods, A. Williams, J. K. Hughes, M. Black and R. Murphy, “Energy and the food system,” *Phillosophical Transactions B,* vol. 27, no. 365, pp. 2991-3006, 2010.

[139] K. Ashley, D. Cordell and D. Mavinin, “A brief history of phosphorus: From the philosopher’s stone to nutrient recovery and reuse,” *Chemosphere,* vol. 84, no. 6, pp. 737-746, 2011.

[140] D. J. Patzelt, S. Hindersin, S. Elsayed, N. Boukis, M. Kerner and D. Hanelt, “Hydrothermal gasification of Acutodesmus obliquus for renewable energy production and nutrient recycling of microalgal mass cultures,” *Journal of Applied Phycology,* vol. 27, pp. 2239-2250, Decemeber 2014.

[141] A. Larasati, G. D. Fowler and N. J. D. Graham, “Chemical regeneration of granular activated carbon: preliminary evaluation of alternative regenerant solutions,” *Environ. Sci.: Water Res. Technol.,* vol. 6, pp. 2043-2056, 2020.

[142] M. Brandenberger, S. Suquet, F. Vogel, R. Bernier-Latman and C. Ludwig, “SunCHem: an integrated process for the hydrothermal production of methane from microalgae and CO2 mitigation,” *Journal of Applied Phycology,* vol. 21, pp. 529-541, 2009.

[143] M. Luo, Y. Yi, S. Wang, Z. Wang, M. Du, J. Pan and Q. Wang, “Review of hydrogen production using chemical-looping technology,” *Renewable and Sustainable Energy Reviews,* vol. 81, no. 2, pp. 3186-3214, 2018.

[144] A. Rahbari, A. Shirazi, M. B. Venkataraman and J. Pye, “A solar fuel plant via supercritical water gasification integrated with Fischer–Tropsch synthesis: Steady-state modelling and techno-economic assessment,” *Energy Conversion and Management,* vol. 184, pp. 636-648, 2019.

[145] M. B. Venkataraman, A. Rahbari, P. v. Eyk, A. W. Weimer, W. Lipiński and J. Pye, “Liquid fuel production via supercritical water gasification of algae: a role for solar heat integration?,” *Sustainable Energy and Fuels,* vol. 5, no. 24, pp. 6269-6297, 2021.

[146] A. T. Wijayanta and M. Aziz, “Ammonia production from algae via integrated hydrothermal gasification, chemical looping, N2 production, and NH3 synthesis,” *Energy,* vol. 174, pp. 331-338, 2019.

[147] P. A. Marrone, “Supercritical water oxidation—Current status of full-scale commercial activity for waste destruction,” *The Journal of Supercritical Fluids,* vol. 79, pp. 283-288, July 2013.

[148] T. Adschiri, Y.-W. Lee, M. Goto and S. Takami, “Green materials synthesis with supercritical water,” *Green Chemistry,* vol. 13, no. 6, pp. 1380-1390, May 2011.

[149] T. Rogalinski, K. Liu, T. Albrecht and G. Brunner, “Hydrolysis kinetics of biopolymers in subcritical water,” *Tim Rogalinski, Kaiyue Liu, Tobias Albrecht, Gerd Brunner,* vol. 46, no. 3, pp. 335-341, 2008.

[150] O. Norouzi, F. Safari, S. Jafarian, A. Tavasoli and A. Karimi, “Hydrothermal gasification performance of Enteromorpha intestinalis as an algal biomass for hydrogen-rich gas production using Ru promoted Fe–Ni/γ-Al2O3 nanocatalysts,” *Energy Conversion and management,* vol. 141, pp. 63-71, 2017.

2.2 ADDITIONAL LITERATURE

As the literature review presented above was originally accepted for publication in August 2023, additional literature has been published or has come to the author's attention. Hence, this section of the thesis aims to summarise these additional works and how they correlate to the original conclusions.

2.2.1 Influence of Biomass Composition

Further studies have been performed to further understand the influence of different components of biomass on SCWG. Khandelwal et al [1], studied the SCWG of glycerol and oleic acid, both known intermediate products in lipid SCWG, observing a significantly reduced gas yield in the fatty acid compared to glycerol or methanol. They claimed that reforming of fatty acids into cyclic ketones and aromatics occurred, as outlined in Section 2.1.2.2.3 of the main literature review, are known to limit gas yield and favour polymerisation reactions, explaining the reduction in gas yield observed. Analysis of the SCWG of canola wastes [2] revealed that the high protein meal had a reduced yield compared to straw and hull. This provides further evidence of the negative influence of protein outlined in Section 2.1.3.1.1 of the main literature review. Additionally, analysis of the SCWG various woody and grassy biomasses found no significant difference in yield, despite clear visual differences [3]. However, no analysis of the composition was performed, emphasising the importance of such analysis when comparing SCWG feedstocks.

2.2.2 Catalysts

Further evidence has been provided for the effectiveness of nickel catalysts at increasing the hydrogen yield for the SCWG of biomass (canola straw [4] and oily sludge [5]), with both showing the influence of support material on the reaction. Khandelwal et al. [4] investigated a series of oxide and carbon-based supports and their influence on the SCWG reaction. They found oxide catalysts ZrO_2 and Al_2O_3 outperformed activated carbon and carbon nanotubes, attributed to greater support-catalyst interaction which ensured thermal stability. They also noted that acidic catalyst supports

supress the WGS reaction, as was noted in other literature [6], so should be considered in selection of supports for hydrogen production. The main literature survey noted that activated carbon supports were advantageous for breaking down proteins [7], however canola straw has minimal protein content, so this impact is not observed. This shows that consideration of the feedstock should be included in support selection.

The literature review presented above outlines $FeCl_3$ as a catalyst of high potential but with limited literature available. However, since publication additional literature on other Lewis acid metal chlorides has been discovered. $CaCl_2$, $ZnCl_2$, $FeCl_3$, $CuCl_2$, $NiCl_2$, $AlCl_3$ were all found effective at increasing hydrogen yield in sewage sludge and its model compounds [8] [9] [10]. $AlCl_3$ was also found to be effective on the macroalga *Enteromorpha prolifera* [11], which contains a high carbohydrate, low protein and low lipid content. This was attributed to the enhanced ring opening and C-C bond opening caused by the Lewis acid and metal ions. This provides further evidence of the potential of Lewis acid catalysts. However, there is still no literature utilising them in a continuous process or on high protein feedstocks such as many microalgae.

2.2.3 Recovery of Inorganic Nutrients

As mentioned in Section 2.1.4.1 of the main literature review, recovery of nutrients is key advantage of SCWG and key to ensuring cost effective operation. Further analysis has since been made on how the inorganic proportions behave in SCWG and how to improve their recovery. Nitrogen salts is known to largely remain in the liquid phase in SCWG [12] but is often bound to organic compounds making it hard to recover. Gong et al. [13] assessed the influence of $CuSO_4$ on nitrogen dispersion in SCWG of cyanobacteria. They observed that $CuSO_4$ suppressed Maillard reactions and promoted deamidation, reducing the nitrogen in the liquid organic carbon, increasing it in the char and aqueous phases. This will increase the recyclability of the nitrogen and as stated in Section 2.1.2.2 of the main literature review, Maillard reaction products are stable and reduce gasification. Thus, this could also help improve gas yields, although the influence on gas yield was not assessed in this study.

In contrary to Nitrogen, phosphorous typically remains in the solid phase bound to the char in SCWG [12], making them more difficult to recover. Wang et al. [14], found that in the SCWG of cyanobacteria, hydroxides increase the phosphorous that remains in the liquid phase from 11% up to in 78%, reducing processing steps for nutrient recovery. Therefore, the use of hydroxide catalysts can increase nutrient recyclability in addition to hydrogen yields. Another advantage of hydrothermal processing, such as SCWG, is the immobilisation of heavy metals in the biochar produced [15] [16]. This allows for recirculation of the aqueous phase, even if the algae are used for bioremediation of water streams [17], without resulting in accumulation that can eventually kill the algae.

2.2.4 SCWG Reaction Models

Machine learning (ML) algorithms have been utilised to predict the gas yields of the SCWG reaction. Khandelwal et al. [18] tested 8 different ML models to predict the SCWG of lignocellulosic biomass and Azadvar et al. [19] tested 4 ML models to predict SCWG of a wider range of feedstocks included algae, food wastes and plastics. Additionally, Santos et al. [20] used linear regression to improve equilibrium calculations of microalgal SCWG without the need for more complex equations of state. They considered influence of reaction conditions and feedstock characteristics to achieve this, although they did not consider the carbohydrate, protein, lipid or lignin contents, which were key factors outlined in the main body of the literature review.

All three studies found temperature to be the most significant factor, with biomass concentration also significant, a high temperature and low biomass concentration favouring hydrogen yield. Pressure was found to be much less significant, being disregarded entirely in the two larger models [18, 19]. This aligns with the work displayed in Sections 2.1.3.3 – 2.1.3.6 of the main literature review. The influence of the ultimate analysis was also studied in these studies, which was not considered in the initial literature review. Both studies also found that a larger hydrogen and lower carbon content in the feedstock was preferable for hydrogen production [18, 19]. This could be attributed to certain components of the biomass, such as aromatic compounds, which have a lower H/C ratio and are known to be difficult to gasify in SCW.

2.2.5 SCWG System Models

In addition to those outlined in Section 2.1.4.2 in the main literature review, new integrated systems have been developed for the SCWG of biomass. Hu et al [21] and Qi et al [22] investigated an integrated system to produce both hydrogen from sewage sludge and organic waste waters respectively. The latter included an evaporation unit to concentrate the feedstock and increase the overall efficiency from 0.8% to 44.88%. Both found that increasing the concentration of feedstock increased the efficiency of the process, contrary to experimental studies, due to the lower pumping power and heating requirement. Liu et al [23] developed an integrated model for power production from SCWG, using a ML algorithm to predict what the produced power will be per given inputs. This found that a high temperature (up to 750°C) and, as with other models, a high biomass concentration was desirable. However, all models refer to equilibrium calculations and don't consider char formation, which can be significant at high concentrations [24], so could be limitations of these models.

2.3 FURTHER DISCUSSION

It is clear from literature that temperature and biomass concentration are key operating conditions that should be considered when analysing SCWG processes. Therefore, for this work, temperature and pressure will also be included as variable when analysing other impacts, such as catalysts. The influence of pressure is known to be far less significant than other operating conditions but high pressures will increase the cost of materials and pumping requirements. Thus, in this work pressures close to the critical point (23 - 25Mpa) were utilised and not considered as variable of interest. Literature shows that reaction time increases gas yields and hydrogen content, often reaching a plateau after a certain length of time. Therefore, it is desirable to have the longest reaction time possible, unless the plateau is reached at all conditions. Consequently, to simplify analysis, it was deemed suitable to set a residence time in this work. The reactor will be designed to maximise reaction time, and tests performed to assess whether a plateau in hydrogen yield or conversion could be observed.

Catalysts are also a key component that influence SCWG outlined in the literature review. Alkali metal salts and transition metals, especially nickel and ruthenium, were the most common and largely the most effective catalysts in the literature. Therefore, it is important to consider a comparison to these catalyst types when suggesting new catalysts or processes. An emerging catalyst type is Lewis acid metal chlorides, which outperformed the more traditional catalysts in some cases. Despite this, literature on these catalysts is rare and none to this author's knowledge is available on microalgae or continuous systems. As a result, investigation into these catalysts is included in this work.

Other factors that were significant in the literature review could not be included in this work. Obtaining microalgal strains of varying composition is greatly difficult without the capacities of a significant algal growth facilities. *Chlorella vulgaris* was chosen to study as its high growth rate and durability make it an easily scalable strain that can be obtained in large quantities with ease. Heating rate could not be considered as, in a continuous system, this would include additional heating apparatus outside of the existing set-up that is not feasible. It is also notable that deionised or distilled water was often utilised as the reaction media in the literature. This is not representative of a real system where, after algal growth, significant quantities of ions will still be present in the water. The impact of this water should be analysed to determine its significance.

2.4 ADDITIONAL REFERENCES

These refer to the references in the additional literature subsection, not the published work presented.

[1] K. Khandelwal, P. Boahene, S. Nanda and A. K. Dalai, “Hydrogen Production from Supercritical Water Gasification of Model Compounds of Crude Glycerol from Biodiesel Industries,” *Energies*, vol. 16, no. 9, 2023 doi:10.3390/en16093746.

[2] K. Khandelwal, S. Nanda, P. Boahene and A. K. Dalai, “Hydrogen production from supercritical water gasification of canola residues,” *Int. J. of Hydrogen Energy*, vol. 49, 2024 doi:10.1016/j.ijhydene.2023.10.228.

[3] J. Dutzi, I. K. Stoll, N. Boukis and J. Sauer, “Screening of ten different plants in the process of supercritical water gasification,” *Sus. Chem. for the Environ.*, vol. 5, 2024 doi:10.1016/j.scenv.2024.100062.

[4] K. Khandelwal and A. K. Dalai, “Catalytic Supercritical Water Gasification of Canola Straw with Promoted and Supported Nickel-Based Catalysts*,” Molecules*, vol. 29, no. 4, p. 911, 2024 doi: 10.3390/molecules29040911.

[5] A. Zandifar, F. Esmaeilzadeh and J. Rodríguez-Mirasol, “Hydrogen-rich gas production via supercritical water gasification (SCWG) of oily sludge over waste tire-derived activated carbon impregnated with Ni: Characterization and optimization of activated carbon production*,” Environ. Pollut.*, vol. 342, 2024. doi: 10.1016/j.envpol.2023.123078

[6] Y. Lu, H. Jin and R. Zhang, “Evaluation of stability and catalytic activity of Ni catalysts for hydrogen production by biomass gasification in supercritical water,” *Carbon Res. Conv*., vol. 2, no. 1, pp. 95-101, 2019.doi:10.1016/j.crcon.2019.03.001

[7] I.-G. Lee, A. Nowacka, C.-H. Yuan, S.-J. Park and J.-B. Yang, “Hydrogen production by supercritical water gasification of valine over Ni/activated charcoal catalyst modified with Y, Pt, and Pd,” *Int, J. of Hydrogen Energy*, vol. 40, no. 36, pp. 12078-12087, September 2015. doi: 10.1016/j.ijhydene.2015.07.112

[8] M. Gong, S. Nanda, H. N. Hunter, W. Zhu, A. K. Dalai and J. A. Kozinski, “Lewis acid catalyzed gasification of humic acid in supercritical water,” *Catal Today*, vol. 291, pp. 13-23, 2017. doi:10.1016/j.cattod.2017.02.017

[9] Z. Li, M. Gong, M. Wang, A. Feng, L. Wang, P. Ma and S. Yuan, “Influence of AlCl3 and oxidant catalysts on hydrogen production from the supercritical water gasification of dewatered sewage sludge and model compounds,” *Int. J. of Hydrog. Energ*y, vol. 46, no. 61, pp. 31262-31274, 2021 doi:10.1016/j.ijhydene.2021.07.028.

[10] M. Gong, Z. Li, M. Wang, A. Feng, L. Wang and S. Yuan, “Effects of Lewis acid on catalyzing gasification of sewage sludge and model compounds in supercritical water,” *Int. J. of Hydrog. Energ*y, vol. 46, no. 13, pp. 9008-9018, 2021 doi:10.1016/j.ijhydene.2020.12.207.

[11] M. Gong, J. Hu, Q. Xu and Y. Fan, “Catalytic gasification of Enteromorpha prolifera for hydrogen production in supercritical water,” *Process Saf. and Environ. Prot*., vol. 175, pp. 227-237, 2023. doi: 10.1016/j.psep.2023.05.027

[12] M. Yan, J. Cui, T. Li, H. Feng, D. Hantoko and E. Kanchanatip, “Transformation and distribution of nitrogen and phosphorus in sewage sludge during supercritical water gasification,” *Fuel*, vol. 332, no. 1, 2023 doi:10.1016/j.fuel.2022.125918.

[13] M. Gong, S. Wang, J. Hu and Y. Fan, “Effect of CuSO4 on the behavior of nitrogen during supercritical water gasification of microalgal biomass*,” J. of Environ. Chem. Eng*., vol. 12, no. 5, 2024 doi:10.1016/j.jece.2024.113737.

[14] C. Wang, X. Ling, C. Wu, C. He, B. Gui and W. Sun, “Evolution of phosphorus with the promotion of KOH in supercritical water gasification of dewatered cyanobacteria from ion perspective,” C*hemosphere*, vol. 327, 327 doi:10.1016/j.chemosphere.2023.138466.

[15] D. M. Paniagua, L. M. M. Krenz, J. A. Libra, N. Korf and V. S. Rotter, “Towards a high-quality fertilizer based on algae residues treated via hydrothermal carbonization. Trends on how process parameters influence inorganics,” *Biochar*, vol. 6, 2024 doi:10.1007/s42773-024-00357-8.

[16] W. Su, M. Zhao, Y. Xing, H. Ma, P. Liu, X. Li, H. Zhang, Y. Wu and C. Xia, “Supercritical water gasification of hyperaccumulators for hydrogen production and heavy metal immobilization with alkali metal catalysts,” *Environ. Res*, vol. 214, 2022 doi:10.1016/j.envres.2022.114093.

[17] M. Chugh, L. Kumar, M. P. Shah and N. Bharadvaja, “Algal Bioremediation of heavy metals: An insight into removal mechanisms, recovery of by-products, challenges, and future opportunities,” *Energy Nexus*, vol. 7, 2022 doi:10.1016/j.nexus.2022.100129.

[18] K. Khandelwal and A. K. Dalai, “Prediction of Individual Gas Yields of Supercritical Water Gasification of Lignocellulosic Biomass by Machine Learning Models,” *Molecule*s, vol. 10, p. 29, 2024 doi:10.3390/molecules29102337.

[19] S. Azadvar and O. Tavakoli, “Data-driven interpretation, comparison and optimization of hydrogen production from supercritical water gasification of biomass and polymer waste: Applying ensemble and differential evolution in machine learning algorithms*,” Int. J. of Hydrog. Energy*, vol. 85, pp. 511-525, 2024 doi:10.1016/j.ijhydene.2024.08.081.

[20] J. S. J, Í. Zelioli, E. G. F, A. Freitas and A. Mariano, “Supercritical water gasification thermodynamic study and hybrid modeling of machine learning with the ideal gas model: Application to gasification of microalgae biomass,” *Energy*, vol. 291, 2024 doi:10.1016/j.energy.2024.130287.

[21] D. Hu, C. Ren, S. Zhang, M. Ma, Y. Chen, B. Chen and L. G. a, “Thermodynamic and environmental analysis of integrated supercritical water gasification of sewage sludge for power and hydrogen production,” *Energy*, vol. 299, 2024 doi:10.1016/j.energy.2024.131568.

[22] X. Qi, Z. Ren, F. Meng, L. Lu, F. Liu, X. Li, H. Jin, Y. Chen and L. Guo, “Thermodynamic and environmental analysis of an integrated multi-effect evaporation and organic wastewater supercritical water gasification system for hydrogen production,” *Appl. Energy*, vol. 357, 2024. doi: 10.1016/j.apenergy.2023.122449

[23] S. Liu, Y. Yang, L. Yu, Y. Cao, X. Liu, A. Yao and A. Yao, “Self-heating optimization of integrated system of supercritical water gasification of biomass for power generation using artificial neural network combined with process simulation,” *Energy*, vol. 272, 2023 doi:10.1016/j.energy.2023.127134.

[24] G. Caputo, M. Dispenza, P. Rubio, F. Scargiali, G. Marotta and A. Brucato, “Supercritical water gasification of microalgae and their constituents in a continuous reactor,” *The J. of Supercrit. Fluids*, vol. 118, pp. 163-170, December 2016 doi:10.1016/j.supflu.2016.08.007.

[25] I.-G. Lee, A. Nowacka, C.-H. Yuan, S.-J. Park and J.-B. Yang, “Hydrogen production by supercritical water gasification of valine over Ni/activated charcoal catalyst modified with Y, Pt, and Pd,” *Int. J. of Hydrog. Energy*, vol. 40, no. 36, pp. 12078-12087, September 2015 doi:10.1016/j.ijhydene.2015.07.112.

[26] H. Ge, L. Yi, Y. Huang, P. Peng, W. Cao, Y.-n. Chen and L. Guo, “Insight into the interconversion mechanisms during the supercritical water gasification of bark,” *Chem. Eng. J,*, vol. 468, 2023 doi:10.1016/j.cej.2023.143683.

CHAPTER 3: EXPERIMENTAL APPARATUS DESIGN, OPERATIONAL AND ANALYTICAL TECHNIQUES

3.1 MICROALGAL GROWTH

To provide a suitable feedstock for SCWG reactions, a significant quantity of microalgal biomass must be acquired. To achieve this, photobioreactors were set up to grow *Chlorella vulgaris* in the School of Biosciences at the University of Birmingham (UoB). This can supply microalgae at minimum cost, a live source of algae that could be used for future experiments and the algal growth water which was used as a reaction medium in SCWG experiments. This also helps increase understanding into the requirements of algal growth, such as light, nutrients and sources of carbon. However, the capacity of algal production available at UoB proved not to be sufficient to generate all the required biomass. Therefore, dried *Chlorella vulgaris* powder outsourced and utilized in experiments in chapter (5-6), while the grown algae were utilized in Chapter 4.

3.1.1 Photobioreactor Set-Up

3.1.1.1 Initial Experiments

To understand the requirements for algal growth and to solve any potentially unforeseen issues with the growth set up, a series of preliminary experiments were completed. This started with a 1.5l (1l working volume) photobioreactor (PBR) and moving on to a 5l (4l working volume) PBR. As a result, a number of features were incorporated into the PBR design which included: A pump system to automatically remove the culture and supply fresh media, saving significant time while keeping the system sterile and free from external contamination; ports to allow addition of other chemicals (in case of pH imbalance) without the need to expose the PBR to external contamination; a flowmeter to ensure a consistent flow was achieved between batches.

After the improved PBR design was constructed, an initial experiment was conducted to increase the concentration of algae and establish a suitable batch time was carried out. 2 parallel PBR systems (PBR1 and PBR2) were set-up with each being inoculated with 40ml of an existing 0.55wt.% *Chlorella vulgaris* culture. Fresh medium was added after 7 days, to compensate for evaporation losses and nutrient uptake. Figure 3.1 shows a clear plateau in algal growth before the additional media was provided and then again after around 14 days of growth. Therefore, a growth period of 14 days, with additional media addition at 7 days was selected.

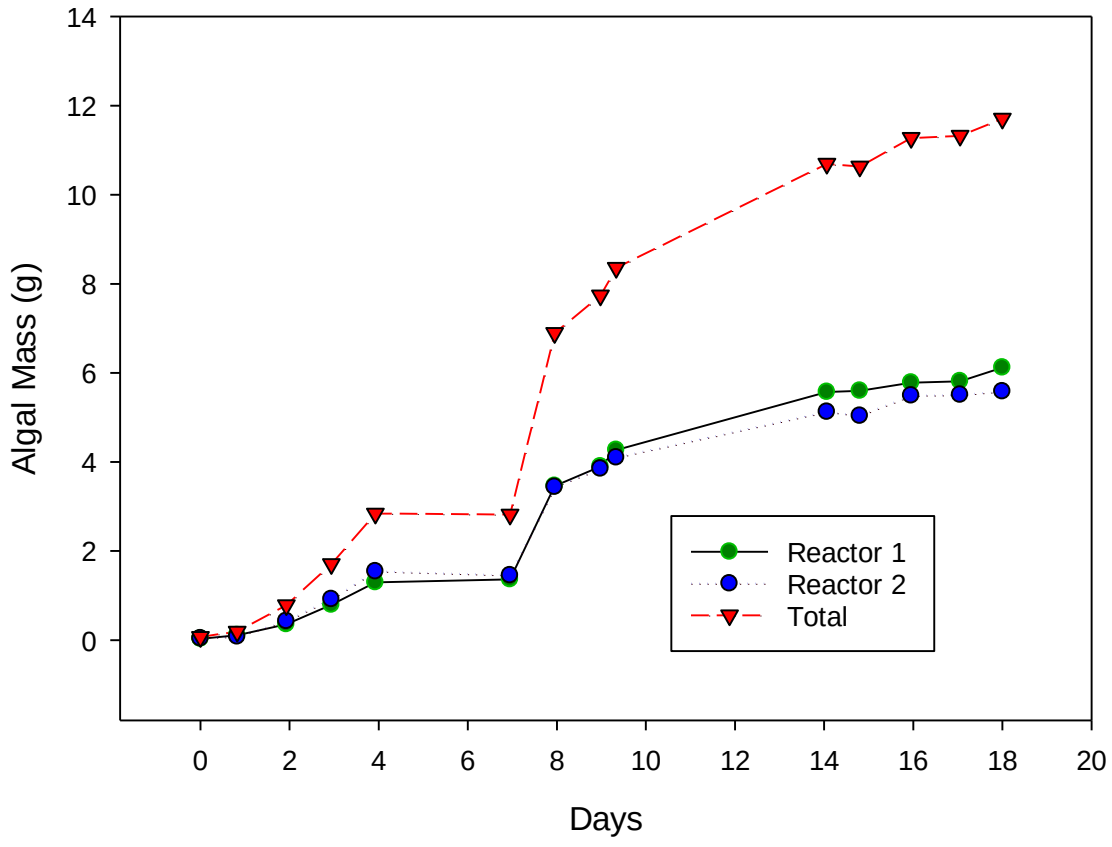

Figure 3.1- Initial algal growth experiment. Variation in dry algal mass of two 4L photobioreactors with medium addition after 7 days.

3.1.1.2 Finalised Reactor Set-up

Chlorella vulgaris was grown simultaneously in two 5L stirred tank vessels, with a working volume of 4L each and impeller speed of 3000rpm. Air (~.04 % CO_2) was filtered through 0.2-micron filters to prevent contamination, before being fed through spargers at the bottom of each vessel at a flowrate of 4L/minute for the two vessels. The PBRs were illuminated with two panels of white LED

lights at a power consumption of 0.81W. To maximise illumination the reactors were surrounded by foil panels, resulting in an illumination on the outside wall of the reactors of 25W m^{-2}. The growth medium used was Chu-13, which was prepared to the concentrations in Table 3.1, adjusted to a pH of 7.5 using 2M sodium hydroxide and sterilised in an autoclave for 20minutes at 121°C.

Table 3.1-Composition of Chu-13 growth medium

Compound	Concentration (mg/l)
Potassium nitrate	400
Dipotassium hydrogen phosphate	80
Calcium chloride dihydrate	107
Magnesium sulphate heptahydrate	200
Ferric citrate	20
Citric acid	100
Cobalt chloride	0.02
Boric acid	5.72
Magnesium chloride tetrahydrate	3.62
Zinc sulphate heptahydrate	0.44
Copper sulphate pentahydrate	0.16
Sodium molybdate	0.084

The culture was grown in two-week cycles, fresh growth media being used increase the volume back to 4L, to account for evaporation losses, at the midpoint (7 days). At the conclusion of these cycles, the culture was emptied down to a remaining volume of 1.4L and 1.8L for PBR1 and PBR2 respectively. This was the maximum volume that can be extracted using the sampling port on the reactors. PBR products are combined and centrifuged at 5000rpm for 5minutes to form an algal pellet. This pellet was then resuspended in 175ml of sterile distilled water and the resulting algae was stored in at 4°C until required. The residual water produced during centrifugation was autoclaved at 120°C for 20 minutes, to kill any residual algae and bacteria. It was then stored in darkness at room temperature until required. Fresh media was then used to make the PBR volume up to 4L and the next cycle has begun. This process was repeated for 28 cycles, a total running time of 13 months. Before the first cycle the initial growth stage outlined in Section 3.1.1.1 was completed.

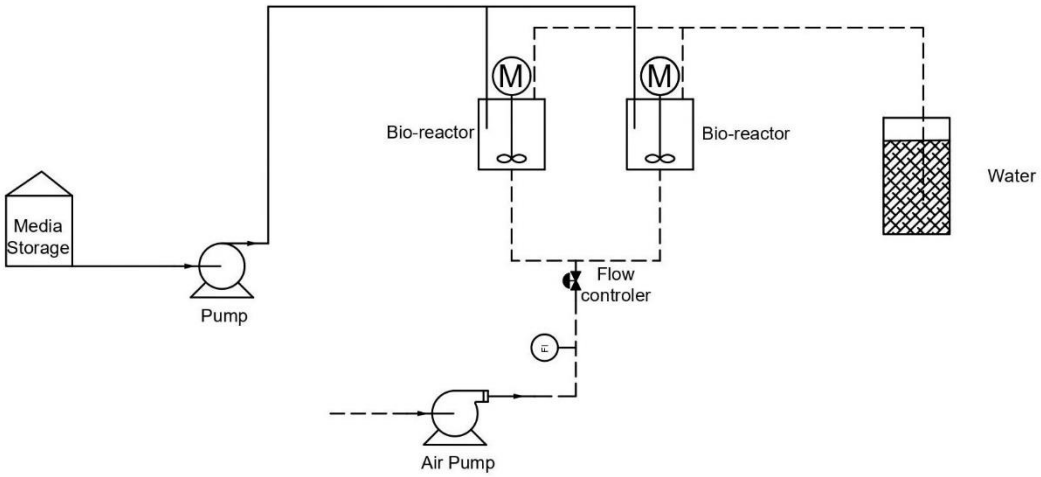

Figure 3.2-Photobioreactor set-up schematic diagram. Dotted line: air, solid line: media

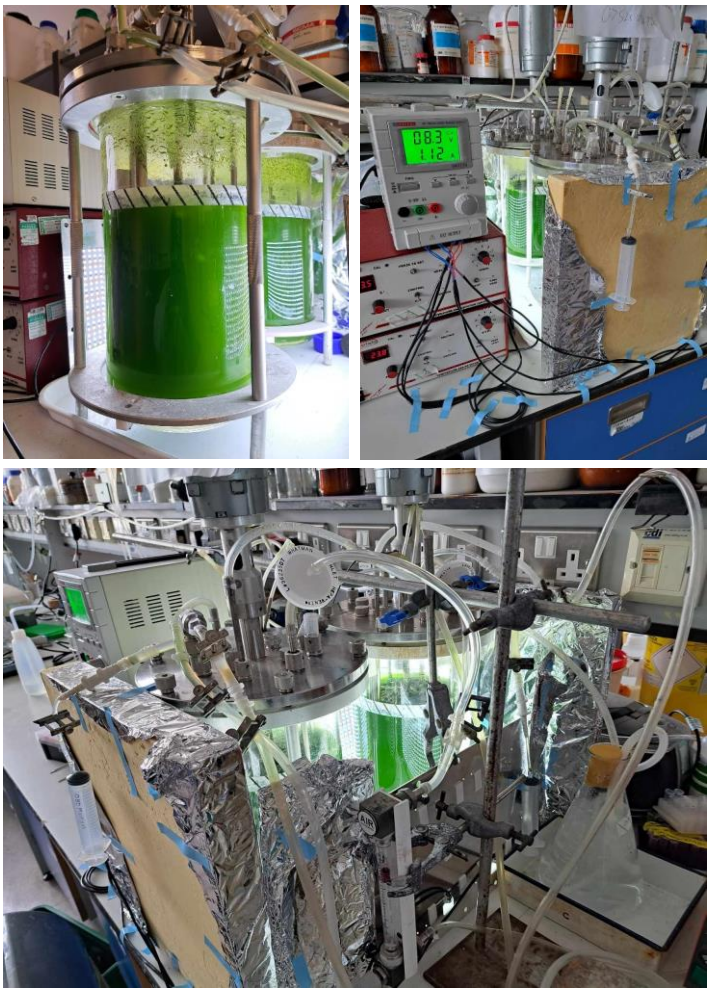

Figure 3-Images of photobioreactor set-up

3.1.2 Analysis Methods

3.1.2.1 Culture Monitoring

Monitoring culture conditions and growth are crucial to ensure that any issues are promptly identified and addressed, enabling optimal growth. Regular monitoring allows for the detection of deviations from the desired conditions, such as changes in temperature, pH, nutrient levels, light or contamination. This proactive approach is essential for maintaining the health and productivity of the culture.

3.1.2.1.1 Growth

To regularly and easily monitor the growth of *Chlorella vulgaris*, a correlation between culture density and an easily measurable factor was developed. Optical density (OD) is a commonly used factor, particularly for *Chlorella vulgaris*, where OD is typically measured at 680 nm [1]. This wavelength corresponds to red light, which is strongly absorbed by green algae like *Chlorella vulgaris*, making it a reliable indicator of biomass concentration. The Calibration Curve Process to establish a correlation between OD_{680} and actual biomass concentration was as follows:

1. Eight suspensions of *Chlorella vulgaris* were prepared, each with a known optical density ranging from 0 to 1 at OD_{680} nm.
2. Each solution was centrifuged at 5000 rpm for 5 minutes to produce an algal pellet, allowing the supernatant to be removed.
3. To remove any residual salts that could affect the dry weight measurement, 100 ml of de-ionized water was added to the algal pellet, and the cells were resuspended.
4. The suspension was centrifuged again under the same conditions, and the supernatant was discarded.

5. The washed algae pellet was transferred to pre-weighed containers by resuspension in deionised water. The samples were then dried at 80°C until no further weight loss was observed, ensuring that all moisture was removed, and only the dry biomass remained.

The resulting calibration, shown in Appendix A, yielded a correlation coefficient (R2) of 0.984, indicating OD_{680} is a reliable proxy for the biomass concentration of this alga. Thus, the resulting concentration of *Chlorella vulgaris* can be calculated by the following equation:

$$Algal\ Concentration\ \left(\frac{g}{l}\right) = 0.162 OD_{680} \quad (1)$$

Growth was measured at the start, the halfway point and the end of the two-week culture cycle by extracting 20ml from each reactor, diluting to a factor of 10 and measuring the optical density in triplicate in a photospectrometer.

3.1.2.1.2 pH and Temperature

The pH of the culture is an important variable as it can limit growth and alter the composition of the algae [2, 3], providing an inconsistent feedstock and increase growing time. Therefore, pH measurements were taken weekly. The pH remained within the range of 8-9.5 so no further action was required. Temperature is also known to impact growth and the composition of the algae [4]. The temperature should be maintained between 20-30°C to prevent growth inhibition [5]. Ideally, a smaller temperature range would be used to ensure a greater consistency but controlling that was difficult with the equipment available, so intervention would only be implemented in the most extreme cases.

3.1.2.2 Characterisation of Microalgae

As outlined in Chapter 2, the composition of the alga can have a significant impact on the SCWG reaction. Therefore, as the algae were grown in several batches, it is important to measure the carbohydrate, protein and lipid content to guarantee consistency between runs and to provide a comparison with similar experiments in literature. Methods were chosen and developed from literature based on limiting time and cost requirements.

3.1.2.2.1 Protein

The Lowry method for protein content analysis outlined by Frølund et al. [6] (adapted from the original method by Raunkjær et al. [7]) was chosen. This involves:

A. Reagent 1: Add 1ml of 57mM copper sulphate solution and 1ml of 124mM sodium tartrate to a 100ml solution of 143mM sodium hydroxide and 270mM sodium carbonate.
1. Reagent 2: Dilute 50ml of Folin's reagent with 60ml de-ionised water.
2. Mix 0.5ml of sample with 0.7ml of pre-prepared reagent 1 and 0.1ml of pre-prepared reagent.
3. Leave at room temperature for 45 minutes.
4. Measure absorption at 750nm in a photospectrometer.
5. Compare the results to known quantities of bovine serum albumin.

3.1.2.2.2 Carbohydrates

The Anthrone method for carbohydrate analysis outlined by Frølund et al. [6] (adapted from an original method by Gaudy [8].) was chosen. This involves:

1. Prepare reagent: 1.25g/l Anthrone in concentrated sulphuric acid.
2. Mix 0.8ml of sample with 1.6ml of pre-prepared reagent.
3. Heat for 14minutes at 100°C, then cooling for 5 minutes at 4°C.
4. Measure the absorbance at 625nm of the solution in a photospectrometer.
5. Compare the results with known quantities of glucose.

3.1.2.2.3 Lipid

To calculate the quantity of lipids, a colorimetric method comparable to the carbohydrate and protein analysis methods was attempted based on work by Mishra et al. [9]. However, unrealistic values of >100wt.% lipid were consistently observed at a range algal concentrations (1-30%), Reactant concentrations (1.2-2.4 g/l vanillin), reaction time (15-120 minutes) and heating methods (oven or heating block). The cause of this was unknown but could relate to interference of the other chemicals within the algae or growth media. Consequently, a gravimetric method was developed.

This method is based upon work by Axelsson and Gentili [10] with an additional sonication step used to break down the algal cell structure, which has been observed to be important in literature [11]. The involves:

1. Centrifuge a known amount of microalgal suspension at 5000rpm for 5 minutes.
2. Add 8ml of a 2:1 chloroform-methanol solution.
3. Place in an ultrasonic bath for 40 minutes at ambient temperatures and 33kHz.
4. Add 2ml of a 7.3g/l sodium chloride in water solution.
5. Return to the ultrasonic bath for 20 minutes.
6. Centrifuge at 350g for 5 minutes, then carefully remove the lower (chloroform and lipid) layer.
7. Pass it through a 2µm glass fibre filter under suction into a pre-weighed vessel. rinsing the filter with 8ml of chloroform to ensure all the lipid is captured.
8. Heat the remaining lipid at 60°C until all the liquid has been removed and place in a desiccator.
9. Once cooled, the vessel is weighed again to obtain the total lipid weight.

To ensure and quantify the accuracy of this method, a set of experiments were performed on model algae made up of its constituent parts. This was achieved by adding a known mass of a model lipid (rapeseed oil) to a mixture of 0.05g model carbohydrate (cellulose) and 0.05g model protein (peptone), which was then processed as outlined above. 13 repeats were completed in a range of 15-65% lipid fraction, the results of which can be found in Appendix B. The error across the whole

dataset had a standard deviation of 8%, meaning there's a 95% the result will fall within 16% of the correct answer. While this may be a significant error in some applications, it will be sufficient for analysing the consistency of the composition of microalgae in this work. It was also notable that this method can be heavily affected by certain aspects of the process such as the phase separation and influence of dust. Therefore, 3 repeats are necessary to be discount any anomalous results that may arise as a result.

3.1.2.3 Growth Water Analysis

As outlined in Chapter 2, the growth medium remaining after algal growth (GW) is likely to be the reaction medium in SCWG systems. Therefore, it is important to know the properties and salt composition of this medium. It is expected that the ions in the media will be those present in the Chu-13 medium at the start of the process (see Table 3.1), only with varying concentrations. A variety of different techniques were employed to ensure all of these ions were detected. Inductively Coupled Plasma Spectroscopy (ICP) used to measure single element ions (Ca^{2+},Co^{2+},Cu^{2+},$Fe^{2+/3+}$,Mg^{2+},Na^{+},Zn^{2+},K^{+}). Ion Chromatography (IC) was used to a measure anion (Cl^{-}, SO_4^{2-}, NO_3^{-},PO_4^{3-}) and some of the cations measured by ICP (Mg^{2+},Na^{+},K^{+}). This was achieved in-house with a Perkin Elmer Optima 8000 ICP-OES for ICP, Thermo Scientific Dionex ICS-200 for anion IC and Thermo Scientific Integrion and cation IC respectively. When an ion was covered by both methods, an average was taken. Molybdate could not be directly measured, so it was assumed that the entire molybdenum content was in the form of molybdate. Due to availability of the equipment, some samples were outsourced to ALS Laboratories (UK) Limited, who analysed the water using ICP and colorimetric techniques.

Centrifugation does not completely remove all of the solid material, thus there was still residual organic material in the GW. This would be gasified along with the main feedstock material so this must be included in any yield calculations during the SCWG experiments. This was calculated by measuring the total organic carbon (TOC), as outlined in Section 3.2.4.1.2. The pH was also measured for each sample.

3.1.3 Results of Algal Growth

3.1.3.1 Algae

The algae were grown in 28 two-week batches, with an average productivity of 0.046g $l^{-1}day^{-1}$. This resulted in each 2-week batch producing an average of 6g of microalgae (dry weight), with a standard deviation of 0.72g. Figure 3.4 shows the produced biomass, for each individual reactor and both combined. This shows a noticeably reduced growth in batches 7-14. Batches 7-14 correspond to summer 2022, where extreme weather resulted in higher temperatures in the reactor, often exceeding 28°C. At these temperatures, the mortality rate of *Chlorella vulgaris* was greatly increased [5], thus reducing the growth. As a result, these batches had a significant variation in growth from the others and were not utilized for within this work.

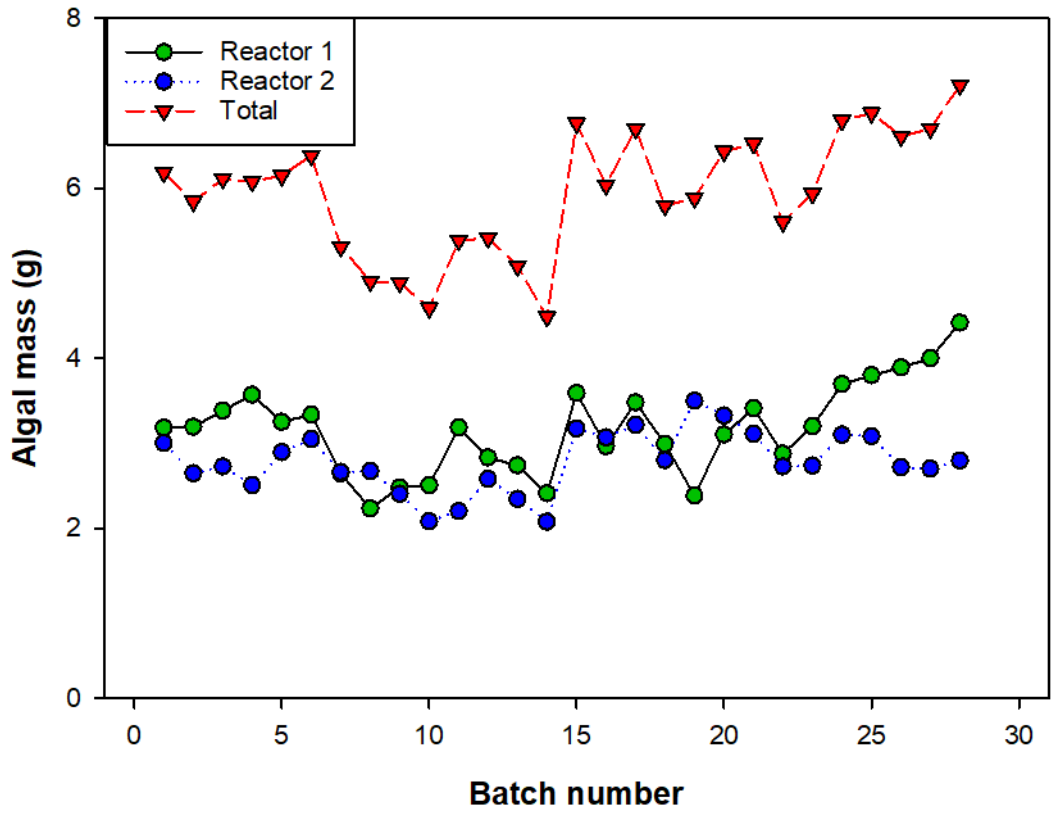

Figure 3.4-Algal mass produced for each 2-week batch growth of Chlorella vulgaris. Grown in two parallel 4L photobioreactors with Chu-13 growth media, a combined air flowrate of 4L and irradiation of 25W m^{-2}.

For use in SCWG experiments, it is imperative that the composition of the algae is consistent in every experiment. Therefore, to test how the composition varied between batches and during storage, 5 samples were characterised. The results, shown in Table 3.2, clearly outline that the composition significantly altered over time, with a reduction in carbohydrate and increase in protein content with longer storage times. A coefficient of variation (COE), defined as the ratio of standard deviation to the mean, of 27% and 16% in the protein and carbohydrate content respectively was observed. Fozer et al. [12] observed significant differences in gas yield with a respective 15% and 8% change in carbohydrate and protein content in the SCWG of *Chlorella vulgaris*. Thus, this difference cannot be assumed to be negligible.

As a result, batches must be combined and dried to make a single homogenous sample to be used in SCWG. However, a total of just 90g of dried biomass was produced across the entire operation of the PBR, which is insufficient for a full program of gasification experiments. Consequently, dried *Chlorella vulgaris* powder was purchased for the experimental program, the source and composition of which is outlined in each experimental chapter.

Table 3.2-Algae characterisation results.

Batch Number	Date of extraction	Days stored	Carbohydrate (wt.%)	Protein (wt.%)	Lipid (wt.%)
22	30/11/2022	0	25.72%	37.08%	37.19%
16	31/08/2022	91	20.49%	44.83%	34.68%
11	21/06/2022	149	19.35%	56.61%	24.03%
5	01/04/2022	230	12.75%	51.56%	35.70%
2	18/02/2022	285	15.35%	52.18%	32.47%

3.1.3.2 Growth Water

The growth water from 11 batches of algal growth were collected and analysed. Table 3.3 displays the pH, TOC and ion content of these batches. In some experiments in this thesis, an artificial growth water was produced, which contained ion concentrations and pH similar to that of the measured samples. This sample and the ion concentrations of initial Chu-13 media are also displayed in Table 3.2. Most of the major components in the GW showed were deemed a consistent ion content and pH, with a CoV less than 25% (0.07, 0.18, 0.18, 0.09, 0.22 for pH, Cl^-,Ca^{2+},PO_4^{3-},K^+ ,Na^+ respectively)

indicating that the standard deviation was less than a quarter of the mean. An exception being sulphate, due to the anomalous result with batch 2. To ensure this batch did not negatively impact the repeatability of experiments, initial SCWG experiments were completed at 550°C, 2wt.% glucose. They found the CoV was <0.1 for all output variables, it was therefore deemed a suitable feedstock and was utilised in the experimental work of Chapter 4. The order of experiments was randomised to ensure that minor variations due to GW composition or other unknown factors was attributed to any of the studied variables.

A comparison of the GW to the initial Chu-13 medium shows a clear decrease in concentration of the nutrients during algal growth. This was most notable with nitrate, which sees a decrease from 245 to < 7mg/l. However, some ions, such as sulphate and potassium, increased during the growth period. This indicates that nitrate was the limiting nutrient in this growth, the depletion of which caused the reduction in growth after a period of time shown in Section 3.1.1.1. Other ions remained in excess and, if the increase concentration through evaporation outweighed the uptake by the algae, an increase in those ions was observed.

Table 3.3- Analysis of algal growth water and Chu-13 media.

Batch	pH	TOC	Concentration of ions (mg/l)												
			Cl^-	NO_3^-	SO_4^{2-}	Ca^{2+}	$Co^{2+/3+}$	$Cu^{+/2+}$	$Fe^{2/3+}$	mg^{2+}	MoO_4^{2-}	PO_4^{3-}	K^+	Na^+	Zn^{2+}
1	8.8	94	30	<7	71	17.9	0.0027	0.04	2.0	24	0.09	9.2	210	65	0.31
2	8.4	109	57	<7	447	26.1	0.0034	0.049	2.5	17	0.12	2.6	210	84	0.2
3	9.5	385	65	<7	68	22.5	0.0036	0.031	2.0	22	0.11	3.8	220	66	0.13
4	8.8	220	62	<7	79	32.3	0.0038	0.034	2.5	25	0.11	4.5	250	60	0.13
5	9.7	202	63	<7	68	25.6	0.004	0.033	2.7	26	0.11	2	240	59	0.2
6	8.5	180	56	<7	75	26.4	0.0042	0.03	2.4	24	0.1	1.2	220	46	0.09
7	8.4	170	54	<7	73	28.6	0.0023	0.023	1.8	26	0.09	0.47	200	43	0.05
8	8.6	169	59	<7	90	30.5	0.0052	0.028	2.6	28	0.1	1.7	260	48	0.07
9	8.0	100	56	1.8	82	20	0.0013	0.027	0.32	21	0.067	12	200	47	0.0087
10	8.2	43	61	3.2	74	17	0.00039	0.015	0.19	20	0.092	9	207	48	0.0074
11	8.4	70	56	3.0	76	17	0.0011	0.025	0.86	21	0.1	11	196	44	0.056
Made	8.5	0	63	2.7	101	21	0	0	2.0	20	0	4	219	43	0
CHU-13	7.5	0	69	245	77.1	39	0.009	0.04	4.5	20.2	0.074	43	190	60	0.1

3.2 SUPERCRITICAL WATER GASIFICATION

3.2.1 Reactor Design Calculations

To prevent plugging, caused by char formation and salt precipitation [13], and ensure a sufficient residence time, careful consideration of the reactor design was required.

3.2.1.1 Practical Constraints

The design was constrained by the equipment that was available or could be purchased within the limits of this project. These limitations are outlined in Table 3.4.

Table 3.4-Equipment constraints

Equipment	Availability	Constraints
Pump	2 Jasco Pu-2086 HPLC pumps	Pressure: 50MPa Flowrate: 20ml/min (each)
Oven	Carbolite Gero LHT	Temperature: 600°C Volume: 128l
Pipework	Swagelok SS316l tubing	Diameter:1/16,1/8,1/4,3/8'' Pressure rating: dependent on diameter Length: availability at the time
Shell and tube heat exchanger	Manufactured in-house	Pressure rating:36MPa Tube Diameter:1/4" Tube length: 6m
Back pressure regulator	Go BP-66	Max Pressure: 68.8MPa

A larger diameter pipe will reduce the chance of plugging due to the greater cavity for flow. Therefore, a ¼'' pipework was selected, as it was the largest available size for which turbulence could be achieved with the pumps available at the required range of temperatures (400-600°C). At the time of construction 24m of this pipework was available, all of which was used to maximise the residence time that can be achieved.

3.2.1.2 Minimum Flowrate

To help minimise the risk of blockage from solid formation in the reactor, the flowrate should remain turbulent for all the required reaction conditions. Due to the complex reactions taking place, it is not possible to know the fluid properties in the reactor. However, as the algae

breaks down into smaller intermediates and gas, the viscosity will decrease. Therefore, for fluid property calculations it was assumed the algae remains solid throughout, ensuring turbulence was being maintained throughout the reactor.

To calculate the minimum flowrate, the slurry density and viscosity within the reactor must be calculated. The density was calculated from the weighted average of water (at a given temperature) and dry algae, shown in equation 2. The viscosity for a microalgae slurry can be found as a function of the volume fraction [14], as shown in equation 3. The volume fraction can be calculated using equation 4 [15]. In the following equations, ρ denotes the density, x the mass fraction of microalgae in the slurry, μ_c is the viscosity of the continuous phase (water), ϕ is the volume fraction and ϕ_m is the maximum packing fraction (0.637). The subscript w, p, a refer the water, algae powder and algae cell respectively.

$$\rho_T = \frac{1}{\frac{x_a}{\rho_p} + \frac{1 - x_a}{\rho_w}} \tag{2}$$

$$\mu = \mu_c \left(1 - \frac{\varphi}{\varphi_m}\right)^{-2} \tag{3}$$

$$\frac{x_a \left(1 - \frac{\rho_w}{\rho_p}\right)}{\left(\frac{x_a}{\rho_p} + \frac{(1-x)}{\rho_w}\right)(\rho_a - \rho_w)} \tag{4}$$

As data was not available for *Chlorella vulgaris*, the density of was inferred from the cell density obtained by Hu [16] using the same ratio to powder density as found for *Chlorella pyrenoidosa* [15]. The water density for a given condition was obtained from NIST databases [17]. A Reynolds number greater than 2500 is required to ensure turbulence is achieved. Therefore, the minimum mass flowrate ($\dot{m}$) can be calculated using equation 5.

$$\dot{m} = \frac{2500\pi\mu d}{4} = 625\pi\mu d \tag{5}$$

3.2.1.3 Reactor Coil design

The SCWG reactor consisted of a coiled length of stainless steel 316l pipework. The coil was designed to minimise dead legs, which can lead to accumulation of solid material, increasing the risk of blockages. Moreover, the coil diameter should be 10 times the pipe diameter to ensure heat transfer is not negatively influenced [18]. A coil diameter of 201mm was selected as this was the largest diameter that was feasible within the oven dimensions. As a result, the diameter was 39.6 times the coil diameter and allows for a large cavity in the centre for thermocouples and greater access for maintenance work. Additionally, K-type thermocouples were placed on the entrance, exit, 6m and 12m intervals along the reactor. Due to the lack of stiffness in the pipework, the shape of the coil was not maintained once installed. As a result, metal supports were added to ensure no upwards sections or contact was observed. This prevents the formation of dead legs and any effect on the heat transfer [19]. Despite careful design, the location of the oven exit required one dead leg to be present in the system. To prevent build-up of solid material, a T junction was included to provide a cavity for this material and an entrance to allow for easy removal.

3.2.1.4 Reactor Length

Despite being a fixed length of coil, a significant proportion of the process fluid would not be at the reaction temperature. Therefore, to calculate the residence time, the length of this proportion is required. As the oven was isothermal at the reaction temperature, the heating rate is very slow close as it approaches the desired temperature. Thus, it was deemed at temperature when it was within 5°C of the target. To calculate the amount length of the pre-heater section, the energy required (*Q*) and average heat transfer coefficient (*U*) are required. These are displayed in equations 6 and 7 [20].

$$Q = \dot{m} x_a \left(C_{pa}\right)(T_{ov} - T_{ro}) + \dot{m}(1 - x_a)\left(H_{T_{ro}} - H_{T_{ov}}\right) \tag{6}$$

$$\frac{1}{U_o} = \frac{1}{\frac{1}{h_o} + \frac{d_o}{2k}\ln\left(\frac{d_o}{d_i}\right) + \frac{d_o}{d_i h_i}} \tag{7}$$

Where *h* is the heat transfer coefficient, *d* is the diameter, *k* is the thermal conductivity and *o* or i indicate the inside or outside of the reactor. *T* is the temperature, where the subscripts *ov* and *ro* refers to the oven room temperatures respectively. The thermal conductivity is a function of temperature and taken to be the average of the reactor temperature and that of the inlet (room) temperature, as shown in equation 8. The internal heat transfer coefficient was assumed to be the same a pure water system and is represented by equations 9a and 9b for laminar and turbulent flow respectively [20]. All cases start at laminar flow and end at turbulent flow, so the h_i was a weighted average of the two. Due to the high temperatures, the influence of radiation cannot be ignored, therefore the outside heat transfer coefficient was taken as a sum of convective and radiative heat transfer coefficients (equations 10 and 11) [21] [20].

$$k = 54 - \frac{3.33}{2} \times 10^{-2}(T_{ro} + T_{ov}) \tag{8}$$

$$h_i = \frac{3.66 k_{water}}{d_i} \tag{9a}$$

$$h_i = 0.0243 Re^{0.8} Pr^{0.4} \frac{k_{water}}{d_i} \tag{9b}$$

$$h_{oc} = C_0 Re^{C_1} Pr^{C_2} \left(\frac{pr_{bulk}}{Pr_{wall}}\right)^{C_3} \tag{10}$$

$$h_{or} = \frac{1}{\left(\frac{1}{\varepsilon_{ov}} + \frac{A_{ov}}{A_r}\left(\frac{1}{\varepsilon_r} - 1\right)\right)(T_{ov} - T_r)} \sigma(T_{ov}^4 - T_r^4) \tag{11}$$

For which, *Re* is the Reynolds number, *Pr* is the Prantl number, *C* is a constant that is determined by the Reynolds number, ε is the emissivity, *A* is the surface area, σ is the Boltzmann's constant and the subscript *r* denotes the reactor. All water and air properties were obtained from NIST databases [17], the emissivity of stainless steel was used [22] and the air flow was assumed to be 1.5m/s, the upper limit of commercial ovens [23]. Using these values, the h_o is in the range 50-70 W $m^{-2}k^{-1}$, h_i is >500 W $m^{-2}k^{-1}$ and the inverse of the conductive

term $\left(1/\frac{d_o}{2k}\ln\left(\frac{d_o}{d_i}\right)\right)$ is approximately 30,000W $m^{-2}k^{-1}$. This shows that the outside heat transfer coefficient is the dominant resistance to heat transfer.

The length of the preheater section (*l*) was then calculated from equation 12, where ΔT_{lm} is the log meant temperature difference.

$$l = \frac{Q}{U_o \pi d \Delta T_{lm}} \tag{12}$$

As the external heat transfer resistance dominates, the flow within the reactor has a minimal impact on heat transfer rate. Therefore, as the length is directly proportional to the heat required. As total heat requirement is a function flowrate into the reactor, the preheater length is proportional to the flowrate (at the same conditions). To ensure the calculations are correct, verification using thermocouples placed at 6m intervals was used. These all confirmed that the calculated lengths fell into the correct 6m section of the pipework. It was not possible to have a more accurate measurement without significant increase in the risks of leaks.

3.2.2 Reactor Set-up

The reactor was a 25m continuous tubular reactor of ¼'' nominal diameter (internal 3.87mm) stainless steel 316l pipework, 24m of which was coiled in a coil diameter of 201mm, located within a Carbolite Gero LHT oven (Figure 3.7). The oven cavity was maintained at the desired reaction temperature. Thermocouples are located on the entrance, exit, 6m along and 12m along the reactor length. The desired feedstock was fed by 2 Jasco Pu-2086 HPLC pumps where each pump provided 50% of the flow (Chapters 4 and 5).

When oxidant was used (Chapter 6), the feed was split and preheated separately. The algal feedstock flows through the existing reactor, whereas the oxidant feed flows through a separate 7.8m stainless steel 316l preheater of 1/8'' nominal diameter (1.75mm internal diameter) that combine with the main reactor after 6m. Due to the influence of oxidant reaction, it was not possible to ensure the residence time as outlined in Section 3.2.1.4. Therefore, as the 2nd preheater has a larger length and smaller diameter, it reached within 20 °C of the oven

temperature in all cases at the point of mixing. This was considered as the start of the reactor in these examples.

The reactor exit stream was cooled to ambient temperatures in a water-cooled shell and tube heat exchanger with 6m of coiled ¼" tube (di =3.87mm) and a shell diameter of 10cm. A GO BP-66 manual back pressure regulator (BPR) was used to maintain the reactor pressure, which was monitored using a Swagelok PGN manual pressure gauge. A pair of 2-micron filters are located in parallel before the BPR and 1 x 0.5-micron filter was located afterwards. The parallel filters are used to ensure the flow and pressure can be maintained when a blockage occurs. A second pressure gauge was used, before the 1-micron filter to monitor for blockages. These can all be seen in the image in Figure 3.8. A gas liquid separator, consisting of a 250mm long, 25mm diameter glass tube, was used to separate the cooled and depressurised gaseous product from the liquid product. The gas flow then flows through 1/8'' pipework to a three-way valve, directing the flow to a bubble column to measure flowrate or a gas bag for sampling. These are shown in the image in Figure 9. A schematic of the one feed and two feed reactor set-ups can be found in Figure 3.5 and Figure 3.6.

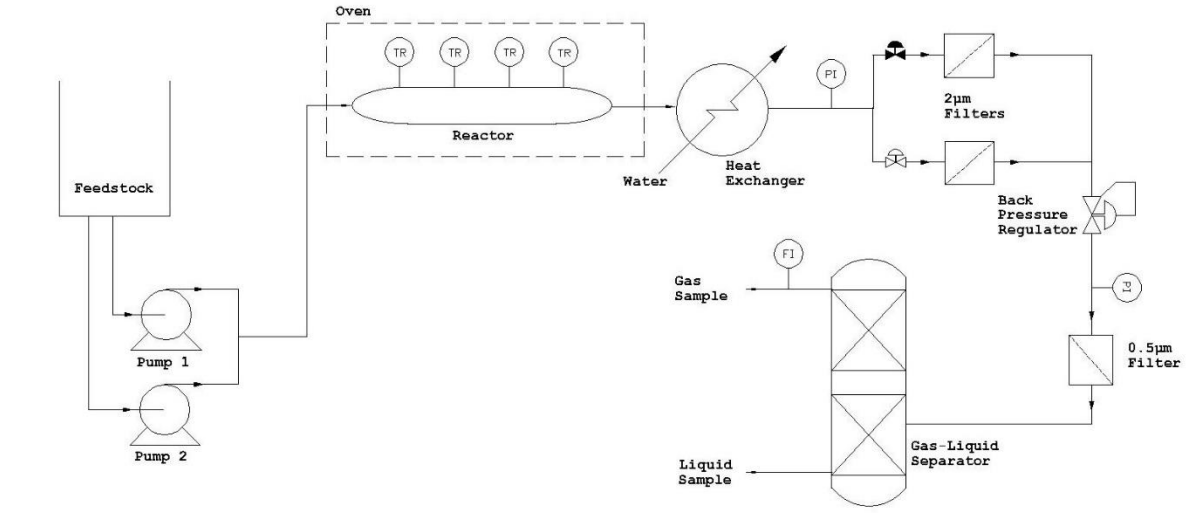

Figure 3.5-Reactor set-up one feed schematic diagram.

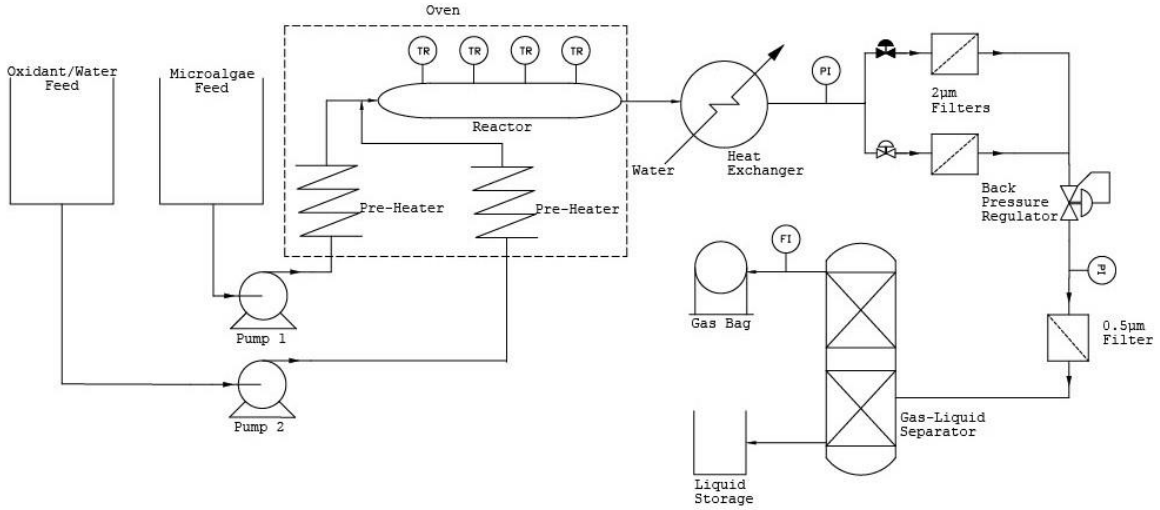

Figure 3.6-Reactor set-up two feeds schematic diagram.

Figure 3.7-SCWG reactor image.

Figure 3.8-SCWG downstream processing image: Part 1

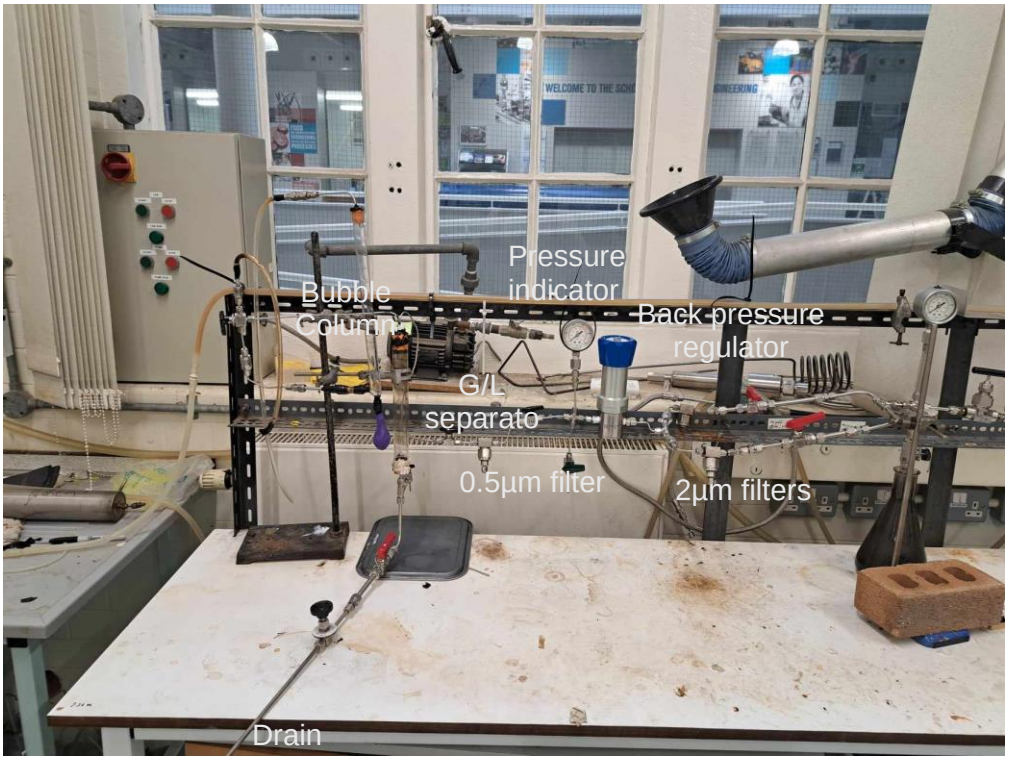

Figure 3.9 SCWG downstream processing image: Part 2

3.2.3 Experimental Procedure

3.2.3.1 Feedstock Preparation

Prior to each experiment, the feedstock was prepared as such:

1. Measure 500ml of desired reaction medium (DW or GW).
2. Weigh the correct quantity of biomass (glucose or *Chlorella vulgaris*) and catalyst to meet a pre-determined concentration.
3. If required, prepare oxidant solution by dilution of 30% hydrogen peroxide in distilled water.
    a. Tubing and glassware for oxidant side should be clean and solution stored under ice to prevent decomposition.
4. Combine the biomass and media, shacking vigorously and keep suspended using a magnetic stirrer.
5. Add the catalyst to the biomass suspension immediately prior to experiment.
    a. Alkaline or acid catalyst are known to alter biomass when used in pre-treatment [24,25], so contact time should be minimised.

3.2.3.2 Operational Procedure

3.2.3.2.1 Pre-Experiment Procedure

Prior to operation of the rig, a series of tests a procures are required to ensure the experiment can progress smoothly and safely. This are as follows:

1. Pressure test at 30Mpa
    a. Ensure no leaks are present in the system, any leaks should be resolved before heating up of the system.
2. Test pumps for flowrate at 10ml/min without pressure and at reaction pressure.
    a. Wear of the pump components can cause the flowrate to differ, recalibration of the software or replacement of the components may be required.

3. Bring the oven to required reaction temperature.
    a. This can take in excess of 2 hours so must be achieved in advance of the experiment.
4. Pump the system at the desired flowrate with distilled water, adjusting the pressure to 23MPa.
5. Once the pressure and temperature have reached a steady state, the experiment can commence.

3.2.3.2.2 Experimental Procedure

Once the above steps have been fulfilled and the feedstock prepared, the main experiment can proceed. The procedure for this is as follows:

1. Pumps operated at the desired flowrate.
2. Reactants allowed to flow through the system until visible changes are observed in the gas/liquid separator.
    a. This can take between 6-10 minutes, depending on the conditions being utilised.
3. This is allowed to flow for a further 3 minutes to allow steady state to be reached in the G/L separator.
4. Flowrate measurements are taken and 50ml of liquid sample is collected.
    a. Flowrate measurements are taken every 2 minutes until 3 have been collected.
    b. Gas samples must be analysed within the day of collection, liquid samples are stored in darkness at 4°C and are analysed within a week.

3.2.3.2.3 Post-Experiment Procedure

Once sufficient samples had been collected, it was important that the system as sufficiently flushed at reaction temperature to remove any organic material that remains and below the critical point to remove any precipitated salts from the system. This will limit any interference that may occur between the experiments. The procedure for this is as follows:

1. Flush with distilled water at 40ml/min for 30 minutes.
2. Switch off the oven and allow to cool while continuing to flush at 40ml/min.
3. Once the oven has cooled below 100°C, the system is switched off

Additionally, after every 10 experiments, the reactor was flushed with propanol to remove any tar that has built up during the process. This prevents clogging of the pipework and BPR.

3.2.4 Analysis Methods

3.2.4.1 Product Analysis

The SCWG process converts the feedstock into three main streams: A gas stream, consisting of H2, CO2, CH4, CO and other short chain hydrocarbons; a liquid stream, consisting of organic intermediates formed from the breakdown of the feedstock and inorganic carbon formed from the CO2 produced during the reaction; a residual phase, consisting of solid char and highly viscous tar, which largely remains on the walls of the reactor, cooler and in the filters. To calculate output variables, such as gas yield or carbon conversion, and understand the causes of any changes in these variables, these streams must be analysed. However, due to their deposition within the system, it was not possible to quantify the residual phase directly.

3.2.4.1.1 Gas

The gas volumetric flowrate was measured using a bubble column, which consisted of a 50ml volumetric cylinder with a surfactant reservoir. The time taken for a bubble to travel a given volume was then used to calculate volumetric flow. Three measurements were taken for each experiment and averaged to ensure accuracy. The gas composition was measured using a Shimazu 2014 Gas chromatography with a thermal conductivity detector (GC-TCD) and a 0.35 mm internal diameter, 20 m Shim Carbon ST column. All samples were measured in triplicate to account for any anomalous analysis. The volumetric fractions of H_2, CH_4, CO, CO_2 and N_2 were measured, the N_2 was used to calculate the quantity of air that has entered the sample. It was assumed that the remaining gas volume was larger hydrocarbons.

3.2.4.1.2 Liquid

To quantify both the Total organic carbon (TOC) and total inorganic carbon (TIC), the Shimadzu TOC-L analyse was used, following a 150x dilution. This dilution was required to minimise machine degradation due to salt deposition and ensure the TOC and TIC were in the instrumental range. Initially, this instrument was not available, so alternative analysis was required. The Spectroquant® TOC Cell test following 100x dilution was utilised for this. To

ensure no influence of the measurement method on the results, it was imperative that the same method was used for an entire dataset.

To identify the compounds that constitute the TOC in the liquid phase, the organic phase was extracted from the sample using a 4:1 ratio of dichloromethane to sample. This was passed through a Thermo Scientific Trace1600-ISQ7610 Gas chromatography-mass spectrometer (GC-MS), using helium as the carrier gas and a Restek Rxi-35Sil MS column with a 0.5 µm film thickness, a 0.25 mm inner diameter and 30 m length. This gave a qualitative assessment of the compounds and could quantify differences of the same compounds between different samples.

3.2.4.2 Calculations

3.2.4.2.1 Gas Yields

The gas yields are important output variables as they quantify the amount of gas produced per unit mass of biomass. This is important to quantify a key product which in this work is hydrogen. Additionally, it is useful for inclusion into wider models, these include the system model in Chapter 6 of this work. The yield is calculated from equation 13. Where ρ is the density, φ is the volumetric concentration in the gas stream, v is the volumetric flow, ($\dot{m}$) is the mass flow and x is the mass fraction. The subscript x indicates the product, b is the biomass and f the feedstock.

$$Y_x = \frac{\rho_x \varphi_x v}{x_b \dot{m}_f} \tag{13}$$

3.2.4.2.2 Carbon Conversion

It is important to know how much of the feedstock has been converted to gas, thus showing to what extent the reaction has progressed. In most literature, carbon gasification efficiency (equation 14) is used as the carbon makes up the backbone of all biomasses hence, this was adopted in Chapter 4. However, subsequent chapters showed the significance of including the TIC into the carbon conversion. Therefore, in these chapters, equation 15 was used to calculate the carbon conversion.

$$Carbon\ Gasification\ Efficiency\ (\%) = \frac{C_{gas}}{C_{Feed}} \tag{14}$$

$$Conversion\ (\%) = \frac{C_{gas} + C_{TIC\ liquid}}{C_{Feed}} \tag{15}$$

3.2.4.2.3 Other Parameters

The SCWG aims to convert the feedstock to a gaseous product, for which the efficiency of this process is key parameter. It is particularly important when comparing to other technologies and performing energy analysis. This is calculated from the higher heating value (HHV) of both products and feedstock, as shown in equation 16.

$$\eta = \frac{\dot{m}_g \sum(HHV_p x_p)}{\dot{m}_f HHV_a x_a} \tag{16}$$

Polymerisation into longer chain compounds, in the form of viscous liquid tar and solid char, are largely undesirable in SCWG as they can reduce the gas yield and cause blockages in the reactor [26]. Therefore, it is important to quantify the amounts of such compounds. However, due to the viscous nature of the tars, much of this remains lined to the reactor and downstream processing, trapping the char in the process hence, it cannot be directly quantified. The residual carbon, calculated by substitution of the known products from the carbon in the feedstock, was used to estimate this.

$$C_{Residual} = C_{Feed} - C_{TOC\ liquid} - C_{TIC\ liquid} - C_{Gas} \tag{17}$$

3.2.5 Initial Tests

3.2.5.1 Flow Tests

The pumps used in this process are reciprocating piston pumps, so the flowrate is calculated as a function of the motor rotational speed. As a result, the flowrate produced varies with fluid viscosity and calibrations within the pump software must be altered to overcome this. However, it was not feasible to recalibrate every experiment; a consistent flow must be achieved for all feedstocks studied. The viscosity of an algal slurry varies with the concentration of the biomass [15], therefore, to ensure that the pump can consistently provide the correct flowrate it must be tested at varying concentrations of algae. The pump flowrate was set to 10ml/min and concentration varied from 0.1 to 30wt.%, the results of which can be found in Appendix C. These tests showed that the effect of the viscosity was negligible up to 5wt.%, but at 10wt.% it was significant. Thus, in this work, no concentration above 5wt.% was used.

3.2.5.2 Residence time tests

It is established in literature that an increase in reaction time (residence time in continuous reactors) increases the conversion of the feedstock and yield of gases, including hydrogen [27, 28, 29, 30]. However, in these cases a plateau is formed, after which a longer residence time had little impact. Therefore, to simplify the number of factors studied in this work, a residence time that maximises yield and conversion at all conditions was selected. To determine this, the conversion and yield was studied for the largest range of residence times possible at the lowest temperature studied (400°C), where the reaction would be slowest.

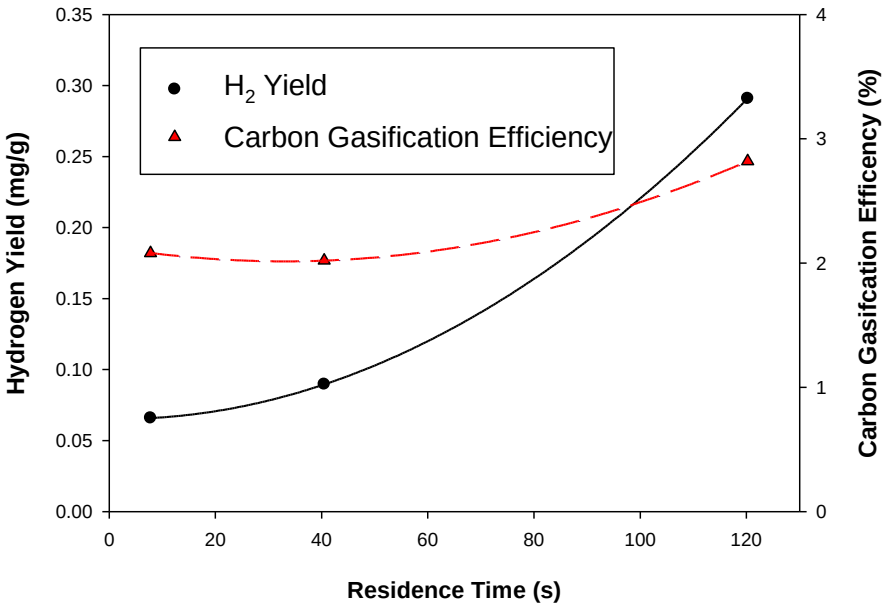

Figure 3.10-Impact of residence time on the hydrogen yield. 2wt.% Chlorella vulgaris, 400°C, Distilled water.

This clearly shows that both hydrogen yield and carbon conversion increase with the residence time for the full range studied. Therefore, the residence time selected was the greatest that could be achieved while remaining turbulent for all reaction conditions in that data set.

3.2.5.3 Catalyst and Oxidant Concentration Tests

The concentration of homogenous catalysts can influence the reaction, generally increasing the effect of that catalyst [31] as with residence time. For work in Chapters 4 and 5, to simplify the experimental plan and significantly reduce the minimum number of experiments, it was decided to maintain a constant catalyst concentration. To determine this concentration, a series of tests was completed at 500°C, 2wt.% and a residence time of 50s. A maximum concentration of 1wt.% was observed in the literature for a continuous system [32, 31], so that was chosen as the maximum concentration.

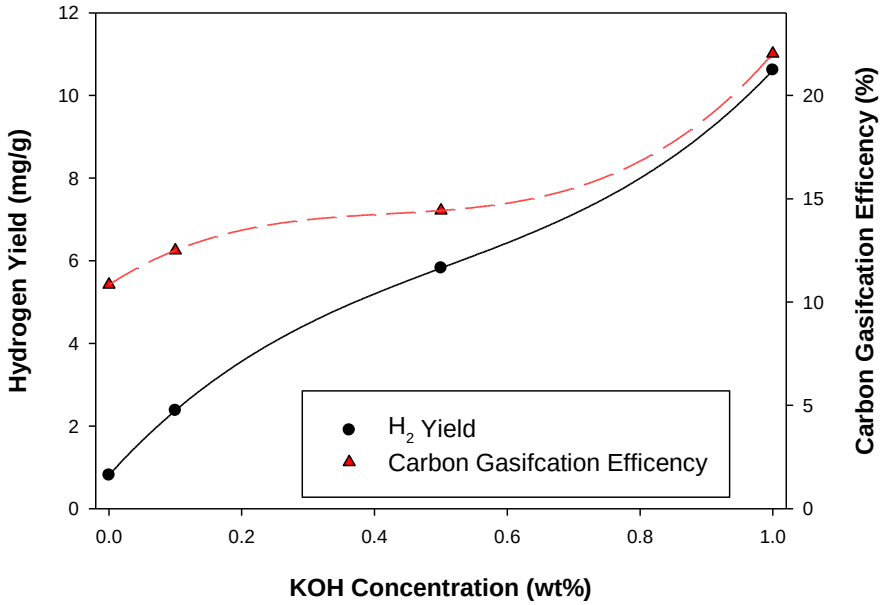

Figure 3.11-Infuence of KOH on hydrogen yield and carbon gasification efficiency. 2wt.% Chlorella vulgaris, 500°C, 50s residence time.

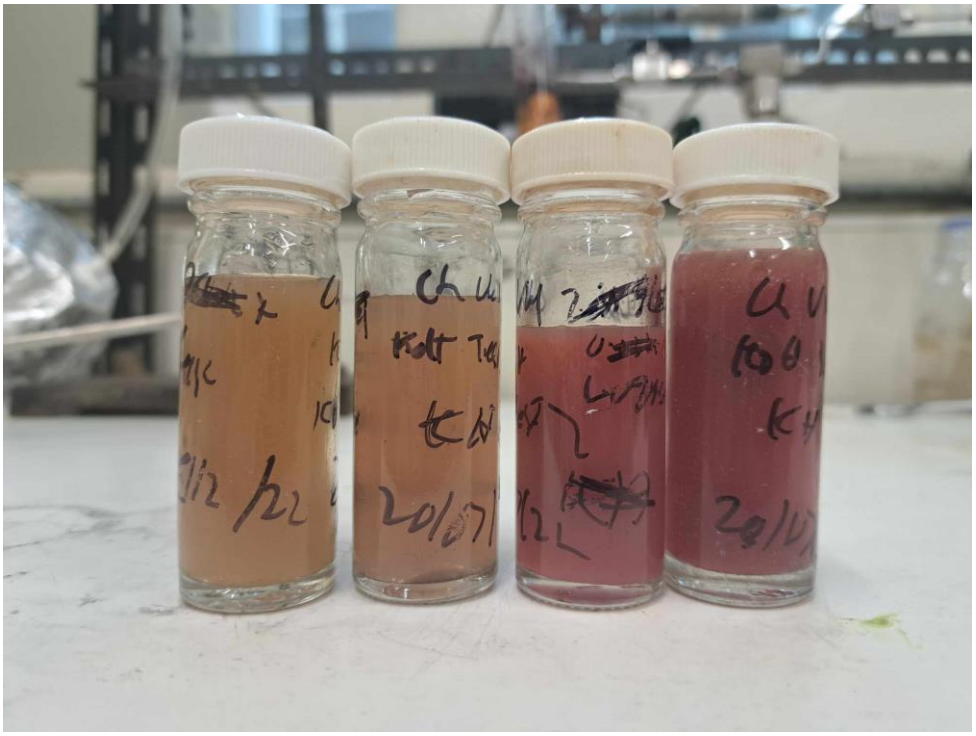

Figure 3.12-Infuence of KOH on liquid product. Left to right, 0%, 0.1%, 0.5%, 1wt.% KOH. 2wt.% Chlorella vulgaris, 500°C, 50s residence time.

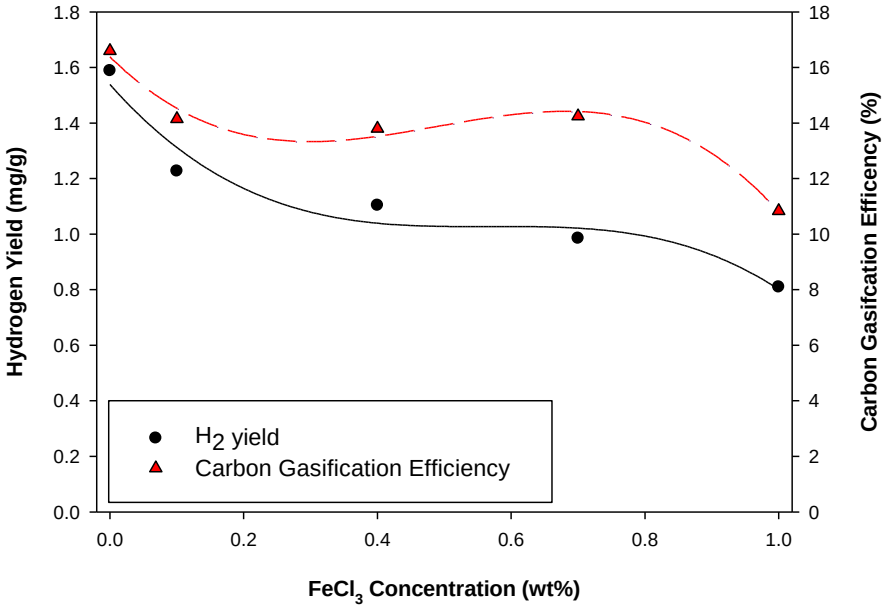

Figure 3.13-Infuence of $FeCl_3$ on hydrogen yield and carbon gasification efficiency. 2wt.% Chlorella vulgaris, 500°C, 50s residence time.

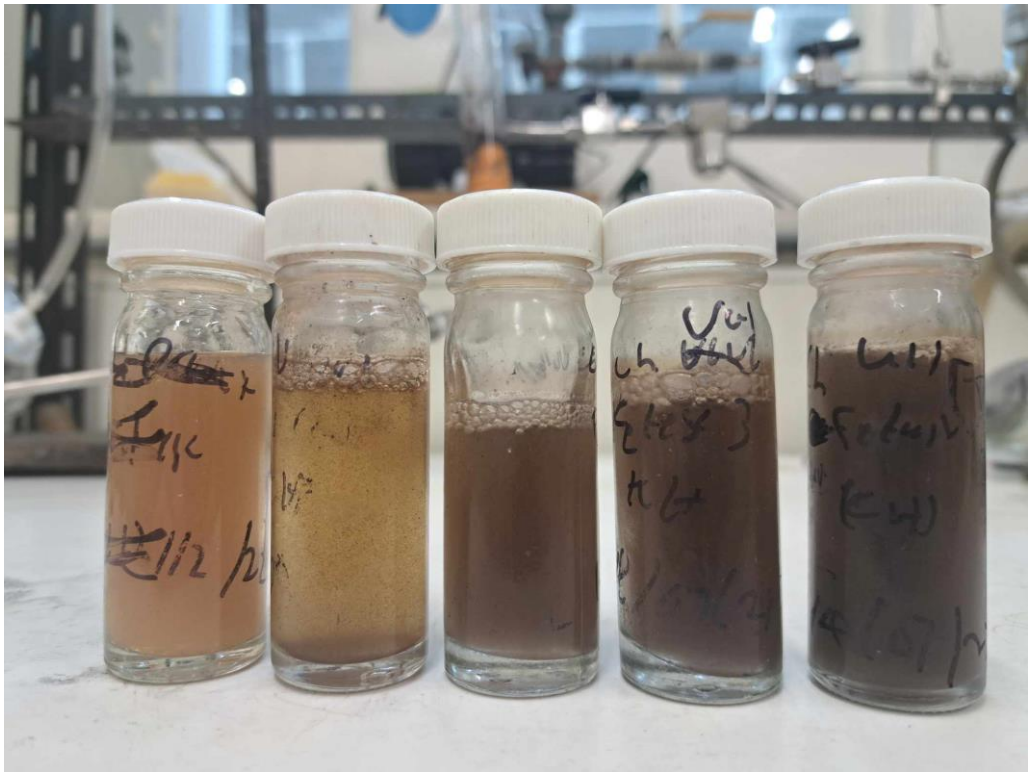

Figure 3.14-Infuence of $FeCl_3$ on liquid product. Left to right, 0%, 0.1%, 0.5%, 1wt.% $FeCl_3$. 2wt.% Chlorella vulgaris, 500°C, 50s residence time.

KOH had a positive impact on hydrogen yield and conversion with liquid product going a noticeable pink colour at elevated concentrations. Conversely, the $FeCl_3$ had a negative impact on hydrogen and CGE, with the liquid phase increasing in small black char particles with an increased concentration. Despite these differences, both show that the catalyst concentration increases the impact on the hydrogen yield, carbon gasification efficiency and the appearance of the liquid phase. Thus, to maximise the impact shown by these catalysts, a concentration of 1wt.% was chosen in both cases.

In this study, heterogeneous catalysts are suspended in the feedstock, thus a concentration must also be selected. However, the solid particles damage the pumping system and can increase viscosity of the fluid. Consequently, a concentration of 0.1wt% was selected to minimise these negative impacts but ensure the effect was as significant as possible.

3.2.5.4 Oxidant Concentrations

It is also important to know the quantity of oxidant to test in Chapter 6, as excessive oxidant is known to be detrimental to hydrogen yield. This was tested at 500°C, 2wt.% *Chlorella vulgaris*, 55s residence time, using the 2nd reactor set-up outlined in Figure 3.6. The oxidant coefficient, the ratio of oxidant to the stoichiometric amount of oxygen for complete oxidation of the feedstock, was the variable used. Due to the desired product being hydrogen, which is oxidised to water, complete oxidation is not desirable, thus an oxidant coefficient up to 0.5 was tested.

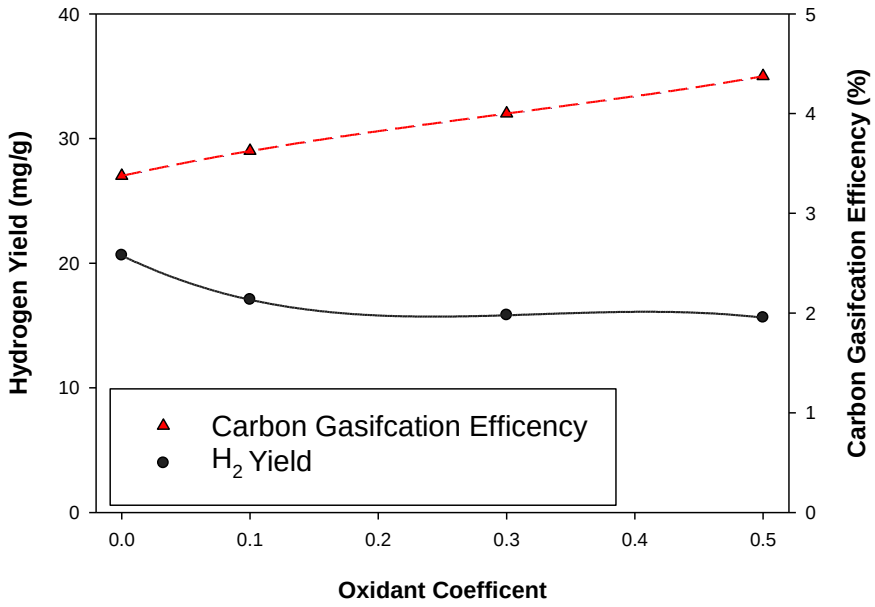

Figure 3.15- Influence of oxidant coefficient on hydrogen yield and carbon gasification efficiency. 2wt.% Chlorella vulgaris, 500°C, 50s residence time.

Figure 3.16- Influence of oxidant coefficient on liquid Product. Left to right, oxidant coefficient 0, 0.5, 0.3, 0.1. 2wt.% Chlorella vulgaris, 500°C, 50s residence time.

These show that the conversion of the carbon increases with oxidant, reducing the colour in the liquid product and the residual carbon. However, they also reduce the hydrogen yield. Therefore, when conversion is low it may be preferable to have higher oxidant concentration. Thus, the full range of 0-0.5 was considered in the optimisation in Chapter 6.

3.2.6 Safety Considerations

The SCWG process has several potential hazards that have to be included in the reactor design. The risk of overpressure due to blockages was significant due to the solid char and salt precipitation, which is exacerbated by high operating pressures. To overcome this, the maximum pressure of the pumps was set to 20% below the maximum operating pressure of the pipework and fittings. Moreover, a pressure relief system was designed to cool vented fluid and separate any or toxic flammable gases for proper disposal in the case of overpressure. Additionally, CO makes up a significant quantity of the gas stream, which is toxic, even at relatively low concentrations. As a result, pressure testing of the equipment was required before every run, to check for potential leaks and CO monitors are employed next to the equipment.

3.3 REFERENCES

[1] J. L. Salgueiro, L. Perez, R. Maceiras, A. Sanchez and A. Cancela, “Bioremediation of Wastewater using *Chlorella Vulgaris* Microalgae: Phosphorus and Organic Matter,” *Int. J. of Environ. Res*., vol. 10, no. 3, pp. 465-470, 2016 doi:10.22059/ijer.2016.58766.

[2] H. Singh, J. L. Varanasi, S. Banerjee and D. Das, “Production of carbohydrate enrich microalgal biomass as a bioenergy feedstock,” *Energy*, vol. 188, 2019 doi:10.1016/j.energy.2019.116039.

[3] N. Chandra, P. Shukla and N. Mallick, “Role of cultural variables in augmenting carbohydrate accumulation in the green microalga Scenedesmus acuminatus for bioethanol production*,” Biocat. and Agric. Biotech*., vol. 26, 2020 doi:10.1016/j.bcab.2020.101632.

[4] F. Han, W. Wang, Y. Li, G. Shen, M. Wan and J. Wang, “Changes of biomass, lipid content and fatty acids composition under a light–dark cyclic culture of *Chlorella pyrenoidosa* in response to different temperature,” *Bioresour. Tech*., vol. 189, p. 182, 2013 doi:10.1016/j.biortech.2012.12.175.

[5] R. Serra-Maiaa, O. Bernard, A. Gonçalves, S. Bensalem and F. Lopes, “Influence of temperature on *Chlorella vulgaris* growth and mortality rates in a photobioreactor,” *Algal Res*., vol. 18, pp. 352-259, 2016 doi:10.1016/j.algal.2016.06.016.

[6] B. Frølund, R. Palmgren, K. Keiding and H. Nielsen, “Extraction of extracellular polymers from activated sludge using a cation exchange resin,” *Water Res.,* vol. 30, no. 8, pp. 1749-1758, 1996 doi:10.1016/0043-1354(95)00323-1.

[7] K. Raunkjær, T. Hvitved-Jacobsen and H. Nielsen, “Measurement of pools of protein, carbohydrate and lipid in domestic wastewater,” *Water Res*., vol. 28, no. 2, pp. 251-262, 1994 doi:10.1016/0043-1354(94)90261-5.

[8] A. F. Gaudy, “Colorimetric determination of protein and carbohydrates,” *Ind. Water Wastes*, vol. 7, pp. 17-22, 1962.

[9] S. K.Mishra, W. I. Suh, W. Farooq, M. Moon, A. Shrivastav, M. S. Park and J.-W. Yang, “Rapid quantification of microalgal lipids in aqueous medium by a simple colorimetric method,” *Bioresour. Tech.,* vol. 155, pp. 330-333, 2014 doi:10.1016/j.biortech.2013.12.077.

[10] M. Axelsson and F. Gentili, “A Single-Step Method for Rapid Extraction of Total Lipids from Green Microalgae*,” PLOS one*, vol. 9, no. 2, 2014 doi:10.1371/journal.pone.0089643.

[11] G. S.Araujo, L. J.B.L.Matos, J. O.Fernandes, S. J.M.Cartaxo, L. R.B.Gonçalves, F. A.N.Fernandes and W. R.L.Farias, “Extraction of lipids from microalgae by ultrasound application: Prospection of the optimal extraction method,” *Ultrason. Sonochemistry*, vol. 20, no. 1, pp. 95-98, 2013 doi:10.1016/j.ultsonch.2012.07.027.

[12] D. Fozer, B. Kiss, L. Lorincz, E. Szekely, P. Mizsey and A. Nemeth, “Improvement of microalgae biomass productivity and subsequent biogas yield of hydrothermal gasification via optimization of illumination,” *Renew. Energy,* vol. 138, pp. 1262-1272, August 2019 doi:10.1016/j.renene.2018.12.122.

[13] R. F. Susanti, J. Kim and K.-p. Yoo, “Supercritical Water Gasification for Hydrogen Production: Current Status and Prospective of High-Temperature Operations,” in Supercritical Fluid Technology for Energy and Environmental Application, Amsterdam, Elsevier, 2014, pp. 111-137.

[14] A. Souliès, J. Pruvost, J. Legrand, C. Castelain and T. I. Burghelea, “Rheological properties of suspensions of the green microalga *Chlorella vulgaris* at various volume fractions,” *Rheologica Acta*, vol. 52, p. 2013, 2013 doi:10.1007/s00397-013-0700-z.

[15] H. Chen, Q. Liao, Q. Fu, Y. Huang, A. Xia, C. Xiao and X. Zhu, “Convective heat transfer characteristics of microalgae slurries in a circular tube flow*,” Int. J. of Heat and Mass Transf.*, vol. 137, pp. 823-834, 2019 doi:10.1016/j.ijheatmasstransfer.2019.03.166.

[16] W. Hu, “Dry Weight and Cell Density of Individual Algal and Cyanobacterial Cells for Algae Research and Development,” University of Missouri- Columbia, 2014.

[17] E. W. Lemmon, I. H. Bell, M. L. Huber and M. O. McLinden, “Thermophysical Properties of Fluid Systems,” in NIST Chemistry WebBook, NIST Standard Reference Database Number 69, P. L. W. Mallard, Ed., Gaithersburg MD, National Institute of Standards and Technology.

[18] D. R. Moss, “Procedure 6-8: Design of Pipe Coils for Heat Transfer,” in Pressure Vessel Design Manua, Elsevier, 22004, p. 336.

[19] J. S. Jayakumar, “Helically Coiled Heat Exchangers,” in Heat Exchangers – Basics Design Applications, Intech, 2012, pp. 312-342.

[20] F. P. Incropera, D. P. Dewitt, T. L. Bergman and A. S. Lavine, “Heat Exchangers,” in Fundimentals of Heat Transfer, John Wiley & Sons, 2007.

[21] R. Chhabra and V. Shankar, Coulson and Richardson's Chemical Engineering, Volume 1B - Heat and Mass Transfer - Fundamentals and Applications (7th Edition), Elsevier, 2018.

[22] H. Y. Nam, K. Y. Lee, J. M. Kim, S. K. Chio, J. H. Park and I. K. Choi, “Experimental study on the emissivity of stainless steel,” 2001.

[23] J. K.Carson, JimWillix and M. F.North, “Measurements of heat transfer coefficients within convection ovens,” *J. of Food Eng*., vol. 72, no. 3, pp. 293-301, 2006 doi:10.1016/j.jfoodeng.2004.12.010.

[24] J. S. Kim, Y. Lee and T. H. Kim, “A review on alkaline pretreatment technology for bioconversion of lignocellulosic biomass,” *Bioresour. Tech.,* vol. 199, pp. 42-48, 2016 doi:10.1016/j.biortech.2015.08.085.

[25] Y. Liu, W. Wang, Y. Wang, L. Liu, G. Li and C. Hu, “Enhanced pyrolysis of lignocellulosic biomass by room-temperature dilute sulfuric acid pretreatment,” *J. of Anal. and Appl. Pyrolysis*, vol. 166, 2022 doi:10.1016/j.jaap.2022.105588.

[26] C. Wang, W. Zhu, H. Zhang, C. Chen, X. Fan and Y. Su, “Char and tar formation during hydrothermal gasification of dewatered sewage sludge in subcritical and supercritical water: Influence of reaction parameters and lumped reaction kinetics,” *Waste Manag.*, vol. 100, pp. 57-65, 2019 doi;10.1016/j.wasman.2019.09.011.

[27] L. Tiong and M. Komiyama, “Supercritical water gasification of microalga *Chlorella vulgaris* over supported Ru,” *The J. of Supercrit. Fluids*, vol. 144, pp. 1-7, 2019 doi:10.1016/j.supflu.2018.05.011.

[28] R. Samiee-Zafarghandi, J. Karimi-Sabet, M. A. Abdoli and A. Karbassi, “Supercritical water gasification of microalga *Chlorella PTCC* 6010 for hydrogen production: Box-Behnken optimization and evaluating catalytic effect of MnO2/SiO2 and NiO/SiO2,” *Renew. Energy*, vol. 126, pp. 189-201, 2018 doi:10.1016/j.renene.2018.03.043.

[29] P. R. Nurcahyani, S. Hashimoto and Y. Matsumura, “Supercritical water gasification of microalgae with and without oil extraction,” *The J. of Supercrit. Fluids*, vol. 165, 2020 doi:10.1016/j.supflu.2020.104936.

[30] A. G. Chakinala, D. W. F. (. Brilman, W. P. v. Swaaij and S. R. A. Kersten, “Catalytic and Non-catalytic Supercritical Water Gasification of Microalgae and Glycerol,” *Ind. and Eng. Chem. Res*., vol. 49, no. 3, pp. 1113-1122, Septemeber 2010 doi:10.1021/ie9008293.

[31] S. Nanda, S. N. Reddy, H. N. Hunter, A. K. Dalai and J. A. Kozinski, “Supercritical water gasification of fructose as a model compound for waste fruits and vegetables,” *The J. of Supercrit. fluids*, vol. 104, pp. 112-121, September 2015 doi:10.1016/j.supflu.2015.05.009.

[32] G. Caputo, M. Dispenza, P. Rubio, F. Scargiali, G. Marotta and A. Brucato, “Supercritical water gasification of microalgae and their constituents in a continuous reactor,” *The J. of Supercrit. Fluid*s, vol. 118, pp. 163-170, December 2016 doi:10.1016/j.supflu.2016.08.007.

CHAPTER 4: THE IMPACT OF THE ALGAL GROWTH WATER ON SUPERCRITICAL WATER GASIFCATION OF *CHLORELLA VULGARIS*

4.1 PUBLICATION: SUPERCRITICAL WATER GASIFICATION OF MICROALGAE: THE IMPACT OF THE ALGAL GROWTH WATER

The research within this chapter subsection was published as journal article in *the Journal of Supercritical Fluids* as cited on the following page. For consistency with the published material, the content remains the same as the journal article.

ABSTRACT

Investigation into the supercritical water gasification (SCWG) of microalgae has largely used deionized water as the reaction medium. However, real systems would use the algal growth water directly, containing ions that have been known to catalyse SCWG (K^+, Na^+, OH^-, Fe^{3+}, Cl^-). Investigation into the effect of the growth water on SCWG was carried out for a range of temperatures (450-550), biomass concentrations (1-3%.wt) and catalysts (KOH, Ru/C), using glucose or *Chlorella vulgaris* as the feedstock was performed. A significant increase in CO_2 and reduction in CO content in the gas was observed without a catalyst and with a Ru/C catalyst. An increase in char/tar was also observed without a catalyst. As a result, the impact of the growth water should be considered for the SCWG of microalgae, in laboratory experiments and the selection of algal growth media in industrial applications.

4.1.1 Introduction

To achieve decarbonisation targets and limit global warming to 1.5°C above pre-industrial levels, carbon removal technologies are expected to be key achieving this, of which bioenergy with carbon capture and storage (BECCS) is expected to be a significant contributor [1]. As a result, deployment of new bioenergy projects is rapidly required. However, the production of many biomass sources can come with negative environmental and social impacts. The use of fertilizers causing eutrophication in waterways [2], the use of pesticides [18] and large monocultures [4] are all damaging to biodiversity. Additionally, the competition for land and fertilizers can have negative impacts on food prices [5].

Microalgae offer an alternative biomass source that can grow 10 times faster than terrestrial plants [6], thus far less land is required. Additionally, they are grown in man-made ponds, meaning arable land or the use of pesticides are not required, and nutrients used are contained so they do not enter waterway. Despite these advantages, the high-water content of microalgae has an adverse effect on the efficiency of conventional energy conversion processes such as thermal gasification or pyrolysis [19]. Therefore, alternative methods of extracting the energy and carbon from the algae is required.

Supercritical water gasification (SCWG) uses water above its critical point (374°C and 22.1MPa) as the reaction medium to form gaseous products (H_2, CH_4, CO, CO_2, and short chain hydrocarbons). The CO_2 can then be captured, leaving a highly combustible gas stream, which can be used for a variety of energy applications. The use of water makes it appropriate for high moisture feeds such as microalgae and the thermophysical properties of supercritical water (SCW) brings other advantages. The low density and viscosity of SCW increases the diffusivity, thus increasing reaction rates [8]. Additionally, the weakened hydrogen bonds, and low dielectric constant allow organic intermediates formed during the reaction, to dissolve and thus prevent recombination to form undesirable tars and chars [9], which limit operability and reduce gas yield.

The SCWG of microalgal biomass has been widely studied for a range of reaction conditions, catalysts, algal strains, and reactor types. These are summarised in Table 4.1. However, in most of these cases, the reactor feedstock is prepared by adding distilled, deionised or what is listed as simply water to dry or concentrated feedstocks to produce the desired concentration. This is not representative of a real-life situation as the addition of deionised water would greatly increase the energy requirement and thus reduce the efficiency of the process. The use of the water used to grow the algae as the reaction medium is a far more realistic scenario. The growth water contains ions remaining from the original growth media, many of which have been known to catalyse SCWG (K^+, Na^+, OH^-, $Fe3^+$, Cl^-) and other ions for which the effect has not been studied. Therefore, this could have a significant impact on the results of the SCWG reaction.

Table 4.1-Supercritical water gasification of microalgae literature summary

Feedstocks	Reactor type	Catalysts	Temp (°C)	Pressure (MPa)	Time (min)	Biomass Conc (wt%)	Reaction Media	Source
Spirulina platensis	Batch	Ru/C Ru/ZrO_2	399-409	30.8-34.5	60-360	2.5-20%	Water	[20]
Chlorella vulgaris *Scenedesmus quadricauda*	Batch	Ni/α- Al_2O_3 Raney nickel	385	26	10-60	5%	Distilled water	[11]
Chlorella vulgaris *Spirulina platensis* *Saccharina latissimi*	Batch	NaOH Nickel/ Al_2O_3	500	36	30	5%	De-ionised water	[22]
Botryococcus braunii *Nannochloropsis oculata* *Tetraselmis chuui*	Batch	Nickel NaCl	400	25	10	4.3%k	De-ionised water	[13]
Chlorella vulgaris Glycerol Amino Acids	Batch and continuous	Ru/TiO_2 $NiMo/Al_2O_3$ $PtPd/Al_2O_3$ $CoMo/Al_2O_3$ Inconel Ni wire K2CO3	400-650	24-25	0.067-2	7.3-10%	Diluted growth water	[24]
Acutodesmus obliquus	Continuous	K2CO3	600-690	28	2.33-2.5	2-20%	Diluted growth water	[15]
Acutodesmus obliquus	Continuous	None	600-650	28	NS	2.5-5%	Growth water	[26]

Nannocloropsis gaditana	Continuous	K_2CO_3 Na_2CO_3	663	24	2.13	1,1.16 %	Water	[27]
Chlorella pyrenoidosa	Batch	Ni (Various supports)	430	13-22	60	16.67%	Water	[18]
Chlorella sp.	Batch, stainless steel	Ni Cu Co Mn Cr All on reduced graphene oxide	380		30	1.4%	De-ionised water	[19]
Chlorella Pyrenoidosa	Batch	Ru/C and Rh/C	380-600	22-55	60	26.6-50%	Water	[30]
Nannochloropsis oculata	Batch	Ni/γAl2O3 Ni/La-γAl2O3	400-500	28	15	NS	De-ionised water	[21]
Chlorella Vulgaris	Batch	Ru (Various supports)	385	26.2	15-120	5.06-10.12%	Distilled water	[32]
Chlorella S.P (Increased Carbohydrate content)	Batch	NiO/SiO_2 MnO_2/SiO_2	355-405	17.5-26.5	15-45	1-8%	Water	[33]
Phaeodactylum tricornutumpr	Continuous	Ru/C	425	30	NS	6.5%	Water	[24]
Chlorella vulgaris	Continuous	None	550	30	2	1.5%	Diluted growth water	[35]
Chlorella S.P Chlorella S.P (Increased Carbohydrate content)	Batch	None	380	22.5	30	4.9%	De-ionised water	[36]
Chlorella vulgaris Chlorella vulgaris (oil removed)	Continuous	None	600	25	0.117-1	1%	Water	[37]
Chlorella pyrenoidosa S. platensis Schizochytrium limacinum Nannochloropsis species	Batch	Pd/C Ru/C Pt/C Rh/C Ir/C	430° C	22-55	60	25-100%	Water	[28]
Spirulina	Continuous	None	550-600	23.5	0.067-0.15	17.5-25%	Water	[39]
Chlorella vulgaris	Continuous	Ru/C	394-420	26-30	Not stated	2.8-14.8%	Diluted growth water	[30]
Chlorella vulgaris hydrochar	Continuous	None	650	30	2	2.5%	Diluted growth water	[31]
Various Cyanobacteria	Batch	None	400-500	22	30	NS	Lake Water	[42]
Various Cyanobacteria	Batch	None	350-450	23	0-60	NS	Lake Water	[33]

The main gas forming reaction in SCWG are steam reforming, water gas shift (WGS) and methanation [34], outlined in equations 1,2,3 below. Steam reforming and WGS are highly desired as they increase the gas yield and produce more hydrogen in place of carbon monoxide, which is toxic and less desirable as a fuel. Methanation is also less desirable as methane contains carbon, so it is more difficult to apply BECCS to this, though it still remains a useful fuel. At mild conditions, decarboxylation reactions are also significant, producing a gas stream of predominantly CO_2 [45] [11].

$$C_xH_yO_z + (x-z)H_2O \rightarrow xCO + \left(\frac{y}{2} + x - z\right)H_2 \quad (1)$$

$$CO + H_2O \rightarrow CO_2 + H_2 \quad (2)$$

$$CO + 3H_2 \rightarrow CH_4 + H_2O \quad (3a)$$

$$CO_2 + 4H_2 \rightarrow CH_4 + 2H_2O \quad (3b)$$

In addition to these, a number of other reactions occur in the liquid phase, which produce a range of intermediates and can have a strong influence on the gas produced. Using real biomass, such as microalgae, these reactions are complex due to the variety of compounds available. However, analysis has been done on model compounds to help understand these reactions. Glucose is a key compound as it forms the building block of many carbohydrates, which are key components in all biomasses (including microalgae). In SCWG, SCW can break down glucose through C-C bond scission into straight chain or cyclic ketones and aldehydes, which are readily broken down into gas, which is desirable. Alternatively, it can easily dehydrate into furfural and other furans, which can dehydrate further into phenol. Both of these are known to be refractory in SCW and have a greater tendency to polymerise into undesirable tar/char [36] [47]. This is summarised in Figiure 1.

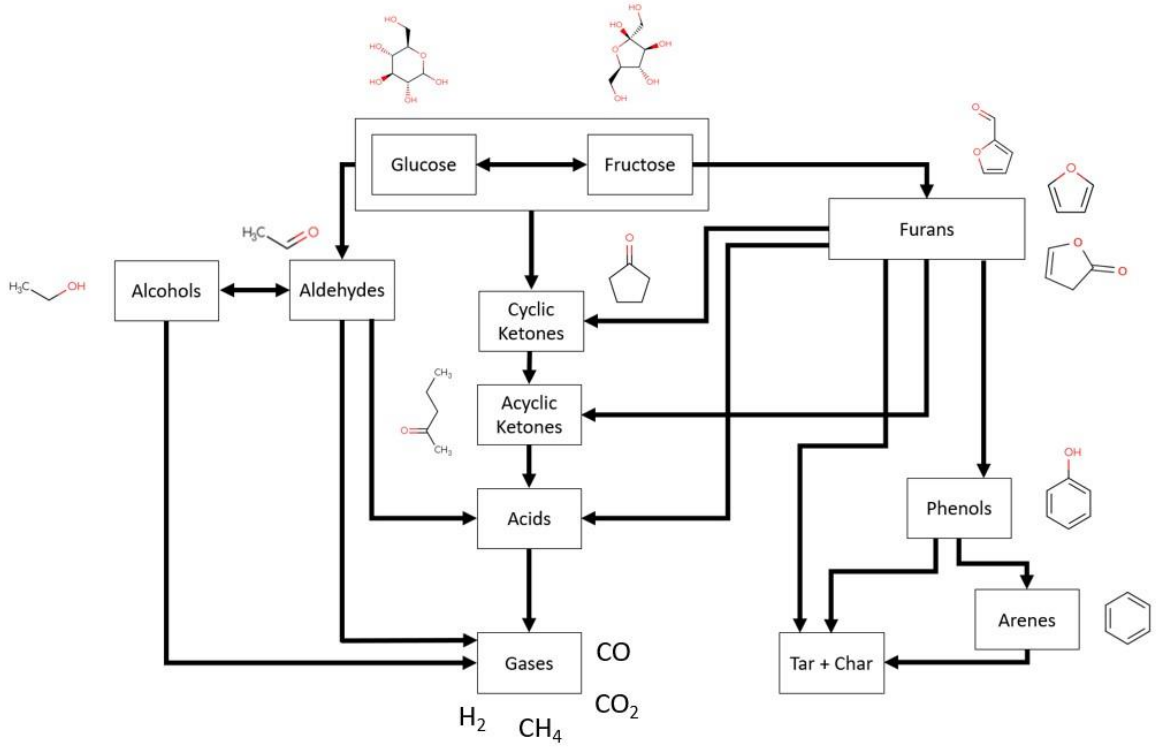

Figure 4.1-Reaction pathways of the supercritical water gasification of glucose [48]

This paper investigates the impact of using algal growth water (GW) compared with distilled water (DW) as the reaction medium in the SCWG of glucose and *Chlorella vulgaris.* Glucose gasification was performed without a catalyst for a range of temperatures (450-550°C) and concentrations (1-3wt.%). Glucose gasification was conducted at 500°C and 2wt.% used a KOH and Ru/C catalysts, to study the effect under catalytic SCWG. These were selected as they represent the most common types of homogenous and heterogenous catalysts [48] Additionally, non-catalytic SCWG of *Chlorella vulgaris* was performed to ensure the effect of using the growth water still applied to algal biomass.

4.1.2 Materials and methods

4.1.2.1 Materials

The microalga (*Chlorella vulgaris)* was grown in two parallel 5L stirred tank vessels, with a working volume of 4 L each (8 L in total). The whole system was sparged with 4 L min^{-1} of air (~.04% CO_2). The reactors are constantly illuminated by two panels of white LED lights with a light intensity at the wall of the reactors of 25 W m^{-2}. The growth medium used is chu13, which is prepared to the specifications shown in Appendix A, with the pH adjusted to 7.5 using 2M sodium hydroxide. The culture was grown for two weeks, with centrifugal separation of algae from the growth medium. The algae was then stored at 4 °C until required and the residual liquid (the growth water (GW)) is autoclaved at 120 °C for 20 minutes, before storing in darkness at room temperature. No further precipitation of the medium was observed, and the composition of the resulting GW was analysed by ALS Laboratories ltd. The GW had an average pH of 9, 200mg/l of organic carbon and the composition of ions displayed in Table 4.2.

Table 4.2-Growth water ion composition

Ion	Average Concentration (mg/l)	Standard deviation
Potassium	220.00	14.14
Sulphate	163.50	189.01
Sodium	68.50	10.79
Chloride	53.75	16.19
Calcium	23.03	3.77
Magnesium	22.25	3.86
Phosphate	4.40	3.29
Iron	2.33	0.36
Zinc	0.21	0.07
Molybdate	0.108	0.013
Copper	0.038	0.008
Cobalt	0.003	0.001
Nitrate	<7	n/a

The carbohydrate content of the microalgae was measured using the Anthrone method and proteins content was measured using the lowry method both outlined in [49]. The lipid content was measured gravimetrically, following sonication for 1 hour at and extraction using a 2:1 mixture of chloroform and methanol. The results of this are displayed in Table .

Table 4.3-Chlorella vulgaris composition

Component	Wt.%
Carbohydrates	15%
Proteins	52%
Lipids	33%

Dry D-glucose (99.5%) powder was obtained from sigma Aldrich. Potassium hydroxide >85% (KOH) was obtained from VWR. Ruthenium (5wt.%) catalyst supported on activated carbon (Ru/C) was obtained from Sigma-Aldrich, with an average particle size of 105.6nm (range of 68.7-169.9). Distilled water (DW) was produced by double distilling tap water in a Cole-Parmer Aquatron A4000D automatic still. Double-lined supelinert gas bags were obtained from Sigma-Aldrich.

4.1.2.2 Supercritical Water Gasification Reactor Set-Up

The reactor consists of a 25 m coiled stainless-steel 316l pipe with an internal diameter of 3.87mm (nominal ¼”), located within a Carbolite Gero LHT oven (max temperature 600°C), which is maintained at the desired reaction temperature. The feedstock solution is kept suspended using a magnetic stirrer to ensure heterogenous elements (algae or Ru/C catalyst) do not settle and the feedstock is homogenous for the whole experiment. This feed is supplied by 2 Jasco Pu-2086 HPLC pumps, which maintain the desired flowrate to ensure a residence time of 32s. The flowrate used was 19.4,20 and 20.914ml/min for 450,500 and 550°C respectively. The reactor exit stream passes through a shell-and-tube heat exchanger to cool it to ambient temperature before flowing through a back pressure regulator (BPR) to maintain the pressure in the reactor and reduce the stream to ambient pressure. The pressure is maintained between 23 and 25MPa. The fluid stream is filtered before and after the BPR using a 2µm and 0.5µm filters respectively, to prevent blockages and solid material entering the liquid product. The filtered stream is admitted to a gas/liquid separator. The gas stream can then be either passed through a bubble column to measure flowrate or collected in a gas sampling bags for analysis. This is shown in Figure .

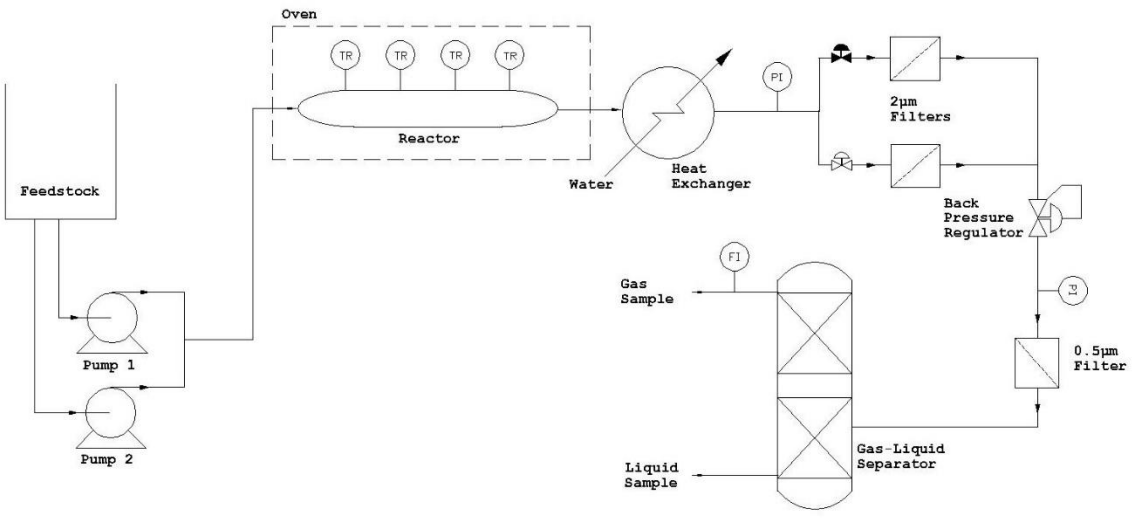

Figure 4.2 -Experimental set-up. Process flow diagram showing equipment used in the experiments.

Initially the oven is allowed to reach the desired temperature; the system is then fed with DW only and the pressure is gradually increased until the required pressure has been met. The correct quantity of feedstock (glucose or microalgae) is mixed with 500 ml of either DW or GW, along with the correct quantity of catalyst (if required) and shaken vigorously to obtain a homogenous mixture is achieved. If microalgae or the Ru/C catalyst is used, the solution is kept homogenous using a magnetic stirrer. The feedstock is then fed into the system until noticeable product is seen in the gas/liquid separator. Three flowrate measurements are taken over the 6 minutes following this, before switching to fill the gas bag until it is sufficiently filled. Samples of the liquid product are withdrawn regularly throughout. Following the reaction, the reactor is flushed with DW for 30minutes at reaction temperature before being allowed to cool. All experiments are repeated for each datapoint.

4.1.2.3 Analysis

The gas product is analysed using a Shimadzu 2014 Gas chromatography with a thermal conductivity detector (GC-TCD) and a 0.35 mm internal diameter, 20 m Shim Carbon ST column to determine the composition of the gas. The liquid product is analysed for total organic carbon (TOC) and which organic compounds were present. TOC was calculated using Spectroquant® TOC Cell test, following a 10x dilution with distilled water. To analyse the organic compounds in the liquid product, they were extracted overnight using a 4:1 ratio of dichloromethane: sample. The extract was passed through a Thermo Scientific Trace1600-ISQ7610 Gas chromatography-mass spectrometer (GC-MS), using helium as the carrier gas and a Restek Rxi-35Sil MS column with a 0.5 µm film thickness, a 0.25 mm inner diameter and 30 m length. The carbon that forms char or tar is calculated for the following equation, where C is the mass of carbon.

$$C_{\frac{tar}{Char}} = C_{Feed} - C_{Liquid} - C_{Gas} \quad (1)$$

Inorganic carbon produced through reaction of CO_2 with an alkaline media has been significant in experiments with hydroxide catalysts previously [40]. However, CO_2 absorbed due to the

increased pH of the GW was found to be negligible, so was not considered in the carbon balance. Analysis of the iron content in the liquid effluent was analysed using Inductively coupled plasma atomic emission spectroscopy (ICP).

The growth water composition (displayed in Table 4.2) was analysed by ICP-MS and colorimetric techniques which were performed by ALS Laboratories (UK) Limited, following dilution 10x with deionised water. All tests are repeated once and a two tailed t-test was performed to compare the gas composition (H_2, CH_4, CO, CO_2 vol.%) and carbon distribution (carbon in gas, liquid, tar/char) results between DW and GW across the whole data set. A p-value is produced for each output variable, which indicates the probability that the two data sets are different. This identifies if the differences observed when GW is used are significant or can be explained by the error observed in the data. A p-value< 0.05 is seen as significant.

4.1.3 Results and discussion

4.1.3.1 Glucose Gasification Without a Catalyst

SCWG of glucose was performed without a catalyst for a range of temperatures (450,500,550°C) at 2wt% glucose and a range of glucose concentrations (1wt.% ,2wt.%, 3wt.%) at 500°C. These were completed with either (DW) or (GW) to evaluate the difference effect of the GW at a range of temperatures and glucose concentrations. The composition of the gas product, total gas yield and distribution of carbon in the products are shown in Figure 4.3.

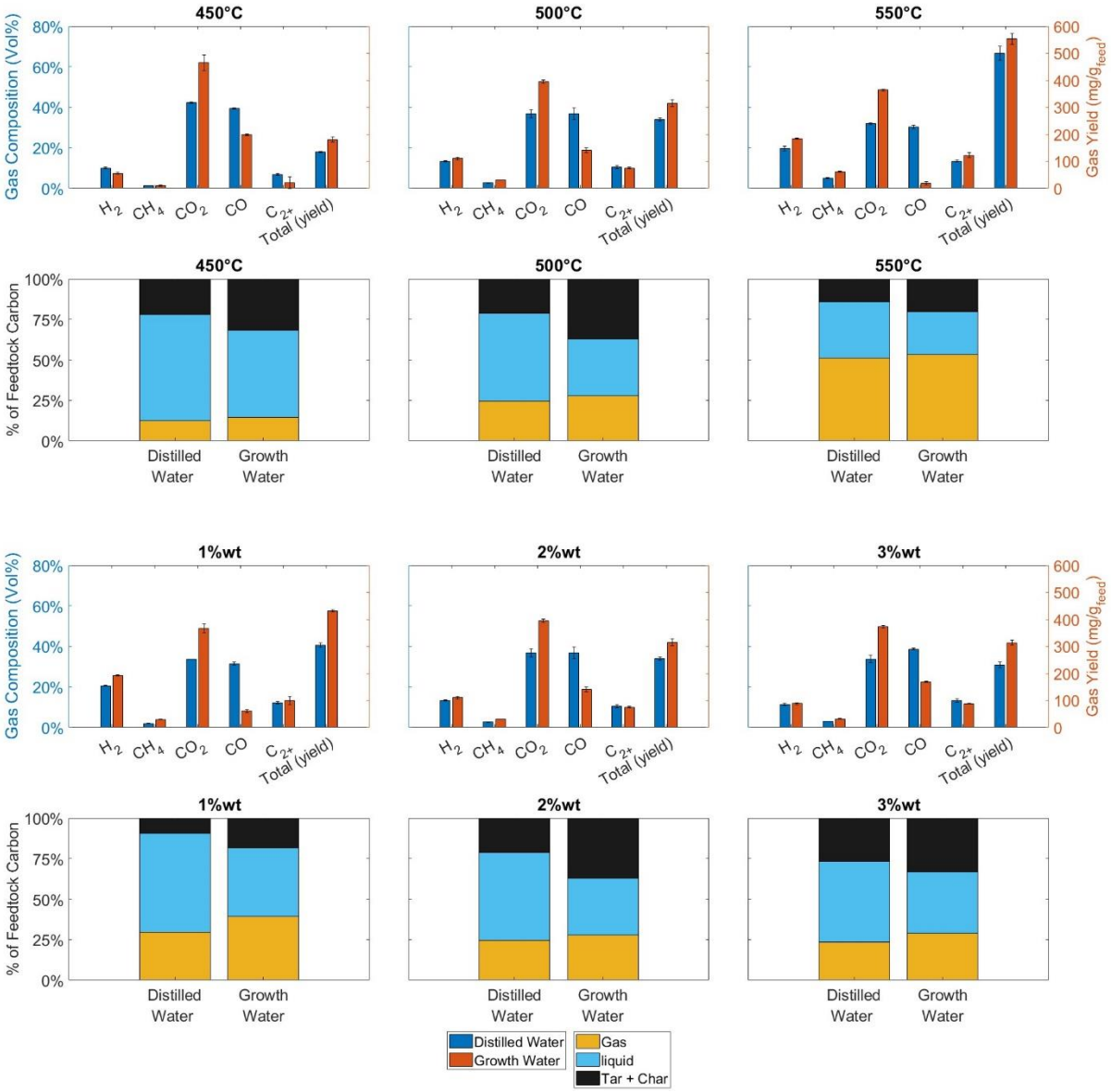

Figure 4.3-Results of the supercritical water gasification of glucose without a catalyst. In all cases: 32s residence time, 23-25MPa pressure. Rows 1,2, 2%wt glucose, temperatures 450-550°C. Rows 3,4, 1-3%wt glucose, temperature 500°C.

These results show a clear decrease in quantity of CO and increase of CO_2 in the gas stream across all the chosen temperatures and glucose concentrations when the GW is used. This is most pronounced when conditions favour gasification (low biomass concentration and high temperature), in which the CO concentration falls from ~30%vol with deionised water to < 8% with the growth water. These differences were shown to have statistical significance as the results of the T-test gave p-values of 0.00001 and 0.0001 for CO and CO_2 concentrations respectively. Increases in H_2, CH_4, and total gas were also observed, but they proved not to be significant in these results (p values of 0.54, 0.08 and 0.22 respectively).

A significant increase in CO_2 and decrease in CO with a less significant increase in total gas yield suggests gas phase reactions being catalysed, namely the water gas shift reaction (WGS). Potassium, sodium, and hydroxide ions are all present in the GW, which have been known to catalyse the WGS reaction in SCWG [22, 51, 52, 53] hence their catalytic influence may be present here. However, an increased WGS would also increase the hydrogen more significantly. Therefore, either the hydrogen is being consumed in subsequent reactions or a different ion in the medium is the cause of this phenomena, or a combination of the two. There are many ions present, many of which have never been specifically studied in SCWG, therefore it is difficult to be certain without further investigation.

There is also a clear decrease in the carbon remaining in the liquid following the reaction and a clear increase in the tar/char produced, when using growth water compared with distilled water. This difference was significant with p values of 0.01 being observed for both carbons remaining in liquid and in the tar/char. A notable increase in tar was observed visually on the filters when growth water is used, indicating the increase in precchar is predominantly due to an increase in tar. However, further work is needed to quantify the tar and char product separately, as this was not possible with the reactor set-up used for these reactions. An increase in the carbon in the gas was also observed but this increase was found to be insignificant (p value of 0.46).

Analysis of the liquid phase at 2 wt.% glucose and 500°C showed that the quantity of furans (furfural, furones and furaldehydes) was reduced by 85% in growth water SCWG compared to distilled water. The use of KOH on xylose, a similar compound to glucose, also showed a large reduction furfural compared with non-catalytic runs [44]. However, in that case the tar/char was lower than the non-catalytic example. Additionally, the quantity of phenols in the liquid product increased by 128% when using GW. Sinag et al. [45], observed similar effect when using KOH as a catalyst in the SCWG of glucose. This shows again, a similar impact to alkali catalysts, indicating the potassium and/or hydroxide ions contribute to the GW effect. However, as outlined later (Section 4.1.3.2), this is not the case when using KOH in study.

Furans such as furfural, and phenols are both known to be refractory in SCWG and precursors to the formation of tars and chars [36] [47]. Therefore, it would be expected that a decrease in furans observed when GW was used would increase the gas and reduce the tars/chars. However, an increase in phenols would have the opposite effect. Consequently, the increase in phenols counteracted most of the positive impact achieved through reduced furans. Additionally, the impact on tars/chars from the phenol increase is greater than from the furan decrease. This indicates that phenols are the main precursors for char formation in the SCWG of glucose. This is likely to be a result of the benzene ring being harder to break than the furan ring [46]. This should be considered when selecting a catalyst to minimise residue and thus reduce the potential for blockages in the reactor.

The formation of phenol in the SCWG of glucose has been proposed in two potential pathways. Through the dehydration and ring closure of furfural [57] [48] or Diels−Alder cycloaddition of a conjugated diene and unsaturated furanone [49]. In both these cases, phenol is the degradation product of a furan (furfural or furanone), so it is likely the GW catalyses one of or both of these reactions, resulting in a lower quantity of furans. The quantity of furfural was reduced by 95% but quantity of furone increased 4-fold. Indicating that the ring dehydration and ring closure of furfural was catalysed by the growth water. Additionally, Iron and chloride ions have been found to be effective dehydration catalysts when reacting pentose to form furfural at milder conditions [50]. Both of these are present in the GW and thus could contribute to this effect or the formation of furfural, thus further increasing the total phenol and tar/char.

The GW contains ions that are known to be corrosive to metals, such as OH^- or Cl^-, which would be expected to be most significant in the subcritical region when heating or cooling the reactor. In this experiment, no visual effects of corrosion were observed and ICP analysis of the liquid effluent showed a minimal increase in iron content when GW was present, thus the corrosion effects in this case were not noticeable. Nonetheless, the potential corrosive effects

of the GW should be considered in reactor design, as differing concentrations of some ions and longer running times could make the effects more significant.

4.1.3.2 Glucose Gasification With a Catalyst

SCWG of glucose was performed with either a homogenous catalyst (KOH) or a heterogenous catalyst (Ru/C). The latter was suspended in the glucose solution to ensure a homogenous feedstock. This was carried out with GW or DW as the reaction media to understand if the effects outlined in Section 4.1.4.1.3.1 still applied when a catalyst is present. The results are shown in Figure 4.4.

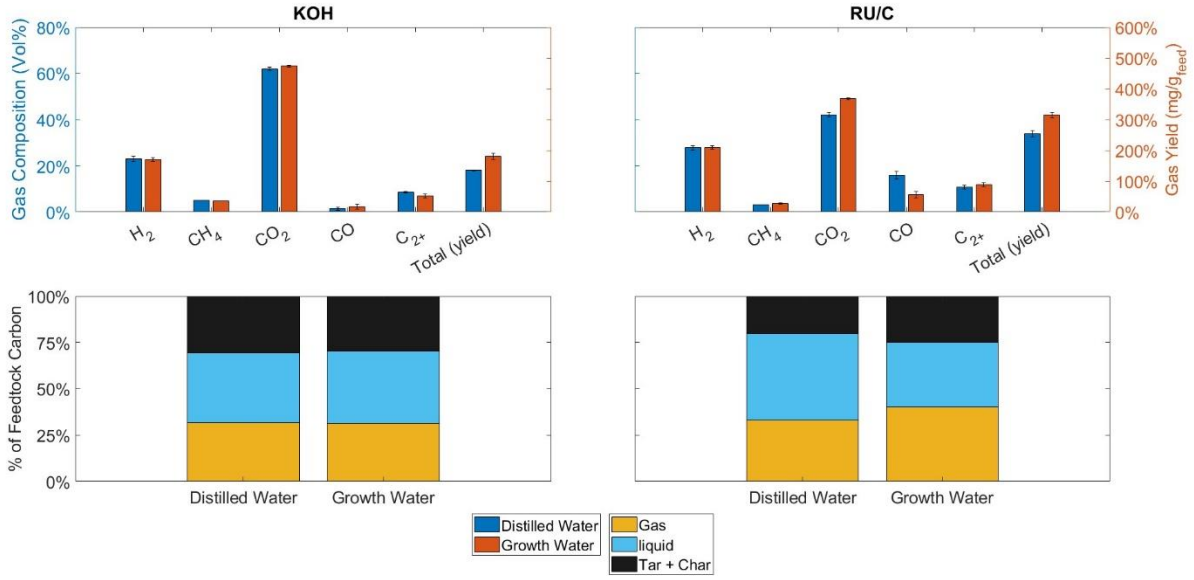

Figure 4.4 Results of the supercritical water gasification of glucose with a catalyst. 32s residence time, 23-25MPa pressure, 500°C temperature, 2wt% glucose, 0.1%wt catalyst concentration.

In the presence of the Ru/C catalyst a similar effect is observed as without a catalyst, a significant decrease in CO and increase in CO_2. Although, in this case less significant than without a catalyst with p-values of 0.02 and 0.01 respectively. This similarly is due to the catalytic activity of Ru/C being a result of hydrogen affinity, allowing it to catalyse reactions such as hydrogenation and steam reforming [45]. This effect of Ru/C catalysts breaks down the organic components but does not significantly catalyse the WGS reaction, resulting in large quantities of CO when DW was used. Therefore, the catalytic effect of the GW on the WGS reaction is still significant.

With Ru/C catalyst the increase in total gas and carbon in the gas stream in GW compared with DW was significant, with the increase in the total tar/char not being significant. This indicates that the carbon that remained in the liquid phase when using DW as the reaction media, which polymerised to tar/char in GW when no catalyst was present, is converted to gas in GW when a ruthenium catalyst is present. As outlined in Section 4.1.3.1, this is expected to be largely made up of furans and phenols, which the hydrogenation activity of Ruthenium is known to be effective at breaking down [45]. A significant decrease in phenol content was observed when Ru/C was present as was established in Section 4.1.4.1.3.1, proved to be the main driver for char/tar production. Thus, the increased degradation of phenol reduced the effect of GW on the tar/char. In this study, contrary to some literature [45], furan content increased in with the addition of Ru/C catalyst. Further evidencing phenol being the key driver in tar/char formation in the SCWG of glucose.

In the liquid product, when Ru/C was present, <1% of the furans were present when GW was used compared with DW, with an increased phenol content also being observed. However, the phenol content was still >3 times lower than without the presence of the Ru/C catalyst. This effect was similar to that observed in non-catalytic runs, except with a greater conversion of furans the majority of which, was furfural. As outlined in Section 4.1.3.1, the GW catalyses the conversion of furfural to phenols. The greater extent to which the furans are reduced when Ru/C is present can be explained by Le Chatelier's principle as the increased conversion of phenol to gas pushes the equilibrium to the phenol side, thus reducing the quantity of furfural. This can explain why the organic carbon that remains in the liquid phase in DW, was converted to gas with Ru/C present but to tar/char without a catalyst in GW. The GW catalyses the dehydration of furfural into phenol which, without a catalyst polymerises into char/tar but is readily gasified in the presence of Ru/C due to the strong hydrogenation activity of ruthenium.

In the presence of KOH, there is no significant difference to the gas composition, gas yield or carbon product distribution. This was carried out at the lowest catalyst concentration observed in the literature [13]. Therefore, in all cases where KOH was used as a catalyst, it is likely that

the observed results would be an accurate representation of a real system, despite not including GW as the reaction medium. This concentration is still over 3 times that of the GW thus indicating that the effect of GW is similar to KOH but lower in magnitude, resulting in it being partially masked when both are present. This adds further evidence that the effect of hydroxide (high pH), and or potassium and sodium ions in the salt are key in the effect of the GW, as proposed in Section 4.1.3.1

There is no significant quantity of furfural or furaldehyde present in the liquid product when KOH catalyst is used, with DW or GW. As a result, a decrease in both phenol and furan content is observed when using GW compared with DW. This indicates that the dominant driver in the catalysis of the dehydration of furfural to phenol is hydroxide or potassium ions in the GW. Despite this, the quantity of phenol was reduced in the presence of KOH, contrary to what was observed by Sinag et al [45]. This could be explained by a shift from furfural formation, towards formation of other intermediates such as aldehydes and ketones, which readily gasified so do not appear in significant quantities in the liquid product. This would explain the increased gas yield in the presence of KOH as they are more readily gasified. This may not have occurred in the experiments by Sinag et al [45] as their set up was in a batch reactor, with a much slower heating rate, which would significantly affect the intermediates formed in the sub-critical phase.

4.1.3.3 Microalgae Gasification

Microalgal biomass contains a quantity of inorganic material (similar to that present in the GW) that is released during the SCWG process. Therefore, to a verify the above results, gasification runs with microalgae must be conducted for comparison. An algal concentration of 0.7 wt.% was suspended in either DW or GW with a temperature of 500 °C. All other conditions matched those in the glucose gasification experiments. The results are displayed in Figure .

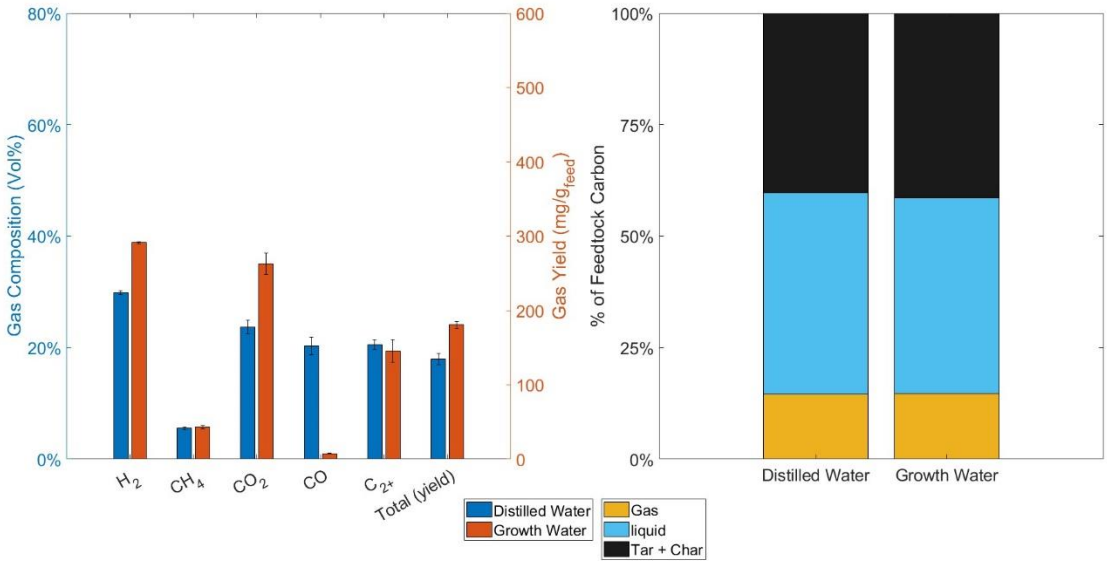

Figure 4.5- Results of the supercritical water gasification of Chlorella vulgaris without a catalyst. 32s residence time, 23-25MPa pressure, 500°C temperature, 0.7wt% biomass

In the SCWG of microalgae, the difference between using GW and DW as the reaction media, was even greater than the glucose examples. As with glucose, the CO reduced and CO_2 increased significantly, with the CO almost completely removed when GW was used. Additionally, the impact on hydrogen and total gas yield was greater than glucose, resulting in a statistically significant increase in hydrogen yield (p-value 0.001), even at this small sample size. However, unlike the glucose example, the carbon balance remained the same, with no significant change in the gas, liquid or tar/car. This indicates an increase in WGS reaction but minimal impact of the intermediate reaction pathway.

Glucose is a model compound representing carbohydrates, but that only typically represents a proportion (10-15% [45] [36] [11]) *of Chlorella vulgaris*. Therefore, the impact on the protein and lipid proportions of the algae is still unclear. This could be explained by the impact on the protein/lipid intermediates being less significant than on the dehydration of furfural. Alternatively, interactions between intermediate products of proteins and carbohydrates are known to produce N-cyclic compounds that are difficult to gasify, form tar/char and are known to be free radical scavengers [36]. Therefore, a possible interpretation is that these reactions dominate in the intermediates and are less impacted by the contents of the GW, thus only the

gas phase reactions are notable. This could explain the low gas and high tar/char yields. As a result, it would then be expected that algal strains with higher carbohydrate content would have a greater impact on the carbon distribution, as the impact of the furfural dehydration would be more significant.

Nonetheless, the large disparity in gas composition confirms the significant impact of the GW on the results of the SCWG of microalgae. Thus, it is important to consider when performing lab-based experiments to best understand the process in a real-life context. Furthermore, this analysis was only performed on one growth medium and one microalga, but different algal strains prefer different concentrations of ions, pH (Hydroxide ions) and growth period. Therefore, the impact of the GW on the reaction would vary. Additionally, the hydroxide ions are formed due to the removal of CO_2 by the alga hence may vary depending on gas feed rate, CO_2 % in gas, and growth rate. Therefore, this should be considered when choosing an alga and growth conditions for SCWG, as to maximise favourable products mainly hydrogen and reduce unwanted products, while minimising additional catalysts required. For example, some blue-green alga (cyanobacteria) can be grown at elevated pH [51], which increases hydroxide ions, which were outlined to have a significant impact on SCWG. Although the impact of the differing compositions of the algal strains [62], and impact on the algal growth must also be accounted for when selecting an alga and growth media.

4.1.4 Conclusion

The use of algal growth water as the reaction medium has a significant impact on the SCWG of glucose and microalgae when no catalyst or Ru/C catalyst are used. Specifically, the CO content in the gas is reduced and the CO_2 content is increased, due to the catalytic activity of potassium, sodium and hydroxide ions present in the media on the water gas shift reaction. Hence, when using an alkali catalyst such as KOH, no significant effect is observed when using the growth water. Additionally, the growth water catalysed the dehydration of furfural to phenol, which resulted in an increased tar/char yield in non-catalytic SCWG of glucose. However, in the presence of either catalyst this was not the case. This was due to the activity

for the breakdown of phenols by Ru/C and the suppression of the formation of furfural by KOH. Consequently, it is important to consider the GW in laboratory experiments to accurately represent real systems, especially if no catalyst or heterogenous metal catalysts (such as Ru/C) are present. Additionally, this impact should be considered in choice of algal strain and growth media, as to maximise desirable products with reduced catalyst requirements.

4.1.5 References

[1] Intergovernmental Panel on Climate Change: Working Group 3, “Climate Change 2022-Mitigation of Climate Change,” Intergovernmental Panel on Climate Change, Geneva, 2022.

[2] M. Dorgham, “Effects of Eutrophication.,” in *Eutrophication: Causes, Consequences and Control*, Dordrecht, Springer, 2014. doi:10.1007/978-94-007-7814-6_3.

[3] F. Geiger and etal, “Persistent negative effects of pesticides on biodiversity and biological control potential on European farmland,” *Basic and Appl. Ecology,* vol. 11, no. 2, pp. 97-105, 2010. doi:10.1016/j.baae.2009.12.001.

[4] M. S. Yahya, M. Syafiq, A. Ashton-Butt, A. Ghazali, S. Asmah and B. Azhar, “Switching from monoculture to polyculture farming benefits birds in oil palm production landscapes: Evidence from mist netting data,” *Ecology and Evolution,* vol. 7, no. 16, p. 6, 2017. doi:10.1002/ece3.3205.

[5] J. Tomei and R. Helliwell, “Food versus fuel? Going beyond biofuels,” *Land Use Policy,* vol. 56, pp. 320-236, 2016. doi:10.1016/j.landusepol.2015.11.015.

[6] M. Benedetti, V. Vecchi, S. Barera and L. Dall’Osto, “Biomass from microalgae: the potential of domestication towards sustainable biofactories,” *Microb Cell Factories,* vol. 17, no. 173, 2018. doi:10.1186/s12934-018-1019-3.

[7] Y. Yoshida, K. Dowaki, Y. Matsumura, R. Matsuhashi, D. Li, H. Ishitani and H. Komiyama, “Comprehensive comparison of efficiency and CO2 emissions between biomass energy conversion technologies—position of supercritical water gasification in biomass technologies,” *Biomass and Bioenergy,* vol. 25, no. 3, pp. 257-272, 2003. doi:10.1016/S0961-9534(03)00016-3.

[8] N. Akiya and P. E. Savage, “Roles of Water for Chemical Reactions in High-Temperature Water,” *Chem. Reviews,* vol. 102, no. 8, pp. 2725-2750, 2002. doi:10.1021/cr000668w.

[9] C. Wang, W. Zhu, H. Zhang, C. Chen, X. Fan and Y. Su, “Char and tar formation during hydrothermal gasification of dewatered sewage sludge in subcritical and supercritical water: Influence of reaction parameters and lumped reaction kinetics,” *Waste Management,* vol. 100, pp. 57-65, 2019. doi:10.1016/j.wasman.2019.09.011.

[10] S. Stucki, F. Vogel, C. Ludwig, A. G. Haiduc and M. Brandenberger, “Catalytic gasification of algae in supercritical water for biofuel production and carbon capture,” *Energy and Environ Sci,* vol. 2, pp. 535-541, 2009. doi:10.1039/B819874H.

[11] L. Tiong, M. Komiyama, Y. Uemura and T. T. Nguyen, “Catalytic supercritical water gasification of microalgae: Comparison of *Chlorella vulgaris* and Scenedesmus quadricauda,” *The J. of Supercrit. Fluids,* vol. 107, pp. 408-413, January 2016. doi:10.1016/j.supflu.2015.10.009.

[12] J. A. Onwudili, A. R. Lea-Langton, A. B. Ross and P. T. Williams, “Catalytic hydrothermal gasification of algae for hydrogen production: Composition of reaction products and potential for nutrient recycling,” *Bioresour. Technol.,* vol. 127, pp. 72-80, January 2013. doi:10.1016/j.biortech.2012.10.020.

[13] V. Krishnan, S. Thachanan, Y. Matsumura and Y. Uemura, “Supercritical Water Gasification on Three Types of Microalgae in the Presence and Absence of Catalyst and Salt,” *Procedia Eng.,* vol. 148, pp. 594-599, 2016. doi:10.1080/15567036.2016.1270375.

[14] A. G. Chakinala and W. P. v. S. a. S. R. A. K. Derk W. F. (Wim) Brilman, “Catalytic and Non-catalytic Supercritical Water Gasification of Microalgae and Glycerol,” *Ind. and Eng. Chem. Res.,* vol. 49, no. 3, pp. 1113-1122, Septemeber 2010. doi:10.1021/ie9008293.

[15] S. Elsayed, N. Boukis, D. Patzelt, S. Hindersin, M. Kerner and J. Sauer, “Gasification of Microalgae Using Supercritical Water and the Potential of Effluent Recycling,” *Chem. Eng. & Tech.,* vol. 39, no. 2, November 2015. doi:10.1002/ceat.201500146.

[16] D. J. Patzelt, S. Hindersin, S. Elsayed, N. Boukis, M. Kerner and D. Hanelt, “Hydrothermal gasification of Acutodesmus obliquus for renewable energy production and nutrient recycling of microalgal mass cultures,” *J. of Appl. Phycology,* vol. 27, pp. 2239-2250, Decemeber 2014. doi:10.1007/s10811-014-0496-y.

[17] G. Caputo, M. Dispenza, P. Rubio, F. Scargiali, G. Marotta and A. Brucato, “Supercritical water gasification of microalgae and their constituents in a continuous reactor,” *The J. of Supercrit. Fluids,* vol. 118, pp. 163-170, December 2016. doi:10.1016/j.supflu.2016.08.007.

[18] L.-F. Xie, P.-G. Duan, J.-L. Jiao and Y.-P. Xu, “Hydrothermal gasification of microalgae over nickel catalysts for production of hydrogen-rich fuel gas: Effect of zeolite supports,” *Int. J. of Hydrog. Energy,* vol. 44, no. 11, pp. 5114-5124, 2019. doi:0.1016/j.ijhydene.2018.09.175.

[19] R. Samiee-Zafarghandi, A. Hadi and J. Karimi-Sabet, “Graphene-supported metal nanoparticles as novel catalysts for syngas production using supercritical water gasification of microalgae,” *Biomass and Bioenergy,* vol. 121, pp. 13-21, 2019. doi:10.1016/j.biombioe.2018.11.035.

[20] P.-G. Duan, S.-C. Li, J.-L. Jiao, F. Wang and Y.-P. Xu, “Supercritical water gasification of microalgae over a two-component catalyst mixture,” *Sci of The Total Environ.,* vol. 630, pp. 243-253, 2018. doi:10.1016/j.scitotenv.2018.02.226.

[21] M. M. Hossain, “Production of H2 from Microalgae Biomass in Supercritical Water Using a Ni/La-γAl2O3 Catalyst,” *Energy Procedia,* vol. 110, pp. 384-389, 2017. doi:10.1016/j.egypro.2017.03.157.

[22] L. Tiong and M. Komiyama, “Supercritical water gasification of microalga *Chlorella vulgaris* over supported Ru,” *The J. of Supercrit. Fluids,* vol. 144, pp. 1-7, 2019. doi:10.1016/j.supflu.2018.05.011.

[23] R. Samiee-Zafarghandi, J. Karimi-Sabet, M. A. Abdoli and A. Karbassi, “Supercritical water gasification of microalga *Chlorella PTCC* 6010 for hydrogen production: Box-Behnken optimization and evaluating catalytic effect of MnO2/SiO2 and NiO/SiO2,” *Renew. Energy,* vol. 126, pp. 189-201, 2018. doi:10.1016/j.renene.2018.03.043.

[24] M. Bagnoud-Velásquez, M. Brandenberger, F. Vogel and C. Ludwig, “Continuous catalytic hydrothermal gasification of algal biomass and case study on toxicity of aluminum as a step toward effluents recycling,” *Catal. Today,* vol. 223, pp. 35-43, 2014. doi:10.1016/j.cattod.2013.12.001.

[25] D. Fozer, B. Kiss, L. Lorincz, E. Szekely, P. Mizsey and A. Nemeth, “Improvement of microalgae biomass productivity and subsequent biogas yield of hydrothermal gasification via optimization of illumination,” *Renew. Energy,* vol. 138, pp. 1262-1272, August 2019. doi:10.1016/j.renene.2018.12.122.

[26] R. Samiee-Zafarghandi, J. Karimi-Sabet, M. A. Abdoli and A. Karbassi, “Increasing microalgal carbohydrate content for hydrothermal gasification purposes,” *Renew.energy,* vol. 116, no. A, pp. 710-719, February 2018. doi:10.1016/j.renene.2017.10.020.

[27] P. R. Nurcahyani, S. Hashimoto and Y. Matsumura, “Supercritical water gasification of microalgae with and without oil extraction,” *The J. of Supercrit. Fluids,* vol. 165, 2020. doi:10.1016/j.supflu.2020.104936.

[28] J. Jiao, F. Wang, P. Duan, Y. Xu and W. Yan, “Catalytic hydrothermal gasification of microalgae for producing hydrogen and methane-rich gas,” *Energy Sources, Part A: Recovery, Util., and Environ. Eff.,* vol. 39, no. 9, pp. 851-860, 2017. doi:10.1080/15567036.2016.1270375.

[29] A. Miller, D. Hendry, N. Wilkinson, C. Venkitasamy and W. Jacoby, “Exploration of the gasification of Spirulina algae in supercritical water,” *Bioresource Tech.,* vol. 119, pp. 41-47, 2012. doi:10.1016/j.biortech.2012.05.005.

[30] G. Peng, F. Vogel, D. Refardt and C. Ludwig, “Catalytic Supercritical Water Gasification: Continuous Methanization of *Chlorella vulgaris*,” *Ind. and Eng. Chem. Res.,* vol. 56, no. 21, pp. 6256-6265, 2017. doi:10.1021/acs.iecr.7b00042.

[31] G. Sztancs, L. Juhasz, B. J. Nagy, A. Nemeth, A. Selim, A. Andre, A. J. Toth, P. Mizsey and D. Fozer, “Co-Hydrothermal gasification of *Chlorella vulgaris* and hydrochar: The effects of waste-to-solid biofuel production and blending concentration on biogas generation,” *Bioresource Tech.,* vol. 302, 2020. doi:10.1016/j.biortech.2020.122793.

[32] H. Zhang, W. Zhu, Z. Xu and M. Gong, “Gasification of cyanobacterial in supercritical water,” *Environ. Tech.,* vol. 35, no. 22, pp. 2788-2795, 2014. doi:10.1080/09593330.2014.922126.

[33] H. Zhang and X. Zhang, “Phase behavior and stabilization of phosphorus in sub- and supercritical water gasification of cyanobacteria,” *The J. of Supercrit. Fluids,* vol. 130, pp. 40-46, 2017. doi:10.1016/j.supflu.2017.07.030.

[34] Q. Yan, L. Guo and Y. Lu, “Thermodynamic analysis of hydrogen production from biomass gasification in supercritical water,” *Energy Convers. and Management,* vol. 47, no. 11-12, pp. 1515-1528, July 2006. doi:10.1016/j.enconman.2005.08.004.

[35] A. G. Chakinala, D. W. F. (. Brilman, W. P. v. Swaaij and S. R. A. Kersten, “Catalytic and Non-catalytic Supercritical Water Gasification of Microalgae and Glycerol,” *Ind. and Eng. Chem. Res.,* vol. 49, no. 3, pp. 1113-1122, Septemeber 2010. doi:10.1021/ie9008293.

[36] N. Wei, D. Xu, B. Hao, S. Guo, Y. Guo and S. Wang, “Chemical reactions of organic compounds in supercritical water gasification and oxidation,” *Water Res.,* vol. 190, 2021. doi:10.1016/j.watres.2020.116634.

[37] C. Zhu, L. Guo, H. Jin, J. Huang, S. Li and X. Lian, “Effects of reaction time and catalyst on gasification of glucose in supercritical water: Detailed reaction pathway and mechanisms,” *Int. J. of Hydrogen Energy,* vol. 41, no. 16, pp. 6630-6639, May 2016. doi:10.1016/j.ijhydene.2016.03.035.

[38] K. Heeley, R. L. Orozco, L. E. Macaskie, J. Love and B. Al-Duri, “Supercritical water gasification of microalgal biomass for hydrogen production-A review,” *Int. J. of Hydrogen Energy,* 2023. doi:10.1016/j.ijhydene.2023.08.081.

[39] K. Raunkjær, T. Hvitved-Jacobsen and P. Halkjær Nielsen, “Measurement of pools of protein, carbohydrate and lipid in domestic wastewater,” *Water Research,* vol. 28, no. 2, pp. 251-262, 1994 doi:10.1016/0043-1354(94)90261-5.

[40] l. J. Sheikhdavoodi, M. Almassi, M. Ebrahimi-Nik, A. Kruse and H. Bahrami, “Gasification of sugarcane bagasse in supercritical water; evaluation of alkali catalysts for maximum hydrogen production,” *J. of the Energy Ins.,* vol. 88, no. 4, pp. 450-458, November 2015. doi:10.1016/j.joei.2014.10.005.

[41] H. Schmieder, J. Abeln, N. Boukis, E. Dinjus, A. Kruse, M. Kluth, G. Petrich, E. Sadri and M. Schacht, “Hydrothermal gasification of biomass and organic wastes,” *The Journal of Supercritical Fluids,* vol. 17, no. 2, pp. 145-153, April 2000 doi:10.1016/S0896-8446(99)00051-0.

[42] S. Nanda, S. N. Reddy, H. N. Hunter, A. K. Dalai and J. A. Kozinski, “Supercritical water gasification of fructose as a model compound for waste fruits and vegetables,” *The Jounal of Supercritical fluids,* vol. 104, pp. 112-121, September 2015 doi:10.1016/j.supflu.2015.05.009.

[43] M. Watanabe, H. Inomata and K. Arai, “Catalytic hydrogen generation from biomass (glucose and cellulose) with ZrO2 in supercritical water,” *Biomass and Bioenergy,* vol. 22, no. 5, pp. 405-410, 2002 doi:10.1016/S0961-9534(02)00017-X.

[44] D. S. Gökkaya, M. Sağlam, M. Yüksel, T. G. Madenoğlu and L. Ballice, “Characterization of products evolved from supercritical water gasification of xylose (principal sugar in hemicellulose),” *Energy Sources, Part A: Recovery, Utilization, and Environ Effects,* vol. 38, no. 11, pp. 1503-1511, 2016. doi:10.1080/15567036.2014.914109.

[45] A. Sinag, A. Kruse and J. Rathert, “Influence of the Heating Rate and the Type of Catalyst on the Formation of Key Intermediates and on the Generation of Gases during Hydropyrolysis of Glucose in Supercritical Water in a Batch Reactor,” *Ind. and eng. chem. res.,* vol. 43, no. 2, pp. 502-508, 2004. doi:10.1021/ie030475.

[46] A. Chuntanapum and Y. Matsumura, “Formation of Tarry Material from 5-HMF in Subcritical and Supercritical Water,” *Ind. Eng. Chem. Res.,* vol. 48, no. 22, pp. 9837-9846, 2009. doi:10.1021/ie900423g.

[47] A. Kruse, T. Henningsen, A. Sınağ and J. Pfeiffer, “Biomass Gasification in Supercritical Water: Influence of the Dry Matter Content and the Formation of Phenols,” *Ind. & Eng. Chem. Res.,* vol. 42, no. 16, pp. 3711-3717, 2003. doi:10.1021/ie0209430.

[48] A. Kruse and E. Dinjus, “Hot compressed water as reaction medium and reactant: 2. Degradation reactions,” *The J. of Supercrit. Fluids,* vol. 41, no. 3, pp. 361-379, 2007. doi:10.1016/j.supflu.2006.12.006.

[49] P. T. Williams and J. Onwudili, “Composition of Products from the Supercritical Water Gasification of Glucose: A Model Biomass Compound,” *Ind. & Eng. Chem. Res.,* vol. 44, no. 23, pp. 8739-8749, October 2005. doi:10.1021/ie050733y.

[50] B. Danon, G. Marcotullio and W. d. Jong, “Mechanistic and kinetic aspects of pentose dehydration towards furfural in aqueous media employing homogeneous catalysis,” *Green Chemistry,* vol. 16, pp. 39-54, 2014. doi:10.1039/C3GC41351A.

[51] M. Haines, A. Vadlamani, W. D. L. Richardson and M. Strous, “Pilot-scale outdoor trial of a cyanobacterial consortium at pH 11 in a photobioreactor at high latitude,” *Bioresource Tech.,* vol. 354, 2022. doi:10.1016/j.biortech.2022.127173.

[52] R. Samiee-Zafarghandi, J. Karimi-Sabet, M. A. Abdoli and A. Karbassi, “Increasing microalgal carbohydrate content for hydrothermal gasification purposes,” *Renewable energy,* vol. 116, no. A, pp. 710-719, February 2018 Doi:10.1016/j.renene.2017.10.020.

4.2 FURTHER DISCUSSION

This work clearly outlines that the algal growth water has a significant influence on SCWG, when compared with distilled water. Separation of the growth media and use of distilled water would result in unnecessary energy losses, thus the application of microalgal SCWG in industry would use the growth water as the reaction medium. Consequently, to ensure the reaction environment is representative of a real system growth water was utilised as the reaction medium in subsequent experimental work. This was either the water remaining after growth of *Chlorella vulgaris,* as outlined in Chapter 3, or a mixture of salts that has an ion content and pH comparable that of the growth water.

CHAPTER 5: ASSESSMENT OF IRON(III) CHLORIDE AS A CATALYST FOR THE PRODUCTION OF HYDROGEN FROM THE SUPERCRITICAL WATER GASIFICATION OF MICROALGAE

The research within this chapter subsection has been accepted for publication as journal article in *Next Energy*. At the time of submission, the paper is in production so cannot be presented in the exact format of the journal. However, for consistency with the published material, the content and structure are identical to the published work.

ABSTRACT

Alkali metal salts and supported transition metals have been the dominant catalysts used to maximise hydrogen production from supercritical water gasification (SCWG). Recently, $FeCl_3$ has emerged as an alternative to these that has been found to be more effective in some cases reported in literature. However, to these authors' knowledge, few studies exist that study this catalyst with none that involve microalgae as the feedstock. Investigation is reported into the effect of $FeCl_3$ on the SCWG of *Chlorella vulgaris* for a range of temperatures (400-600°C) and biomass concentrations (1-3wt.%), with comparisons made to other catalysts (KOH, Ru/C and their combinations). A significant decrease in hydrogen yield, carbon conversion and energy efficiency was observed with the addition of $FeCl_3$, due to a reduced pH which supressed the water gas shift reaction and catalysed of char forming reactions. This was in contrary to Ru/C and KOH catalysts, where those outcomes increased. Additionally, when $FeCl_3$ was used with Ru/C, the ruthenium was poisoned, nullifying its positive effects. Consequently, $FeCl_3$ is not a suitable catalyst for hydrogen production from microalgae, either alone or in conjunction with a ruthenium catalyst.

5.1 INTRODUCTION

To limit global warming to 1.5°C above pre-industrial levels, carbon removal technologies are expected to be key to which, bioenergy with carbon capture and storage (BECCS) is expected to be a major contributor [1]. Consequently, deployment of new bioenergy projects is rapidly required. However, biomass production often results in negative environmental and social impacts. Large monocultures [2], the use of pesticides [3] and fertilizer run off causing eutrophication in waterways [4] are all damaging to biodiversity. Additionally, food prices can be impacted by the competition for land and fertilizers [5].

Microalgae requires far less land than other biomass sources as it can grow 10 times faster than terrestrial plants [6]. Additionally, the use of pesticides or arable land are not required, and nutrients used are contained so they do not enter waterways. Despite this, the high-moisture content of microalgae has an adverse effect on the efficiency of conventional energy conversion processes such as thermal gasification or pyrolysis [7]. Therefore, alternative methods of extracting the energy and carbon from the algae are required.

Supercritical water gasification (SCWG) produces a gaseous product consisting of H_2, CH_4, CO, CO_2, and short chain hydrocarbons, using water above its critical point (374°C and 22.1MPa) as the reaction medium. The CO_2 can then be captured for storage, leaving a highly combustible gas stream, which can be used for a variety of energy applications, making this an ideal BECCS process. Additionally, hydrogen, expected to be key resource in decarbonising many hard to abate sectors, replacing existing fossil fuels [8], can be separated out from this gas stream.

The use of water makes it appropriate for high moisture feeds such as microalgae and the thermophysical properties of supercritical water (SCW) brings other advantages. The low viscosity and density of SCW increases the diffusivity, resulting in increased reaction rates [9]. Additionally, the low dielectric constant and weakened hydrogen bonds allow organic

intermediates formed during the reaction to dissolve, reducing recombination to form tars and chars [10], which are undesirable as they limit operability and reduce gas yield.

It is well documented that higher temperatures and lower biomass concentrations are preferable for maximising biomass conversion and hydrogen yield in SCWG [11]. However, in real systems the increased energy losses [12] and cost of equipment required with extreme temperatures can limit the feasibility of the process. Therefore, catalysts are often employed, to maximise yields at milder conditions. The catalysts used in literature on the SCWG of various biomass feedstocks is shown in Table 5.1 and Table 5.2. A more detailed description of how each catalyst performs can be found in a previous literature study by these authors [11].

Table 5.1- Heterogenous catalysts used in the supercritical water gasification of biomass.

Catalyst	Supports used	Feedstocks used	Sources
Ni	• Al_2O_3 • SiO_2 • Al_2O_3- SiO_2 • ZrO_2 • Zeolite • Activated Carbon • Graphene Oxide • Hydrotalcite • No support	• *Chlorella vulgaris* • *Scenedesmus quadricauda* • *Spirulina platensis* • *Nannochloropsis oculata* • *Chlorella sp.* • *Chlorella pyrenoidosa* • *Enteromorpha intestinalis* • Glucose • Fermentation stillage • Cellulose • Xylan • Lignin • Bark • Oleic Acid • Switchgrass Biocrude • Xylose • Valine • Sugarcane bagasse • Fructose • Sewage sludge, • Sawdust • Rice straw • *Enteromorpha prolifera*	[15] [16] [17] [18] [19] [20] [21] [22] [23] [24] [25] [26] [27] [28] [20] [15] [19] [29] [20] [30] [31] [32] [33] [34] [35] [36]
Ru	• Al_2O_3 • ZrO_2 • Zeolite • Activated carbon • TiO_2 • No Support	• *Chlorella vulgaris* • *Enteromorpha intestinalis* • *Laminaria digitata* • *Laminaria hyperborea* • *Saccharina latissimi* • *Alaria esculenta* • *Spirulina platensis* • *Phaeodactylum tricornutumpr* • *Chlorella pyrenoidosa* • *Nannochloropsis species* • *Schizochytrium limacinum* • Glucose • Cellulose • Fructose • Xylan • Pulp • Alkali lignin • Bark • Fermentation stillage • Xylose • Oleic acid • switchgrass biocrude	[37] [20] [19] [26] [38] [23] [33] [39] [40] [37] [41] [37] [42] [40] [20] [19] [26] [43] [44] [31] [24] [34]
Co-Mo	• Al_2O_3	• *Chlorella vulgaris*	[31]
Pt-Pd	• Al_2O_3	• *Chlorella vulgaris*	[31]
Co	• Graphene oxide	• *Chlorella sp* • Switchgrass Biocrude	[28] [24]
Cu	• Graphene oxide • No support	• *Chlorella sp* • Methanol	[28] [45]
Cr	• Graphene oxide	• *Chlorella sp*	[28]
Mn	• Graphene oxide	• *Chlorella sp*	[28]
Fe	• No support	• Banana Stem • Lignin • Cellulose	[34] [46]

Table 5.2-Homogenous catalysts used in the supercritical water gasification of biomass.

Catalyst	Feedstocks used	Source
KOH	• Sawdust • Straw • Sewage sludge • Lignin • Glycine • Glucose • Catechol • Fructose • Xylose • Cellulose • Sugarcane bagasse • *Enteromorpha prolifera*	[29] [47] [26] [48] [49] [36]
NaOH	• *Chlorella vulgaris* • *Spirulina platensis* • *Saccharina latissimi* • Fructose • Sugarcane bagasse	[29] [48] [16] [50]
K_2CO_3	• *Nannochloropsis gaditana* • *Acutodesmus obliquus* • Sawdust • Straw • Sewage sludge • Lignin • Glycine • Glucose • Catechol • Xylose • Sugarcane bagasse • Cauliflower residue • Acorn • Tomato residue • Hazelnut shell • Glycerol • *Enteromorpha prolifera*	[51] [49] [29] [26] [31] [52] [53] [30] [54] [36]
Na_2CO_3	• *Nannochloropsis gaditana* • Leucine • Glutamic acid • Glycine	[51]
$KHCO_3$	• Sugarcane bagasse	[29]
$NaHCO_3$	• Sugarcane bagasse	[29]
Trona ($Na_2CO_3 \cdot NaHCO_3 \cdot 2H_2O$)	• Cauliflower residue • Acorn • Tomato residue • Hazelnut shell	[52]
$FeCl_3$	• Humic acid • Food waste	[55] [56] [57] [58]
$AlCl_3$	• Humic acid • *Enteromorpha prolifera* • Guaiacol • Alanine • Glycerol	[36] [59] [58]

Table 5.1 and Table 5.2 show that the majority of the research has been focused on alkali metal salts (most commonly KOH, NaOH, K_2CO_3) as homogenous catalysts or supported transition metal catalysts (most commonly nickel or ruthenium). However, a machine learning model by Li et al. [58], predicted that a $FeCl_3$ catalyst would produce the highest hydrogen yields, surpassing that of nickel, ruthenium, and alkali metal salts. The body of literature for $FeCl_3$ and other iron catalysts used in this model is far less extensive than the aforementioned catalysts and no research to date considers the SCWG of microalgae specifically. Therefore, the reliability of this model at predicting catalyst performance on microalgae is limited, but it does suggest that $FeCl_3$ has the potential to be an effective catalyst. It also has a lower cost much lower cost associated than ruthenium catalysts (over 10x to that of Ru/C catalysts with 5wt.% metal loading) and is similar in cost to alkali metal salts [59].

Gong et al. [53] used $FeCl_3$ to catalyse the SCWG of humic acid. They found that it was more effective than alkali salts (K_2CO_3) and heterogenous metal catalysts (alumina-silica supported nickel) at increasing hydrogen yield and the total gas yield. Also, analysis of the chars produced suggested an increase in steam reforming and ring opening reactions. A positive impact of $FeCl_3$ on hydrogen yield was also observed in the SCWG of Athabasca bitumen or food waste [60] [54] and the hydrothermal liquefaction of peat [61].

In other fields, $FeCl_3$ has been employed as a catalyst due its strong Lewis acidity. These include the Aza-Diels–Alder Reaction of dienes and imines [62], hydrothermal carbonisation of biomass [63] [64] [65] and amide bond formation [66]. Red mud (38% Fe_2O_3) increased the hydrogen yield in the SCWG of sunflower stalk, corncob and leather waste [67], more effectively than Raney nickel, but not the alkali catalyst (K_2CO_3). Additionally, Fe_3O_4 was successfully used to catalyse the water gas shift reaction, but it was less effective than metal catalysts (Ru/C and Pd/ $LaCoO_3$) [68].

However, to this authors knowledge $FeCl_3$ has never been applied algal feedstocks, which differ greatly in composition to humic acid, bitumen or peat. Moreover, existing work only considers batch processes with long reaction times, which are not representative of potential

industrial scenario. This paper assesses the effectiveness of $FeCl_3$ as a catalyst for the production of hydrogen from the continuous SCWG of microalgae. SCWG of the microalga *Chlorella vulgaris* was performed with and without an $FeCl_3$ catalyst for a range of temperatures (400-600°C) and concentrations (1-3wt.%). As previous work found that the growth medium can significantly impact the SCWG reaction [69], the reaction media used was the algal growth water (GW), obtained after two weeks of growth, to ensure that the experiments are as close to a realistic industrial scenario as possible. Comparisons with alkali salt (KOH) and transition metal (Ru/C) catalysts were also performed.

5.2 MATERIALS AND METHODS

5.2.1 Materials

The microalga used was *Chlorella vulgaris* obtained as a spray dried powder from Sevenhills Wholefoods. The composition of the microalgae was provided by the supplier and the elemental analysis (C, H, N, S) was performed using a CE Instruments EA1110 elemental analyser, the remaining weight was assumed to be oxygen content, these are shown in Table 5.3.

Table 5.3-Composition of Chlorella vulgaris feedstock.

Component	Composition (wt%)
Carbohydrates	24.4
Proteins	64.5
Lipids	1.8
Ash	9.3
C	49.1
H	6.48
O	33.92

The algal growth water, used as the reaction medium, was obtained by growing *Chlorella vulgari*s in two parallel 5L stirred tank vessels, with a working volume of 4 L each (8l in total). The whole system was sparged with 4 L min-1 of air (~.04% CO_2). The reactors were constantly illuminated by two panels of white LED lights with a light intensity at the wall of the reactors of 25 W m^{-2}. The growth medium used was chu-13, as outlined in Chapter 3, with the

pH adjusted to 7.5 using 2M sodium hydroxide. The culture was grown for two weeks, with centrifugal separation of algae from the growth medium. The GW was autoclaved at 120 °C for 20 minutes, before storing in darkness at room temperature until required. No further precipitation of the medium was observed, and the composition of the resulting GW was analysed by Inductively Coupled Plasma Spectroscopy (Perkin Elmer Optima 8000 ICP-OES) and Ion Chromatography (Thermo Scientific Dionex ICS-200 and Integrion for anion and cations respectively). The GW had an average pH of 8.4 ,132mg/l of organic carbon, 200mg/l of inorganic carbon and the composition of ions displayed in Table 5.4. The feedstock pH becomes 2 and 13.5 when FeCl3 and KOH are used respectively. The feedstock pH is unaffected by the Ru/C catalyst.

Table 5.4-Growth water ion composition.

Ion	Average Concentration (mg/l)	Standard deviation
Potassium	222	26
Sulphate	78	6.5
Sodium	48	5
Chloride	58	3
Calcium	25	17
Magnesium	24	3
Phosphate	5	0.5
Iron	1.6	0.2
Zinc	0.06	0.05
Molybdate	0.1	0.01
Copper	0.03	0.001
Cobalt	0.0029	0.001
Nitrate	2.57	1

Potassium hydroxide >85% (KOH), Hydrochloric acid 37.5% (HCL) and Iron (III) Chloride >98.5% ($FeCl_3$) were obtained from VWR. Ruthenium (5wt.%) catalyst supported on activated carbon (Ru/C) was obtained from Sigma-Aldrich. Iron (III) Chloride is an anhydrous powder, with a purity >98.5%, which is dissolved I the reaction media before use as a catalyst. Distilled water (DW) was produced by double distilling tap water in a Cole-Parmer Aquatron A4000D automatic still. Double-lined superliners gas bags were obtained from Sigma-Aldrich.

5.2.2 Supercritical Water Gasification Set-up

The continuous reactor consisted of a 25 m coiled stainless-steel 316l pipe with an internal diameter of 3.87mm (nominal ¼”), located within a Carbolite Gero LHT oven (max temperature 600°C), which was maintained at the desired reaction temperature. The feedstock solution was kept suspended using a magnetic stirrer to ensure that heterogenous elements (algae or Ru/C catalyst) did not settle and the feedstock was homogenous for the whole experiment. The feedstock solution was supplied by 2 Jasco Pu-2086 HPLC pumps, which maintain the desired flowrate to achieve a 45 s residence time. The flowrates used were 20.75,16.87, 16.62 and 15.58 ml/min for 400, 500, 530 and 600 °C respectively. The reactor exit stream passed through a shell-and-tube heat exchanger to cool it to ambient temperature, before flowing through a back pressure regulator (BPR) to maintain the pressure in the reactor and reduce the stream to ambient pressure. The pressure was maintained between 23 and 25MPa. The fluid stream was filtered before and after the BPR using 2µm and 0.5µm filters respectively, to prevent blockages and solid material entering the liquid product. The filtered stream was admitted to a gas/liquid separator. The gas stream can then be either passed through a bubble column to measure flowrate or collected in a gas sampling bags for analysis. This is shown in Figure 5.1.

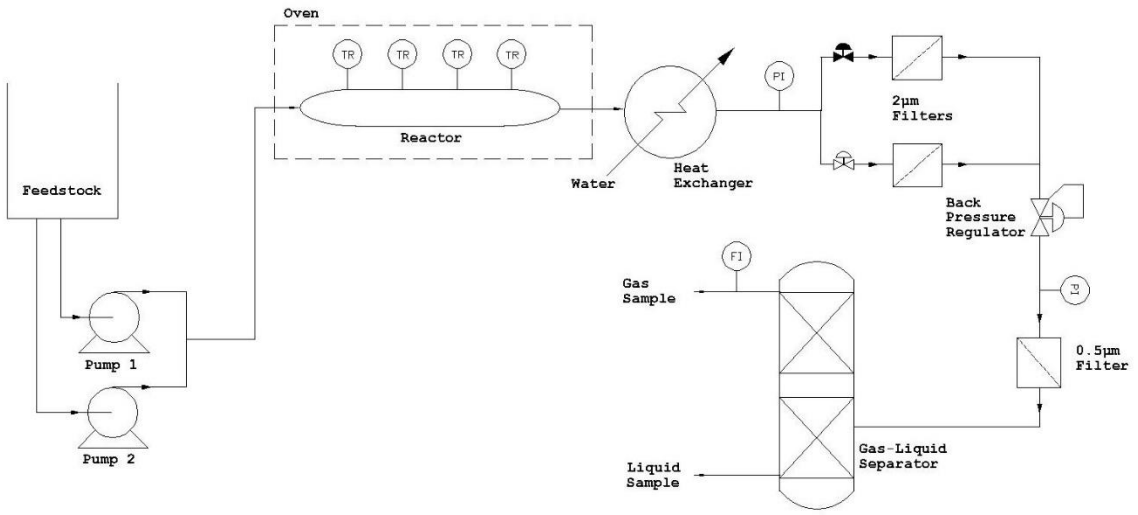

Figure 5.1-Experimental set-up. TR, PI and FI are sensors for temperature, pressure and flowrate respectively.

Upon feedstock preparation, the correct quantity of microalgae was added to 500 ml of GW, along with the correct quantity of catalyst (if added) and shaken vigorously until a homogenous mixture was achieved. The solution was kept homogenous using a magnetic stirrer. Initially the system was fed with DW until the required reaction conditions have been met. The feedstock was then fed into the system until noticeable product is seen in the gas/liquid separator. 3 flowrate measurements were taken across the 6 minutes following this, before switching to fill the gas bag, until the bag is sufficiently filled. The liquid product is sampled regularly throughout. Following the experiment, the reactor is flushed with DW for 30 minutes at reaction temperature before being allowed to cool.

5.2.3 Analysis

The composition of the gas product is analysed using a Shimazu 2014 Gas chromatography with a thermal conductivity detector (GC-TCD) and a 0.35 mm internal diameter, 20 m Shim Carbon ST column. In the liquid phase, total organic carbon (TOC) was calculated using Spectroquant® TOC Cell test, following a 10-fold dilution with distilled water. Total inorganic carbon (TIC) is measured using a Shimadzu TOC-L following overnight extraction of organic components using a 4:1 vol: vol ratio of dichloromethane: sample. The residual carbon, that can be used to estimate the quantity of tar/char, is calculated from the following equation, where *C* is the mass of carbon in the designated stream.

$$C_{Residual} = C_{Feed} - C_{TOC\ liquid} - C_{TIC\ liquid} - C_{Gas} \quad (1)$$

The percentage to which the feedstock is converted to gas in SCWG is often shown as carbon gasification efficiency (CGE), however, much of the carbon dioxide produced remains in the liquid as inorganic carbon. This is particularly the case with alkaline catalysts such as KOH, where the CO_2 can react to form carbonates [27]. Therefore, the true conversion of the carbon in the feedstock is given by the following equation:

$$Conversion\ (\%) = \frac{C_{gas} + (C_{TIC\ liquid} - C_{TIC\ feedstock})}{C_{Feed}} \quad (2)$$

Due to the same phenomenon, the CO_2 yields include the TIC that remains in the liquid. The energy efficiency of the gasification is defined as the energy in the gas stream, compared with that in the feedstock, as shown by equation, where ethane was used to represent the C_{2+} compounds.

$$Energy\ efficency\ (\%) = \frac{\dot{m}_{H2}HHV_{H2} + \dot{m}_{CH4}HHV_{CH4} + \dot{m}_{CO}HHV_{CO} + \dot{m}_{C2+}HHV_{C2+}}{\dot{m}_{algae}HHV_{algae}} \quad (3)$$

The $FeCl_3$ is dissolved into the reaction media, so should have a minimal effect on pumping power and heat recover, thus the energy efficiency in this work refers to the reaction only.

5.2.4 Design of Experiments

To assess the impact of $FeCl_3$ as a catalyst and study interactions with other operating conditions, a design of experiments was used, with temperature (400-600°C), biomass concentration (1-3wt.%) and catalyst (no catalyst, 1wt.% $FeCl_3$) as the chosen factors. A custom design that considers these factors, any interactions and the quadratic nature of the continuous variables was chosen. The hydrogen yield, carbon conversion, energy efficiency and gas yields (H_2, CH_4, CO, CO_2, C_{2+}) were chosen as response variables. All experimental data points were repeated in duplicate. The results are fit to a model using a standard least squares method for each of the response variables, with any factors or combination of factors removed if they have a *p*-value <0.05 (deemed insignificant [70]) The logworth was calculated to quantify the significance of each factor. Logworth was calculated using the *p*-value for each factor using the following equation:

$$Logworth = -log_{10}(p) \quad (4)$$

To easily demonstrate whether the impact a factor is positive or negative, a directional logworth was used. This can be calculated using the following equation.

$$Direction\ Logworth = Logworth * \begin{Bmatrix} +impact, & 1 \\ -impact, & -1 \end{Bmatrix} \quad (5)$$

The model was then deemed to be suitable if there was no significant difference between the error from model and the error between repeats, signified by a lack of fit *p*-value >0.05. Additionally, an R^2 term was produced for each model to show the proportion of the response that can be attributed to the model.

Following this, experiments at 500°C, 2wt.% were also completed with either KOH, Ru/C, or a combination of the catalysts to compare the impact of $FeCl_3$ to the most common catalysts reported in the literature and establish any synergy between the catalysts. It was not possible to combine $FeCl_3$ and KOH as the precipitation formed could not be pumped effectively using the existing pumps. This data point was chosen as it represents the midpoint of the data. The lower temperature (400°C) was not considered as the very low conversion achieved makes it an undesirable condition for maximising hydrogen yield.

5.3 THEORY

Water gas shift (WGS), methanation and steam reforming are the main gas forming reactions in SCWG [71] (equations 6,7 and 8). Decarboxylation reactions, also key gas forming reactions, are dominant at milder conditions [29] [13] but are less relevant for hydrogen production as they do not contribute to the production of hydrogen or any other fuel gas. Steam reforming is desirable as it increases the total conversion of intermediates and produces hydrogen. WGS is also desirable as it increases hydrogen and removes the less desirable carbon monoxide. Methanation is not desirable for hydrogen production as it removes hydrogen and is harder to include BECCS but may be desirable in some contexts as methane is still a useful fuel.

$$CO + H_2O \rightarrow CO_2 + H_2 \tag{6}$$

$$CO + 3H_2 \rightarrow CH_4 + H_2O \tag{7a}$$

$$CO_2 + 4H_2 \rightarrow CH_4 + 2H_2O \tag{7b}$$

$$C_xH_yO_z + (x - z)H_2O \rightarrow xCO + \left(\frac{y}{2} + x - z\right)H_2 \tag{8}$$

Other reactions occur in the liquid phase, which produce a range of intermediates and can strongly influence the gas produced. These reactions can include hydrolysis, C-C bond scission and decomposition reactions which break down the biomass into small molecules that are more readily gasified. It can also include other reactions such as the Maillard reaction and polymerisations, which can lead to more stable compounds or tar/char, which leads to lower conversion and potential blocking of the reactor [36, 11, 23].

5.4 RESULTS AND DISCUSSION

5.4.1 Assessment of $FeCl_3$

SCWG of *Chlorella vulgaris* was completed with and without a FeCl*3* (1wt.%) catalyst for a range of temperatures (400-600°C) and a range of algae concentrations (1-3wt. %). For the yield of each of the gases produced (H_2, CH_4, CO, CO_2 and C_{2+}), carbon distribution (carbon conversion, total organic carbon and residual carbon) and energy efficiency. The standard least squares method was used to fit model to predict how each output variable is affected by each factor or any of their interactions. The resulting models are shown in equations 9-16, where *T*= temperature (°C), x= biomass concentration (wt.%) and *C*= catalysts (1 for $FeCl_3$,0 for no catalyst). The directional; logworth of each factor is displayed in Table 5.5. The results are displayed visually in Figure 5.2 and Figure 5.3. The R^2 values for all output variables are >0.8, indicating an acceptable representation of the data [20].

$$H_2Yield(\frac{mg}{g}) = 2.1T - 1.8x - 0.8C - 1.7T \times x$$
$$-0.9C \times T + 1C \times x + 1T \times x \times C + 0.74x^2 + 2.09 \quad (9)$$

$$Carbon\ Conversion(\%) = 0.13T - 0.06C - 0.04T \times x + 0.27 \quad (10)$$

$$Energy\ Efficency(\%) = 0.1T - 0.07x - -0.07T \times x$$
$$+0.04T^2 + 0.11 \quad (11)$$

$$Residual\ Carbon\ (\%) = -0.04T + 0.09x + 0.1C - 0.04C \times x + 0.04T \times x + 0.42 \quad (12)$$

$$CH_4Yield\ (\frac{mg}{g}) = 13.8T - 5.2x - 6.1T \times x + 6.3T^2 + 7.82 \quad (13)$$

$$CO\ Yield\left(\frac{mg}{g}\right) = 17.8T - 7.8x + 7.8C + 7.4C \times T - 10.4C \times x - 9.09T \times x \times C + 28.4 \quad (14)$$

$$CO_2\ Yield(\frac{mg}{g}) = 71.7T - 108.2C - 60.3C \times T + 389.5 \quad (15)$$

$$C_{2+}Yield(\frac{mg}{g}) = 31.8T - 17.4x - 18.3T \times x - 5.7C \times T + 34.5 \quad (16)$$

Where:

$T = \frac{(temperature\ (℃) - 500)}{100}$, $x = (Biomass\ Concentration(wt\%) - 2, C = \frac{FeCl_3 \rightarrow 1}{No \rightarrow -1}$

*Table 5.5-Logworth of each factor of the model. T, x, C represent temperature, biomass concentration and catalyst respectively. * Represents an interaction between the factors. Black squares indicate when the factor was not significant.*

Output variable	**Logworth**									**R^2**
	T	**x**	**C**	**T*x**	**T*C**	**C*x**	**T*x*C**	**x^2**	**T^2**	
H_2 Yield	10.7	-7.5	-4.2	-6.5	-3.7	3.9	3.6	1.34	NS	0.94
Conversion	10	NS	-4.7	-1.9	NS	NS	NS	NS	1	0.84
Energy Efficiency	12.3	-6	NS	-5.3	NS	NS	NS	NS	1.3	0.91
Residual carbon	-1.7	5	7.7	1.4	NS	-1.3	NS	NS	NS	0.81
CH_4 Yield	12.6	-4	NS	-4.3	NS	NS	NS	NS	2.2	0.9
CO_2 Yield	4.9	NS	-9	NS	NS	3.4	NS	NS	NS	0.82
C_{2+} yield	11.6	-5.7	NS	-5.4	-1.4	NS	NS	NS	NS	0.9
CO Yield	5.1	-1.3	2	NS	1.5	-2	-1.6	NS	NS	0.8

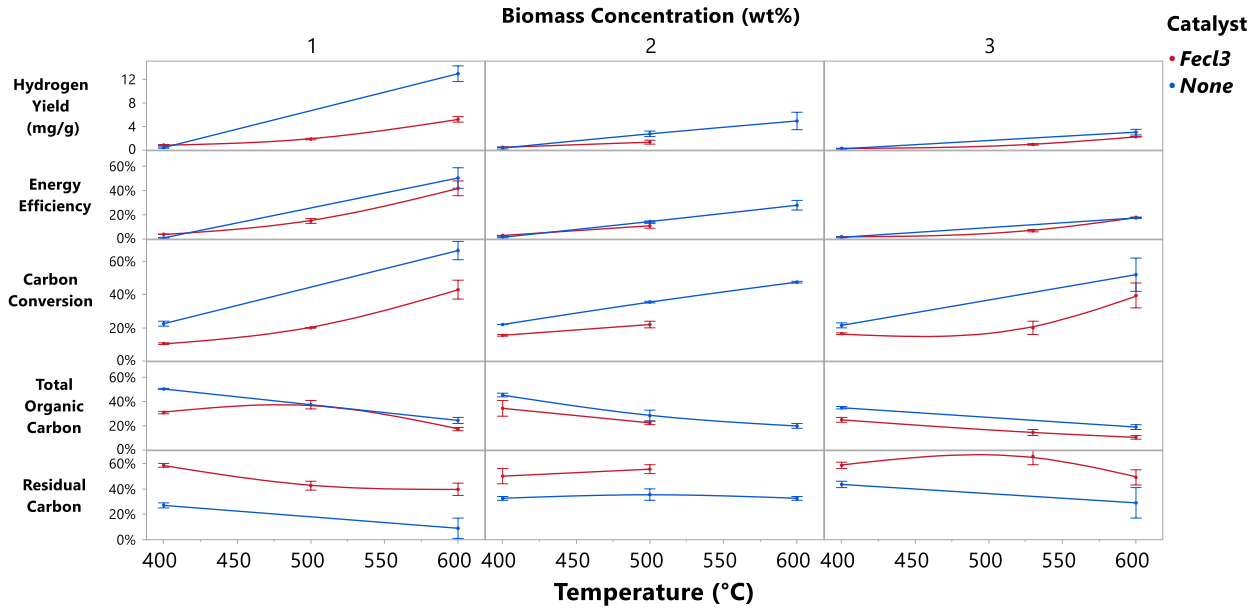

Figure 5.2-Hydrogen yield, Energy efficiency and carbon distribution comparison for FeCl3 as a catalyst. 45s residence time, 1-3%wt Chlorella vulgaris, 400-600°C, 1%wt catalyst. The error bars represent 1 standard error from the mean.

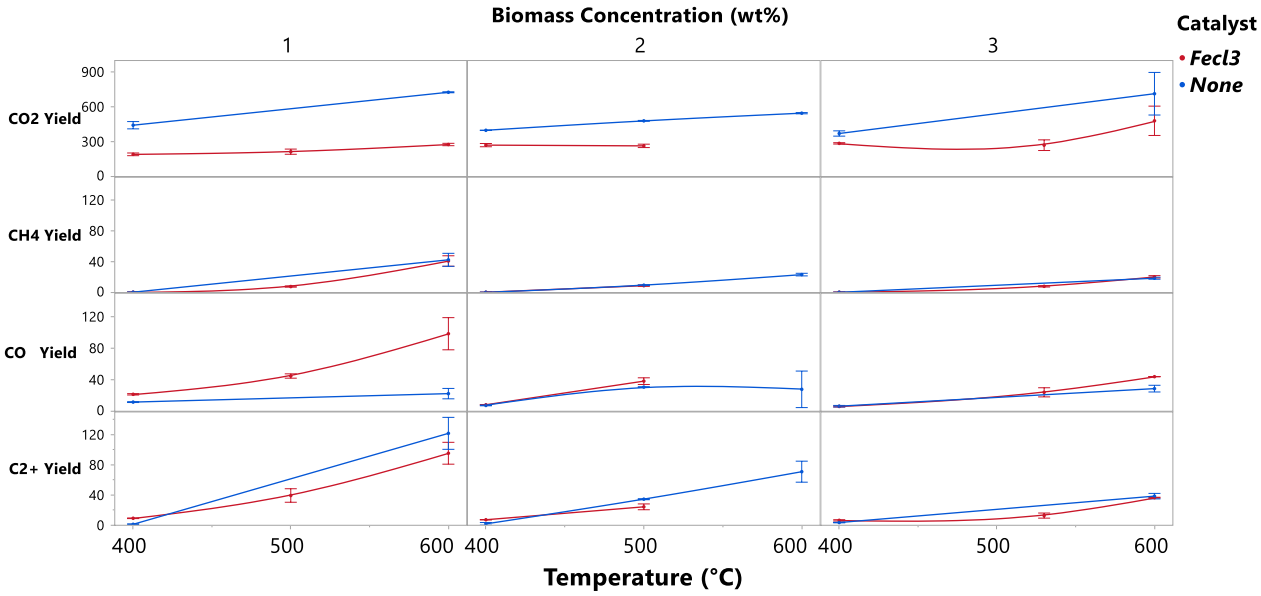

Figure 5.3-Non-hydrogen gas yields in mg/g of feedstock. 45s residence time, 1-3%wt Chlorella vulgaris, 400-600°C, 1%wt catalyst. The error bars represent 1 standard error from the mean.

This shows that while temperature and biomass concentration are the most significant factors, the $FeCl_3$ catalyst still has a significantly negative impact on hydrogen yield. There is also a significant negative impact of the (temperature*catalyst) interaction and positive impact of the (concentration*catalyst) interaction. This suggests that the negative impact is greater at higher temperatures and lower biomass concentrations. Figure 5.2 clearly shows this impact as the difference between the two plots is greater for 1wt.% biomass and at higher temperatures.

The most extreme effect was observed at 1wt.% and 600°C where a H_2 yield was 4.8g mg^{-1} with $FeCl_3$ compared with 12.7g mg^{-1} without a catalyst. Additionally, a significant negative impact on CO_2 yield and positive impact on CO yield was observed. Similarly to that observed with the hydrogen yield, these impacts are more significant at lower biomass concentrations and higher temperatures. These effects indicate a suppression of the WGS reaction (equation 6).

A potential explanation is the impact of pH on the reaction. The Lewis acid nature of $FeCl_3$ makes the feedstock a pH of approximately 2 when $FeCl_3$ is used, compared to 8.4 without a catalyst. This is significant as the hydroxide ions are known to catalyse the WGS reaction, by the formation of formate as an intermediate [52]. A lower pH reduces the availability of OH^- ions to participate in that reaction, thus reducing the rate at which the CO is converted. During the reaction when $FeCl_3$ is present, the pH increases (see Appendix D). However, the increase in pH is reduced at higher temperatures and lower biomass concentrations. The pH at 600°C and 1wt.% remained at 2.6 after the reaction, whereas at 400°C and 3wt.% it rose to 7, despite both starting at 2. This likely to be a result of precipitation of the $FeCl_3$, which is subsequently bound the produced char. As more char is favoured at lower temperatures and larger biomass concentrations, a greater amount of the $FeCl_3$ is lost in the process. This would explain why the impact on the WGS is greater at lower temperatures and larger biomass concentrations.

$FeCl_3$ also has a significant negative effect on the conversion of feedstock carbon to gas and a positive effect on the residual carbon remaining, with the latter showing that the catalyst was the most significant factor. Unlike the gas yields mentioned above, the impact of the catalyst on these factors had no significant interactions with the temperature or biomass concentration. This is also clearly shown in Figure 5.2, indicating that $FeCl_3$ reduces the conversion to gas and increases the amount of tar/char produced. From observations during the experiments, a noticeable increase in solid material in the filters was observed with the catalyst, suggesting that this increase is due to increased char. However, due to equipment limitations, the char alone could not be quantified.

The Lewis acid nature of $FeCl_3$ is known to increase the rate of polymer crosslinking and graphitisation reactions [72], which has resulted in it being a common catalyst in hydrothermal carbonisation of biomass [63, 64, 65]. An increase in acid sites of zeolite supports was also found to increase char yield on the SCWG of *Chlorella pyrenoidosa* [23]. Therefore, the Lewis acid nature of $FeCl_3$ is a likely source of the increased char in this work. Additionally, iron salts are known to enhance graphitisation reaction in oxygen free reactions with biomass, through the formation of iron carbide, which can further catalyse further formation of solid carbon [73]. It is likely that was also a factor in this work and shows iron itself is also a contributor to char production. The char produced is far more stable in SCW than other organic intermediates, thus is it postulated to be the main driver behind the reduced carbon conversion shown in this work.

Analysis of the organic liquid phase, shown in Appendix E, shows a clear decrease in both aromatic and N-heterocyclic compounds when $FeCl_3$ is present. Both are known to be undesirable for gas production in SCWG, favouring the formation of tars or chars [11]. Despite these lower concentrations, an increase in char and decrease in gas was observed. This could be resulting from the catalysis of polymerisation reaction by $FeCl_3$ removing these compounds form the liquid stream and depositing them as char.

Lewis acids, including iron chloride, has been found to be an effective catalysts in polycondensation reactions by easing the nucleophilic attack on alcohol groups [74], this is the main mechanism in phenol polymerisation [75] and as it applies to the alcohol group it will also be applicable on phenol derivatives such as cresol. Phenolic compounds, such as phenol or cresol were the most common aromatic compounds observed in the liquid phase. Similarly, metal chlorides were found to the activate polymerisation of pyridines and its derivatives [76]. Pyridine and it's derivates are the most common N-cyclic compound observed in the liquid phase. Thus, the catalytic effect of $FeCl_3$ on the polymerisation of these compounds, is expected to be a major contributor the negative effect on gas yield and increased char observed in this work.

Moreover, due to the lower concentrations of aromatics and N-heterocyclic compounds, Le Chatelier's principle dictates that reactions are favoured to produce these intermediates, reducing the concentration of other intermediates that are more readily gasified and leading to the observed lower gas yield. It is important to note that at supercritical conditions, when pressures are near the critical point, that the solubility of inorganic components greatly decreases [77], so much of the catalyst will precipitate out of solution. However, the Lewis acid nature of $FeCl_3$ is still apparent in solid form [78] and many solid catalysts with Lewis acid sites have been used in supercritical water applications before [79, 23]. Therefore, as the reactor is designed to keep particles suspended, the effects outlined above are still valid even though the catalyst is no longer in solution. However, fouling of the catalyst from the formed chars will now be a factor and the catalytic activity will be greatly reduced further along the reactor.

Additionally, there are operability challenges that arise from the use of $FeCl_3$ as a catalyst. Increased char formation will also limit the recyclability of the catalyst as precipitated $FeCl_3$, which will occur at supercritical conditions [9], will be bound to the char and difficult to separate. Also, the presence of cl- ions will increase the corrosion in the subcritical region, which is a major issue with SCWG and will increase costs of the process [80].

The findings reported here are on the contrary to what was observed by Gong et al. [53], Rana et al [60] and Yan et al [54], who all found that $FeCl_3$ increased hydrogen yield and carbon conversion on the SCWG of humic acid, bitumen and food waste respectively. However, this disparity can be explained when looking at differences between these experiments and this work. Humic acid and food waste are acidic in nature [81], making the non-catalytic experiments acidic, contrary to this work where the feedstock is mildly basic. This makes the decrease in pH caused by the $FeCl_3$, less significant.

Also, Gong et al. [53, 55] suggested that iron chloride such as $FeCl_3$ catalysed ring opening reactions, which resulted in the observed increased conversion. Microalgae, mostly consists of proteins, lipids and carbohydrates [11]. Hence, while rings are formed as intermediates, the

positive impact of increased ring openings will be reduced when compared with a compounds like humic acid and bitumen are large molecules with many rings. Despite this, Gong et al. [56, 34], found that other Lewis acid metal chlorides (AlCl3), were still effective at increasing the hydrogen yield for the amino acid alanine, glucose the macroalga *Enteromorpha prolifera*. Thus, this is not likely to be the major cause of this disparity.

The biomass concentration used in existing studies on $FeCl_3$ [53, 60, 55, 56] and other lewis acid metal chlorides [55, 56, 34, 57], were all batch experiments. Consequently, they utilised a greater biomass concentration (5-35wt.%), catalyst loadings (5-10wt.%) and longer reaction times (>30minutes), which are not feasible in continuous system. Such biomass concentrations would increase pumping energy and cost due to specialist pumps being required [82], while also having an increased plugging risk due to the greater char formation. Similarly, such high catalyst loading would have a high plugging risk due to precipitated salts and would increase corrosion [82]. Consequently, to these authors' knowledge no SCWG work has used more than 1%wt of a homogenous catalyst in a continuous system. It is these difference that can show the disparity shown in performance of Lewis acid catalysts in SCWG.

Gong et al. [56] observed that at low concentrations (<2wt.%), minimal impact on hydrogen yield was observed with a metal chloride catalyst ($AlCl_3$) in the SCWG of sewage sludge, with the hydrogen yield increasing exponentially with catalyst concentration. Also, as discussed above, the higher biomass concentration reduces the negative impacts on hydrogen yield. Thus, it appears at higher concentrations and catalyst loading, the positive influence of metal ions at breaking down the biomass outweighs the negative influence of pH.

Furthermore, minimal CO is observed at these longer residence times, even without a catalyst [55], which was significant in this work. This indicates that the gas phase reactions (WGS and methanation) have progressed to near equilibrium. Consequently, the influence of a catalyst known to catalyse these reactions is reduced, negating some of the negative impacts of the high pH observed in this work. Therefore, as continuous operation is key to ensure heat

recovery and efficient operation [82], $FeCl_3$ is not feasible for enhancing hydrogen yield in the SCWG of microalgae in a realistic system.

Despite the decrease in conversion to gas, the CH_4 yield, C_{2+} yield and energy efficiency are not significantly affected by the $FeCl_3$. This indicates that the $FeCl_3$ is increasing the yield of short chain alkanes such methane and ethane from the reduced intermediates available. An increase in C-O bond cleavage is known to increase alkane formation from intermediates such as alcohols, acids, and aldehydes in SWCG [83]. Increased C-O bond cleavage has been observed from $FeCl_3$ in hydrothermal carbonisation of biomass [63], thus it is likely that the catalyst favoured that pathway in this work also resulting in increased alkane yield for the intermediates available.

Another point of interest is that a high proportion of the feedstock carbon (up to 38%) remained as inorganic carbon in the liquid phase, when a catalyst was not used. The quantity of inorganic carbon significantly reduced when $FeCl_3$ was used, where in some cases less inorganic carbon was measured than in the feedstock. This difference can be explained by the lower pH in the $FeCl_3$ examples, as the solubility of inorganic carbon is reduced. This is important to outline as, to these authors' knowledge, other SCWG research has not measured TIC. Therefore, incorrect conclusions about conversion and CO_2 yield may be formed due to the differing TIC values going undetected.

Figure 5.2 and Figure 5.3 show that the error observed between repeats was greater at increased temperatures. Previous work outlined that the impact of algal growth water was greater at increased temperatures [69]. This indicates that the reaction is more sensitive to changes in media composition at increased temperatures. Therefore, while steps were taken to reduce this, slight changes due to batch variation pr run to run contamination, could have resulted in this error. This highlights the importance of run randomisation and doing repetitions to ensure this error is accounted for.

5.4.2 Comparison to Other Catalysts

To compare how the effect of $FeCl_3$ compares to other catalysts and to see if there are any interactions between catalyst types, a series of SCWG experiments were completed at 500°C and 2wt.% algal concentration. KOH and Ru/C were chosen to represent alkali metal salt and supported transition metal catalysts respectively. As shown in Table 5.1 and Table 5.2, these represent the most common homogenous and heterogenous catalysts respectively. The yields of each of the gas, energy efficiency and carbon product distribution for no catalyst, each catalyst individually, $FeCl_3$ with Ru/C and KOH with Ru/C are displayed in Figure 5.4.

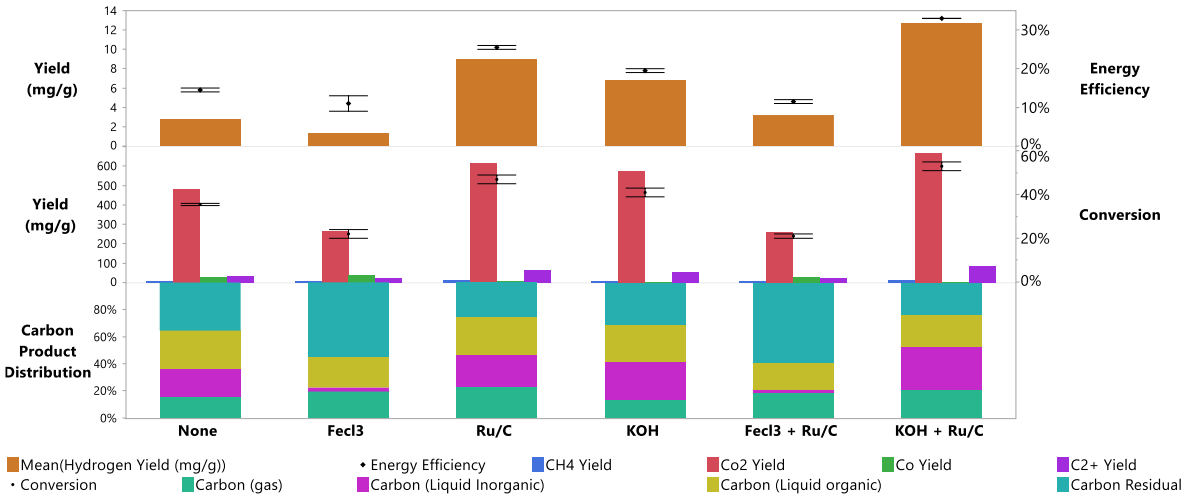

Figure 5.4-Gas Yields, Carbon Product Distribution and Energy Efficiency Comparison for Different Catalysts. 45s residence time, 2%wt Chlorella vulgaris, 500°C, 1%wt catalyst. Energy efficiency and conversion are represented by icons, the remaining factors are represented by bars. The error bars represent 1 standard error from the mean.

For the single catalysts, it is clear that both Ru/C and KOH have positive impacts on carbon conversion, energy efficiency, hydrogen yield and reducing the tar/char. Ru/C was the most effective increasing the hydrogen yield, conversion, and efficiency from 2.72 to 8.96mg g^{-1}, 35.5 to 47% and 14 to 25% respectively. The increased conversion and reduced tar/char indicates an increased C-C bond scission, while the high hydrogen yield and significantly reduced CO yield suggest an enhancement of the WGS reaction in both cases. These are desirable features of a catalyst for hydrogen production from SCWG as they maximise the quantity of hydrogen produced, the overall energy produced and minimise char/tar production

that significantly affect operability. These are all contrary to that observed in for $FeCl_3$ (Section 5.3.1), thus the latter is not a suitable catalyst for hydrogen production in SCWG of microalgae.

Using $FeCl_3$ in conjunction with Ru/C produced results similar to $FeCl_3$, reducing the conversion (35.5 to 23%) energy efficiency (14.5 to 11.5%) and increasing the tar/char produced (35.5 to 58.5%) when compared to an absence of catalyst. The difference was even greater when compared with Ru/C alone. While there was a minor increase in hydrogen yield (2.72 to 3.20mg g^{-1}) this indicates that the negative impacts of the $FeCl_3$ outweighs the positive effects of Ru/C. Chloride ions are a known poison for ruthenium catalysts [84], as a consequence the activity of the Ru/C is greatly reduced by the presence of $FeCl_3$, leading to the observed effect of the $FeCl_3$ dominating. On the contrary, when the Ru/C and KOH catalysts are used in conjunction, a positive effect was observed. The conversion, hydrogen yield, energy efficiency were all increased, compared to the best performing catalyst (Ru/C) alone (47 to 53%, 8.96 to 12.5mg g^{-1}, 25 to 33%) with the tar/char reduction (25 to 23%). This suggests no negative interactions between the catalysts, unlike when alumina supported transition metal (Ni/A_2O_3) was used along with a hydroxide homogenous catalyst (NaOH) [14], where a reaction between the catalyst resulted in lower gas yield than either catalyst alone. Therefore, the carbon supported ruthenium catalyst in conjunction with KOH appears to be the optimum catalyst option.

The quantity of inorganic carbon in the liquid phase was also significantly affected by the catalysts used. As discussed in section 5.3.1, the low pH caused by $FeCl_3$ reduces the inorganic carbon, while KOH had the opposite effect. The latter effect has been attributed to the reaction of CO_2 with the hydroxide to form carbonates [14]. Due to the heterogeneous nature of Ru/C, it does not impact the pH and thus has a negligible impact on the inorganic carbon. Due to Le Chatelier's principle, removal of CO_2 into carbonate form will move the equilibrium of any CO_2 forming reactions to the right. This increases steam reforming and decarboxylation, which are involved in the breakdown of intermediates into gas, thus increasing the carbon conversion. Additionally, this would increase the WGS reaction,

increasing the hydrogen yield and reducing CO content in the gas. Therefore, this could contribute to the positive effects shown by KOH and the negative effects caused by $FeCl_3$.

5.4.3 pH Analysis

In Sections 5.4.1 and 5.4.2, it was suggested that the low pH, caused by $FeCl_3$, was a major driver into the undesirable effects observed when it was used as catalyst. This effect was attributed to the opposite effect to that of alkaline media, which are widely known to have positive effects on the WGS reaction in SCWG [11]. However, SCWG literature is less established on the effect of an acidic environment. To confirm this hypothesis, a series of experiments were performed at a range of pH (1-13). A temperature of 500°C, algal concentration of 1%wt and residence time of 45s was used. To ensure no influence from other factors, distilled water was used, with the pH being adjusted by the addition of NaOH or HCL.

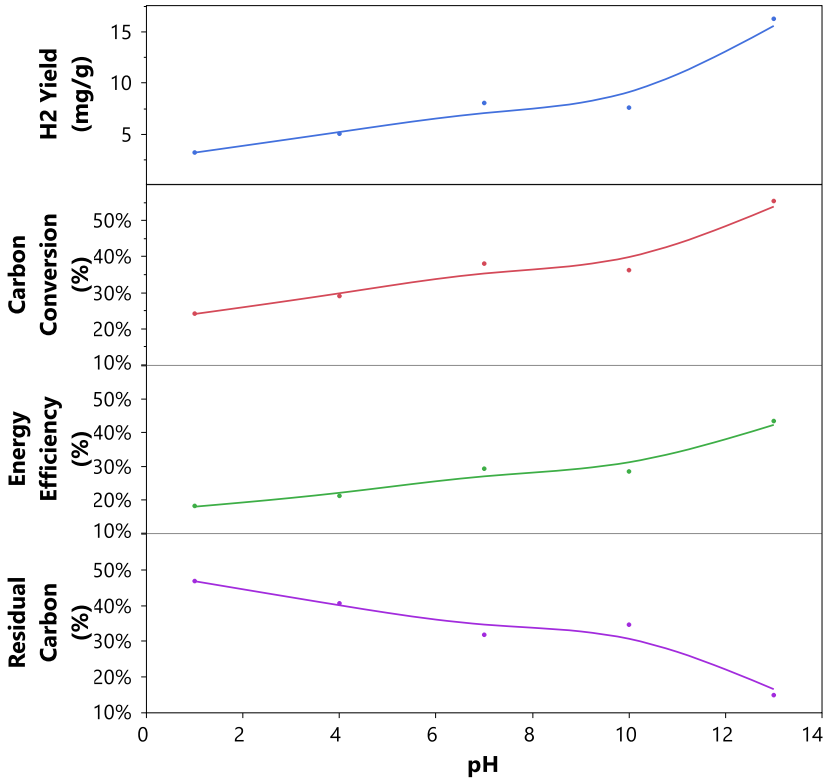

Figure 5.5-Effect of pH on the Main Output Variables. 1%wt Chlorella vulgaris, 500°C, 45s residence time.

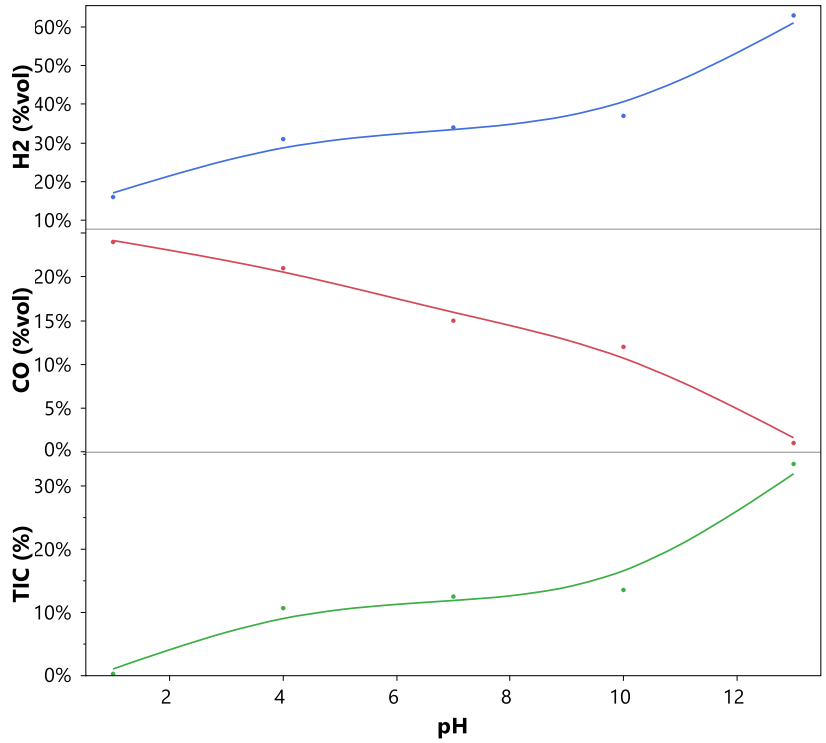

Figure 5.6-Effect of pH on the CO and H2% in gas and inorganic carbon in the liquid. 1%wt Chlorella vulgaris, 500°C, 45s residence time.

Figure 5.6 clearly shows an increase in the Hydrogen concentration in the gas stream and a reduction in CO as the pH increases. This clearly shows how the WGS reaction is catalysed when the pH is elevated and suppressed when the pH is low, further evidencing the influence of pH on the WGS reaction. As outlined in Section 5.4.1, a driver of this phenomena could be the concentration of hydroxide ions, which would be greater at a higher pH and reduced at a low pH. Hydroxide ions are known to form formate intermediates, which leads to a greater rate of the WGS reaction [52]. Additionally, the at higher pH, a greater amount of the carbon remains in the liquid phase as inorganic carbonates. As stated in Section 5.4.2, this removes CO_2 from the reaction, thus favouring CO_2 producing reactions such as WGS.

Figure 5.5 clearly shows that the increasing the pH also increases the carbon conversion and reduces the residual carbon, indicating a reduced amount of tar/char. This cannot be directly attributed to the impact of the WGS outlined above, as that is a gas phase reaction and would not directly impact either char formation or conversion. This suggests acidic environment catalyses char forming reactions, regardless of whether this is a Lewis acid ($FeCl_3$) or acids that dissociate on solution (HCl). This is established in hydrothermal carbonisation reactions, where both $FeCl_3$ [65] [63]and HCL [85] have been used to increase polymerisation in hydrothermal conditions.

Furthermore, the removal of CO_2 from the gas stream at elevated pH would also increase reactions that convert organic intermediates into CO_2, such as steam reforming, will be favoured. This will also contribute to the increased carbon conversion. As a result, strongly suggests that the reduced pH caused by the $FeCl_3$ is the major contributor to the undesirable effects observed in this study. This emphasises the importance of pH in SCWG reactions, that should be considered for proposed homogenous catalysts.

5.5 CONCLUSION

In the SCWG of the microalga *Chlorella vulgaris* $FeCl_3$ is an unsuitable catalyst for hydrogen production. The Lewis acid nature of the $FeCl_3$ catalyst catalyses the formation of char and reduces the pH of the feedstock, suppressing the WGS reaction. As a result, the total conversion of carbon to gas and yield of hydrogen are significantly reduced. Also, chloride ions poison ruthenium, so $FeCl_3$ cannot be used in conjunction with ruthenium catalysts. KOH and Ru/C both had a positive impact on hydrogen yield, energy efficiency, conversion to gas and minimised char formation, with an increased effect when used simultaneously. Therefore, a combination of KOH and Ru/C is the preferred catalyst for hydrogen production form algal biomass using SCW. Whereas the unsuitability of $FeCl_3$ is further shown by its antagonistic effect on the catalytic efficacy of Ru/C.

5.6 REFERENCES

[1] Intergovernmental Panel on Climate Change: Working Group 3, “Climate Change 2022-Mitigation of Climate Change,” Intergovernmental Panel on Climate Change, Geneva, 2022.

[2] M. S. Yahya, M. Syafiq, A. Ashton-Butt, A. Ghazali, S. Asmah and B. Azhar, “Switching from monoculture to polyculture farming benefits birds in oil palm production landscapes: Evidence from mist netting data,” *Ecology and Evolution,* vol. 7, no. 16, p. 6, 2017. doi:10.1002/ece3.3205.

[3] F. Geiger, J. Bengtsson, F. Berendse, W. W. Weisser, M. Emmerson, M. B. Morales, P. Ceryngier, J. Liira, T. Tscharntke, C. Winqvist, S. Eggers, R. Bommarco, T. Pärt, V. Bretagnol, M. Plantegenest, L. W. Clement, C. Dennis, C. Palmer, J. J. Onate and I. Guerrero, “Persistent negative effects of pesticides on biodiversity and biological control potential on European farmland,” *Basic and Appl. Ecology,* vol. 11, no. 2, pp. 97-105, 2010. doi:10.1016/j.baae.2009.12.001.

[4] M. Dorgham, “Effects of Eutrophication.,” in *Eutrophication: Causes, Consequences and Control*, Dordrecht, Springer, 2014. doi:10.1007/978-94-007-7814-6_3.

[5] J. Tomei and R. Helliwell, “Food versus fuel? Going beyond biofuels,” *Land Use Policy,* vol. 56, pp. 320-236, 2016. doi:10.1016/j.landusepol.2015.11.015.

[6] M. Benedetti, V. Vecchi, S. Barera and L. Dall’Osto, “Biomass from microalgae: the potential of domestication towards sustainable biofactories,” *Microb Cell Factories,* vol. 17, no. 173, 2018. doi:10.1186/s12934-018-1019-3.

[7] Y. Yoshida, K. Dowaki, Y. Matsumura, R. Matsuhashi, D. Li, H. Ishitani and H. Komiyama, “Comprehensive comparison of efficiency and CO2 emissions between

biomass energy conversion technologies—position of supercritical water gasification in biomass technologies," *Biomass and Bioenergy,* vol. 25, no. 3, pp. 257-272, 2003. doi:10.1016/S0961-9534(03)00016-3.

[8] Committee on Climate Change, "Hydrogen in a Low-Carbon Economy," Committee on Climate Change, London, 2018.

[9] N. Akiya and P. E. Savage, "Roles of Water for Chemical Reactions in High-Temperature Water," *Chem. Reviews,* vol. 102, no. 8, pp. 2725-2750, 2002. doi:10.1021/cr000668w.

[10] C. Wang, W. Zhu, H. Zhang, C. Chen, X. Fan and Y. Su, "Char and tar formation during hydrothermal gasification of dewatered sewage sludge in subcritical and supercritical water: Influence of reaction parameters and lumped reaction kinetics," *Waste Management,* vol. 100, pp. 57-65, 2019. doi:10.1016/j.wasman.2019.09.011.

[11] K. Heeley, R. L. Orozco, L. E. Macaskie, J. Love and B. Al-Duri, "Supercritical water gasification of microalgal biomass for hydrogen production-A review," *Int. J. of Hydrogen Energy,* vol. 49 Part A, pp. 310-336, 2023. doi:10.1016/j.ijhydene.2023.08.081.

[12] A. Nurdiawati, I. N. Zaini, A. R. Irhamna, D. Sasongkod and M. Aziz, "Novel Configuration of Supercritical Water Gasification and Chemical Looping for Highly-Efficient Hydrogen Production from Microalgae," *Renew. and Sustain. Energy Rev.,* vol. 112, pp. 369-381, 2019 doi:10.1016/j.rser.2019.05.054.

[13] L. Tiong, M. Komiyama, Y. Uemura and T. T. Nguyen, "Catalytic supercritical water gasification of microalgae: Comparison of *Chlorella vulgaris* and Scenedesmus quadricauda," *The J. of Supercrit. Fluids,* vol. 107, pp. 408-413, January 2016. doi:10.1016/j.supflu.2015.10.009.

[14] J. A. Onwudili, A. R. Lea-Langton, A. B. Ross and P. T. Williams, “Catalytic hydrothermal gasification of algae for hydrogen production: Composition of reaction products and potential for nutrient recycling,” *Bioresource Tech.,* vol. 127, pp. 72-80, January 2013 doi:10.1016/j.biortech.2012.10.020.

[15] S. Adamu, H. Binous, S. A. Razzak and M. M. Hossain, “Enhancement of glucose gasification by Ni/La2O3-Al2O3 towards the thermodynamic extremum at supercritical water conditions,” *Renew. Energy,* vol. 111, pp. 399-409, 2017 doi:10.1016/j.renene.2017.04.020.

[16] Y. Lu, S. Li, L. Guo and X. Zhang, “Hydrogen production by biomass gasification in supercritical water over Ni/γAl2O3 and Ni/CeO2-γAl2O3 catalysts,” *Int. J. of Hydrog. Energy,* vol. 35, no. 13, pp. 7161-7168, 2010 doi:10.1016/j.ijhydene.2009.12.047.

[17] H. T. Nguyen, E. Yoda and M. Komiyama, “Catalytic supercritical water gasification of proteinaceous biomass: Catalyst performances in gasification of ethanol fermentation stillage with batch and flow reactors,” *Chem. Eng. Sci.,* vol. 109, pp. 197-203, April 2014 doi:10.1016/j.ces.2014.01.036.

[18] P. Azadi, S. Khan, F. Strobel, F. Azadi and R. Farnood, “Hydrogen production from cellulose, lignin, bark and model carbohydrates in supercritical water using nickel and ruthenium catalysts,” *Applied Catalysis B: Environ.,* Vols. 117-118, pp. 330-338, May 2012 doi:10.1016/j.apcatb.2012.01.035.

[19] M. M. Hossain, “Production of H2 from Microalgae Biomass in Supercritical Water Using a Ni/La-γAl2O3 Catalyst,” *Energy Procedia,* vol. 110, pp. 384-389, 2017. doi:10.1016/j.egypro.2017.03.157.

[20] R. Samiee-Zafarghandi, J. Karimi-Sabet, M. A. Abdoli and A. Karbassi, “Supercritical water gasification of microalga *Chlorella PTCC* 6010 for hydrogen production: Box-

Behnken optimization and evaluating catalytic effect of MnO2/SiO2 and NiO/SiO2," *Renew. Energy,* vol. 126, pp. 189-201, 2018. doi:10.1016/j.renene.2018.03.043.

[21] E. A. Youssef, G. Nakhla and P. A. Charpentier, "Oleic acid gasification over supported metal catalysts in supercritical water: Hydrogen production and product distribution," *Int. J. of Hydrog. Energy,* vol. 36, no. 8, pp. 4830-4842, April 2011 doi:10.1016/j.ijhydene.2011.01.116.

[22] A. J. Byrd, S. Kumar, L. Kong, H. Ramsurn and R. B. Gupta, "Hydrogen production from catalytic gasification of switchgrass biocrude in supercritical water," *Int. J. of Hydrog. Energy,* vol. 36, no. 5, pp. 3426-3433, March 2011 doi:10.1016/j.ijhydene.2010.12.026.

[23] L.-F. Xie, P.-G. Duan, J.-L. Jiao and Y.-P. Xu, "Hydrothermal gasification of microalgae over nickel catalysts for production of hydrogen-rich fuel gas: Effect of zeolite supports," *Int. J. of Hydrog. Energy,* vol. 44, no. 11, pp. 5114-5124, 2019. doi:0.1016/j.ijhydene.2018.09.175.

[24] D. S. Gökkaya, M. Sağlam, M. Yüksel, T. G. Madenoğlu and L. Ballice, "Characterization of products evolved from supercritical water gasification of xylose (principal sugar in hemicellulose)," *Energy Sources, Part A: Recovery, Util., and Environ. Effects,* vol. 38, no. 11, pp. 1503-1511, 2016 doi:10.1080/15567036.2014.914109.

[25] I.-G. Lee, A. Nowacka, C.-H. Yuan, S.-J. Park and J.-B. Yang, "Hydrogen production by supercritical water gasification of valine over Ni/activated charcoal catalyst modified with Y, Pt, and Pd," *Int. J. of Hydrog. Energy,* vol. 40, no. 36, pp. 12078-12087, September 2015 doi:10.1016/j.ijhydene.2015.07.112.

[26] R. Samiee-Zafarghandi, A. Hadi and J. Karimi-Sabet, "Graphene-supported metal nanoparticles as novel catalysts for syngas production using supercritical water

gasification of microalgae," *Biomass and Bioenergy,* vol. 121, pp. 13-21, 2019. doi:10.1016/j.biombioe.2018.11.035.

[27] l. J. Sheikhdavoodi, M. Almassi, M. Ebrahimi-Nik, A. Kruse and H. Bahrami, "Gasification of sugarcane bagasse in supercritical water; evaluation of alkali catalysts for maximum hydrogen production," *J. of the Energy Ins.,* vol. 88, no. 4, pp. 450-458, November 2015. doi:10.1016/j.joei.2014.10.005.

[28] Y. Che, L. Yi, W. Wei, H. Jin and L. Guo, "Hydrogen production by sewage sludge gasification in supercritical water with high heating rate batch reactor," *Energy,* vol. 238, no. A, 2022 doi:10.1016/j.energy.2021.121740.

[29] A. G. Chakinala, D. W. F. (. Brilman, W. P. v. Swaaij and S. R. A. Kersten, "Catalytic and Non-catalytic Supercritical Water Gasification of Microalgae and Glycerol," *Ind. and Eng. Chem. Res.,* vol. 49, no. 3, pp. 1113-1122, Septemeber 2010. doi:10.1021/ie9008293.

[30] T. Yoshida and Y. Matumura, "Gasification of cellulose, xylan, and lignin mixtures in supercritical water," *Ind. and Eng. Chem. Res.,* vol. 40, no. 23, pp. 5469-5474, 2001 doi:10.1021/ie0101590.

[31] O. Norouzi, F. Safari, S. Jafarian, A. Tavasoli and A. Karimi, "Hydrothermal gasification performance of Enteromorpha intestinalis as an algal biomass for hydrogen-rich gas production using Ru promoted Fe–Ni/γ-Al2O3 nanocatalysts," *Energy Convers. and Manag.,* vol. 141, pp. 63-71, June 2017 doi:10.1016/j.enconman.2016.04.083.

[32] A. Kumar and S. N. Reddy, "Subcritical and supercritical water in-situ gasification of metal (Ni/Ru/Fe) impregnated banana pseudo-stem for hydrogen rich fuel gas mixture," *Int. J. of Hydrog. Energy,* vol. 45, no. 36, pp. 18348-18362, 2020 doi:10.1016/j.ijhydene.2019.08.009.

[33] V. Krishnan, S. Thachanan, Y. Matsumura and Y. Uemura, “Supercritical Water Gasification on Three Types of Microalgae in the Presence and Absence of Catalyst and Salt,” *Procedia Eng.,* vol. 148, pp. 594-599, 2016. doi:10.1080/15567036.2016.1270375.

[34] M. Gong, J. Hu, Q. Xu and Y. Fan, “Catalytic gasification of Enteromorpha prolifera for hydrogen production in supercritical water,” *Process Safety and Environmental Protection,* vol. 175, pp. 227-237, 2023.

[35] L. Tiong and M. Komiyama, “Supercritical water gasification of microalga *Chlorella vulgaris* over supported Ru,” *The J. of Supercrit. Fluids,* vol. 144, pp. 1-7, 2019. doi:10.1016/j.supflu.2018.05.011.

[36] C. Zhu, L. Guo, H. Jin, J. Huang, S. Li and X. Lian, “Effects of reaction time and catalyst on gasification of glucose in supercritical water: Detailed reaction pathway and mechanisms,” *Int. J. of Hydrogen Energy,* vol. 41, no. 16, pp. 6630-6639, May 2016 doi:10.1016/j.ijhydene.2016.03.035.

[37] R. Cherad, J. Onwudili, U. Ekpo, P. Williams, A. R. Lea-Langton, M. Carmargo-Valero and A. Ross, “Macroalgae supercritical water gasification combined with nutrient recycling for microalgae cultivation,” *Environ. Process and Sustain. energy,* pp. 186-185, 2013 doi:10.1002/ep.11814.

[38] S. Stucki, F. Vogel, C. Ludwig, A. G. Haiduc and M. Brandenberger, “Catalytic gasification of algae in supercritical water for biofuel production and carbon capture,” *Energy and Environ. Sci,* vol. 2, pp. 535-541, 2009. doi:10.1039/B819874H.

[39] M. Bagnoud-Velásquez, M. Brandenberger, F. Vogel and C. Ludwig, “Continuous catalytic hydrothermal gasification of algal biomass and case study on toxicity of aluminum as a step toward effluents recycling,” *Catal. Today,* vol. 223, pp. 35-43, 2014. doi:10.1016/j.cattod.2013.12.001.

[40] J. Jiao, F. Wang, P. Duan, Y. Xu and W. Yan, “Catalytic hydrothermal gasification of microalgae for producing hydrogen and methane-rich gas,” *Energy Sources, Part A: Recovery, Util., and Environ. Eff.,* vol. 39, no. 9, pp. 851-860, 2017. doi:10.1080/15567036.2016.1270375.

[41] G. Peng, F. Vogel, D. Refardt and C. Ludwig, “Catalytic Supercritical Water Gasification: Continuous Methanization of *Chlorella vulgaris*,” *Ind. and Eng. Chem. Res.,* vol. 56, no. 21, pp. 6256-6265, 2017. doi:10.1021/acs.iecr.7b00042.

[42] P.-G. Duan, S.-C. Li, J.-L. Jiao, F. Wang and Y.-P. Xu, “Supercritical water gasification of microalgae over a two-component catalyst mixture,” *Sci. of The Total Environ.,* vol. 630, pp. 243-253, 2018. doi:10.1016/j.scitotenv.2018.02.226.

[43] J. B. Gadhe and R. B. Gupta, “Hydrogen production by methanol reforming in supercritical water: Catalysis by in-situ-generated copper nanoparticles,” *Int. J. of Hydrog. Energy,* vol. 32, no. 13, pp. 2374-2381, 2007 doi:10.1016/j.ijhydene.2006.10.050.

[44] F. L. P. Resende and P. E. Savage, “Effect of Metals on Supercritical Water Gasification of Cellulose and Lignin,” *Ind. Eng. and Chem. Res.,* vol. 49, no. 6, pp. 2694-2700, 2010 doi:10.1021/ie901928f.

[45] M. B. García-Jarana, J. R. Portela, J. Sánchez-Oneto, E. J. M. d. l. Ossa and B. Al Duri. 2, “Analysis of the Supercritical Water Gasification of Cellulose in a Continous System Using Short Residence times,” *Appl. Sci.,* vol. 10, no. 15, p. 5185, 2020 doi:10.3390/app10155185.

[46] S. Nanda, S. N. Reddy, H. N. Hunter, A. K. Dalai and J. A. Kozinski, “Supercritical water gasification of fructose as a model compound for waste fruits and vegetables,” *The J. of*

Supercrit. fluids, vol. 104, pp. 112-121, Septemeber 2015 doi:10.1016/j.supflu.2015.05.009.

[47] H. Schmieder, J. Abeln, N. Boukis, E. Dinjus, A. Kruse, M. Kluth, G. Petrich, E. Sadri and M. Schacht, “Hydrothermal gasification of biomass and organic wastes,” *The J. of Supercrit. Fluids,* vol. 17, no. 2, pp. 145-153, April 2000 doi:10.1016/S0896-8446(99)00051-0.

[48] M. Watanabe, H. Inomata and K. Arai, “Catalytic hydrogen generation from biomass (glucose and cellulose) with ZrO2 in supercritical water,” *Biomass and Bioenergy,* vol. 22, no. 5, pp. 405-410, 2002 doi:10.1016/S0961-9534(02)00017-X.

[49] G. Caputo, M. Dispenza, P. Rubio, F. Scargiali, G. Marotta and A. Brucato, “Supercritical water gasification of microalgae and their constituents in a continuous reactor,” *The J. of Supercrit. Fluids,* vol. 118, pp. 163-170, December 2016. doi:10.1016/j.supflu.2016.08.007.

[50] T. Madenoğlu, M. Saglam, M. Yüksel and L. Ballice, “Hydrothermal gasification of biomass model compounds (cellulose and lignin alkali) and model mixtures,” *The J. of Supercrit. Fluids,* vol. 115, pp. 79-85, September 2016 doi:10.1016/j.supflu.2016.04.017.

[51] S. Elsayed, N. Boukis, D. Patzelt, S. Hindersin, M. Kerner and J. Sauer, “Gasification of Microalgae Using Supercritical Water and the Potential of Effluent Recycling,” *Chem. Eng. & Tech.,* vol. 39, no. 2, November 2015. doi:10.1002/ceat.201500146.

[52] A. Sinag, A. Kruse and J. Rathert, “Influence of the Heating Rate and the Type of Catalyst on the Formation of Key Intermediates and on the Generation of Gases during Hydropyrolysis of Glucose in Supercritical Water in a Batch Reactor,” *Ind. and eng. chem. res.,* vol. 43, no. 2, pp. 502-508, 2004. doi:10.1021/ie030475.

[53] M. Gong, S. Nanda, M. J. Romero, W. Zhu and J. A. Kozinski, “Subcritical and supercritical water gasification of humic acid as a model compound of humic substances in sewage sludge,” *The J. of Supercrit. Fluids,* vol. 119, pp. 130-138, 2017 doi:10.1016/j.supflu.2016.08.018.

[54] M. Yan, H. Su, D. Hantoko, E. Kanchanatip, F. B. S. Hamid, S. Zhang, G. Wang and Z. Xu, “Experimental study on the energy conversion of food waste via supercritical water gasification: Improvement of hydrogen production,” *Int. J. of Hydrogen Energy,* vol. 44, no. 10, pp. 4664-4673, 2019 doi:10.1016/j.ijhydene.2018.12.193.

[55] M. Gong, S. Nanda, H. N. Hunter, W. Zhu, A. K. Dalai and J. A. Kozinski, “Lewis acid catalyzed gasification of humic acid in supercritical water,” *Catalysis Today,* vol. 291, pp. 13-23, 2017.

[56] M. Gong, Z. Li, M. Wang, A. Feng, L. Wang and S. Yuan, “Effects of Lewis acid on catalyzing gasification of sewage sludge and model compounds in supercritical water,” *Int. J. of Hydrog. Energy,* vol. 46, no. 13, pp. 9008-9018, 2021 doi:10.1016/j.ijhydene.2020.12.207.

[57] Z. Li, M. Gong, M. Wang, A. Feng, L. Wang, P. Ma and S. Yuan, “Influence of AlCl3 and oxidant catalysts on hydrogen production from the supercritical water gasification of dewatered sewage sludge and model compounds,” *Int. J. of Hydrog. Energy,* vol. 46, no. 61, pp. 31262-31274, 2021 doi:10.1016/j.ijhydene.2021.07.028.

[58] J. Li, L. Pan, M. Suvarna and X. Wang, “Machine learning aided supercritical water gasification for H2-rich syngas production with process optimization and catalyst screening,” *Chem. Eng. J.,* vol. 426, 2021 doi:10.1016/j.cej.2021.131285.

[59] Merk, 12 02 2024. [Online]. Available: https://www.sigmaaldrich.com/GB/en. [Accessed 12 02 2024].

[60] R. Rana, S. Nanda, J. A. Kozinski and A. K. Dalai, “Investigating the applicability of Athabasca bitumen as a feedstock for hydrogen production through catalytic supercritical water gasification,” *J. of Environ. Chem. Eng.,* vol. 6, no. 1, pp. 182-189, 2018 doi:10.1016/j.jece.2017.11.036.

[61] H. Li, S. Hurley and C. (. Xu, “Liquefactions of peat in supercritical water with a novel iron catalyst,” *Fuel,* vol. 90, no. 1, pp. 412-420, 2011 doi:10.1016/j.fuel.2010.09.004.

[62] R. Tomifuji, K. Maeda, T. Takahashi, T. Kurahashi and S. Matsubara, “FeCl3 as an Ion-Pairing Lewis Acid Catalyst. Formation of Highly Lewis Acidic FeCl2+ and Thermodynamically Stable FeCl4– To Catalyze the Aza-Diels–Alder Reaction with High Turnover Frequency,” *Org. Lett.,* vol. 20, no. 23, pp. 7474-7477, 2018 doi:10.1021/acs.orglett.8b03249.

[63] L. T. Tran, H. T. Hoang, M. Q. Nguyen, N. D. Dao and T. H. T. Vu, “Effect of FeCl3 Catalyst on Chemical Properties of Hydrochar Produced by Hydrothermal Carbonization of Dragon Fruit Stem (Hylocereus undatus,” *Bioenergy Res.,* vol. 15, pp. 1996-2005, 2022 doi:10.1007/s12155-022-10424-2.

[64] S. B. A. Hamid, S. J. Teh and Y. S. Lim, “Catalytic hydrothermal upgrading of alpha-cellulose using iron salts as a Lewis acid,” *Bioresources,* vol. 10, no. 3, pp. 5974-5986, 2015 doi:10.15376/biores.10.3.5974-5986.

[65] K. MacDermid-Watts, E. Adewakun, O. Norouzi, T. D. Abhi, R. Pradhan and A. Dutta, “Effects of FeCl3 Catalytic Hydrothermal Carbonization on Chemical Activation of Corn Wet Distillers’ Fiber,” *ACS Omega,* vol. 6, no. 23, pp. 14875-14886, 2021 doi:10.1021%2Facsomega.1c00557.

[66] Basavaprabhu, K. Muniyappa, N. R. Panguluri, P. Veladia and V. V. Sureshbabu, “A simple and greener approach for the amide bond formation employing FeCl3 as a catalyst,” *A new J. of Chem.,* no. 10, 2015 doi:10.1039/C5NJ01047K.

[67] J. Yanik, S. Ebale, A. Kruse, M. Saglam and M. Yüksel, “Biomass gasification in supercritical water: II. Effect of catalyst,” *Int. J. of Hydrog. Energy,* vol. 33, no. 17, pp. 4520-4526, 2008 doi:10.1016/j.ijhydene.2008.06.024.

[68] T. Sato, R. Watanabe, C. Fukuhara and N. Itoh, “Effect of water density on heterogeneous catalytic water gas shift reaction in the presence of Ru/C, Pd/LaCoO3 and Fe3O4 in supercritical water,” *The J. of Supercrit. Fluids,* vol. 97, no. 211-216, 2015 doi:10.1016/j.supflu.2014.12.003.

[69] K. Heeley, R. L. Orozco, Z. Shah, L. E. Macaskie, J. Love and B. Al-Duri, “Supercritical water gasification of microalgae: The impact of the algal growth water,” *The J. of Supercrit. Fluids,* vol. 205, 2024 doi:https://doi.org/10.1016/j.supflu.2023.106143.

[70] B. Chalermsinsuwan, Y.-H. Li and K. Manatura, “Optimization of gasification process parameters for COVID-19 medical masks using response surface methodology,” *Alexandria Engineering Journal,* vol. 62, pp. 335-347, 2023.

[71] Q. Yan, L. Guo and Y. Lu, “Thermodynamic analysis of hydrogen production from biomass gasification in supercritical water,” *Energy Convers. and Management,* vol. 47, no. 11-12, pp. 1515-1528, July 2006. doi:10.1016/j.enconman.2005.08.004.

[72] Y. Cai, Y. Hu, L. Song, S. Xuan, Y. Zhang, Z. Chen and W. Fan, “Catalyzing carbonization function of ferric chloride based on acrylonitrile–butadiene–styrene copolymer/organophilic montmorillonite nanocomposites,” *Polym. Degradation and Stab.,* vol. 92, no. 3, pp. 490-496, 2007 doi:10.1016/j.polymdegradstab.2006.08.029.

[73] R. D. Hunter, M. Takeguchi, A. Hashimoto, K. M. Ridings, S. C. Hendy, D. Zakharov, N. Warnken, J. Isaacs, S. Fernandez-Muñoz, J. Ramirez-Rico and Z. Schnepp, “Elucidating the Mechanism of Iron-Catalyzed Graphitization: The First Observation of Homogeneous Solid-State Catalysis,” *Advanced Materials,* 2024 doi:10.1002/adma.202404170.

[74] A. Kirchberg, S. Wegelin, L. Grutke and M. A. R. Meier, “Unexpected performance of iron(III)chloride in the polymerization of renewable 2,3-butanediol and the depolymerization of poly(ethylene terephthalate),” *RSC Sustain.,* vol. 2, pp. 435-444, 2024 doi:10.1039/D3SU00388D.

[75] I. Gallegos, J. Kemppainen, J. R. Gissinger, M. Kowalik, A. v. Duin, K. E. Wise, S. Gowtham and G. M. Odegard, “Establishing Physical and Chemical Mechanisms of Polymerization and Pyrolysis of Phenolic Resins for Carbon-Carbon Composites,” *Carbon Trends,* vol. 12, 2023 doi:10.1016/j.cartre.2023.100290.

[76] W. Sassi, R. Msaadi, J.-Y. Hihn and R. Zrelli, “Effect of pyridine as advanced polymeric inhibitor for pure copper: adsorption and corrosion mechanisms,” *Polymer Bulletin,* vol. 78, pp. 4261-4280, 2020 doi:doi.org/10.1007/s00289-020-03311-3.

[77] H. Weingärtner and E. U. Franck, “Supercritical Water as a Solvent,” *Angewandte Chemie Int. Edit.,* vol. 44, no. 18, pp. 2672-2692, 2005 doi:10.1002/anie.200462468.

[78] M. M. Heravi, M. Ebrahimzadeh, H. A. Oskooie and B. Baghernejad, “FeCl3: Highly Efficient Catalyst for Synthesis of α-Amino Nitriles,” *Chinese J. of Chemistry,* vol. 28, no. 3, pp. 480-482, 2010 doi:10.1002/cjoc.201090100.

[79] M. Akizuki and Y. Oshima, “Solid Acid/Base Catalysis in Sub- and Supercritical Water,” *Ind. Eng. Chem. Res.,* vol. 57, no. 16, pp. 5495-5506, 2018 doi:10.1021/acs.iecr.8b00753.

[80] P. A. Marrone and G. T. Hong, “Corrosion control methods in supercritical water oxidation and gasification processes,” *The J. of Supercrit. Fluids,* vol. 51, no. 2, pp. 83-103, 2009 doi:10.1016/j.supflu.2009.08.001.

[81] C. Ghinea, L. C. Apostol, A. E. Prisacaru and A. Leahu, “Development of a model for food waste composting,” *Environ Sci Pollut Res Int,* vol. 26, no. 4, pp. 4056-4069, 2019 doi:10.1007/s11356-018-3939-1.

[82] B. R. Pinkard, D. J. Gorman, K. Tiwari, E. G. Rasmussen, J. C. Kramlich, P. G. Reinhall and I. V. Novosselov, “Supercritical water gasification: practical design strategies and operational challenges for lab-scale, continuous flow reactors,” *Heliyon,* vol. 5, no. 2, 2019 doi:10.1016/j.heliyon.2019.e01269.

[83] P. Azadi, E. Afif, F. Azadia and R. Farnood, “Screening of nickel catalysts for selective hydrogen production using supercritical water gasification of glucose,” *Green Chem.,* vol. 14, no. 6, pp. 1766-1777, 2012 doi:10.1039/C2GC16378K.

[84] J. Li, P. M. Kitano, T.-N. Ye, M. Sasase, T. Yokoyama and H. Hosono, “Chlorine-Tolerant Ruthenium Catalyst Derived Using the Unique Anion-Exchange Properties of 12 CaO·7 Al2O3 for Ammonia Synthesis,” *ChemCatChem,* vol. 9, no. 15, pp. 3078-3083, 2017 doi:10.1002/cctc.201700353.

[85] E. García-Bordejé, E. Pires and J. M. Fraile, “Parametric study of the hydrothermal carbonization of cellulose and effect of acidic conditions,” *Carbon,* vol. 123, pp. 421-432, 2017 doi:10.1016/j.carbon.2017.07.085.

5.7 FURTHER DISCUSSION

This work clearly shows that $FeCl_3$ is not a suitable catalyst for the SCWG of *Chlorella vulgaris* at the range of conditions used. As the conditions are limited by the available equipment an

expansion on these is not feasible in this study. Therefore, Lewis acid catalysts, such as $FeCl_3$ are not considered in subsequent work. KOH and Ru/C were both found to be effective catalysts in this work, with the hydrogen yield and conversion being the greatest when both were used to together. This shows that there is no negative reaction between the two catalysts, contrary to that observed in Chapter 2 when alumina supports were used along with hydroxide catalysts. Therefore, the use of these catalysts will be included along with temperature, biomass concentration and the use of oxidant to find the optimum conditions for hydrogen production and carbon capture for the SCWG of microalgae.

CHAPTER 6: ASSESSMENT OF THE OPTIMAL REACTION CONDITIONS AND CATALYST COMBINATIONS FOR THE PRODUCTION OF CARBON NEGATIVE HYDROGEN FROM THE SUPERCRITICAL WATER GASIFICATION OF MICROALGAE

This research within this chapter has been submitted for publication in the *Journal of Environmental Chemical Engineering* after the application of corrections recommended by reviewers following an initial submission. For consistency, the content and structure of this chapter has been presented as is in the submission.

ABSTRACT

Supercritical water gasification of microalgae offers a solution to hydrogen production that can simultaneously capture carbon from the atmosphere as both CO_2 and solid biochar, without some of the negative environmental impacts of other biomass sources. Investigation into the influences of temperature (400-600°C), biomass concentration (1-3wt.%), Oxidant Coefficient (0-0.5), heterogenous catalysts (Ru/C) and homogenous catalysts (KOH, 0-1wt.%) was carried out by integrating experimental results into a system model in ASPEN plus®. High temperatures and ruthenium catalyst were found to be preferable for both experimental and whole system approaches at maximising hydrogen yield and efficiency. However, despite being favourable in the reaction, low concentrations were not favourable in the integrated system, due to differences in heat recovery and pumping power. Similarly, the influence of oxidant and KOH showed a more complex influence on the whole system than is currently understood in SCWG reactions. As a result, a maximum hydrogen yield of 12.7mg/g was achieved, with 38% and 30% of the carbon being captured as gas and solid respectively, at 600°C, 2wt.% algae, 1wt. % KOH, Ru/C catalyst and a 0.3 oxidant coefficient.

6.1 INTRODUCTION

To limit global warming and forestall the crossing of catastrophic environmental tipping points, carbon removal technologies are expected to be key to which, bioenergy with carbon capture and storage (BECCS) is expected to be a major contributor [1]. Consequently, deployment of new bioenergy projects is rapidly required. However, biomass production often results in negative environmental and social impacts. Large monocultures [2], the use of pesticides [3] and fertilizer run off, causing eutrophication in waterways [4], are all damaging to biodiversity. Additionally, food prices can be impacted by the competition for land and fertilizers [5].

Microalgae requires far less land than other biomass sources as it can grow 10 times faster than terrestrial plants [6]. Additionally, the use of pesticides or arable land are not required, and nutrients used are contained so they do not enter waterways. Despite these advantages, the high-moisture content of microalgae has an adverse effect on the efficiency of conventional energy conversion processes such as thermal gasification or pyrolysis [7]. Therefore, alternative methods of extracting the energy and carbon from the algae are required.

Supercritical water gasification (SCWG) produces a gaseous product consisting of H_2, CH_4, CO, CO_2, and short chain hydrocarbons, using water above its critical point (374°C and 22.1MPa) as the reaction medium. The CO_2 can then be easily captured for storage [8], leaving a highly combustible gas stream, which can be used for a variety of energy applications, making this an ideal BECCS process. The char formed in the reaction can also be utilised in construction materials, to further enhance the carbon sequestered [9]. Additionally, hydrogen, expected to be key resource in decarbonising many hard to abate sectors, replacing existing fossil fuels [10], can be separated out from this gas stream.

The use of water makes it appropriate for high moisture feeds such as microalgae and the thermophysical properties of supercritical water (SCW) brings other advantages. The low viscosity and density of SCW increases the diffusivity, resulting in increased reaction rates [11]. Additionally, the low dielectric constant and weakened hydrogen bonds allow the organic

intermediates formed during the reaction to dissolve, thereby reducing their recombination into tars and chars [12], which can limit operability and lower gas yield.

Water gas shift (WGS), methanation and steam reforming are the main gas forming reactions in SCWG [13] (equations 1, 2 and 3). Decarboxylation reactions, also key gas forming reactions, are dominant at milder conditions [14, 15] but are less relevant for hydrogen production as they do not contribute to the production of hydrogen or any other fuel gas. Steam reforming is desirable as it increases the total conversion of intermediates and produces hydrogen. WGS is also desirable as it increases hydrogen and removes the less desirable carbon monoxide. Methanation is not desirable for hydrogen production as it removes hydrogen and is harder to include carbon capture but may be desirable in some contexts as methane is still a useful fuel.

$$CO + H_2O \rightarrow CO_2 + H_2 \quad (1)$$

$$CO + 3H_2 \rightarrow CH_4 + H_2O \quad (2a)$$

$$CO_2 + 4H_2 \rightarrow CH_4 + 2H_2O \quad (2b)$$

$$C_xH_yO_z + (x - z)H_2O \rightarrow xCO + \left(\frac{y}{2} + x - z\right)H_2 \quad (3)$$

Other reactions occur in the liquid phase, which produce a range of intermediates and can strongly influence the gas produced. These reactions can include hydrolysis, C-C bond scission and decomposition reactions which break down the biomass into small molecules that are more readily gasified. SCWG can also include other reactions such as the Maillard reaction and polymerisations, which can lead to more stable compounds or tar/char, which leads to lower conversion and potential blocking of the reactor [16, 17, 18].

A variety of factors can have an influence on a SCWG reaction. Temperature is the most influential, with a higher temperature favouring a higher hydrogen yield and conversion of biomass to gas [17]. This is attributed to the thermodynamic favourability of endothermic reactions that break down biomass and produce gas, such as steam reforming and hydrolysis

[19, 20, 21]. Biomass concentration is also a highly influential factor, with a high biomass concentration known to reduce the hydrogen yield and conversion while increasing tar/char [17]. This is due to the lower concentration of water, which is a key reactant in many reactions that break down the biomass and produce gas, such as steam reforming or the WGS reaction [22]. Additionally, polymerisation reactions are known to follow 2nd order kinetics, so tar/char compounds form far more rapidly at higher concentrations [23].

Catalysts can be used to enhance the reaction, with two main types of catalysts being utilised in SCWG. Heterogenous catalysts, consisting of a support impregnated with a transition metal, most commonly ruthenium and nickel [17]. The ability of these catalysts to adsorb hydrogen, allows them to catalyse hydrogen containing reactions [24]. These include hydrogenation reactions that can help reduce the quantity of some refractory components, as well as methanation and WGS reactions. This results in an increase in conversion and hydrogen yield in a number of examples in the literature. [25, 26, 27] Homogenous catalysts, consisting of alkali salts, such as KOH or $NaCO_3$ are commonly used [17] and are effective at increasing hydrogen yield. This is attributed to the catalysis of the WGS by the formation of a formate intermediate [24]. Iron chloride was also suggested to be an effective catalyst [28], but previous work proved that it was not effective for algae gasification [29].

The addition of an oxidant, such as hydrogen peroxide, can also be used to enhance the performance of a SCWG system. The oxidant can perform ring opening and depolymerisation reactions, breaking down compounds that are often stable in SCWG, such as chars and aromatics [30]. As a result, increasing the concentration of oxidant was found to increase the conversion of carbon to gas for phenol, naphthalene, sewage sludge and textile wastewaters [31, 32, 33, 34] all of which, are known to be difficult to gasify in SCW. However, oxidation of the desired products such as hydrogen and methane can occur, which in some cases reduces the yield of those gases [31, 33, 34]. In other cases, [35, 32], when a small amount of oxidant is added (less than half the stoichiometric quantity for full oxidation), the increase in conversion outweighs these negative effects, increasing the yields of hydrogen and methane. As a result,

the use of oxidant can be useful for increasing the conversion of the feedstock and potentially increasing hydrogen yields. Despite this, to the authors' knowledge, no study of the effect of oxidant on the SCWG of microalgae has been reported to date.

In a real industrial process the reactor does not exist independently; an integrated system of pumps, heat transfer equipment and other processing steps will also be included. As a result, the ideal operating conditions may not be the same as those in the reaction alone. A whole system model is required to properly optimise the process. For example, Magdelin et al. [36] found that a higher biomass loading was required to make their hydrogen production facility energetically feasible, when considering a whole process with downstream processing. Moreover, these models can be used to test novel configurations [37, 38, 39, 40, 41] and to perform techno economic assessments on new processes [42, 43]. However, these often use equilibrium models to calculate the reactor outputs. These can differ greatly from real experimental work [14, 44], especially at less favourable conditions and cannot assess the ability of a catalyst to affect the overall results. Therefore, a model that incorporates real experimental data is required. To these authors' knowledge, such a model is not available in the literature for any SCWG process.

This paper assesses the impact of reaction conditions, catalysts and oxidant on the SCWG of microalgae; selecting the optimal conditions for hydrogen production and carbon capture. SCWG of the microalga *Chlorella vulgaris* was performed for a range of temperatures, biomass concentrations, catalyst concentrations, catalyst combinations and oxidant concentrations to assess the impact of these factors and any interactions. These results were incorporated into a full system model, produced on ASPEN plus®, to account for the effects of reaction conditions on the other components in a real system. The optimal conditions for hydrogen production were selected and comparison made between this system, experimental results and equilibrium models.

6.2 MATERIALS AND METHODS

6.2.1 Materials

The microalga used was *Chlorella vulgaris* obtained as a spray dried powder from Sevenhills Wholefoods. The composition of the microalga was provided by the supplier and the elemental analysis (C, H, N, S) was performed using a CE Instruments EA1110 elemental analyser; the remaining weight was assumed to be oxygen content, these are shown in Table 6.1.

Table 6.1-Composition of Chlorella vulgaris feedstock.

Component	**Composition (wt.%)**
Carbohydrates	24.4
Proteins	64.5
Lipids	1.8
Ash	9.3
C	49.1
H	6.48
O	33.92
N	10.19
S	0.31

The reaction medium was created to represent that of the algal growth water (GW) that remained following a growth cycle, as previous work found GW to have a significant impact on the reaction [45]. The composition of which, shown in Table 6.2, was chosen to be comparable to that observed after 2 weeks of growth of *Chlorella vulgaris* in Chu 13 media (as outlined in previous work [45]). The algal growth water (without the addition of catalyst) had a pH of 8.5, which rose to 13.3 and 13.6 with addition of 0.5 wt.% and 1 wt.% KOH respectively. The feedstock pH was unaffected by the Ru/C catalyst.

Table 6.2-Growth water ion composition.

Ion	Concentration (mg/l)
Potassium	219
Sulphate	101
Sodium	43
Chloride	63
Calcium	21
Magnesium	20
Phosphate	4
Iron	2
Nitrate	2.7

Potassium hydroxide >85% (KOH) and hydrogen peroxide (H_2O_2) 30 wt.% were obtained from VWR. Ruthenium (5 wt.%) catalyst supported on activated carbon (Ru/C) was obtained from Sigma-Aldrich. Distilled water (DW) was produced by double distilling tap water in a Cole-Parmer Aquatron A4000D automatic still. Double-lined superliners gas bags were obtained from Sigma-Aldrich.

6.2.2 Supercritical Water Gasification Reactor Set-up

The continuous plug flow reactor system consisted of 2 preheaters and a main reactor, all made with coiled stainless-steel 316l pipes. The oxidant or water preheater had an internal diameter of 1.75 mm (nominal ⅛") and a length of 7.8 m. The preheater for the main feedstock, had an internal diameter of 3.87 mm (nominal ¼") and a length of 6 m. Similarly, the main reactor was 19-m long and an internal diameter of 3.87 mm (nominal ¼"). All preheaters and the main reactor were located within a Carbolite Gero LHT oven (max temperature 600°C, capacity 220L), which was maintained at the desired reaction temperature.

The feedstock was split to ensure a consistent residence time unaffected by the heating effects of the oxidation reactions before reaching reaction temperature. A feed to oxidant/ water split of 3:2 was used for 400°C and 3:1 for all other conditions. The feedstock solution was kept suspended using a magnetic stirrer to ensure that heterogenous elements (algae or Ru/C catalyst) did not settle and the feedstock was homogenous for the whole experiment. The

feedstock solution and water/oxidant stream were each supplied by a Jasco Pu-2086 HPLC pump, which maintained the desired flowrate to achieve a 55 s residence time. The total flowrates used were 32.95, 19.73 and 15.84 ml/min for 400, 500 and 600°C respectively.

The reactor exit stream passed through a shell-and-tube heat exchanger to cool it to ambient temperature, before flowing through a back pressure regulator (BPR) to maintain the pressure in the reactor at 23 – 25 MPa and reduce the exit stream to ambient pressure. The fluid stream was filtered before and after the BPR using 2µm and 0.5µm filters respectively, to prevent blockages and solid material entering the liquid product before being admitted to a gas/liquid separator. The gas stream was either passed through a bubble column to measure flowrate or collected in a gas sampling bags for analysis. The reactor set-up is shown in Figure 6.1.

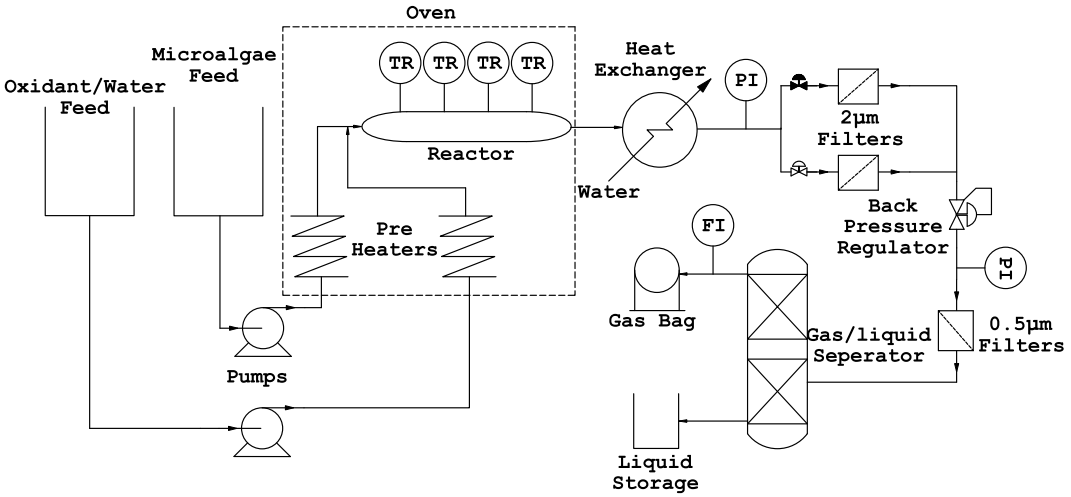

Figure 6.1-Experimental set-up. TR, PI and FI are sensors for temperature, pressure and flowrate respectively.

Upon feedstock preparation, the correct quantity of microalgae was added to 500 ml of GW, along with the correct quantity of catalyst (if added) and shaken vigorously until a homogenous mixture was achieved. GW is used as this was found to be more representative a real system in previous studies [45]. The concentration of ions in the GW, microalgae and catalyst quoted are the feed to the reactor, so the concentrations in the feedstock were adjusted accordingly to account for the split flowrate. The solution was kept homogenous using a magnetic stirrer. Initially DW was pumped through the system until the required reaction conditions were met.

The feedstock was then fed to the system at a given flowrate until noticeable product was flowing in the gas/liquid separator. 3 flowrate measurements were taken during the 10 minutes following this before switching to fill the gas bag with sample sufficient for gas analysis. The liquid product was sampled at regular intervals too. Following the experiment, the reactor was flushed with DW for 30 minutes at reaction temperature before flushing for at least 2 further hours during cooling, to clean the system of residual organic material and inorganic precipitate.

6.2.3 Analysis of Experimental Work

Composition of the gas product was analysed using a Shimazu 2014 Gas chromatography with a thermal conductivity detector (GC-TCD) and a 0.35 mm internal diameter, 20 m Shim Carbon ST column. In the liquid phase, total organic carbon (TOC) and total inorganic carbon (TIC) were measured using a Shimadzu TOC-L, following a 150-fold dilution. The residual carbon, that can be used to estimate the quantity of tar/char, was calculated from the following equation, where *C* is the mass of carbon in the designated stream.

$$C_{Residual} = C_{Feed} - C_{TOC\ liquid} - C_{TIC\ liquid} - C_{Gas} \quad (4)$$

To allow for a reasonable comparison between compositions and other literature, the gas yield of each product is calculated as shown in equation 5, where v, x and ρ are the volumetric flowrate, volumetric percentage in the product gas and density of the given gas.

$$Yield\ of\ Gas\ x = \frac{v_x x_x \rho_x}{\dot{m}_{algae}} \quad (5)$$

The percentage to which the feedstock is converted to gas in SCWG is often shown as carbon gasification efficiency (CGE); however, much of the carbon dioxide produced remains in the liquid as inorganic carbon (bicarbonate and carbonate ions). This was particularly the case with alkaline catalysts such as KOH, having a significant impact on the gasification efficiency [29]. Therefore, the true conversion of the carbon in the feedstock is given by the following equation:

$$Conversion\ (\%) = \frac{C_{gas} + C_{TIC\ liquid}}{C_{Feed}} \quad (6)$$

Due to the same phenomenon, the CO_2 yields include the TIC that remains in the liquid. The energy efficiency of the gasification is defined as the energy in the gas stream, compared with that in the feedstock, as shown by equation 7, where $\dot{m}$ is the mass flowrate, *HHV* is the higher heating value, and the subscript denotes compound to which it refers to. The *HHV* of ethane was used to represent the C_{2+} compounds in this study.

$$Energy\ efficency\ (\%) = \frac{\dot{m}_{H2}HHV_{H2} + \dot{m}_{CH4}HHV_{CH4} + \dot{m}_{CO}HHV_{CO} + \dot{m}_{C2+}HHV_{C2+}}{\dot{m}_{algae}HHV_{algae}} \quad (7)$$

6.2.4 Design of Experiments

To assess the impact of key factors in SCWG, study their interactions and produce a relationship that describes key output variables as a function of these factors, a design of experiments was used. Temperature (400 - 600 °C), biomass concentration (1 - 3wt.%), Ru/C catalyst (no catalyst, 0.05 wt.%), KOH concentration (0 - 1wt.%) and oxidant coefficient (ratio of the concentration of oxidant (H_2O_2) to that of a stoichiometric oxidation reaction, 0 - 0.5) as the chosen factors. Pressure was maintained within the range of 22.5 - 25MPa, with 23 MPa being the target pressure, as it has a minor impact on SCWG [17]. Similarly, as it was established to be the highest residence time that produces the highest gas yields [67, 44, 29], the residence time was kept constant at the highest possible value where the reactor remains turbulent for all conditions (55 s). A custom design that considers these factors, any interactions and quadratic effects was used. The hydrogen yield, carbon conversion, residual carbon and energy efficiency were the main response variables. Other gas yields (CH_4, CO, CO_2, C_{2+}), TOC and TIC were also considered for use in the system model in Section 6.3.2. All experimental data points were repeated in at least once.

The results were fit to a model for each of the response variables. For all but CO yield, a linear regression with standard least squares approach was used. For CO yield, the distribution of the residuals was not normal, thus a linear regression was not suitable. For

this variable, an exponential regression was fit using a backwards elimination method. Any factors or interactions were removed if they had an effect p-value <0.05 (deemed insignificant). The logworth was calculated to quantify the significance of each factor. Logworth was calculated using the *p*-value for each factor using the following equation:

$$Logworth = -log_{10}(p) \tag{8}$$

To clearly demonstrate whether the impact a factor is positive or negative, a directional logworth was used. This can be calculated using the following equation.

$$Direction\ Logworth = Logworth * \begin{Bmatrix} +impact, & 1 \\ -impact, & -1 \end{Bmatrix} \tag{9}$$

The model was then deemed to be suitable if there was no significant difference between the error from model and the error between repeats, signified by a lack of fit *p*-value >0.05. Additionally, an R^2 term was produced for each model to show the proportion of the response that can be attributed to the model.

6.2.5 System Model

To understand how the factors outlined in Section 6.2.4 would impact a real system, a whole system model to process 100 tonnes per day of microalgae (dry weight) was constructed in ASPEN Plus®. This was chosen to represent a smaller sized industrial biomass energy facility [49], a feasible first facility. Two models were produced, the equilibrium model, which utilises Gibbs free minimisation to calculate outlet gas composition, which is comparable to literature. The other model, the experimental model, which uses the relationships produced in this study to predict the gas yields. The schematics for these reactor systems and the process flow diagrams from ASPEN Plus® can be found in figures 6.2,6.3 and 6.4,6.5 respectively.

The equilibrium model utilises a Gibbs free energy minimisation approach, to calculate the products of the SCWG reaction (SCWG in Figure 6.4) based in the thermodynamic pathway of the elements in the feedstock, using the built in RGIBBS reactor module in ASPEN Plus®. To allow this module to work, a yield reactor was also included in the model to split the biomass

into its elemental components (COMPONEN in Figure 6.4). This step is purely for calculation as the RGIBBS Reactor cannot handle the algal feedstock directly and would not exist in a real system. The real system duty would be a sum of these two hypothetical reactors. Due to the limitations of the PRSK method with ionic compounds, nitrogen leaves the reactor as nitrogen gas, in contrary to ammonium ions observed in real experiments [56]. This was accounted for by an additional reactor (N2 in Figure 6.), that converts all the nitrogen gas to ammonia. To estimate char formation, which is not accounted for in equilibrium models, this was assumed to be 10% to correlate to the fixed carbon in the biomass [54]. Sulphur content was also assumed to become solid, as was commonly observed in the literature [57].

In the experimental model, which incorporates the experimental data, the equilibrium reactor (SCWG in Figure 6.) is replaced with an RYIELD reactor (REACTOR in Figure 6.). The gas yields, char yield, TOC and TIC are defined by the experimental results in Section 6.3 (equations 14, 18-22, 23-24). The char is assumed to be solid carbon, equal to the residual carbon calculated from the experimental work. The TOC is assumed to be 100% phenol and TIC assumed to be 100% calcium carbonate. As with the equilibrium model, 100% of the sulphur and ash are assumed to leave the reactor as solid. The removal of phenols is important to ensure recyclability of nutrients and can be easily achieved with activated carbon filters [58], thus it is assumed 100% of the phenol is removed with the solid material in the solid separator (SS). It is assumed that 100% of the nitrogen leaves as ammonia.

In comparison to the equilibrium system, the component reactor (COPONEN in Figure 6.) and nitrogen reactor (N2 in Figure 6.) are no longer needed. Also, due to the assumptions made, elements in and out of the reactor may not balance, thus an additional stream (BALIN in Figure 6.) is added to ensure this is the case, which is removed following the reactor (BALANCES in Figure 6.). A significant proportion of the CO_2 is produced as TIC, so an additional reactor is included to react this with HCL (ACIDR in Figure 6.), allowing the CO_2 to be captured. Due to limitations of the thermodynamic methods available, the solid carbonate could not be included in the HPSEP module, thus it was removed with the solid material and recombined in the

reactor. In a real system, this carbonate would remain in an aqueous phase. Moreover, in this model, an exothermic reaction was observed at all observed conditions, so an additional heater (STHEX3 in Figure 6.) was required to capture this energy and feed it to the steam turbine.

For both cases, all components apart from the reactor, were mostly identical. As Figure 6.4 and 6.5 show, the outlet stream of the reactor is cooled (COOL1 and COOL2), with the heat being recovered by the feed (HEX5 and HEX6), before passing into the separation units. Two flash separators, at reaction and ambient pressures (HPSEP and LPSEP), separate flammable gases and CO_2 respectively from the liquid. The flammable gas stream then passes through a separator to separate a proportion of the hydrogen from the stream (H2SEP). The remaining flammable gases are burned (COMPUST), using air at 1% excess of oxygen, with the heat being used to provide the remaining heat for the feed stream (HEXBURN1 and HEXBURN2) and if required, the reactor duty (HEXBURN3). The remaining hot, pressured gas stream is passed through a combined cycle gas turbine (TURB is the gas turbine and ST the steam turbine), to produce electrical power.

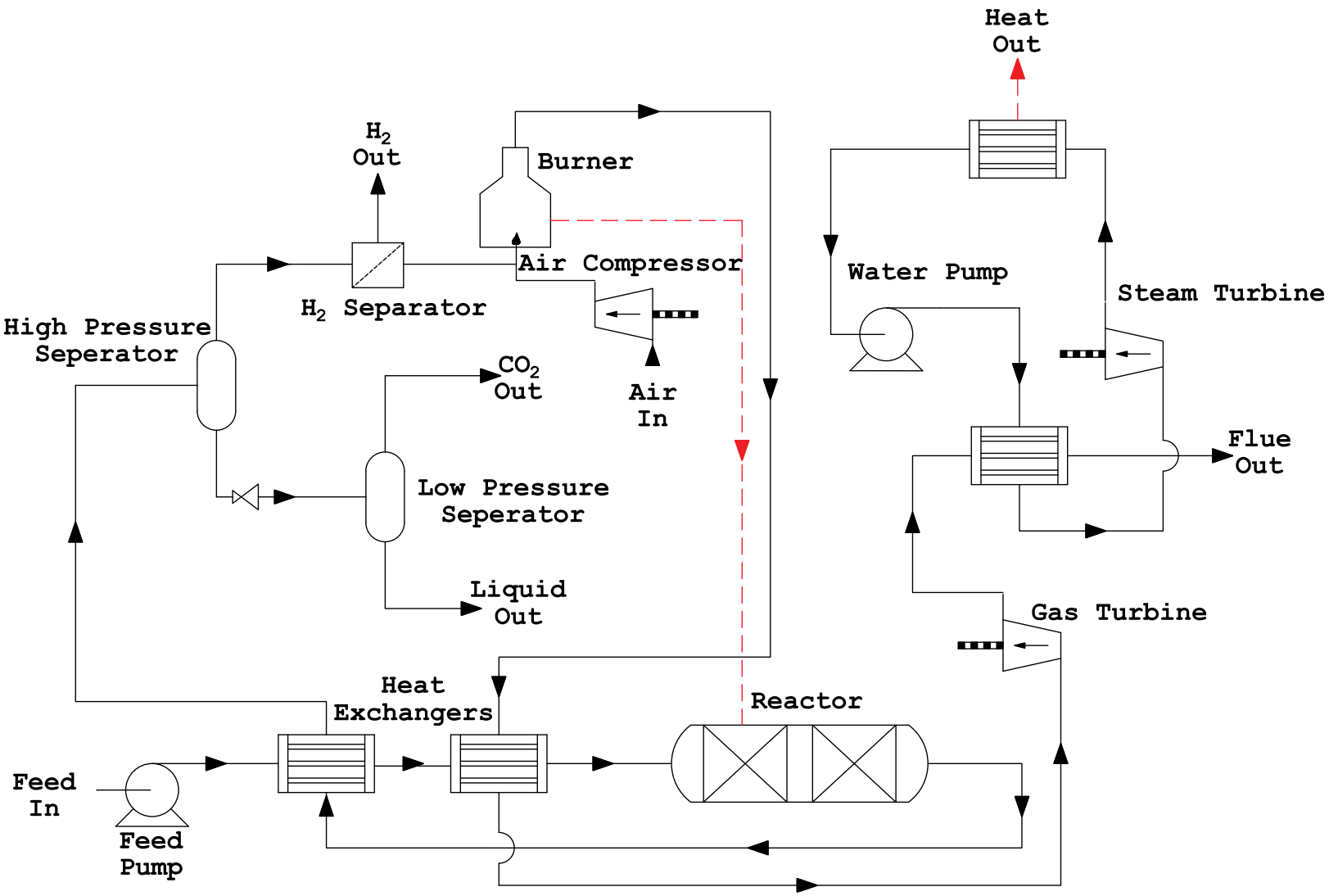

Figure 6.2-Modelled System for the Supercritical Water Gasification of Microalgae, with a equilibrium reactor. Black solid line is the process flow, red dashed line is heat.

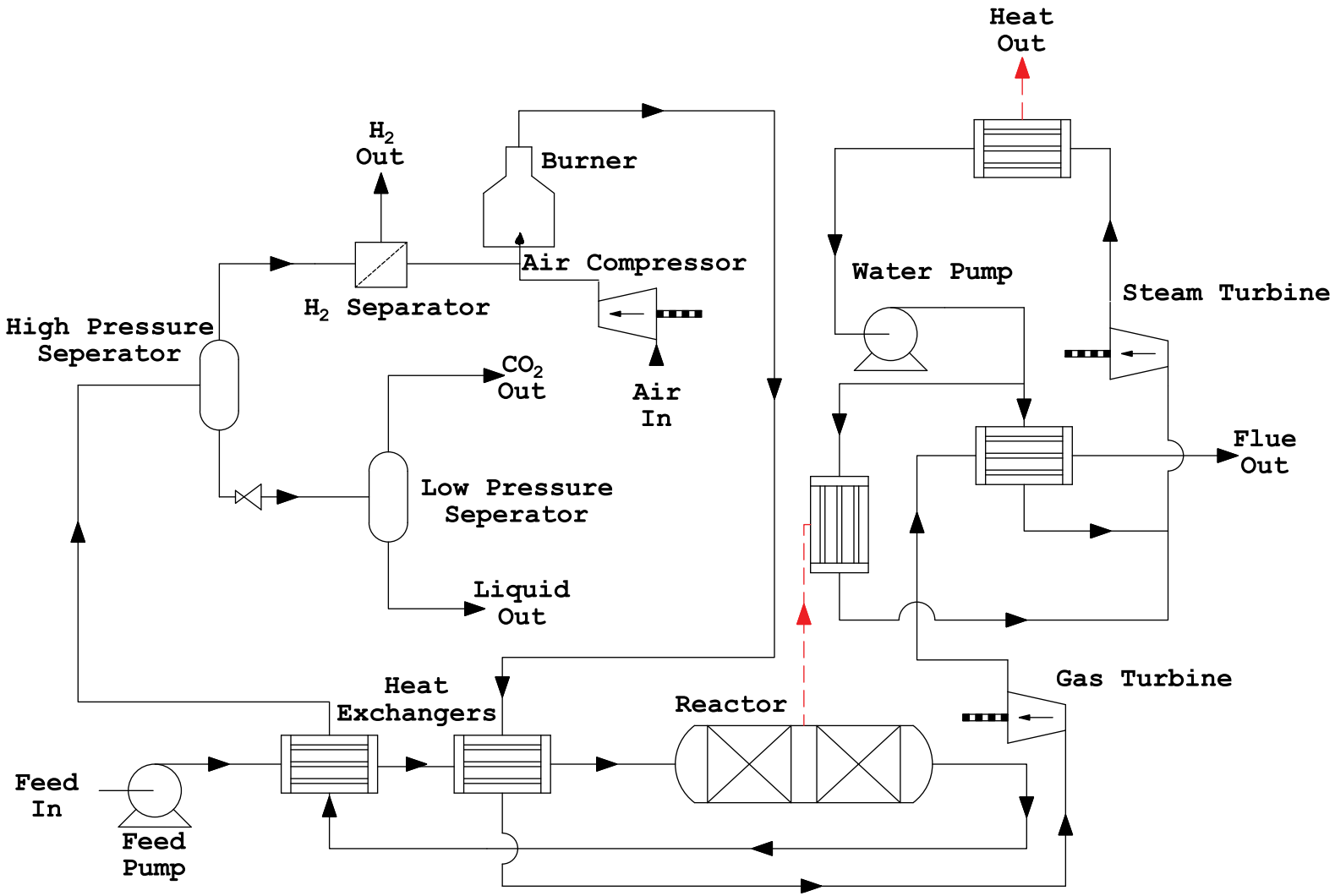

Figure 6.3-Modelled System for the Supercritical Water Gasification of Microalgae, with a reactor modelled on experimental data. Black solid line is the process flow, red dashed line is heat

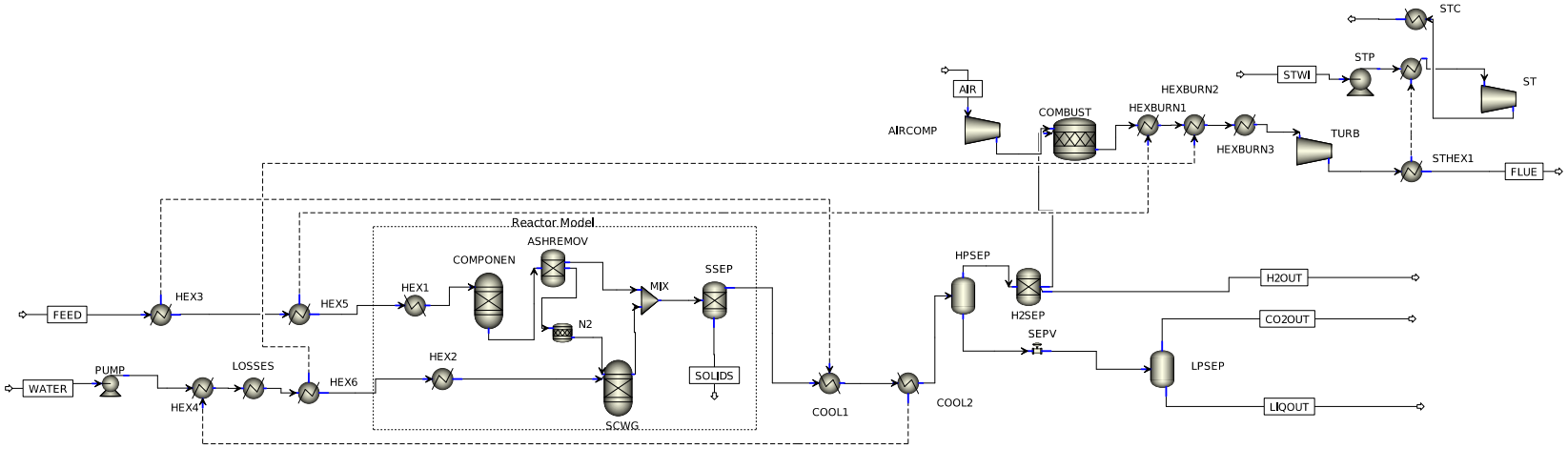

Figure 6.4-Equilibrium system model ASPEN PLUS® flowsheet.

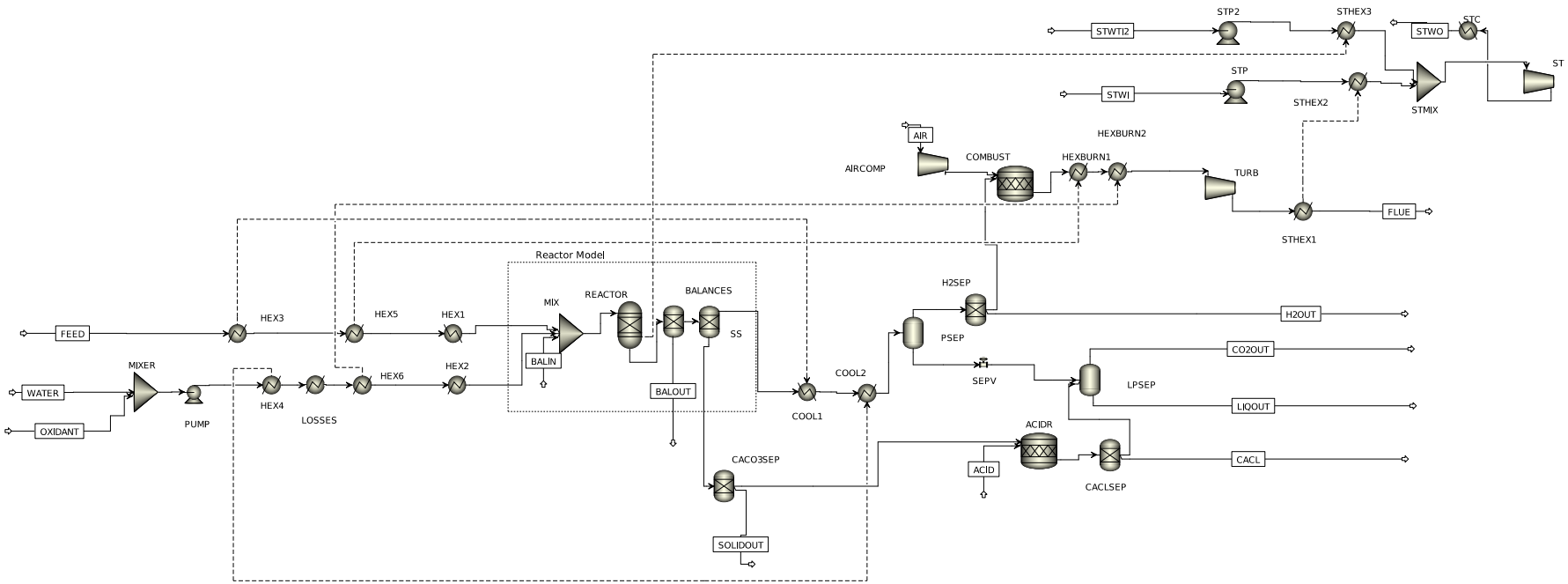

Figure 6.5-System model including experimental data ASPEN PLUS® flowsheet

The REFPROP method, which utilises the thermodynamic properties in the NIST database [54], was utilised when possible due to the greater accuracy compared with predictive models. However, the compounds and conditions it can be used for are limited. Consequently, it was only used for the gas separation (COOL1, COOL2, HPSEP and SEPV). For the rest of the model, a predictive Soave–Redlich–Kwong (PSRK) equation of state was used as the property method, due to its greater accuracy around the critical point of both water and CO_2 [55]. The isentropic efficiencies of compressors and turbines were set at 72% and the efficiencies of the pumps were 80% [56]. To ensure the process is energetically self-sufficient, the percentage separation of hydrogen from the flammable gas stream was selected to ensure the work provided by the two turbines matched that of the feed pump and air compressor. Due to the high pressure of the gas stream, 87% of the hydrogen can be separated into a high purity gas stream, without further energy input [57]. Thus, this was selected as the maximum hydrogen separation.

Heat losses from the system were assumed to be mostly from the pipelines, assuming a 100 m of pipework of 100 mm outside diameter hot pipework, with 20 mm of mineral wool insulation [58]. The flowrate and pressure in the steam turbine were optimised for each scenario using the ASPEN Plus® optimisation module, with a maximum pressure set at 250 bar [59]. Pressure losses in the system were assumed to be negligible. Due to the low concentrations used (<3 wt.%), the effect of biomass concentration on the pumping power was not considered. Also, sedimentation can be used to concentrate the algae to the concentration used in this study [60], so energy for harvesting was not considered. A minimum temperature difference of 10°C was chosen as a higher heating rate is preferable for gasification [17]. Investigation into the effect of a recycle in the G/L separator and elevated pressure to increase carbon capture was performed as this has been known to increase carbon capture [8]. However, the parasitic load of the recycle pump was found to counteract any potential capture benefits (shown in Appendix F), so was not considered.

The model is assessed based on the hydrogen yield, energy efficiency and carbon capture. The hydrogen yield is calculated as outlined in Section 6., using the H2OUT stream as the hydrogen produced. The model can produce (or consume) both electrical and thermal energy. However, the excess heat produced is not at a sufficient temperature to be used in the reaction or a steam turbine. This could be used for other applications, such as district heating or other industrial processes [66], but that will depend on the location of the facility. Consequently, the energy efficiency is either defined as the energy in the hydrogen and the net-work by all the pumps and turbines or with both electrical and thermal energy as shown in equations 10 and 11. In addition to the carbon dioxide stream, the char produced can also be used for carbon storage by incorporation into construction materials [9]. Therefore, the carbon capture is done as either gas only or gas and carbon, as shown in equations 12 and 13, for which it assumed that 90% of the char can be recovered.

$$Energy\ efficency\ (\%) = \frac{\dot{m}_{H2OUT} HHV_{H2} + \sum W}{\dot{m}_{FEED} HHV_{algae}} \tag{10}$$

$$Energy\ efficency\ including\ heat\ (\%) = \frac{\dot{m}_{H2OUT} HHV_{H2} + \sum W + Q_{STC}}{\dot{m}_{FEED} HHV_{algae}} \tag{11}$$

$$Carbon\ capture\ (gas)(\%) = \frac{C_{CO2OUT}}{C_{Feed}} \tag{12}$$

$$Carbon\ capture\ (Total)(\%) = \frac{C_{CO2OUT} + 0.9 \times C_{SOLIDOUT}}{C_{Feed}} \tag{13}$$

Where *W* is the work, *Q* is the heat duty, and the subscripts refer the stream/block in Figure 6.4 or Figure 6.5.

6.3 RESULTS AND DISCUSSION

6.3.1 SCWG Experimental Results

The continuous supercritical water gasification of *Chlorella vulgaris* was completed to study the impacts of reaction conditions (temperature and biomass concentration), catalysts (KOH, Ru/C) and use of oxidant. A temperature range 400 – 600 °C, biomass concentration of 1 – 3 wt.%, KOH concentration of 0 -1 wt.% and oxidant coefficient of 0 - 0.5 were used. Due to the heterogenous nature of the catalyst, Ru/C was considered a categorical variable with two levels (yes/no). To ensure the effects of all factors and interactions could be considered and all experiments were repeated at least twice to account for anomalous results, a total of 43 experiments were completed. The results are shown in Table 6.3.

Table 6.3-Experimental results for the SCWG of Chlorella vulgaris in a continuous system. Factors studied: Temperature(400-600°C), Biomass concentration (1-3wt.%), KOH Concentration (0-1wt.%), Oxidant Coefficient (0-0.5) and Ru/C Catalysts (Yes or no). All data points repeated at least once.

Experiment	Factors					Response Variables								
						Gas Yields (mg/g)					Carbon Balance			
	Temperature (°C)	Biomass Concentration (wt.%)	KOH Concentration (wt.%)	Ru/C	Oxidant Coefficient	H_2	CH_4	CO_2	CO	C_{2+}	Carbon Conversion	Total Organic Carbon	Residual Carbon	Energy Efficiency
1	500	2	0	No	0	2.58	9.33	273	47.38	38.18	27%	36%	37%	16%
2	600	1	0	No	0	10.02	55.52	421	112.12	169.65	70%	23%	7%	68%
3	500	2	0.5	No	0.25	8.46	11.61	548	2.04	56.83	42%	38%	20%	23%
4	600	3	0.5	Yes	0.5	4.90	14.14	712	0.85	36.15	48%	14%	38%	16%
5	600	1	0	Yes	0.25	16.50	53.20	862	1.67	146.22	81%	9%	10%	61%
6	400	3	0	Yes	0.25	0.70	0.84	340	17.26	9.78	22%	58%	19%	4%
7	600	3	0.5	No	0.25	4.61	16.69	564	7.89	48.14	43%	9%	48%	20%
8	500	2	1	No	0	9.29	14.77	310	0.13	74.98	32%	33%	35%	28%
9	400	3	0	No	0	0.07	0.34	178	5.45	2.65	11%	26%	63%	1%
10	400	1	0.5	No	0.25	5.92	0.84	403	1.24	30.50	28%	61%	11%	12%
11	500	2	0	No	0.5	2.99	11.92	350	76.56	47.83	36%	41%	23%	21%
12	400	1	0	Yes	0	1.31	0.77	212	9.71	6.39	14%	53%	33%	3%
13	400	3	0.5	Yes	0	1.69	0.58	249	0.05	11.09	16%	33%	51%	4%
14	600	3	0.5	No	0.25	4.15	14.96	540	4.26	27.54	38%	12%	50%	14%
15	600	1	1	No	0.5	19.12	49.54	693	0.55	155.29	72%	8%	19%	64%
16	600	1	1	No	0.5	19.17	56.80	704	0.00	172.14	77%	9%	14%	70%
17	400	3	1	No	0.5	3.28	0.89	505	0.17	15.25	31%	39%	30%	6%
18	600	3	0.5	Yes	0.5	4.71	16.54	675	2.05	49.82	49%	14%	37%	20%
19	500	2	0	No	0	2.28	8.76	278	48.12	38.54	28%	36%	37%	16%
20	400	1	0.5	No	0.25	5.15	0.66	403	0.22	25.46	27%	48%	26%	10%
21	600	1	0	No	0	14.35	59.47	595	40.47	174.13	75%	22%	3%	70%
22	600	3	1	Yes	0.25	5.34	18.57	616	1.79	55.11	47%	8%	45%	22%
23	600	1	0	Yes	0.25	16.99	59.10	800	2.32	169.58	82%	2%	16%	69%
24	600	1	0.5	Yes	0	21.53	43.23	741	0.56	189.71	80%	4%	16%	72%
25	400	3	1	No	0.5	2.74	0.62	510	0.11	16.37	31%	37%	32%	6%

26	600	3	1	Yes	0.25	5.57	18.17	642	0.53	39.79	45%	6%	49%	18%
27	400	1	0.5	Yes	0.5	8.01	4.93	734	0.03	47.86	50%	19%	31%	18%
28	400	3	0	No	0	0.22	0.49	188	5.86	2.62	12%	26%	62%	1%
29	400	3	0.5	Yes	0	1.98	0.66	253	0.32	13.87	17%	32%	51%	5%
30	500	2	1	No	0	9.24	15.44	407	0.40	82.51	39%	34%	27%	30%
31	400	1	0	Yes	0.25	1.50	0.89	315	31.12	15.27	23%	45%	32%	6%
32	500	2	0	No	0.5	3.43	10.26	405	86.66	55.40	41%	37%	22%	23%
33	600	1	0.5	Yes	0	19.69	45.94	616	7.68	176.30	71%	10%	19%	69%
34	400	1	0.5	Yes	0.5	7.10	4.01	687	0.05	34.06	45%	29%	27%	14%
35	400	1	0.5	Yes	0.5	7.45	5.05	700	0.13	38.04	46%	31%	22%	16%
36	600	3	0	Yes	0	5.86	22.06	620	1.76	52.43	47%	16%	37%	23%
37	600	3	0	Yes	0	4.08	16.50	546	2.68	48.43	41%	17%	41%	19%
38	400	1	0	Yes	0	1.63	1.27	195	7.76	11.53	14%	51%	35%	5%
39	400	3	0	Yes	0.25	0.65	0.63	358	18.17	0.00	22%	54%	24%	1%
40	500	2	0.5	No	0.25	8.32	10.98	443	0.00	71.25	38%	32%	30%	26%
41	400	3	0	Yes	0.25	0.53	0.63	345	16.25	7.20	22%	52%	26%	3%
42	400	1	1	Yes	0.25	13.10	3.73	427	0.91	42.39	32%	43%	26%	20%
43	400	1	1	Yes	0.25	11.61	4.60	349	0.00	41.80	27%	36%	37%	19%

A model was produced to represent how each output variable would be impacted by each of the factors, and any interactions between the factors. The main output variables are H_2 yield, carbon conversion, energy efficiency and residual carbon, the other gas yields, TOC and TIC are also included as they are used to inform the model in Section 6.3.2. The resulting models are shown in equations 14 -23. Due to the complex nature of these results, a variety of visualisation has been used to display them. The relative impact of each factor (directional logworth) and accuracy of the model fit (R^2) can be found in Table . The impact that the interactions between the factors on hydrogen yield, efficiency, carbon conversion and residual carbon, are displayed in figures 6.6-6.8. These figures show for each output variable how a factor may be influenced by other factors, displaying visually what is shown in Table 6.4. Simplified plots that display the impact of single factors, keeping the remaining factors constant, is displayed in the subsequent Sections 6.3.1.1-6.3.1.3. An experimental data vs model prediction plot can be found in Appendix H.

$$H_2Yield\left(\frac{mg}{g}\right) = 8.6 + 3.7T - 4.5x + 2.8K + 1.0R - 2.5T \times x - 0.8T \times K$$
$$-1.9C \times K + 0.4T \times R - 0.7x \times R - 0.8K^2 - 0.4O^2 \quad (14)$$

$$Carbon\ Conversion(\%) = 43 + 18.5T - 9.3x + 1.7K + 4.9O + 2.9R - 7.9T \times x - 4.3T \times O$$
$$-1.3C \times O + 0.144O \times R - 0.027K^2 \quad (15)$$

$$Energy\ Efficency(\%) = 25.6 + 18.2T - 14.3x + 3.2K + 1.2R - 10.6T \times x - 1.7x \times K$$
$$-2.2T \times x \quad (16)$$

$$Residual\ carbon\ (\%) = 31.1 - 1.9T + 11.8x + 2.2K - 3.8O + 4.6T \times x + 4.8T \times O$$
$$-3.9C \times O + 2.4K \times O - 6x \times R + 2.9K \times R \quad (17)$$

$$CH_4Yield\ \left(\frac{mg}{g}\right) = 9.6 + 16.6T - 8.8x - 8.3T \times x - 1.8T \times K + 1.5x \times K - 1.6x \times O$$
$$-0.84T \times R + 0.8x \times R + 0.9O \times R + 7.1T^2 + 2.7K^2 \quad (18)$$

$$CO\ Yield\left(\frac{mg}{g}\right) = \exp\left(\begin{matrix}0.1 + 0.9T - 2.6K + 0.6T \times K + \\ 0.9x \times O - 0.4T \times R + 0.8K \times R + K^2\end{matrix}\right) \quad (19)$$

$$C_{2+}Yield\left(\frac{mg}{g}\right) = 63.3 + 45T - 35.8x + 8.6K + 2.7R - 27.7T \times x - 3.5x \times K$$
$$-6.4T \times x \quad (20)$$

$$CO_2\ Yield\left(\frac{mg}{g}\right) = 134 + 118T - 24x + 60O + 25R - 23.7T \times x$$
$$-24x \times K - 23.4T \times O - 24.6x \times O + 20.7T \times R - 10.9x \times R - 26.8K \times R$$
$$+9.9O \times R + 64.7T^2 \quad (21)$$

$$CO_2\ Yield(inc\ TIC)\left(\frac{mg}{g}\right) = 519 + 140.1T - 37.5x + 23.5K + 87.4O + 49.7R - 28.9T \times x$$
$$-50T \times O - 29.5x \times O + 26.1K \times O + 31.6T \times R - 33.8K \times R + 28.8O \times R - 71.07K^2 \quad (22)$$

$$TOC(\%) = 36 - 17T - 3x - 4K - 2R + 3T \times x$$
$$-3x \times K + 6.5x \times O + 6x \times R - 2.6K \times R - 1.4O \times R - 2.3O^2 \quad (23)$$

$$TIC(\%) = 18 + T - 1.5x + 2.5K + 0.7R + 1.4O - 1.8T \times K$$
$$-0.9C \times O + O \times R - 2.5K^2 \quad (24)$$

Where:

$T = \frac{(temperature\ (℃) - 500)}{100}$, $x = (Biomass\ Concentration(wt\%) - 2)$,

Table 6.4-Directional logworth of each factor on the carbon conversion, energy efficiency and gas yields. Where: T=temperature, x=biomass concentration, K=KOH concentration, O =oxidant coefficient, R is Ru/C catalyst.

Output variable	**Directional Logworth**																		R^2
	T	**x**	**K**	**O**	**R**	**T*x**	**T*K**	**T*O**	**T*R**	**x*K**	**C*O**	**x*R**	**K*O**	**K*R**	**O*R**	**T^2**	**x^2**	**K^2**	**O^2**	
H_2 Yield	20.2	-22.8	16.1		7.6	-16.1	-3.5		1.8	-10.2		-3.6						-2.2	-2.2	0.99
Carbon Conversion	25.1	-16.1	1.7	9.2	5.3	-13.4		-7.6			-1.6				1.2			-1.6		0.98
Energy Efficiency	28.9	-25.3	5.75		1.8	-20.9		-4.0		-2.0										0.99
Residual carbon	-1.6	14.6	1.6	-4.6		5.6		5.7			-4.3	-7.1	1.7	2.6						0.92
CH_4 Yield	27.3	-18.6				-19.3	-2.9		-1.2	1.7	-2.7	1.1			1.8	8.5		3		0.99
CO_2 Yield	16.8		-2.6	10.6	3.2	-3.1		-3.1	2.6	1.7	-2.8	-1.0		-3.1	1	3.5				0.96
CO_2 Yield (inc TIC)	14.3	-3.4	1.4	10	5.5	-2.2		-5	2.5		-2.4		1.5	-2.3	2.6			-3.4		0.95
CO Yield	3.2		-27.7				1.74		-1.5		4.2			4.0				2.4		0.96
C_{2+} yield	25.8	-22.4	4.9		1.3	-18.7		-3.7		-1.2										0.98
TOC	-20.5	-4.3	-4.9		-2	3.6				-2.1	8.3	8		-2.5	-1.6	-4.2			-2.6	0.96
TIC	2.3	-3.9	6.2	3.5	1.5		-3.5				-1.6				2.3			-3.2		0.86

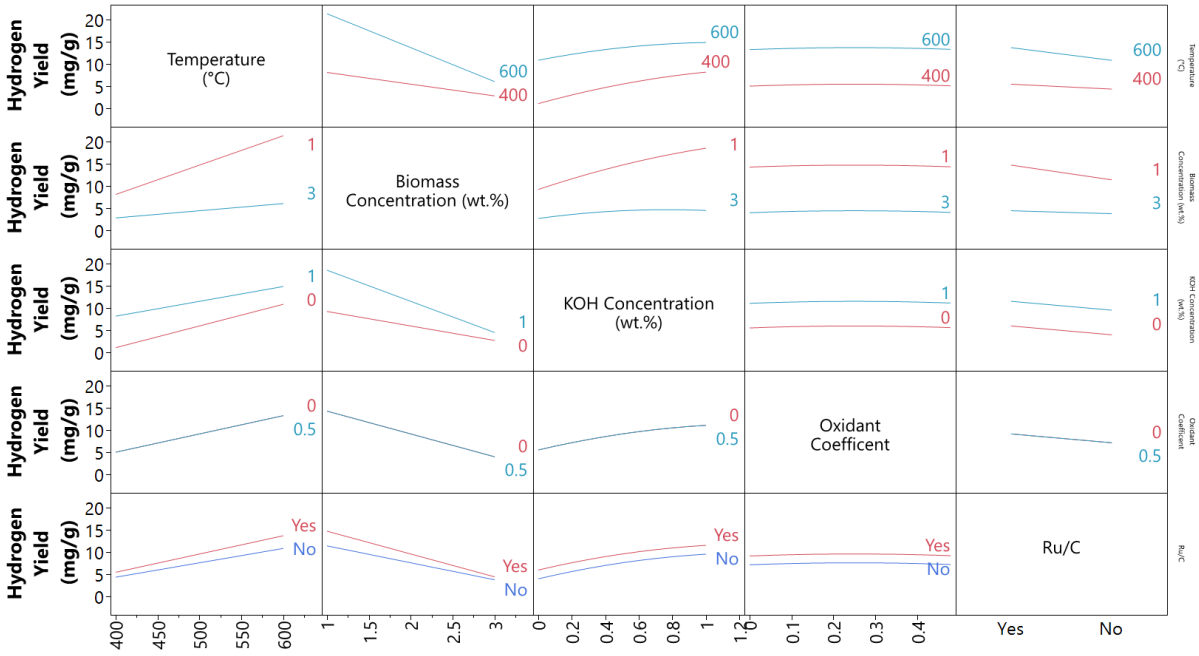

Figure 6.6 - Interaction between factors on the hydrogen yield. When comparing 2 variables, continuous variables are kept at their midpoint or off value (500°C, 2wt. % biomass, 0.5wt. % KOH, 0.25 oxidant ratio and no Ru/C catalyst. X axis refers to the variable of outlined in that column, the 2 curves refer to two values of the variable in that row.

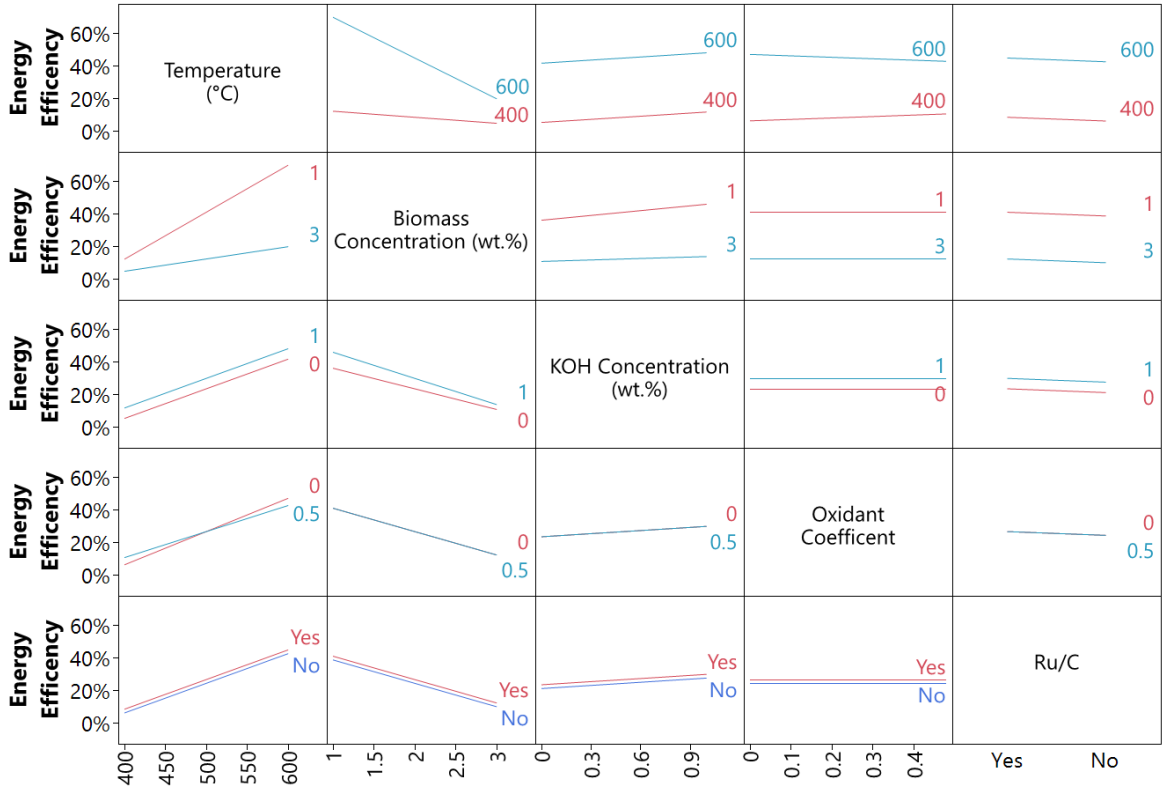

Figure 6.7 - Interaction between factors on the energy efficiency. When comparing 2 variables, continuous variables are kept at their midpoint or off value (500°C, 2wt. % biomass, 0.5wt. % KOH, 0.25 oxidant ratio and no Ru/C catalyst. X axis refers to the variable of outlined in that column, the 2 curves refer to two values of the variable in that row.

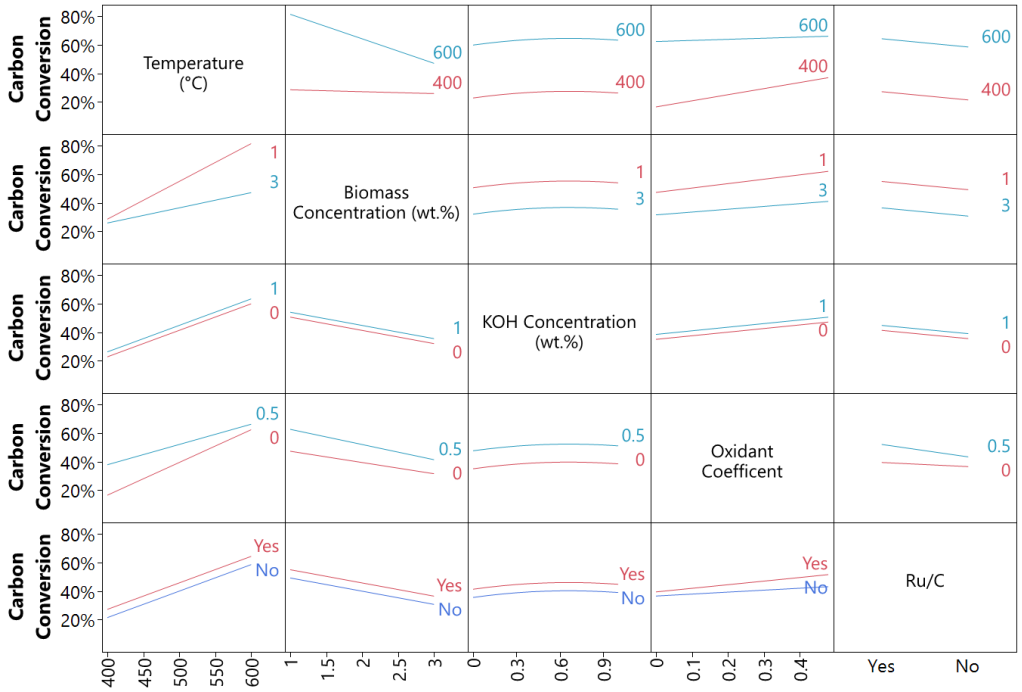

Figure 6.8 -Interaction between factors on the carbon conversion. When comparing 2 variables, continuous variables are kept at their midpoint or off value (500°C, 2wt. % biomass, 0.5wt. % KOH, 0.25 oxidant ratio and no Ru/C catalyst. X axis refers to the variable of outlined in that column, the 2 curves refer to two values of the variable in that row.

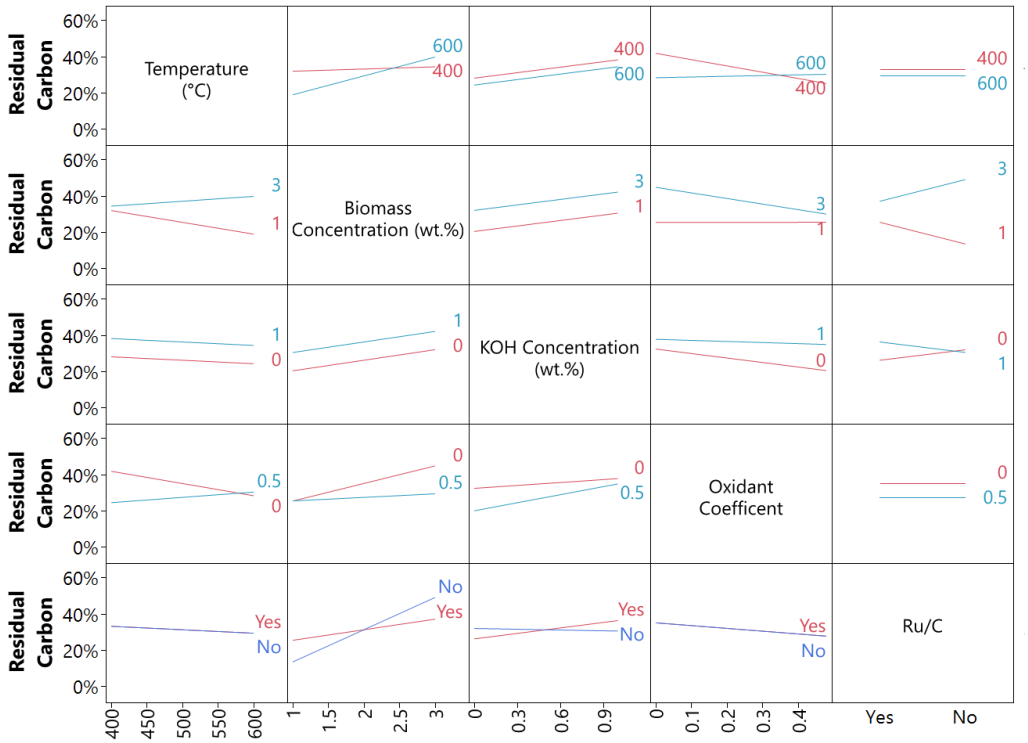

Figure 6.9 - Interaction between factors on the residual carbon. When comparing 2 variables, continuous variables are kept at their midpoint or off value (500°C, 2wt. % biomass, 0.5wt. % KOH, 0.25 oxidant ratio and no Ru/C catalyst. X axis refers to the variable of outlined in that column, the 2 curves refer to two values of the variable in that row.

6.3.1.1 *Impact of Reaction Conditions*

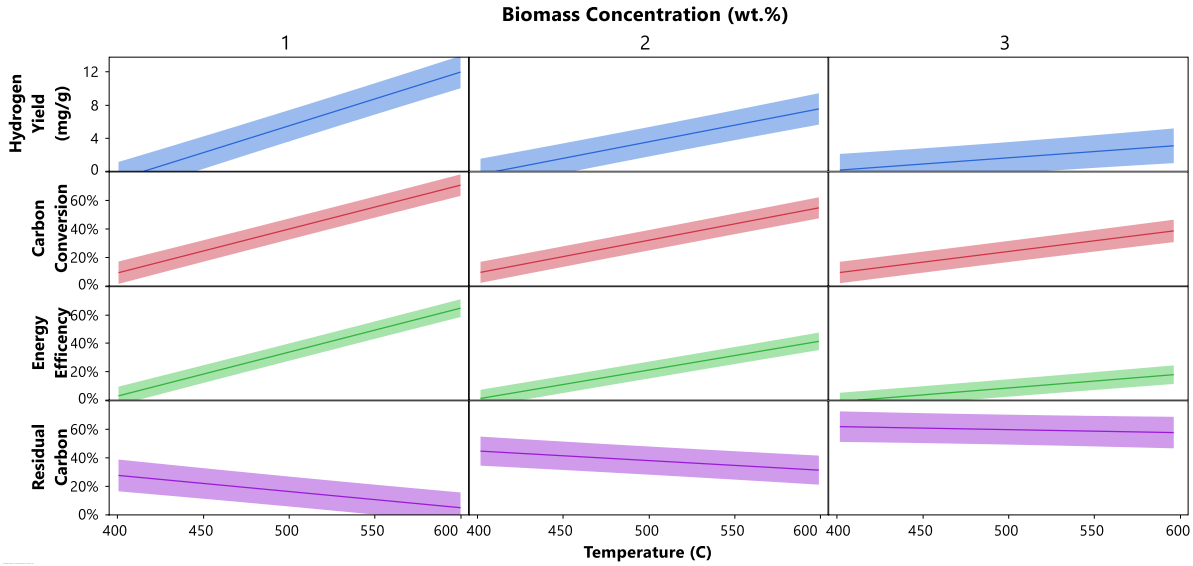

Figure 6.10 -Impact of temperature and biomass concentration on hydrogen yield, carbon conversion, energy efficiency and residual carbon. No catalyst or oxidant. The solid line represents the model output, the shaded area represents the 95% confidence bounds.

The temperature and biomass concentration were the most significant factors observed in SCWG of *Chlorella vulgaris*. Temperature was the most significant factor on the hydrogen yield, carbon conversion and energy efficiency, having a positive impact on all three response variables. Biomass concentration was the 2nd most significant factor for hydrogen yield, carbon conversion and energy efficiency, with increased biomass concentration having a negative impact on all three. Also, biomass concentration was the most significant factor on residual carbon, having a positive impact. Temperature had a significant negative impact on this, but the significance was 9 times lower than that of biomass concentration.

It is favourable to maximise hydrogen production, conversion and efficiency, while trying to minimise tar/char production may also be preferable due to decreased plugging effects. Therefore, this shows that a higher temperature and lower biomass concentration is preferable to maximise the desirability of the process. These all align with previous experimental [14, 62, 53], kinetic [23] and equilibrium studies [36, 50, 63, 64, 65] as outlined in Section 6.1. Additionally, this shows that the biomass concentration is the main driving force towards the polymerisation reactions that lead to the formation

of char/tars in the residual carbon. Polymerisation of aromatic compounds in SCW, a known tar/char precursor, is known to be heavily influenced by concentrations [66], due to an increased likelihood of contact and recombination. This is likely to be the cause of the effect shown in this study.

There was also a significant interaction between temperature and biomass concentration, the interaction being the 3rd most significant factor on hydrogen yield, carbon conversion, energy efficiency and the 2nd most significant factor on residual carbon. The interaction factor was in the opposite direction to temperature and the same direction as concentration; thus, the impact of temperature was greater at lower biomass concentrations and the impact of concentration was greater at higher temperatures. This is evident in the difference in gradients observed in Figure 6.. A possible explanation with this could lie with the greater significance of concentration on polymerisation reactions. If a greater proportion of the organic carbon is being polymerised with higher concentrations, a lower quantity is available to be gasified. Thus, the change due the temperature will be reduced as these compounds are known to be more stable in SCW.

6.3.1.2 Impact of Catalysts

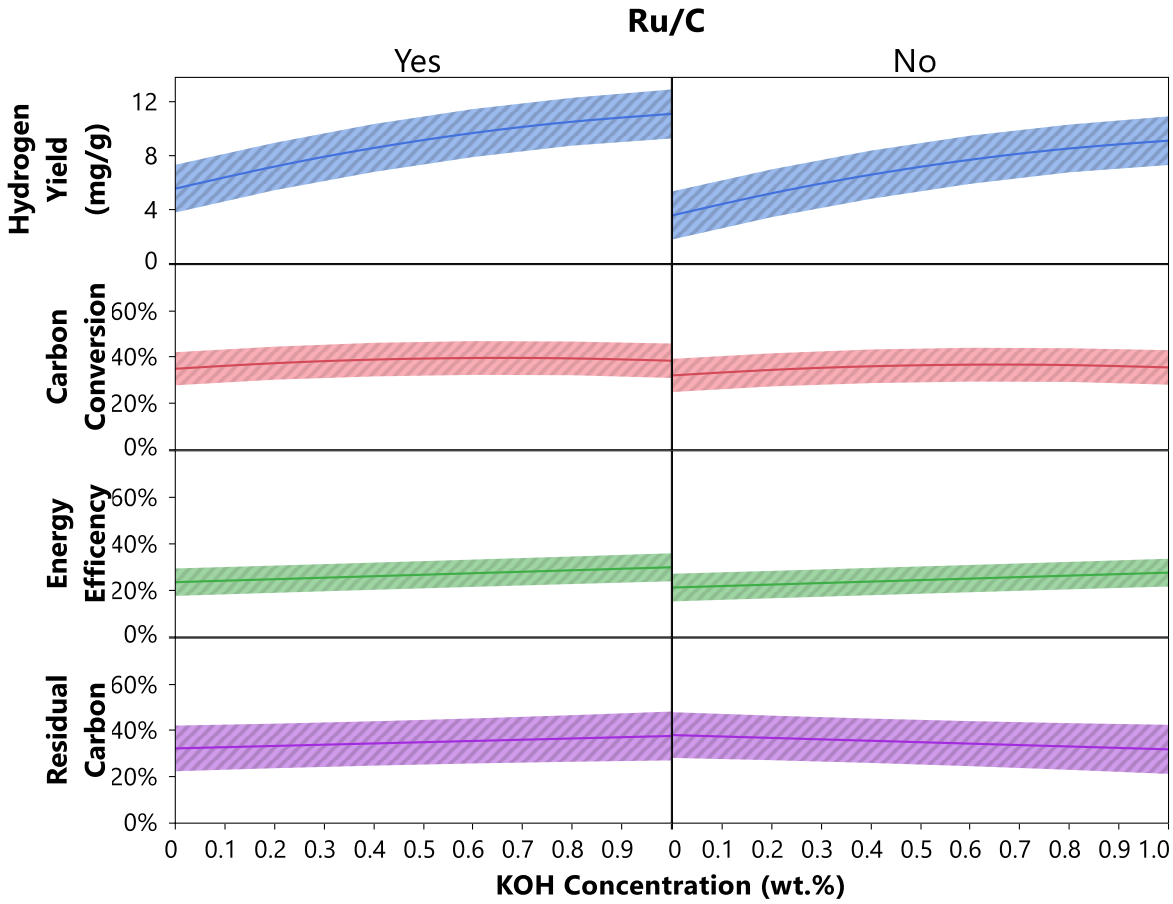

Figure 6.11-Impact of KOH and Ru/C catalysts on Hydrogen Yield, carbon conversion, energy efficiency and residual carbon. 500°C, 2wt%, no oxidant. The solid line represents the model output, the shaded area represents the 95% confidence bounds.

KOH has a significantly positive impact on all of the main output variables especially on the hydrogen yield, for which KOH is the most effective factor after the temperature and biomass concentration. This is expected, as KOH is known to a catalyse the WGS reaction [17], converting the CO produced into hydrogen and CO_2, thus increasing the hydrogen yield. A significant negative interaction with both temperature and biomass concentration was also observed, indicating the effect of KOH diminished at higher temperatures and biomass concentrations. This can be explained in terms of the pH and TIC content in the liquid products following SCWG. A significantly greater drop in pH (displayed in Appendix G) from over 13 in the feedstock to less than 8.5 in the liquid product was observed and, as shown in Table 6.4, KOH had a significant positive influence on the percentage of the carbon that is present as inorganic carbon in the liquid phase. This is because the KOH is

reacting with the CO_2 produced to form carbonates [69]. At higher temperature and biomass concentrations, more CO_2 is being produced, removing the hydroxide from the reaction and reducing its relative effects.

A significant negative quadratic effect was also observed on hydrogen yield, indicating that the rate of increase in hydrogen with respect to KOH concentration decreased above 0.5 wt.%. A major contributor to this is that, after a certain concentration, the WGS reaction cannot be catalysed any further as there is no CO remaining. At the midpoint of the KOH concentration range (0.5 wt.%), minimal CO was observed in the gas stream (<2 vol.%), so the WGS has already been catalysed to its full extent at this point. Despite this, increasing the concentration of KOH still increased the hydrogen yield for the full range of this study. A possible explanation of this could be the reaction of the produced CO_2 with the KOH, as stated above, removing CO_2 from the gas stream. Due to Le Chatelier's principle, this pushes forward any reaction containing CO_2 as a product, which includes steam reforming and some intermediate decarboxylation reactions, which increases the breakdown of intermediates, increasing the overall hydrogen yield. It is this effect and a similar effect due to the removal of CO from the gas stream, that could explain how KOH also had a significant positive impact on carbon conversion and energy efficiency.

Ru/C, like KOH, had a significant positive impact on the hydrogen yield, carbon conversion and energy efficiency. Therefore, both were effective catalysts for enhancing the SCWG of *Chlorella vulgaris*. Moreover, there was no synergic effects, negative or positive, between these catalysts. Consequently, both can be used together without impacting the effects of the other. This is clearly shown in figures 6.6-6.8 and 6.11, where the hydrogen yield, carbon conversion and energy efficiency are clearly greater with both catalysts than each individually. Thus, simultaneous use of both types of catalysts is recommended for SCWG. Although, in a real system, costs consideration of using both catalysts, especially Ru/C must also be considered.

The impact on residual carbon, and thus tar/char production, differs from that of the other output variables. KOH has a significant positive impact on residual carbon, indicating that it leads to the

polymerisation of intermediates to form tar/chars. This can be attributed to the elevated pH which has been known to increase the formation of tar/char through the catalysis of the dehydration of furfural to form phenols [45, 24], known precursors to tar/chars [70, 16]. Ruthenium was only found to have a significant impact on residual carbon as an interaction with concentration, of which it was negative. This indicates that Ru/C reduces the tar/char formation, but this impact is only significant at higher concentrations. Thus, Ru/C could be used to help reduce the issue with large char/tar yields with more concentrated feedstocks, allowing for a greater throughput of a reactor. However, at these higher concentrations, deactivation due to coking would be an issue that must be considered.

It is also notable there was a significant interaction between the catalysts for this, indicating that the increase of char due to KOH was greater when Ru/C was present. This suggests that the production precursors to tar/char production catalysed by the KOH catalyst are favoured with Ru/C. As a result, consideration of the ideal KOH concentration when using both catalysts may have to consider operation issues that may occur as a results of increased residual material. Nonetheless, the unwanted impacts on the residual carbon are less significant than the positive impacts observed on the yield, efficiency and conversion. Thus, both are still effective catalysts for SCWG of microalgae.

6.3.1.3 Impact of Oxidant

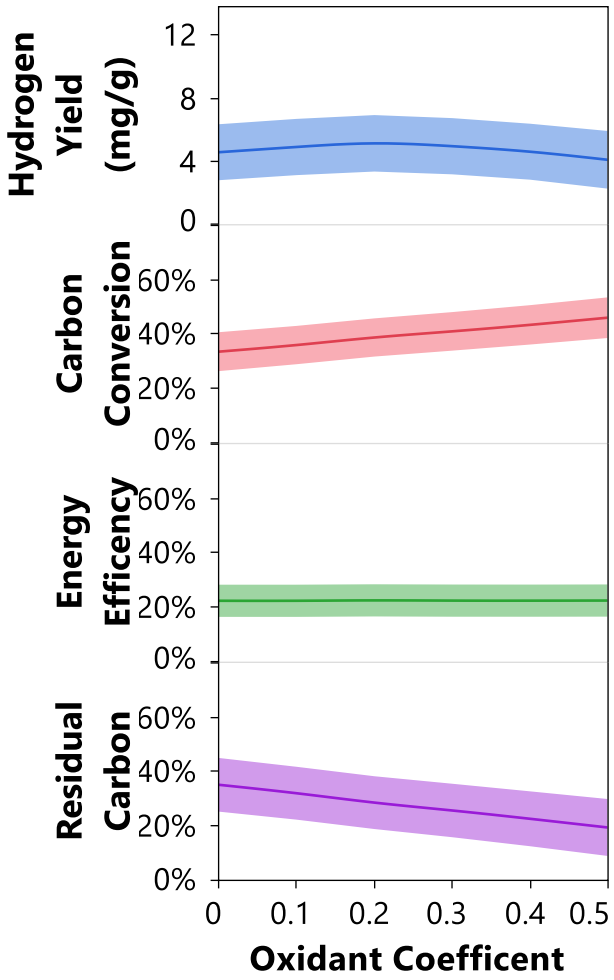

Figure 6.12-Impact of oxidant on hydrogen Yield, carbon conversion, energy efficiency and residual carbon. 500°C, 2wt%, no catalyst. The solid line represents the model output, the shaded area represents the 95% confidence bounds.

Oxidant had a significant impact on increasing the carbon conversion and reducing the residual carbon. This impact was greater than either catalyst, but less significant than the reaction conditions. This is expected as the presence of oxidant in SCW is known to react with organic compounds, breaking them down to produce carbon dioxide. This is known to occur even with stable compounds such as phenol or naphthalene [71]. Additionally, Oxidation releases heat which aids the gasification rate as well as biomass conversion [72]. In both cases, this effect was more significant at higher biomass concentrations and lower temperatures. This is due to the greater amount of carbon that remains either in the liquid as stable organic compounds or has polymerised into larger molecules. These can be broken down by the oxidant, thus increasing the difference in conversion and reducing

residual carbon. At more favourable conditions, a greater proportion of the organic intermediates would have been converted to gas, so the impact of the oxidant would be reduced.

The impact of the oxidant coefficient on the hydrogen yield was observed to be of a negative quadratic nature, with a maximum at 0.2. As a result, increasing the oxidant coefficient initially increased the hydrogen yield but started reducing it beyond 0.2. This indicates that at low concentrations (oxidant coefficient < 0.2), the breakdown of normally stable organic intermediates by the oxidant creates compounds that are more readily gasified, resulting in an increased hydrogen yield. However, oxidant will also react with the hydrogen produced, which after a 0.2 oxidant coefficient begins to reduce the hydrogen yield. The impact of oxidant on the efficiency is only significant in a negative interaction with temperature. Thus, at higher temperatures the use of oxidant can reduce the energy efficiency of the process. This is due the greater proportion of energy rich gases being produced and a greater conversion. Consequently, the negative impact of oxidising the energy rich gases, such as hydrogen and methane, is increased and the positive impact of a higher conversion is reduced.

As a result, oxidant can be useful at increasing the operability by reducing the tars/chars formed and removing unwanted organic intermediates. It can also increase hydrogen yield at when smaller quantities of oxidant are added (~ 0.2 oxidant coefficient). However, it can reduce energy efficiency at higher temperatures, where the positive impacts on conversion are also reduced. As stated in Section 6.3.1.1, higher temperatures are preferable for the SCWG of microalgae and lower temperatures are unlikely to be used in a real system due to their very low conversions and yields. Therefore, it is likely that the positive impacts of oxidant may not be utilised in a real system. Although, the elevated losses at higher temperatures and lower biomass concentrations in full system may alter this, a full system model is required to assess this (as is addressed in Section 6.3.2).

6.3.2 SCWG System Model Results

6.3.2.1 Comparison to Equilibrium Values

To assess how the experimental model differs from an equilibrium model, that are commonly utilised in the literature, 2 models were simulated for the range of biomass concentrations and temperatures studied in the experimental work in Section 6.3.1 (1 -3 wt.%, 400 – 600 °C), with either an equilibrium reactor (Figures 6.2 and 6.4) or using the experimental data (Figures 6.3 and 6.5). The resulting hydrogen yield, efficiency and carbon capture is displayed in Figure 6.13 and Figure 6.14, where the experimental data is either displayed for no catalyst or at the catalyst combination expected to maximise the hydrogen yield (1 wt.% KOH, Ru/C and 0.25 oxidant coefficient).

Additionally, it was notable that the reactor in the experimental model was exothermic but endothermic when utilising the Gibbs free minimisation approach in the equilibrium model. This is largely due to the organic proportion that remains in the liquid phase (assumed to be phenol), which were not considered in equilibrium models and greater char formation in the experimental work. The formation of these products from biomass constituents such as glucose are exothermic [73], so counteract the endothermic nature of the gas forming and bond scission reactions.

This is an important limitation of equilibrium models as, while theoretically the system would reach equilibrium at longer reaction times, a reaction time longer than those studied in this work would largely be impractical, due to the slow flowrates/large pipework required. Therefore, it is important to understand the nature of the reaction at a given condition, to guarantee a reactor is designed appropriately (heated or cooled), ensuring safe operation and efficient performance.

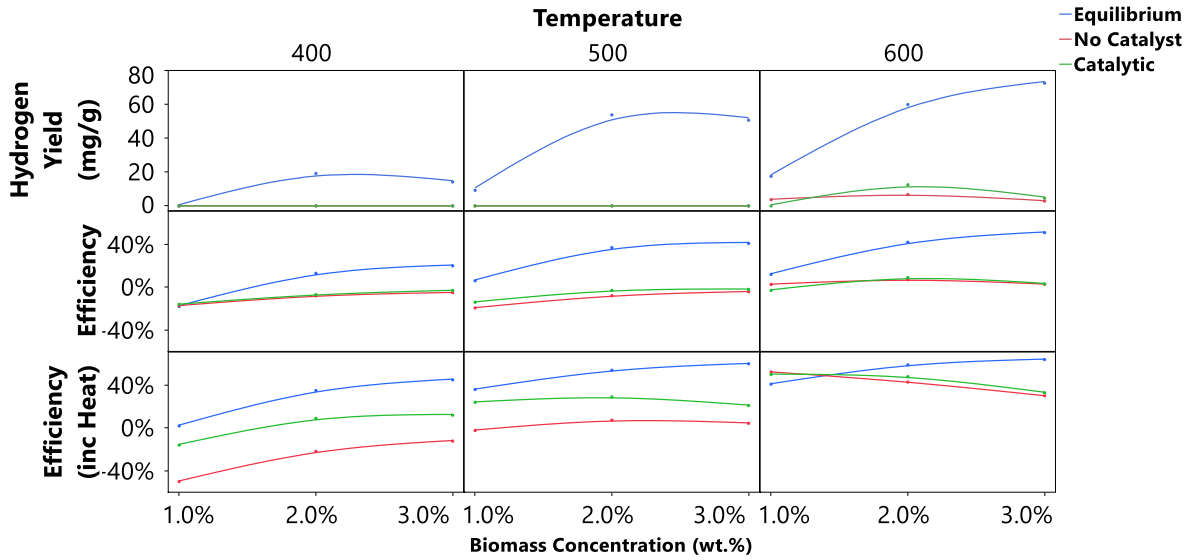

Figure 6.13- Comparison of the Hydrogen Yield and Energy Efficiency of Equilibrium Model to Experimental model. Results displayed are from a system model using a Gibbs free minimisation reactor (blue) and a system model busing experimental data as the reactor (red no catalyst, green catalyst)

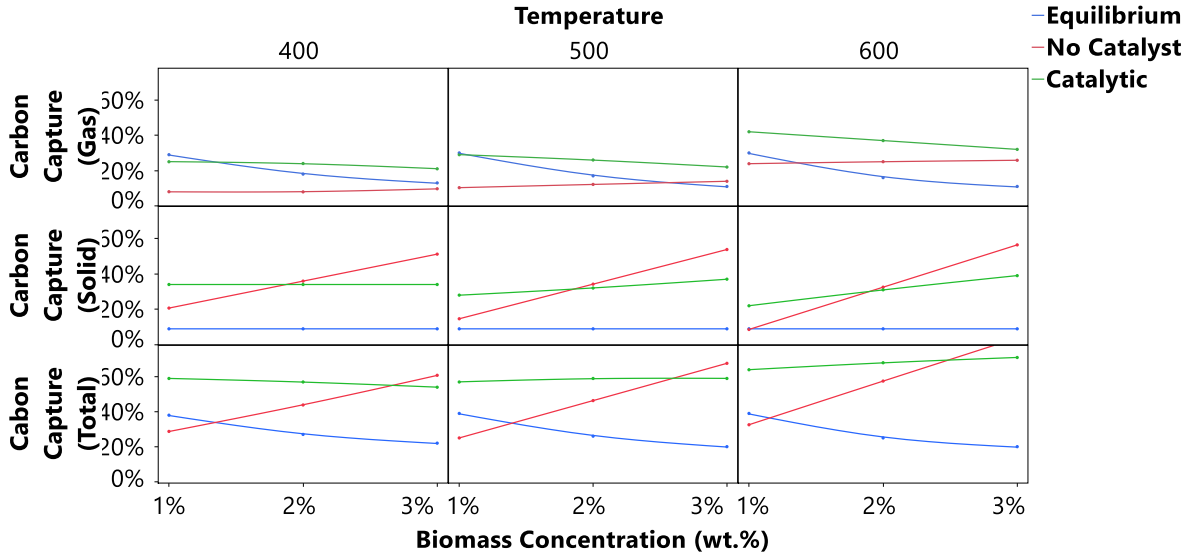

Figure 6.14- Comparison of the Carbon Capture of Equilibrium Model to Experimental model. Results displayed are from a system model using a Gibbs free minimisation reactor (blue) and a system model busing experimental data as the reactor (red no catalyst, green catalyst)

This data clearly shows a disparity between the equilibrium data and the experimental work. The hydrogen yield and efficiency are significantly greater for the equilibrium model than experimental work, even when catalytic activity is at a maximum. This is most notable at higher biomass concentrations, where at 600°C and 3 wt.% where the hydrogen yield is 72mg/g for the equilibrium model and 4.6 or 12.5mg/g for the non-catalytic and catalytic experimental models. This is driven by the larger carbon conversion and hydrogen content in the gas achieved in the equilibrium model. This is most evident at higher biomass concentrations as polymerisation reactions are more significant at these temperatures as the residual carbon was greater than 20%, reaching 63% in some cases, of the feedstock carbon when the maximum concentration was utilised. This is not accounted for in the equilibrium reactor, as the residual carbon is assumed to be the fixed carbon (10%).

It is also notable that the equilibrium model resulted in both higher hydrogen yield and efficiency with a greater biomass concentration, due to the reduced losses from increased pumping power and larger heating requirement for increased water flow. However, this was not the case in experimental models, where the hydrogen yield and efficiency peaked at 2 wt.%. This is because the negative influence of biomass concentration on these outputs in real experiments is more significant to that of equilibrium models. This is a result of the influence of biomass concentration on the kinetics of reactions, most notably the reactions that form of organic intermediates and char, which reduce the overall efficiency and gas yields.

The carbon capture achieved also showed a significant variation between the experimental studies and equilibrium. The experimental results achieved a much higher char yield than that expected from the fixed carbon in the microalgae, due to the influence of polymerisation reactions on char formation [29], which were not considered in the equilibrium models. A greater amount of gas carbon capture was also achieved in the catalytic experimental model. This is due to the reaction to form carbonate, which due to the limit of carbon dioxide solubility in water, allows a greater amount of carbon to be captured from the gas stream [74]. These differences emphasise the importance of considering

experimental work when analysing SCWG systems and understanding any limitations of experimental models.

For all cases, both equilibrium and experimental, the hydrogen yield and efficiency increase with temperature. This shows that in this system, the heat losses and increased specific heat capacity at elevated temperatures is negligible in comparison to the increased in gas yields and hydrogen selectivity. It was also notable that, even with catalysts, a negative efficiency was observed for 400 and 500 °C. This indicates that more energy was needed to heat and power the system than was produced and thus resulted in no hydrogen being produced. As a result, operation at these conditions would not be suitable, so evaluation of the factors in the following Section would only be considered at 600 °C.

6.3.2.2 Consideration of Factors

The experimental model was operated at 600 °C for a range of biomass concentrations (1 - 3 wt.%), KOH concentrations (0 – 1 wt.%), Oxidant coefficients (0 - 0.5) and with or without Ru/C catalyst. To analyse the model outcomes, a regression model was fit to the resulting data, with the response variables of hydrogen yield, efficiency and carbon capture. The standard least squares method was used for the carbon capture, with all variables with a p-value greater than 0.05 being removed. However, due to a lack of normally distributed response variables this could not be applied the other variables. A backwards elimination approach with Cauchy or gamma output distribution was used for efficiency and hydrogen yield respectively. A directional Logworth was produced to assess the impact of each factor on this system model and the interaction plot are outlined in Table 6.5 and figures 6.15-6.17 respectively.

Table 6.5-Directional logworth of each factor on the carbon conversion, energy efficiency and carbon capture of the system model based on experimental data. Where: T=temperature, x=biomass concentration, K=KOH concentration, O =oxidant coefficient, R is Ru/C catalyst.

Output Variable	Directional Logworth													R^2
	C	K	O	R	C*K	C*O	C*R	K*O	K*R	O*R	C^2	K^2	O^2	C*O*R	
H_2 Yield	14		7	19	-1	-12	6			8	-46	5	-11		0.921
Energy Efficiency	39		15	13	-3	-1			2	10	-71	14	-9	3	0.944
Energy Efficiency (inc heat)	-41	16	12	34	-7	-4			-13	22	-30		-22	5	0.954
Carbon Capture (gas)	-182	67	194	224	-75	-29	-47		-127	129	-23		-114		0.997
Carbon Capture (Solid)	337	175	-232	-16		-199	-248	158	179						0.999
Carbon Capture (Total)	296	182	-92	214	-73	-221	-238	143	85	125	-20		-110		0.999

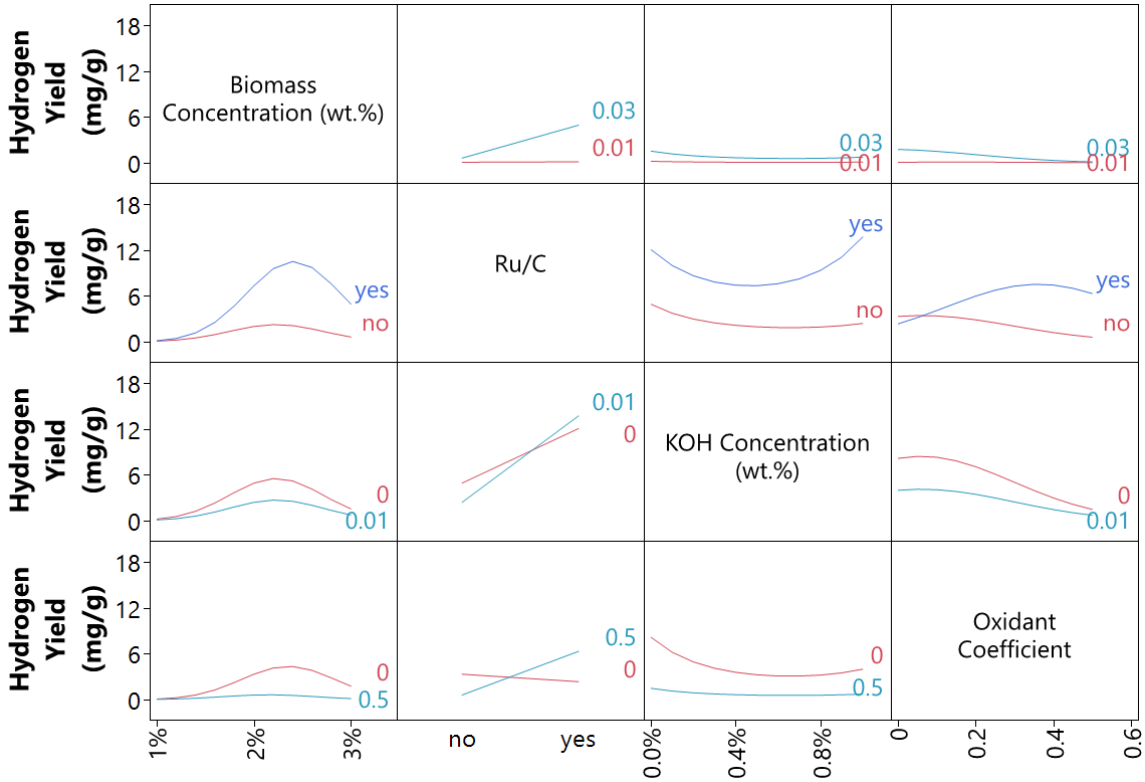

Figure 6.15 -Interaction between factors on the hydrogen yield of the system model based on experimental data. When comparing 2 variables, continuous variables are kept at their midpoint or off value (500 °C, 2 wt.% biomass, 0.5 wt.% KOH, 0.25 oxidant ratio and Ru is on Yes). X axis refers to the variable of outlined in that column, the 2 curves refer to of the variable in that row.

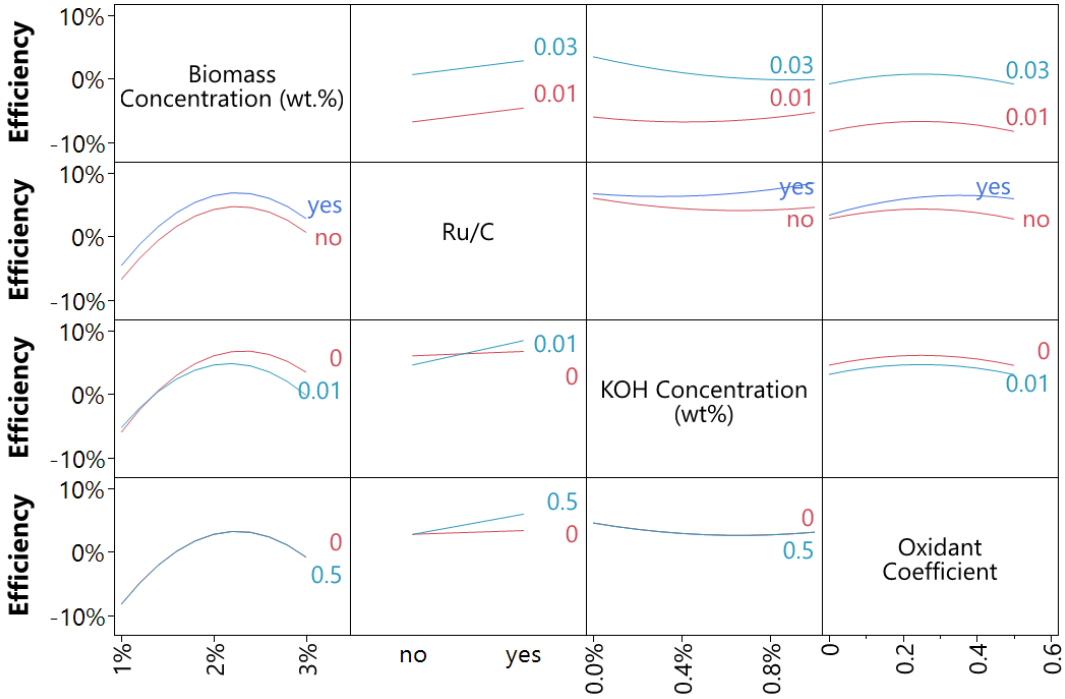

Figure 6.16-Interaction between factors on the efficiency of the system model based on experimental data. When comparing 2 variables, continuous variables are kept at their midpoint or off value (500 °C, 2 wt.% biomass, 0.5 wt.% KOH, 0.25 oxidant ratio and Ru is on Yes). X axis refers to the variable of outlined in that column, the 2 curves refer to the two values of the variable in that row.

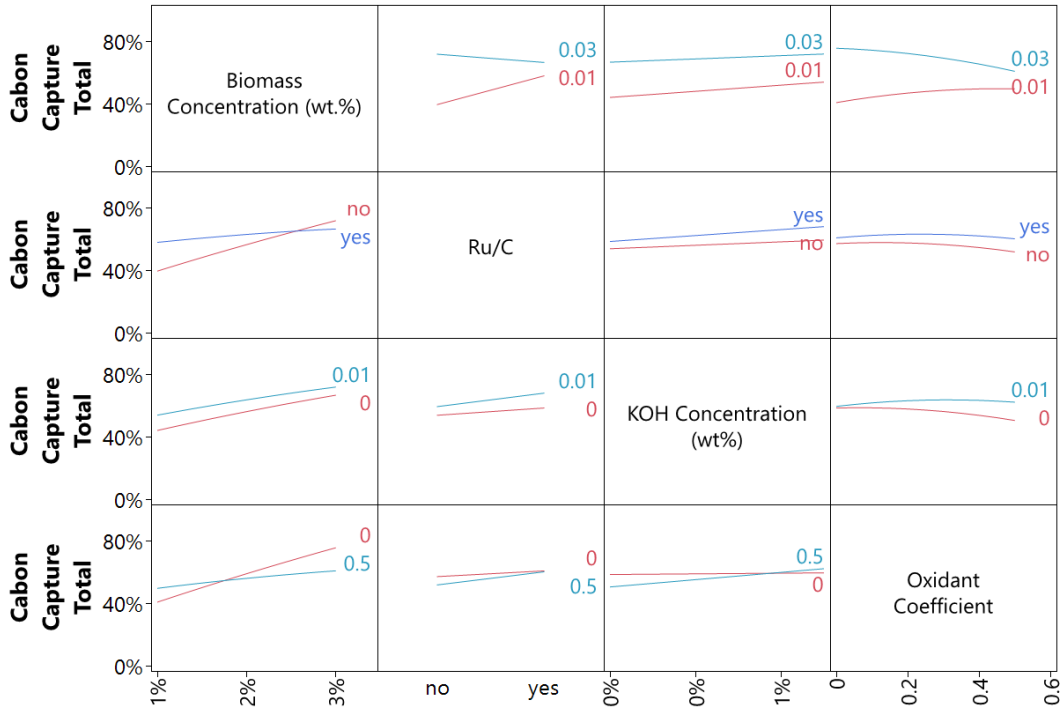

Figure 6.17-Interaction between factors on the Carbon Capture of the system model based on experimental data. When comparing 2 variables, continuous variables are kept at their midpoint or off value (500°C, 2wt.% biomass, 0.5wt.% KOH, 0.25 oxidant ratio and Ru is on Yes). X axis refers to the variable of outlined in that column, the 2 curves refer to the variable in that row.

6.3.2.2.1 Biomass Concentration

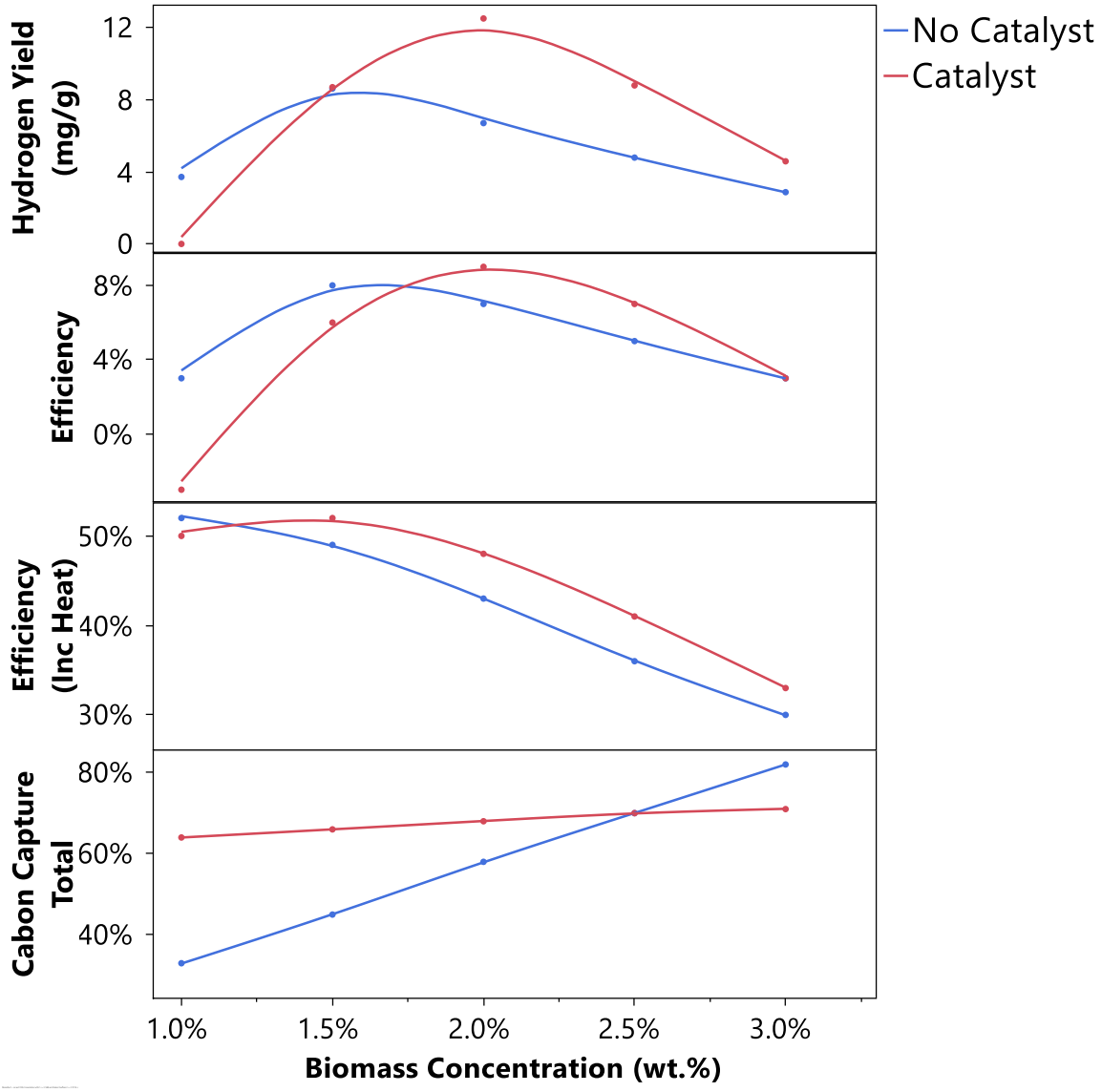

Figure 6.18-Influence of Biomass Concentration on Hydrogen Yield, Efficiency and Carbon Capture of the System Model Using Experimental Data. All data points are for 600°C, Catalyst refers to 1wt.% KOH, Ru/C and 0.25 oxidant coefficient.

The negative quadratic effect of the biomass concentration was the most significant factor on both hydrogen yield and efficiency. There is also an additional positive effect of the biomass concentration. As a result, a parabolic curve is clearly shown in Figure 6.18, with a maximum around 2 wt.% with catalysts and 1.5 wt.% without. This differs from that observed in the experimental work, where a lower biomass concentration was preferable for both hydrogen yield and efficiency. The disparity is due to the increased water flowrate required at lower concentrations, which increases pumping power and heating requirements. However, much of this heat is recovered as lower grade

heat at the exit of the steam turbine, so if this is utilised effectively, the overall efficiency is greatest at low biomass concentrations.

The biomass concentration had a strongly significant positive interaction with Ru/C regarding the hydrogen yield. Consequently, the resulting hydrogen yield was more sensitive to biomass concentration when a Ru/C catalyst was utilised; this can be observed clearly in Figure 5.15 and Figure 6.18 by the sharper curve observed when Ru/C was present. As a catalyst is favourable for achieving high yields, this makes selection of the optimum biomass concentration more critical. Moreover, there was a significant negative interaction with oxidant, indicating that positive impact of the higher concentration was reduced when adding a greater amount of oxidant. This interaction was not observed in the reaction alone, hence, was function of the effects of the system as a whole. As the positive influence of concentration is as a result of a reduction in hydrogen being utilised to heat the reaction, which is undermined by the addition of oxidant. This could be explained by the difference in enthalpy of reaction. Oxidation of organic compounds, such as intermediates formed in the SCWG, is highly exothermic [75], so more oxidant increases the enthalpy of reaction of the process. This excess heat is recovered by the steam turbine, thus reducing the amount of hydrogen required to heat the process. As a result, those advantages of a more concentrated feedstock are reduced.

The amount of carbon captured increased with the biomass concentration, which was the most significant factor, as clearly displayed in Figure 6.16. This was driven by the increased char formation, which, as outlined in Section 6.3.1.1, was significantly dependent on the biomass concentration. Notably the biomass concentration decreased the carbon captured in the gas, attributed to lower gas yield and limited CO_2 solubility due to the lower water flowrates at higher concentration. However, this is less significant than the influence on the solid carbon, resulting in an overall increase in the carbon captured. Moreover, there was significant negative interactions with Ru/C and oxidant system, which reduced the influence of concentration, on the carbon capture. Both

are known to break down char and char precursors, which, in Section 6.3.1, was found to reduce the influence of concentration of the char formation.

6.3.2.2.2 Impact of Catalysts

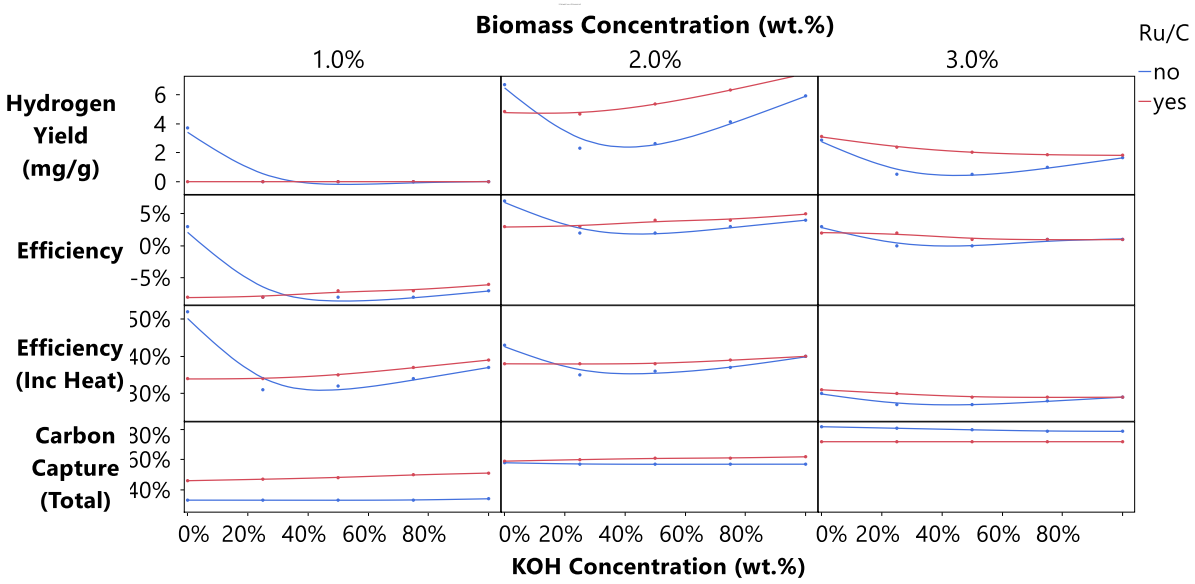

Figure 6.19 -Influence of Catalysts on Hydrogen Yield, Efficiency and Carbon Capture of the System Model Using Experimental Data. All data points are for 600°C and 0 oxidant.

Ru/C had a strong positive impact on both hydrogen yield and efficiency, the most significant after concentration in both cases, including when the low-grade heat recovery was included. This corresponds to the increased gas yields and carbon conversion observed in the experimental results. Therefore, it is still favourable to use Ru/C catalysts when the whole system is considered. Ru/C has a significant positive interaction with oxidant coefficient, indicating that when oxidant was used, the Ru/C catalyst had a bigger effect on hydrogen yield and efficiency. A similar impact was observed on the carbon conversion and methane formation, suggesting that the intermediates more readily formed in the presence of oxidant, are precursors to methane formation. Higher methane yield reduces the requirement for hydrogen to be burned in this system, so influences both efficiency and hydrogen yield.

Despite having significant positive impacts on the hydrogen yield, efficiency and carbon conversion, only a positive quadratic term and some interactions were significant for KOH in the model. As a result, higher hydrogen yields and efficiencies were observed at low and high KOH concentration,

with a lower value at the midpoints. An influence on this effect could be the reduction of CO and methane yields at high temperatures, observed in the experimental work, which were burned to provide heat for the input stream. Consequently, a greater proportion of the hydrogen was required to be burned to meet the heating requirements. At low KOH concentrations, the increased conversion was not significant enough to overcome this difference but as the KOH concentration increased, this dominates causing an increase in yield and efficiency.

Ru/C has positive impact on the gaseous carbon captured but reduces the solid carbon, especially at higher biomass concentrations as there is a strong negative interaction between concentration and Ru. Consequently, at low concentrations, where the majority of the captured carbon was gaseous, ruthenium had a positive impact on captured carbon but at higher concentrations the opposite was observed. Therefore, the effectiveness of Ru in increasing captured carbon depends on the concentration utilised and whether solid or gaseous carbon is preferable for a given scenario.

When Ru/C was not present, KOH increased the carbon capture in the gas phase. This is due to increased carbonate formation, which remains in the liquid phase and is subsequently reacted with acid to convert back into gaseous form. Therefore, as the gaseous carbon that is capture is limited by solubility, this is increases the amount of the carbon that can be captured from the gas stream. However, this impact was negated when Ru/C was present, due to the negative interaction between the two on the reaction CO_2 yield shown in Table . This could be due to catalytic effect of Ru on CO_2 methanation, which is enhanced when KOH is present due to the higher H_2 and CO_2 concentrations. Overall, the KOH did increase the carbon capture, due to an increase in solid carbon. However, this increase could be as a result of tar formation, which is known to be catalysed by hydroxide catalysts [45] and is far more difficult to recover and utilise than char. Therefore, the solid carbon recovery may be lower than predicted and the effect of KOH on it is reduced.

6.3.2.2.3 Oxidant

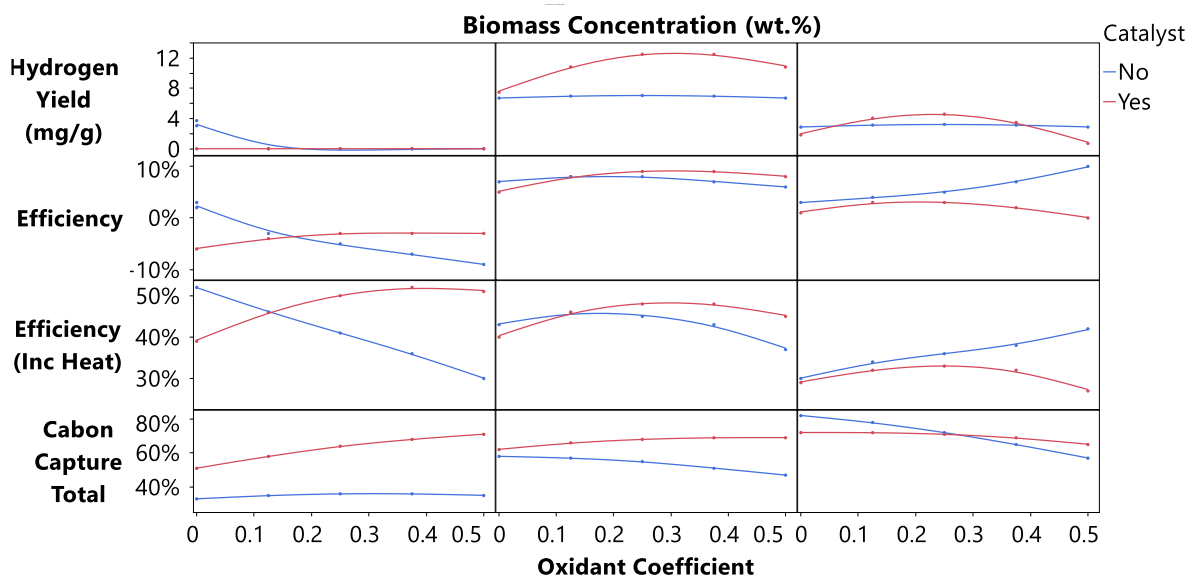

Figure 6.20 Influence of Oxidant Coefficient on Hydrogen Yield, Efficiency and Carbon Capture of the System Model Using Experimental Data. All data points are for 600 °C, Catalyst refers to 1 wt.% KOH, Ru/C and 0.25 oxidant coefficient.

A significant positive impact and negative quadratic impact of the oxidant coefficient is observed on the hydrogen yield and energy efficiency, with or without the heat recovery. This shows that the oxidant can increase the yield and efficiency up to a maximum point above which, the reduction of hydrogen yield in the reaction becomes more significant. This is shown by the concave parabolic curves in Figure 6.20. This differs from the experimental results, where only the quadratic term was significant (see Table 4), showing that in the model a greater quantity of oxidant is preferred than in reaction alone. This can be attributed to the greater conversion observed, as outlined in Section 6.3.2.2.1, a greater exothermic nature of the reaction. A greater conversion increases the quantity of other flammable gases, such as methane or CO, reducing the amount of hydrogen utilised to heat the process. Similarly, a greater heat of reaction is not captured in the experimental work directly but increase the power in the steam turbine, reducing the hydrogen burned.

Additionally, there was a significant interaction with Ru/C and concentration, positive and negative respectively. Therefore, the impact of the oxidant is more significant when Ru/C is present and that higher oxidant coefficients are preferable. As outlined in Section 6.3.2.2.2, Ru/C is preferable for high yields and efficiency, so a higher oxidant coefficient is likely to be preferable. The effect of

interaction of oxidant coefficient and concentration on efficiency is dependent on the catalyst used. If Ru/C is used, then there is a negative interaction, making a higher oxidant concentration preferable at lower concentrations. The opposite effect is observed without Ru/C catalyst. The reaction itself had no interaction between oxidation and any other factor considered here, emphasising the difference that can occur in a full system and the importance of system models to determine this.

The oxidant coefficient increases the carbon capture in the gaseous phase and decreases the carbon capture in the solid phase. This is achieved to a greater extent at lower biomass concentrations and in the presence of Ru/C catalyst. This is because of the oxidation of intermediate products into CO_2 that results in higher gas yield and lower char formation, as outlined in section 6.3.1.3. Consequently, oxidant increases carbon capture at lower concentrations where gaseous carbon dominates the carbon capture but reduces it at elevated concentration.

6.3.2.2.4 Optimal conditions

To assess the optimal conditions, the experimental system model was run at the optimal conditions for a range of criteria. These include optimal reaction conditions for hydrogen yield or efficiency and the optimal conditions for the model to maximise hydrogen yield, efficiency and carbon capture. These are displayed in Table 6.6.

Table 6.6- System model results for a series of optimisation criteria. All results were performed at 600 °C.

Optimisation criteria	Inputs				Outputs					
	Concentration (wt.%)	KOH Concentration (wt.%)	Ru/C	Oxidant coefficient	H2 Yield (mg/g)	Efficiency	Efficiency (inc. heat)	Carbon Capture (gas)	Carbon Capture (Solid)	Carbon Capture (Total)
Reaction H_2 Yield	1	1	Yes	0.2	0	-4%	49%	40%	21%	62%
Model H_2 Yield	2	1	Yes	0.3	12.7	9%	49%	38%	30%	68%
Reaction Efficiency	1	1	Yes	0	0	-6%	39%	32%	19%	51%
Model Efficiency	3	0	No	0.5	2.9	10%	42%	23%	34%	57%
Model Efficiency (inc. heat)	1.2	1	Yes	0.37	0.99	1%	53%	44%	25%	68%
Carbon Capture	3	0	no	0	2.87	3%	30%	26%	56%	82%
Carbon Capture (gas)	1	1	Yes	0.5	0	-3%	51%	46%	17%	63%

This data shows clearly how the optimal conditions for the reaction differ from that of the whole system. The optimal reaction conditions for hydrogen yield gave a yield of 0 in the system model. Similarly, the optimal reaction conditions for energy efficiency produced a -6% efficiency without including heat and just a 39% efficiency when the low-grade heat is included, significantly lower than the highest efficiencies of 10% and 53% respectively. This is driven by the increased energy required for pumping of the fluid and thermal energy required to heat a greater flow of water, which outweighs and reaction benefits at these conditions, due to the low biomass concentration used. This emphasises the importance of considering a whole system when optimising SCWG reactions.

The optimal conditions for hydrogen yield (2 wt.%, 600 °C, Ru/C, 1 wt.% KOH and 0.3 oxidant coefficient) also produced a high efficiency, 1% and 4% off the maximum achieved values for without and with heat recovery respectively. It also produced a high carbon capture of 68%, of which more than half is in the gas phase. This is an ideal solution to the aims of this work as, it maximises hydrogen yield but also produces a significant amount of gaseous and solid carbon, thus allowing carbon to be captured by either storage or incorporation into materials, depending on the availability at the given location. This is not the case when process optimisation is based on the efficiency, where the hydrogen yield was greatly reduced. This is due to a greater quantity of other flammable gases (CH_4, CO, C_{2+}) which produced a greater quantity of electricity, which may be more desirable in some cases but doesn't favour hydrogen production as is the focus of this study.

Optimisation based upon carbon capture differs greatly depending on whether the required carbon is in gaseous form or solid carbon is considered. When gaseous carbon only is considered, a negative efficiency is observed, meaning electrical power is required to achieve this. This seems unfeasible as a solution to simply produce more CO_2, given a self-sufficient process is easily feasible. When solid carbon is also considered, 82% of the feedstock carbon can be theoretically captured, the majority of which is in solid form. In this scenario, some hydrogen yield is also achieved, and the process is self-sufficient. In a scenario, where biochar becomes a product of significance in a particular area, for example a local cement plant requires significant amounts of biochar to reduce

their overall emissions [72], then then these conditions (3wt.%, 600°C, no catalyst, no oxidant) could be suitable. However, the impact on operability of the increased char formation must be considered for this be suitable.

6.4 CONCLUSION

Incorporating experimental results into a whole system model, high temperatures and use of Ru/C catalyst was found to enhance hydrogen yield and efficiency, as was observed in the reaction alone. However, low biomass concentrations (1wt.%) were found to not be preferable, and KOH was only preferable at 0 and 1 wt.%. This differs greatly from the experimental work, due to the greater water flow which increased the pumping and heating required, or the influence of the catalyst on other gaseous products such as methane. Additionally, oxidant was found to be preferable for the efficiency of the system and at small quantities (oxidant coefficient <0.3), the hydrogen yield in the system increased. A greater amount of oxidant was preferable in the system than the reaction alone, due to the positive impact on the enthalpy of reaction, which would be recovered through the steam turbine. This also showed that up to 82% of the feed carbon could be captured as either carbon dioxide or solid char, while still remaining energetically self-sufficient. Overall, this work showed the importance of combining both experimental work and system models, showing the feasibility of a carbon negative hydrogen production from the supercritical water gasification of microalgae.

6.5 REFERENCES

[1] Intergovernmental Panel on Climate Change: Working Group 3, “Climate Change 2022-Mitigation of Climate Change,” Intergovernmental Panel on Climate Change, Geneva, 2022.

[2] M. S. Yahya, M. Syafiq, A. Ashton-Butt, A. Ghazali, S. Asmah and B. Azhar, “Switching from monoculture to polyculture farming benefits birds in oil palm production landscapes: Evidence from mist netting data,” *Ecology and Evolution*, vol. 7, no. 16, p. 6, 2017. doi:10.1002/ece3.3205.

[3] F. Geiger, J. Bengtsson, F. Berendse, W. W. Weisser, M. Emmerson, M. B. Morales, P. Ceryngier, J. Liira, T. Tscharntke, C. Winqvist, S. Eggers, R. Bommarco, T. Pärt, V. Bretagnol, M. Plantegenest, L. W. Clement, C. Dennis, C. Palmer, J. J. Onate and I. Guerrero, “Persistent negative effects of pesticides on biodiversity and biological control potential on European farmland,” *Basic and Appl. Ecology*, vol. 11, no. 2, pp. 97-105, 2010. doi:10.1016/j.baae.2009.12.001.

[4] M. Dorgham, “Effects of Eutrophication.,” in Eutrophication: Causes, Consequences and Control, Dordrecht, Springer, 2014. doi:10.1007/978-94-007-7814-6_3.

[5] J. Tomei and R. Helliwell, “Food versus fuel? Going beyond biofuels,” *Land Use Policy*, vol. 56, pp. 320-236, 2016. doi:10.1016/j.landusepol.2015.11.015.

[6] M. Benedetti, V. Vecchi, S. Barera and L. Dall’Osto, “Biomass from microalgae: the potential of domestication towards sustainable biofactories,” *Microb Cell Factories*, vol. 17, no. 173, 2018. doi:10.1186/s12934-018-1019-3.

[7] Y. Yoshida, K. Dowaki, Y. Matsumura, R. Matsuhashi, D. Li, H. Ishitani and H. Komiyama, “Comprehensive comparison of efficiency and CO2 emissions between biomass energy conversion technologies—position of supercritical water gasification in biomass technologies,” *Biomass and Bioenergy*, vol. 25, no. 3, pp. 257-272, 2003. doi:10.1016/S0961-9534(03)00016-3.

[8] J. A. Withag, J. R. Smeets, E. A. Bramer and G. Brem, “System model for gasification of biomass model compounds in supercritical water – A thermodynamic analysis,” *The Journal of Supercritical Fluid*s, vol. 61, pp. 157-166, 2012 doi:doi.org/10.1016/j.supflu.2011.10.012.

[9] S. A. Miller, E. V. Roijen, P. Cunningham and A. Kim, “Opportunities and challenges for engineering construction materials as carbon sinks,” *RILEM Tech. Lett*., vol. 6, pp. 105-118, 2021 doi:https:10.21809/rilemtechlett.2021.146.

[10] Committee on Climate Change, “Hydrogen in a Low-Carbon Economy,” Committee on Climate Change, London, 2018.

[11] N. Akiya and P. E. Savage, “Roles of Water for Chemical Reactions in High-Temperature Water,” *Chem. Review*s, vol. 102, no. 8, pp. 2725-2750, 2002. doi:10.1021/cr000668w.

[12] C. Wang, W. Zhu, H. Zhang, C. Chen, X. Fan and Y. Su, “Char and tar formation during hydrothermal gasification of dewatered sewage sludge in subcritical and supercritical water: Influence of reaction parameters and lumped reaction kinetics,” *Waste Management*, vol. 100, pp. 57-65, 2019. doi:10.1016/j.wasman.2019.09.011.

[13] Q. Yan, L. Guo and Y. Lu, “Thermodynamic analysis of hydrogen production from biomass gasification in supercritical water,” *Energy Convers. and Management*, vol. 47, no. 11-12, pp. 1515-1528, July 2006. doi:10.1016/j.enconman.2005.08.004.

[14] A. G. Chakinala, D. W. F. (. Brilman, W. P. v. Swaaij and S. R. A. Kersten, “Catalytic and Non-catalytic Supercritical Water Gasification of Microalgae and Glycerol,” *Ind. and Eng. Chem. Res.,* vol. 49, no. 3, pp. 1113-1122, Septemeber 2010. doi:10.1021/ie9008293.

[15] L. Tiong, M. Komiyama, Y. Uemura and T. T. Nguyen, “Catalytic supercritical water gasification of microalgae: Comparison of *Chlorella vulgaris* and Scenedesmus quadricauda,” *The J. of Supercrit. Fluids*, vol. 107, pp. 408-413, January 2016. doi:10.1016/j.supflu.2015.10.009.

[16] C. Zhu, L. Guo, H. Jin, J. Huang, S. Li and X. Lian, “Effects of reaction time and catalyst on gasification of glucose in supercritical water: Detailed reaction pathway and mechanisms,” I*nt. J. of Hydrogen Energy*, vol. 41, no. 16, pp. 6630-6639, May 2016 doi:10.1016/j.ijhydene.2016.03.035.

[17] K. Heeley, R. L. Orozco, L. E. Macaskie, J. Love and B. Al-Duri, “Supercritical water gasification of microalgal biomass for hydrogen production-A review,” *Int. J. of Hydrog. Energy*, vol. 49 Part A, pp. 310-336, 2023. doi:10.1016/j.ijhydene.2023.08.081.

[18] L.-F. Xie, P.-G. Duan, J.-L. Jiao and Y.-P. Xu, “Hydrothermal gasification of microalgae over nickel catalysts for production of hydrogen-rich fuel gas: Effect of zeolite supports*,” Int. J. of Hydrog*. Energy, vol. 44, no. 11, pp. 5114-5124, 2019. doi:0.1016/j.ijhydene.2018.09.175.

[19] H. Tang and K. Kitagawa, “Supercritical water gasification of biomass: thermodynamic analysis with direct Gibbs free energy minimization,” *Chem. Eng. J.*, vol. 106, no. 3, pp. 261-267, 2005. doi: 10.1016/j.cej.2004.12.021

[20] O. Norouzi, F. Safari, S. Jafarian, A. Tavasoli and A. Karimi, “Hydrothermal gasification performance of Enteromorpha intestinalis as an algal biomass for hydrogen-rich gas production using Ru promoted Fe–Ni/γ-Al2O3 nanocatalysts,” *Energy Convers. and Manag*., vol. 141, pp. 63-71, June 2017 doi:10.1016/j.enconman.2016.04.083.

[21] A. Kruse, “Supercritical water gasification*,” Biofuels, Bioproducts and Biorefining*, vol. 2, no. 5, pp. 415-437, 2008. doi: 10.1002/bbb.93

[22] A. Kruse and N. Dahmen, “Water – A magic solvent for biomass conversion,” *The J. of Supercrit. Fluids*, vol. 96, pp. 36-45, January 2015. doi: 10.1016/j.supflu.2014.09.038

[23] Q. Guan, C. Wei and P. E. Savage, “Kinetic model for supercritical water gasification of algae,” *Physical Chemistry Chemical Physics*, vol. 14, no. 9, pp. 3140-3147, 2012. Doi: 10.1039/C2CP23792J

[24] A. Sinag, A. Kruse and J. Rathert, “Influence of the Heating Rate and the Type of Catalyst on the Formation of Key Intermediates and on the Generation of Gases during Hydropyrolysis of Glucose in Supercritical Water in a Batch Reactor,” *Ind. and eng. chem. res*., vol. 43, no. 2, pp. 502-508, 2004. doi:10.1021/ie030475.

[25] R. Samiee-Zafarghandi, J. Karimi-Sabet, M. A. Abdoli and A. Karbassi, “Supercritical water gasification of microalga *Chlorella PTCC* 6010 for hydrogen production: Box-Behnken optimization and evaluating catalytic effect of MnO2/SiO2 and NiO/SiO2,” *Renewable Energy*, vol. 126, pp. 189-201, 2018. doi: 10.1016/j.renene.2018.03.043

[26] P.-G. Duan, S.-C. Li, J.-L. Jiao, F. Wang and Y.-P. Xu, “Supercritical water gasification of microalgae over a two-component catalyst mixture,” *Sci. of The Total Environ.*, vol. 630, pp. 243-253, 2018. doi: 10.1016/j.scitotenv.2018.02.226

[27] R. Samiee-Zafarghandi, A. Hadi and J. Karimi-Sabet, “Graphene-supported metal nanoparticles as novel catalysts for syngas production using supercritical water gasification of microalgae,” *Biomass and Bioenergy*, vol. 121, pp. 13-21, 2019. Doi: 10.1016/j.renene.2018.03.043

[28] J. Li, L. Pan, M. Suvarna and X. Wang, “Machine learning aided supercritical water gasification for H2-rich syngas production with process optimization and catalyst screening,” *Chem. Eng. J.,* vol. 426, 2021 doi:10.1016/j.cej.2021.131285.

[29] K. Heeley, R. Orozco, I. Sheppard, L. Macaskie, J. Love and B. Al-Duri, “Assessment of Iron(iii) Chloride as a Catalyst for the Production of Hydrogen from the Supercritical Water Gasification of Microalgae*,” Next Energy*, 2024.

[30] T. Yoshida and Y. Oshima, “Partial Oxidative and Catalytic Biomass Gasification in Supercritical Water: A Promising Flow Reactor System,” *Ind. Eng. Chem. Res*., vol. 43, no. 15, pp. 4097-4101, 2004 doi:10.1021/ie034312x.

[31] Q. Guan, C. Wei, H. Shi, C. Wu and X.-S. Chai, “Partial oxidative gasification of phenol for hydrogen in supercritical water,” *Appl. Energy*, vol. 88, no. 8, pp. 2612-2616, 2011. Doi: 10.1016/j.apenergy.2011.01.021

[32] Y. Wang, S. Wang, G. Zhao, Y. Guo and Y. Guo, “Hydrogen production by partial oxidation gasification of a phenol, naphthalene, and acetic acid mixture in supercritical water,” *Int. J. of Hydrog. Energy*, vol. 41, no. 3, pp. 2238-2246, 2016. doi: 10.1016/j.ijhydene.2015.12.115

[33] L. Qian, S. Wang, S. Wang, S. Zhao and B. Zhang, “Supercritical water gasification and partial oxidation of municipal sewage sludge: An experimental and thermodynamic study,” *Int. J. of Hydrog. Energ*y, vol. 46, no. 1, pp. 89-99, 2021 doi:10.1016/j.ijhydene.2020.09.200.

[34] W. Gong, L. Huang, L. Guo, Z. Zhou, F. Zhao, Y. Li, J. Li and C. Qi, “Catalytic gasification of textile wastewater treatment sludge for hydrogen production in supercritical water with K2CO3/H2O2: Reaction variables, mechanism and kinetics,” *Int. J.of Hydrog. Energy*, vol. 48, no. 78, pp. 30310-30322, 2023 doi:10.1016/j.ijhydene.2023.04.160.

[35] M. B. García-Jarana, J. R. Portela, J. Sánchez-Oneto, E. J. M. d. l. Ossa and B. A.-D. 2, “Analysis of the Supercritical Water Gasification of Cellulose in a Continous System Using Short Residence times,” *Appl. Sci.,* vol. 10, no. 15, p. 5185, 2020 doi:10.3390/app10155185.

[36] M. Magdeldin, T. Kohl and M. Järvinen, “Process modeling, synthesis and thermodynamic evaluation of hydrogen production from hydrothermal processing of lipid extracted algae integrated with a downstream reformer conceptual plant,” *Biofuels*, vol. 7, no. 2, pp. 97-116, January 2016. Doi: 10.1080/17597269.2015.1118785

[37] A. Nurdiawati, I. N. Zaini, A. R. Irhamna, D. Sasongkod and M. Aziz, “Novel Configuration of Supercritical Water Gasification and Chemical Looping for Highly-Efficient Hydrogen Production from Microalgae,” *Renew. and Sustain. Energy Rev*., vol. 112, pp. 369-381, 2019 doi:10.1016/j.rser.2019.05.054.

[38] M. Aziz, “Integrated hydrogen production and power generation from microalgae,” *Int. J. of Hydrog. Energy*, vol. 41, no. 1, pp. 104-112, 2016. doi: 10.1016/j.ijhydene.2015.10.115

[39] M. Aziz, “Modeling of efficiently-integrated algal gasification, nitrogen production, ammonia synthesis, and power generation,” *Energy Procedi*a, vol. 160, pp. 627-632, 2019. Doi: 10.1016/j.egypro.2019.02.222

[40] A. G. Haiduc, M. Brandenberger, S. Suquet, F. Vogel, R. Bernier-Latman and C. Ludwig, “SunCHem: an integrated process for the hydrothermal production of methane from microalgae and CO2 mitigation*,” J. of Appl. Phycology*, vol. 21, pp. 529-541, 2009. doi: 10.1007/s10811-009-9403-3

[41] A. T. Wijayanta and M. Aziz, “Ammonia production from algae via integrated hydrothermal gasification, chemical looping, N2 production, and NH3 synthesis,” *Energ*y, vol. 174, pp. 331-338, 2019. doi: 10.1007/s10811-009-9403-3

[42] A. Rahbari, A. Shirazi, M. B. Venkataraman and J. Pye, “Solar fuels from supercritical water gasification of algae: Impacts of low-cost hydrogen on reformer configurations,” *Applied Energy*, vol. 228, 2021. Doi: 10.1016/j.apenergy.2021.116620

[43] A. Onigbajumo, A. Taghipour, J. Ramirez, G. Will, T.-C. Ong, S. Couperthwaite, T. Steinberg and T. Rainey, “Techno-economic assessment of solar thermal and alternative energy integration in supercritical water gasification of microalgae,” *Energy Conv. and Manag.*, vol. 230, 2021.doi: 10.1016/j.enconman.2020.113807

[44] S. Adamu, H. Binous, S. A. Razzak and M. M. Hossain, “Enhancement of glucose gasification by Ni/La2O3-Al2O3 towards the thermodynamic extremum at supercritical water conditions,” *Renew. Energy*, vol. 111, pp. 399-409, 2017 doi:10.1016/j.renene.2017.04.020.

[45] K. Heeley, R. L. Orozco, Z. Shah, L. E. Macaskie, J. Love and B. Al-Duri, “Supercritical water gasification of microalgae: The impact of the algal growth water,” *The J. of Supercrit. Fluids*, vol. 205, 2024 doi:https://doi.org/10.1016/j.supflu.2023.106143.

[46] A. Miller, D. Hendry, N. Wilkinson, C. Venkitasamy and W. Jacoby, “Exploration of the gasification of Spirulina algae in supercritical water,” *Bioresource Tech.*, vol. 119, pp. 41-47, 2012. doi: 10.1016/j.biortech.2012.05.005

[47] L. Tiong and M. Komiyama, “Supercritical water gasification of microalga *Chlorella vulgaris* over supported Ru,” *The J. of Supercrit. Fluid*s, vol. 144, pp. 1-7, 2019. doi:10.1016/j.supflu.2018.05.011.

[48] R. Samiee-Zafarghandi, J. Karimi-Sabet, M. A. Abdoli and A. Karbassi, “Supercritical water gasification of microalga *Chlorella PTCC* 6010 for hydrogen production: Box-Behnken optimization and evaluating catalytic effect of MnO2/SiO2 and NiO/SiO2,” *Renew. Energy*, vol. 126, pp. 189-201, 2018. doi:10.1016/j.renene.2018.03.043.

[49] EPA, “Biomass CHP Catalog,” 2007.

[50] O. Yakaboylu, J. Harinck, K. G. Smit and W. d. Jong, “Supercritical Water Gasification of Biomass: A Detailed Process Modeling Analysis for a Microalgae Gasification Process,” *Ind. and Eng. Chem Res* .vol. 54, no. 21, pp. 5550-5562, May 2015. doi: 10.1021/acs.iecr.5b00942

[51] A. Rahbari, M. B. Venkataraman and J. Pye, “Energy and exergy analysis of concentrated solar supercritical water gasification of algal biomass,” Applied Energy, vol. 228, pp. 1669-1682, 2018 doi:10.1016/j.apenergy.2018.07.002.

[52] S. Y. Bircan, H. Kamoshita, R. Kanamori, Y. Ishida, K. Matsumoto, Y. Hasegawa and K. Kitagawa, “Behaviour of heteroatom compounds in hydrothermal gasification of biowaste for hydrogen production,” *App. Energy, vol*. 88, no. 12, pp. 4874-4878, 2011 doi:10.1016/j.apenergy.2011.06.031.

[53] S. Elsayed, N. Boukis, D. Patzelt, S. Hindersin, M. Kerner and J. Sauer, “Gasification of Microalgae Using Supercritical Water and the Potential of Effluent Recycling,” C*hem. Eng. & Tech*., vol. 39, no. 2, November 2015. doi:10.1002/ceat.201500146.

[54] National Institute of Standards and Technology, “hermophysical Properties of Fluid Systems,” 2023. [Online]. Available: https://webbook.nist.gov/chemistry/fluid/. [Accessed 2024 08 15].

[55] F. G. Ortiz, P. Ollero, A. Serrera and A. Sanz, “Thermodynamic study of the supercritical water reforming of glycerol,” *Int J. of Hydrog. Energ*y, vol. 36, no. 15, pp. 8994-9013, 2011 doi:10.1016/j.ijhydene.2011.04.095.

[56] P. M. Ruya, R. Purwadi and S. S. Lim, “Supercritical water gasification of sewage sludge for power generation– thermodynamic study on auto-thermal operation using Aspen Plus,” *Energy Conv. and Manag.,* vol. 206, 2020 doi: https:10.1016/j.enconman.2019.112458.

[57] M. Cholewa, R. Dürrschnabel, N. Boukis and P. Pfeifer, “High pressure membrane separator for hydrogen purification of gas from hydrothermal treatment of biomass,” *Int. J. of Hydrog. Energy*, vol. 43, no. 29, pp. 13294-13304, 2018 doi:10.1016/j.ijhydene.2018.05.031.

[58] D. K. Sarkar, “Steam Generators,” in Thermal Power Plan design and Operation, Elsevier, 2015 doi:10.1016/B978-0-12-801575-9.00002-0, pp. 39-89.

[59] M. Ebrahimi and A. Keshavarz, “CCHP Technology,” in Combined Cooling, Heating and Power, 2015 doi:10.1016/B978-0-08-099985-2.00002-0, pp. 35-91 .

[60] J. J. Milledge and S. Heaven, “A review of the harvesting of micro-algae for biofuel production,” *Reviews in Environ. Sci. and Bio/Technology*, vol. 12, pp. 165-178, 2012 doi:I 10.1007/s11157-012-9301-z.

[61] Y. Ammar, S. Joyce, R. Norman, Y. Wang and A. P. Roskilly, “Low grade thermal energy sources and uses from the process industry in the UK,” *Appl. Energy*, vol. 89, no. 1, pp. 3-20, 2012 doi:10.1016/j.apenergy.2011.06.003.

[62] A. Miller, D. Hendry, N. Wilkinson, C. Venkitasamy and W. Jacoby, “Exploration of the gasification of Spirulina algae in supercritical water*,” Bioresource Tech.*, vol. 119, pp. 41-47, 2012. doi:10.1016/j.biortech.2012.05.005.

[63] A. C. D. Freitas and R. Guirardello, “Thermodynamic Analysis of Supercritical Water Gasification of Microalgae Biomass for Hydrogen and Syngas Production,” *Chem. Eng. Trans*, vol. 32, 2013. doi:10.3303/CET1332093

[64] C. Yang, S. Wang, Y. Li, Y. Zhang and C. Cui, “Thermodynamic analysis of hydrogen production via supercritical water gasification of coal, sewage sludge, microalga, and sawdust,” *Int.l J. of Hydrog, Energy*, vol. 46, no. 34, pp. 18042-18050, 2021. doi: 10.1016/j.ijhydene.2020.06.198

[65] J. Gomes, J. Mitoura and R. Guirardello, “Thermodynamic analysis for hydrogen production from the reaction of subcritical and supercritical gasification of the C. Vulgaris microalgae,” *Energy*, vol. 260, 2022. doi: 10.1016/j.energy.2022.125030

[66] Y. Matsumura, T. Nunoura, T. Urase and K. Yamamoto, “Supercritical water oxidation of high concentrations of phenol,” *J. of Hazard. Mat.*, vol. 73, no. 3, pp. 245-254, 2000. doi: 10.1016/S0304-3894(99)00187-9

[67] A. A.-H. Mourad, A. F. Mohammad, A. H. Al-Marzouqi, M. Altarawneh, M. H. Al-Marzouqi and M. H. El-Naas, “Carbon dioxide capture through reaction with potassium hydroxide and reject brine: A kinetics study,” *Int. J. of Greenhouse Gas Control*, vol. 120, 2022.

[68] N. Wei, D. Xu, B. Hao, S. Guo, Y. Guo and S. Wang, “Chemical reactions of organic compounds in supercritical water gasification and oxidation,” *Water Res.,* vol. 190, 2021. doi:10.1016/j.watres.2020.116634. doi: 10.1016/j.ijggc.2022.103768

[69] Y. Wang, S. Wang, G. Zhao, Y. Guo and Y. Guo, “Hydrogen production by partial oxidation gasification of a phenol, naphthalene, and acetic acid mixture in supercritical water,” *Int. J. of Hydrog. Energy*, vol. 41, no. 4, pp. 2238-2246, 2016. doi: 10.1016/j.ijhydene.2015.12.115

[70] N. Wei, B. Hao, D. Xu, X. Liu, M. Ma and Y. Guo, “Partial oxidation gasification kinetics of indole in supercritical water for hydrogen production,” *Fuel Processing Tech.*, vol. 236, 2022 doi:10.1016/j.fuproc.2022.107377. doi: 10.1016/j.fuproc.2022.107377

[71] H.-H. Lam, T.-M.-T. Nguyen, T.-A.-S. Do, T.-H. Dinh and T. Dang-Bao, “Quantification of total sugars and reducing sugars of dragon fruit-derived sugar-samples by UV-Vis spectrophotometric method,” IOP Conf. Ser.: *Earth Environ. Sci*., vol. 947, 2021 doi:10.1088/1755-1315/947/1/012041.

[72] M. Legan, A. Ž. Gotvajn and K. Zupan, “Potential of biochar use in building materials,” *J. of Environ. Manag*., vol. 309, 2022 doi:10.1016/j.jenvman.2022.114704.

CHAPTER 7: CONCLUSIONS AND RECOMMENDATIONS FOR FURTHER WORK

The overall aim of this research was to maximise the hydrogen produced from the SCWG, while ensuring significant carbon capture. This was achieved by considering a range of factors, which are known to influence SCWG, as is outlined in Chapter 2. A full range of reaction conditions were considered, within the limits of the available equipment (400 - 600°C and 0.7 - 3wt.% biomass). Additionally, the main three catalyst types studied in the literature and the influence of oxidant concentration (H_2O_2) were considered. These include alkali metal salts (KOH), transition metals (Ru/C) and Lewis acid metal chlorides ($FeCl_3$). Moreover, the use of growth water as the reaction medium ensured a realistic reaction environment and the whole system modelling ensured parasitic losses were considered.

This study found an optimal hydrogen yield of 12.7mg/g of microalgae at 600°C, 2wt.% algae, 1wt.% KOH, the presence of a Ru/C catalyst and oxidant coefficient of 0.3. At these conditions, 38% and 30% of the feedstock carbon were captured as CO_2 and char respectively, which represents 83% of the maximum recoverable carbon under the range of conditions studied. Thus, successfully maximising the hydrogen yield while ensuring significant carbon capture was achieved.

To achieve this, the objectives outlined in Chapter 1 were fully met. Details of this and any suggestions for further work are outlined as follows:

1. *Set-up appropriate experimental apparatus and procedures.*

A continuous SCWG reactor rig was designed, constructed and successfully operated for the entirety of the experimental program of this work. The reactor was designed to have the maximum length possible, ensuring longer residence times (>30s) could be reached, with other features included to ensure operability. These include flowrate selection to maintain turbulence preventing plugging in the reactor and parallel filters to allow for continuous operation in the event of filter blockage.

Following the discovery of a significant influence of the algal growth water on the SCWG reaction in Chapter 4, GW was used as the reaction medium in subsequent chapters to better represent an industrial system. Moreover, experimental procedures were developed to clean the reactor of residual organic and inorganic material between experiments, minimising their interference on the subsequent experiments.

Additionally, an experimental apparatus to grow *Chlorella vulgaris* was designed, tested and operated for 56 weeks. This included development of appropriate methods for monitoring growth and characterising of the carbohydrate, protein and lipid content of the resulting biomass. This provided feedstock for the results in Chapter 4 and the growth water used as a reaction medium in Chapters 4 and 5. However, due to the required quantity of biomass, the grown microalgae was insufficient for all investigations, hence *Chlorella vulgaris* powder was purchased could not be used for subsequent works.

In future work, the reactor design could be adjusted to increase the scope of the study. Chapter 6 showed that the hydrogen yield increased with temperature for the entire range studied. Therefore, capabilities of achieving temperatures above 600°C would be preferable to see the extent of this trend. Moreover, the experimental model in Chapter 6 predicted that the reaction is exothermic but due to the isothermal nature of this reactor, the extent of this could not be measured. Introducing this capability would increase the reliability of energy calculations in future work. Due to the limitations of algal growth capabilities in this study, the influence of varying outlet GW concentrations and pH on the growth of microalgae could not be studied. Further work looking into potential synergistic impacts on algal growth and the resulting GW of alterations to the initial growth media could help optimise the growth period and reduce the catalytic requirement in the SCWG reaction.

2. *Investigate new and existing catalyst combinations.*

The literature review, conducted in Chapter 2, observed that alkali metal salts were common homogeneous catalysts and transition metals were common heterogenous catalysts in SCWG. Lewis acid metal chlorides were also known to be effective, with $FeCl_3$ being predicted to the most effective catalyst in a screening of potential SCWG catalysts. However, little research has been done on these catalysts and no research to date has looked at microalgae SCWG in a continuous system.

Analysis of $FeCl_3$ as a catalyst for SCWG of *Chlorella vulgaris* found that it reduced the hydrogen yield, carbon converted to gas and the energy efficiency. These effects were attributed to the reduction in pH, which suppressed the WGS reaction and catalysed polymerisation reactions increasing char formation, outweighing any potential benefits observed in other work. This was more significant at the lower biomass concentrations, catalyst loadings and reaction times in this study than those observed in the literature. Analysis of alkali metal salts (KOH) and transition metals (Ru/C) found that they were both effective catalysts at increasing hydrogen yield, with the highest yield being observed when both were used together. Consequently, these two catalysts were selected for a more in-depth analysis in Chapter 6.

In this study, recovery and deactivation of the catalysts were not considered. This is important to help limit costs of the SCWG, so further work should consider this element of catalyst selection and operation. This is particularly important with ruthenium catalysts, due to their high costs and scarcity. This work showed that alkali catalysts, while very effective at increasing the WGS reaction and hydrogen yield, also increased tar formation which is problematic for operability. Further work investigating the use of two stage catalyst systems would be of interest as alkali could be added later into the process, focusing the catalytic activity on the gaseous products.

3. *Investigate the influence of different factors on the SCWG reaction*.

Analysis of the impact of reaction conditions showed a significantly higher conversion, efficiency and hydrogen yield at high temperatures and low biomass concentrations. Additionally, the use of a Ru/C and KOH catalysts were found to be effective at increasing those factors. These findings align closely with the consensus in the literature. Notable advancements on the literature lie with the study of interactions between these factors and the influence of oxidant.

Oxidant was effective at increasing the breakdown of refractory intermediates, increasing the conversion and, at oxidant coefficients <0.2, increasing hydrogen yield. Increasing the oxidant further oxidised gaseous products like hydrogen and methane, reducing hydrogen yield and energy efficiency. Interaction between temperature and biomass concentration meant the influence of the other operating conditions on hydrogen yield, energy efficiency and conversion, was more significant at higher temperatures and lower biomass concentrations. Significant interactions were also found between these operating conditions, the catalyst and oxidant. These interactions are important to include when selecting the optimal conditions for hydrogen production. However, no interaction was found for these output variables between the two catalysts, allowing them to be used in tandem with no adverse effects.

This work offered a comprehensive study of reaction conditions, catalysts and oxidant, the majority of which, were used to the full range of operability of a real system. An exception being the temperature, which was limited by the oven and pipework available. Process streams above 600°C are common in many industries, so a greater temperature could be feasible. As this work found that a greater temperature increased hydrogen yield for the full range studied, it would be desirable to study the full extent of this effect. Thus, future work should consider temperatures above 600°C. Additionally, the heterogenous catalyst was delivered as a suspension in the feedstock. This was required due to special limitations of the heating system and is suitable for assessing the influence of a catalyst. However, it is not a desirable method in an industrial process due to difficulty recovering the catalyst. Further work should apply heterogeneous catalysts in fixed or fluidised bed systems.

4. *Study the influence of different factors on the SCWG System.*

Two system models were produced in ASPEN plus®, one using a theoretical equilibrium reactor and one reactor using experimental data. These showed a clear disparity, emphasising the importance of using experimental data. The study also showed that hydrogen yield and efficiency was greater at higher temperatures and ≤500°C energy self-sufficiency was not possible. Due to variations in reaction enthalpy, heating requirements, pumping power and influence of the separation process, the whole system produced some noticeable differences from the reactor alone.

Low biomass concentrations, despite being preferred in the reaction, were detrimental to hydrogen yield and efficiency. Consequently, a parabolic relationship was observed for these output variables, with 2wt.% being the favourable concentration. KOH concentration was also parabolic in its influence with lower and higher KOH concentrations being preferable. Ru/C and oxidant had similar relationships to the reaction alone, although a higher oxidant concentration was preferable in the whole system than the reaction alone. Carbon capture was maximised at high biomass concentrations and without any catalyst or oxidant. However, at these conditions the hydrogen yield is significantly lower than can be achieved and 70% is in the form of char. Therefore, these would only be favourable if the biochar was the desired product, rather than hydrogen as in this study.

Higher temperatures, use of catalysts and oxidant were all found to be preferable conditions for producing carbon negative hydrogen from the SCWG of microalgae. However, high temperatures increase the costs of reactor materials and shorten equipment lifetimes. Addition of new materials (catalysts and oxidant) will also increase costs, particularly with ruthenium catalysts which are expensive. Therefore, an economic study on the findings of this work would be of interest. Such work should analyse how factors such as temperature and catalysts effect costs, finding an economic optimum and comparing it to the optimum found in this study. Inclusion of a life cycle assessment to study how the environmental impact varies with these factors would also be of interest. A comparison could then be performed between this process and other hydrogen production methodologies in terms of economic, environmental and resource depletion impacts.

APPENDICES

A- Optical Density and Concentration Relationship

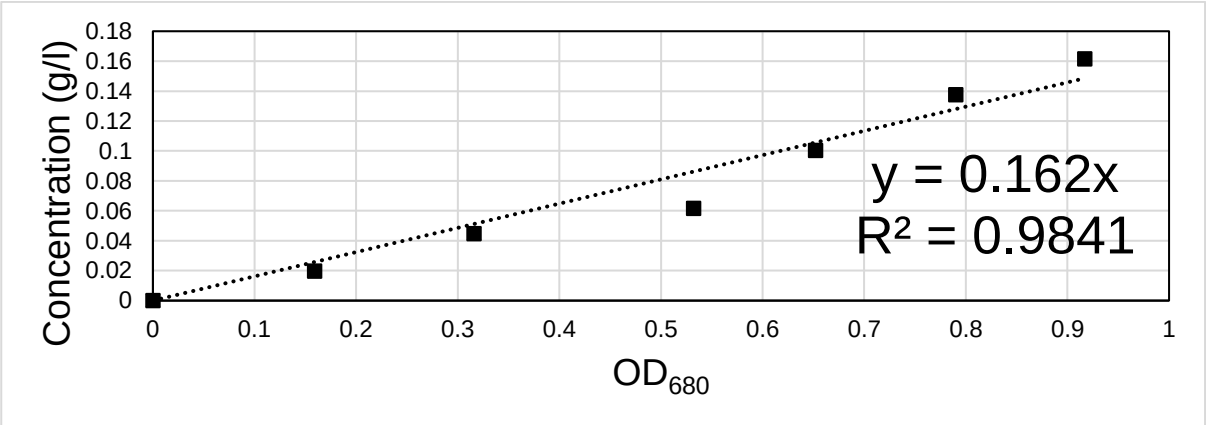

Calibration curve for determining the relationship between optical density and concentration of Chlorella vulgaris suspension.

B- Lipid Measurement Verification

Verification of lipid measurement method. A model compound containing 0.05g of cellulose, 0.05g of protein(peptone) and a known quantity of lipid (rapeseed oil) was tested.

Sample	Mass of oil added (g)	Lipid %	Measured oil (g)	error (%)
1	0.0178	15%	0.0185	4%
2	0.0206	17%	0.0223	8%
3	0.0769	43%	0.0775	1%
4	0.0798	44%	0.0756	-5%
5	0.0209	17%	0.0203	-3%
6	0.0217	18%	0.0233	7%
7	0.0415	29%	0.0355	-14%
8	0.0537	35%	0.0572	7%
9	0.0601	38%	0.06	0%
10	0.1012	50%	0.1167	15%
11	0.0897	47%	0.0967	8%
12	0.1958	66%	0.183	-7%
13	0.1854	65%	0.1968	6%

C- PUMP FLOWRATE TESTING

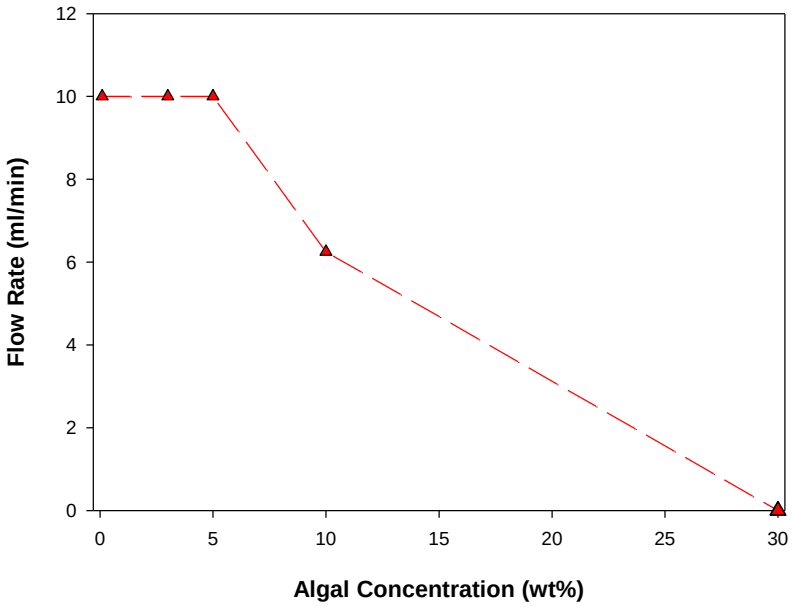

Testing of pump flowrate at different algal concentrations. For all datapoints, pump flowrate was set at 10ml/min.

D. pH of the Liquid Product

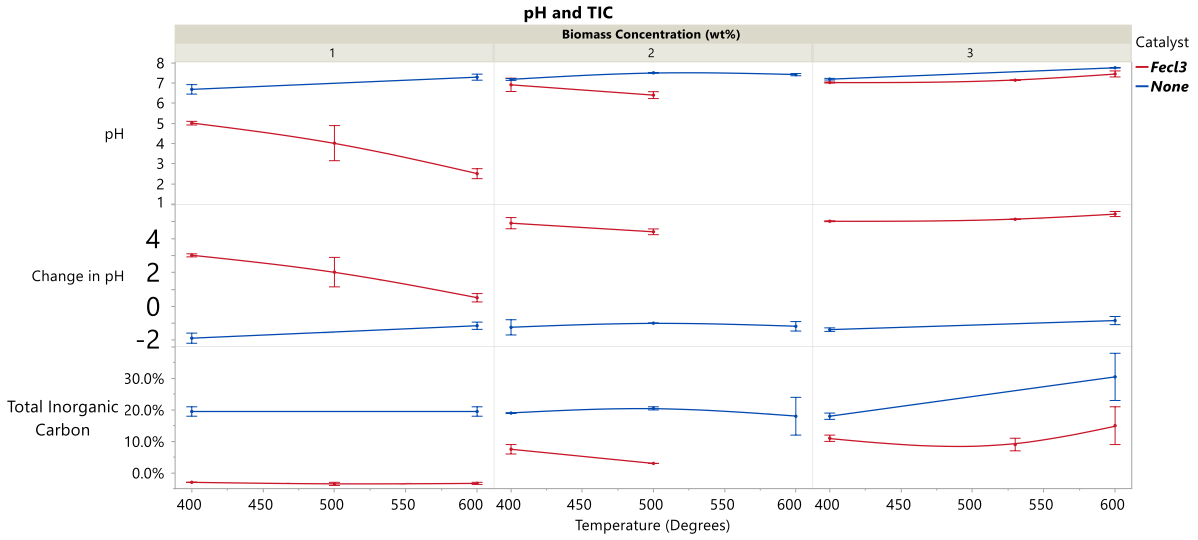

pH and inorganic carbon. 45s residence time, 1-3%wt Chlorella vulgaris, 400-600°C, 1%wt catalyst. The error bars represent 1 standard error from the mean.

The TIC follows an exponential relationship with pH, with an R^2 of 0.823, as shown by following equation and figure.

$$TIC = -0.036 + 0.00014e^{pH}$$

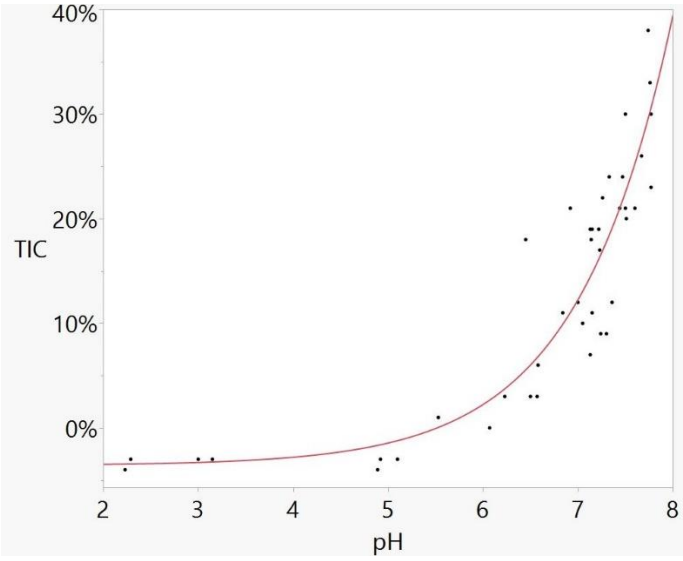

Correlation of inorganic carbon and pH. 45s residence time, 1-3%wt Chlorella vulgaris, 400-600°C, 0-1wt.%. The error bars represent 1

pH as a function of temperature, concentration and $fecl_3$ catalyst can be found in below equation with a 0.95 R^2.

$$pH = -0.17 + 0.96x - 0.74C - 0.36T \times x - 0.41C \times T + 0.72C \times x + 0.37T \times x \times C - 0.49x^2 + 6.83$$

Logworth of factors affecting the pH of liquid stream as outline by the above equation.

Source	Logworth
Biomass Concentration(1,3)	9.915
Catalyst	9.583
Catalyst*Biomass Concentration	7.532
Catalyst*Temperature	4.507
Catalyst*Temperature*Biomass Concentration	3.139
Temperature*Biomass Concentration	3.026 ^
Biomass Concentration*Biomass Concentration	2.466
Temperature(400,600)	1.400 ^

E. ORGANIC LIQUID ANALYSIS

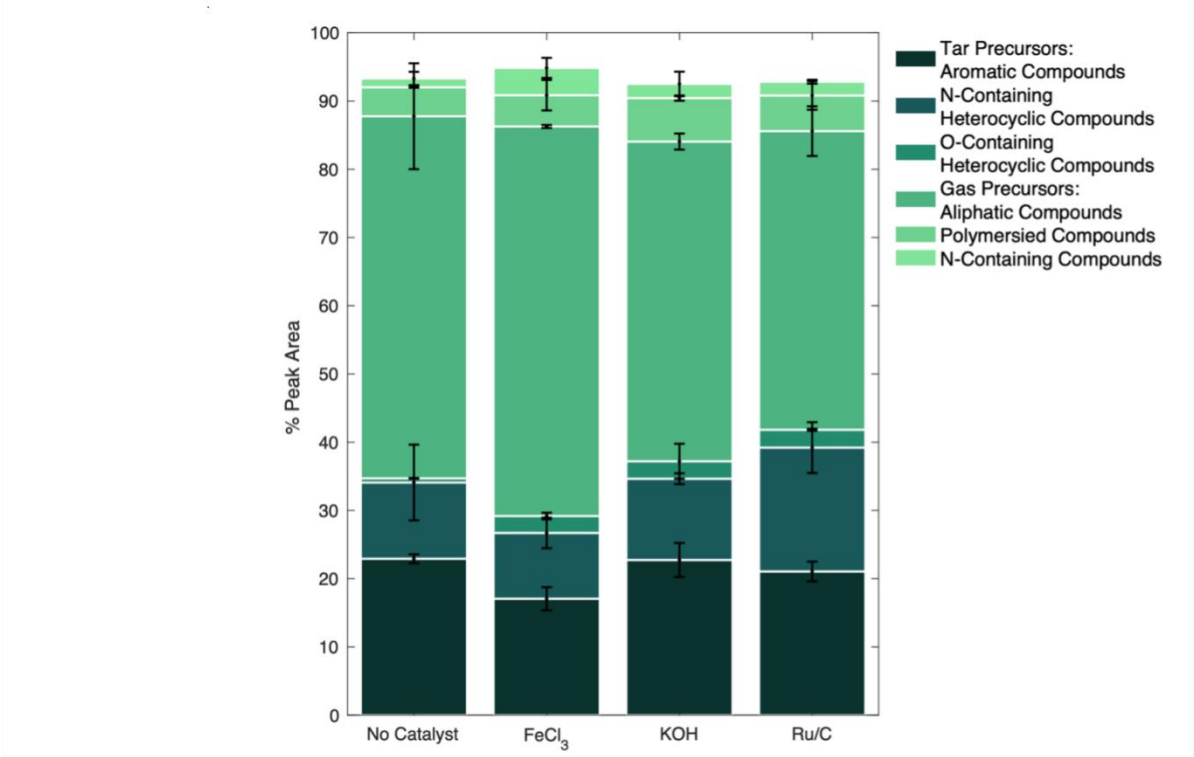

Figure -Composition of organic carbon in liquid stream.

F. Investigation into Recycle Rate and Pressure

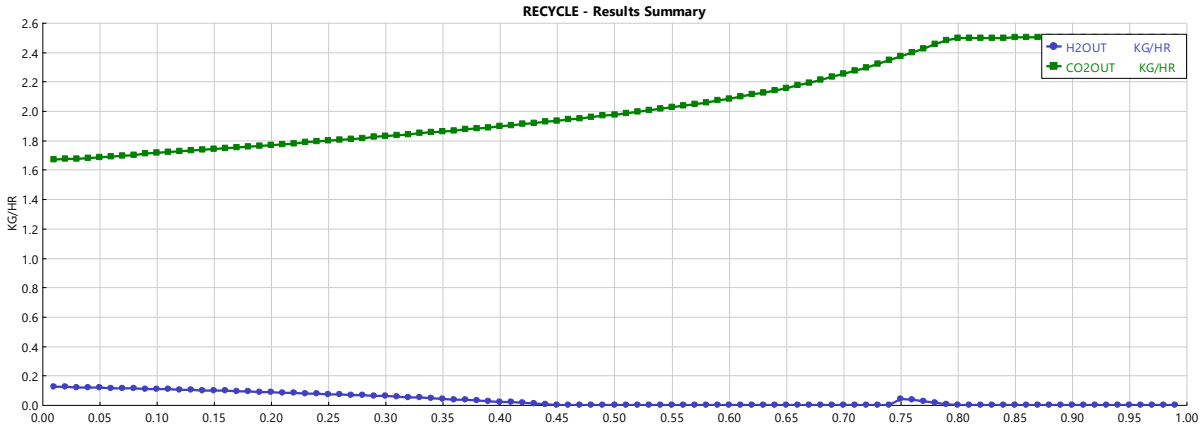

Investigation into recycle ratio at 300bar. Effect of recycle ratio of liquid effluent (x axis) on the hydrogen yield and carbon capture. Performed using equilibrium model at 600°C, 2wt% biomass, reaction pressure 23MPa, HP separator pressure 30MPa.

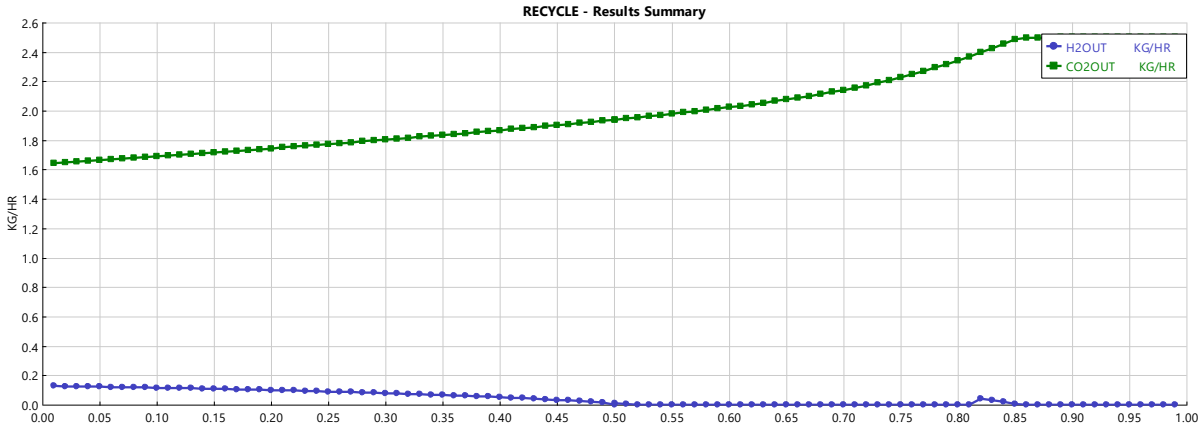

Investigation into recycle ratio at 230bar. Effect of recycle ratio of liquid effluent (x axis) on the hydrogen yield and carbon capture. Performed using equilibrium model at 600°C, 2wt% biomass, reaction pressure 23MPa, HP separator pressure 23MPa

G. pH Change and Influence of KOH

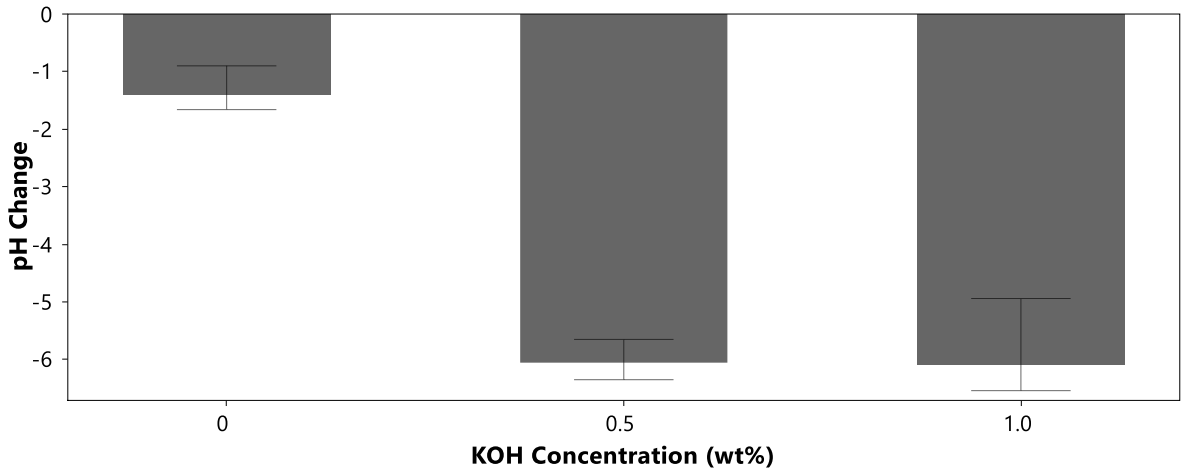

Mean pH changes from feedstock to liquid product following SCWG of Chlorella vulgaris. Error bars refer to the range of the data.

H. Actual vs Predicted Plots

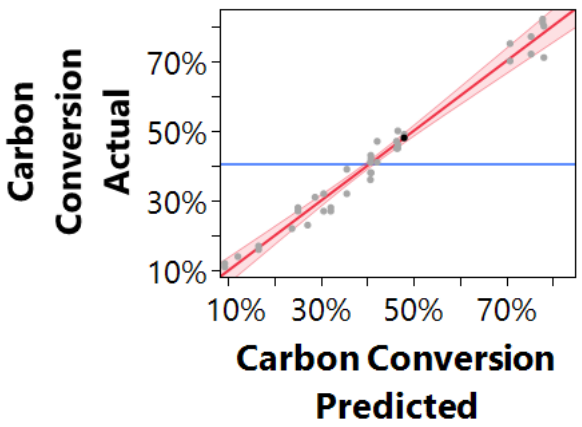

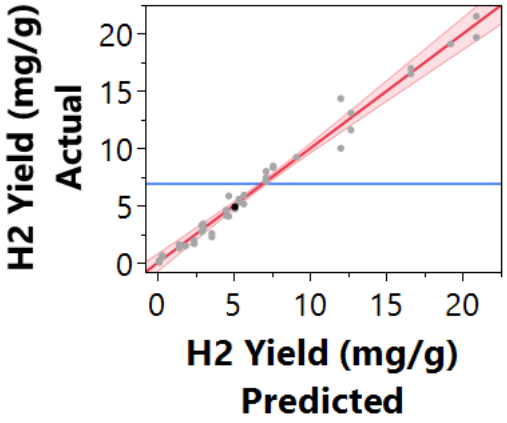

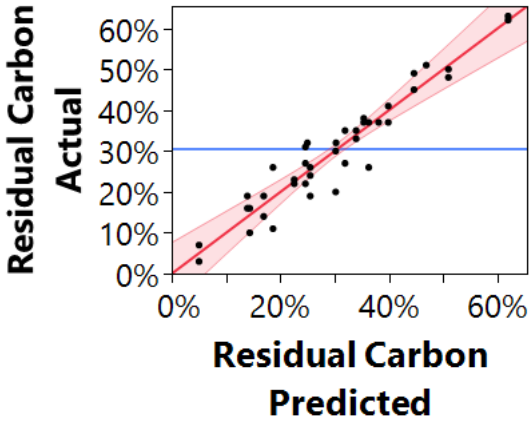

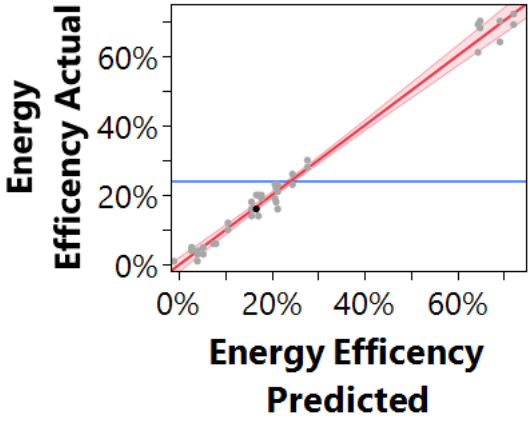

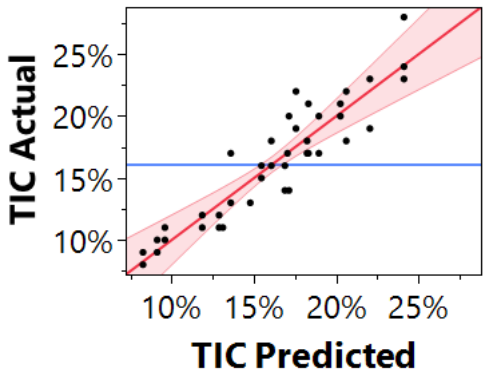
TIC Actual
25%
20%
15%
10%
10% 15% 20% 25%
TIC Predicted

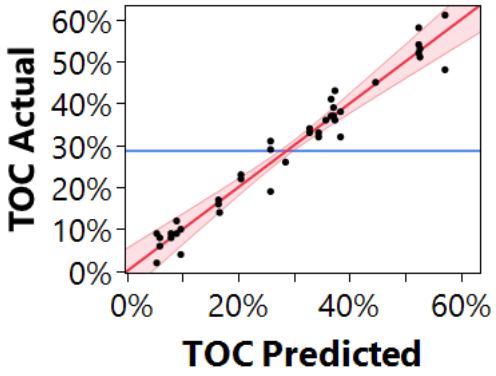
TOC Actual
60%
50%
40%
30%
20%
10%
0%
0% 20% 40% 60%
TOC Predicted

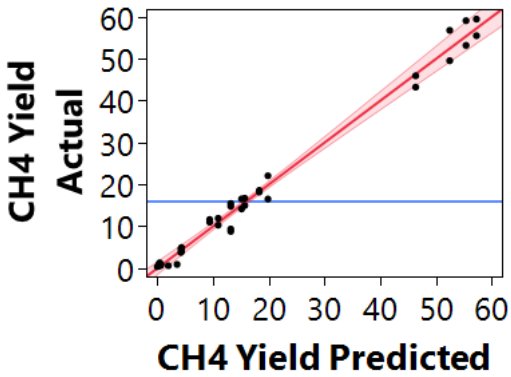
CH4 Yield Actual
60
50
40
30
20
10
0
0 10 20 30 40 50 60
CH4 Yield Predicted

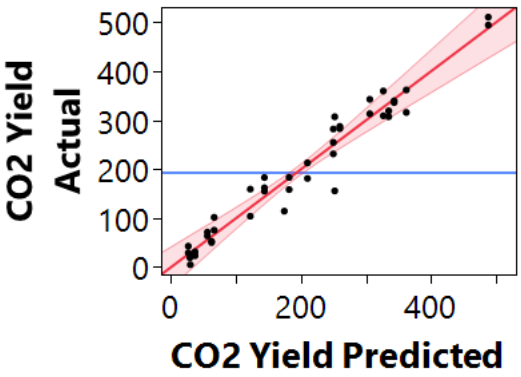
CO2 Yield Actual
500
400
300
200
100
0
0 200 400
CO2 Yield Predicted

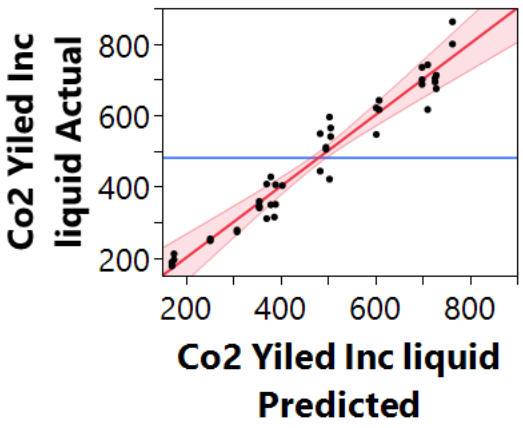
Co2 Yiled Inc liquid Actual
800
600
400
200
200 400 600 800
Co2 Yiled Inc liquid Predicted

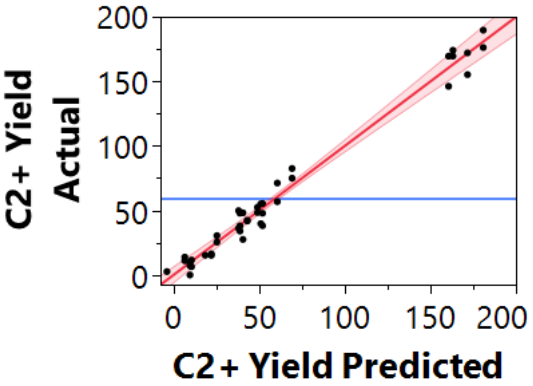
C2+ Yield Actual
200
150
100
50
0
0 50 100 150 200
C2+ Yield Predicted

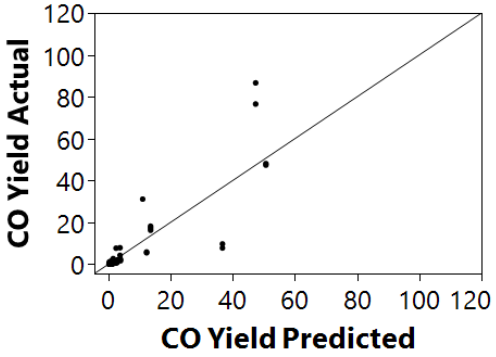
CO Yield Actual
120
100
80
60
40
20
0
0 20 40 60 80 100 120
CO Yield Predicted